Exploring the Production, Biological Activity and Preclinical Safety of Antimicrobial Spirotetronates Isolated from Marine Microorganisms

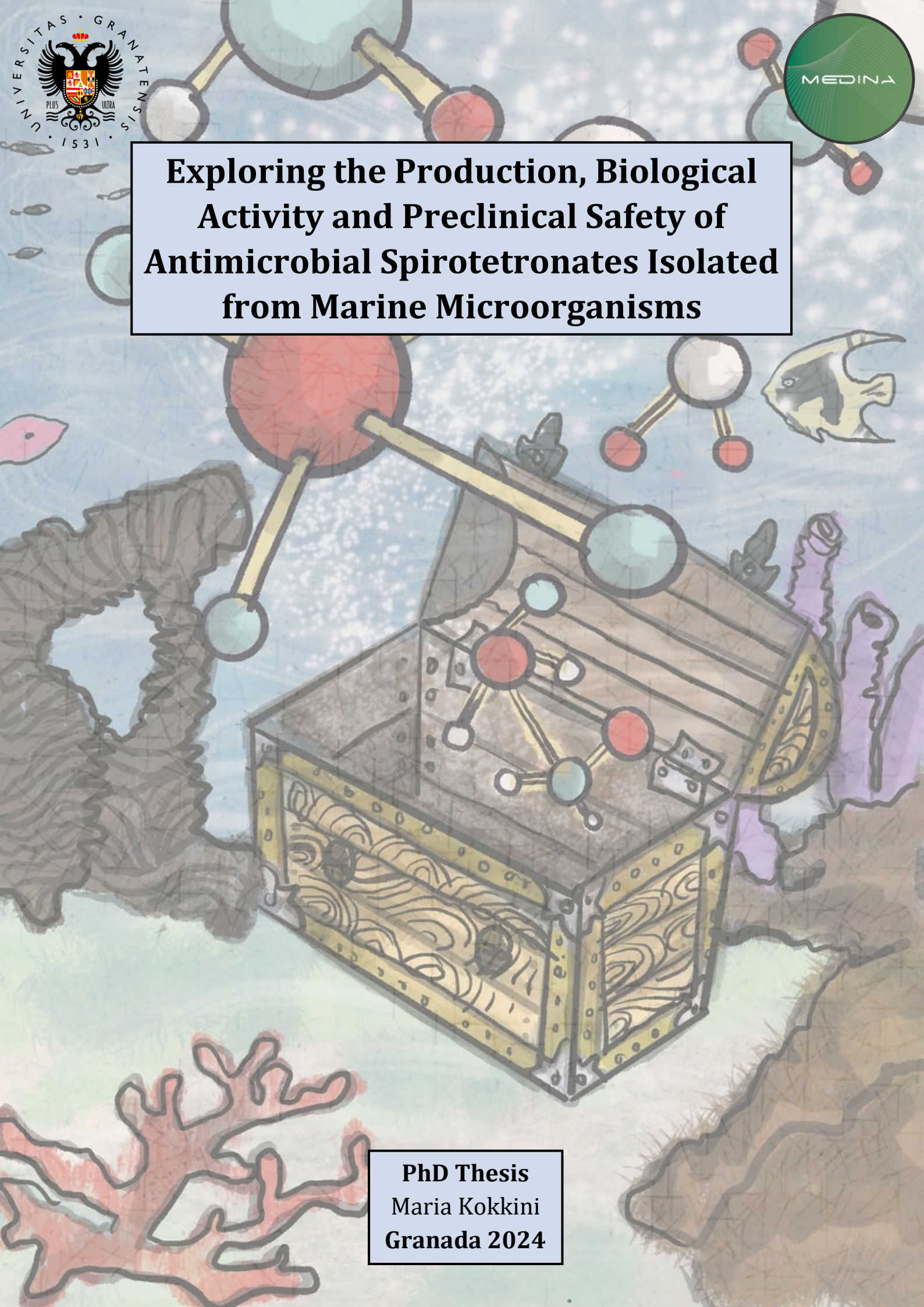

PhD Thesis
Maria Kokkini
Granada 2024

Universidad de Granada

Doctoral programme in Pharmacy

Exploring the production, biological activity and preclinical safety of antimicrobial spirotetronates isolated from marine microorganisms

PhD Thesis

Maria Kokkini

Supervisors

Olga Genilloud Rodríguez

José Fernando Reyes Benítez

Granada 2024

Editor: Universidad de Granada. Tesis Doctorales
Autor: María Kokkini
ISBN: 978-84-1195-406-8
URI: https://hdl.handle.net/10481/94654

“A scientist in his laboratory is not a mere technician:
he is also a child confronting natural phenomena
that impress him as though they were fairy tales.”

~ Marie Sklodowska Curie

"It is the tension between creativity and skepticism
that has produced the stunning and unexpected
findings of science."

~Carl Sagan

Στην οικογένεια μου

The present doctoral thesis has been conducted in the Chemistry Department of Fundación MEDINA under the supervision of Dr. José Fernando Reyes Benítez and Dr. Olga Genilloud Rodríguez within the research area of New Therapeutic Targets of the Doctoral Program in Pharmacy (B15.56.1) at the School of Doctoral Studies in Health Sciences of the University of Granada. This research work has been funded by the European Union Horizon 2020 Marie Skłodowska-Curie Actions - Innovative Training Networks (EU-H2020-MSC-ITN): MarPipe project, Grant Agreement no: 721421, **"**Improving the flow in the pipeline of the next generation of marine biodiscovery scientists**".**

Three secondments have been conducted within the MarPipe project:

-Secondment in ABS-int company under the supervision of Dr Thomas Vanagt,

where training was carried out on ¨Law, Policy and Business¨

08/10/2019-18/10/2019, Brugge, Belgium

-Secondment in KU Leuven under the supervision of Prof. Peter de Witte,

where studies were carried out on toxicity evaluation of secondary metabolites against zebrafish eleuthero embryos.

25/01/2020-07/02/2020, Leuven, Belgium

-Secondment in the Marine Biodiscovery Centre, Department of Chemistry, University of Aberdeen under the supervision of Dr Rainer Ebel (interrupted by the COVID-19 pandemic),

where studies were carried out on metabolomic profiling and molecular networking of microbial extracts by bioinformatics tools (MetaboAnalyst, GNPS).

10/02/2020-17/04/2020, Aberdeen, Scotland, UK

The results from this thesis were published in the following peer-reviewed journals:

Kokkini, M.; Oves-Costales, D.; Sánchez, P.; Melguizo, Á.; Mackenzie, T.A.; Pérez-Bonilla, M.; Martín, J.; Giusti, A.; de Witte, P.; Vicente, F.; et al. New Phocoenamicin and Maklamicin Analogues from Cultures of Three Marine-Derived Micromonospora Strains. Mar. Drugs 2023, 21, 443. https://doi.org/10.3390/md21080443

Kokkini, M.; González Heredia, C.; Oves-Costales, D.; de la Cruz, M.; Sánchez, P.; Martín, J.; Vicente, F.; Genilloud, O.; Reyes, F. Exploring Micromonospora as Phocoenamicins Producers. Mar. Drugs 2022, 20, 769. https://doi.org/10.3390/md20120769

Other scientific publications during PhD period:

Pérez-Bonilla, M.; Oves-Costales, D.; De la Cruz, M.; Kokkini, M.; Martín, J.; Vicente, F.; Genilloud, O.; Reyes, F. Phocoenamicins B and C, New Antibacterial Spirotetronates Isolated from a Marine Micromonospora sp. Mar. Drugs 2018, 16, 95. https://doi.org/10.3390/md16030095

Contributions to scientific conferences and meetings:

Exploring Micromonospora species. XVI International Symposium on Marine Natural Products. 2019. Portugal.

Minor phocoeanamicin analogues from cultures of the marine actinomycete *Micromonospora* sp.. BIOPROSP_19. University of Tromso, Norway. 2019. Norway.

New Antibacterial spirotetronates from marine actinomycete Micromonospora *chaiyaphumensis*. 10th European conference on Marine Natural Products. 2017. Greece.

Agradecimientos

Pasar por este doctorado ha sido toda una aventura, y pasaron épocas que por distintas razones personales, dudé que llegaría hasta aquí escribiendo los agradecimientos. Y no podría haberlo hecho sin un montón de gente que ha estado ahí para mí en cada paso del camino.

Primero de todo, ha sido una suerte contar con Fernando Reyes y Olga Genilloud como mis directores de tesis. Fernando, su insistencia en la excelencia y su disposición para explorar nuevas ideas han ampliado enormemente mi conocimiento. Su habilidad para ver más allá de los datos y encontrar la historia que merece ser contada ha enriquecido no solo mi tesis, sino también mi forma de ver el mundo. Y Olga, su creatividad y su enfoque innovador ha sido la guía que me ha hecho sentir capaz para enfrentarme a los desafíos que encontraba. Juntos, Fernando y Olga, han creado un ambiente de aprendizaje que valora tanto el rigor como la creatividad. Gracias por cada momento de orientación, crítica constructiva y aliento. Este logro es también un reflejo de vuestro compromiso como educadores y mentores.

No puedo dejar de mencionar a una figura clave: mi tutor, Rafael Salto, interesándose no solo por mi progreso académico sino también por mi bienestar general. Gracias, Rafael por tu disposición en todo momento para prestarme tu ayuda. Este viaje ha sido más llevadero gracias a tu apoyo.

Next, I would like to thank all MarPipe IPs for their precious advice and the moments we shared during our wonderful meetings. Special thanks to Prof. Peter de Witte for the warm hospitality in KU Leuven and of course Dr Rainer Ebel and Prof. Marcel Jaspars for showing me Scotland and Highlands and making me feel like home in the difficult situation of the pandemic.

A mis compañeros de trabajo. Cada uno de vosotros ha jugado un papel fundamental en hacer de nuestro lugar de trabajo no solo un espacio profesional sino también un lugar donde la solidaridad, el apoyo mutuo y las risas son parte del día a día. Eli, Carlos, Isa, Paqui, Mercedes, Ignacio, Nacho, Rubén, Pili, Germán, Thomas, Fran y todo MEDINA, gracias por los momentos compartidos. No podría haber pedido un mejor equipo para tener a mi lado. Dani Oves, gracias por introducirme en el mundo de microbiología y siempre ayudándome contestando a mis preguntas. Gloria y Jesús, he aprendido muchísimas cosas de vosotros, gracias por conocerme a Mr Gilson, la mariposa y mucho más.

Un especial agradecimiento a Mercedes y Pepe, que me hicieron sentir que no estaba sola desde mi llegada a España. Y por supuesto, a mis compañeros y amigos Javi, Cari, Ángeles y Dani, los cuales se han convertido en una parte muy importante de mi vida. Espero que sepáis cuánto aprecio

y valoro el tiempo y las experiencias compartidas. Javi, gracias por tus sabios consejos y tu ayuda en el laboratorio. Cari, gracias por estar allí e introducirme al mundo de metabolómica que se ha convertido en una pasión. Ángeles, fuiste una inspiración y siempre dispuesta a ayudarme con los ensayos y mucho más. Y Dani, mi primer amigo en España, gracias por todo, necesitaría muchas páginas para expresar cuánto me has ayudado.

The MarPipe project has been one of the most enriching experiences of my academic career, and this is largely due to my extraordinary project partners. You have been more than just colleagues; you have been fellow adventurers on a journey that, while full of uncertainties, was also filled with moments of joy and satisfaction. MarPipes, Alejandro, Arianna, Menia, Anky, Daniel, Kevin, Grant, Sloane, Yannick, Jane and Florent, thank you for all the wonderful moments we shared, I'm very lucky to have had you as my group.

Στην οικογένεια μου, Πόπη, Δημήτρη, Σήφη και Γιάννη, που πιστέψατε σε μένα ακόμα κι όταν εγώ οχι. Στους φίλους μου, Μπουμπού, Άννα, Στέλλα, Ισιδωράκι, Νεφέλη, Νατάσα, Τόνια, Τίνα, Πετρούλα, Νίκο κ Δίωνα που πάντα ήσαστε εκεί, ακόμα και από μακριά.

Un especial gracias a la gente del maravilloso grupo de "Cenes y yo"! Luci, gracias por dibujar la increíble portada de esta tesis y Ali, gracias por ayudarme con los gráficos del artículo en un momento de desesperación! Laly y Sole, gracias por estar allí en mis peores y mejores momentos, no lo habría hecho sin vosotras. Gracias Laly por ser parte de los altibajos y por las incontables horas de compañía y Sole, has sido más que una amiga, gracias por tu apoyo, ya sea en persona o a través de la pantalla, compartiendo ese espacio que tanto nos ayudó. Y por último, gracias Alfon por tu amor, paciencia y comprensión todos estos años, hicieron que este viaje no solo fuera posible, sino también alegre y han cambiado mi vida.

Table of Contents

Abstract

Historically, natural products (NPs) have played a major role in the discovery of antibiotics. They offer special characteristics in comparison with synthetic compounds, which carry both advantages and challenges for the drug discovery process. Over the past few years, new technological and scientific advances have reinforced the field of NP discovery and the discovery of new antibiotics, contributing to the fight against Antimicrobial Resistance (AMR). The marine environment bears a treasure chest of bioactive compounds and marine actinomycetes have proven to be one of the most prolific producers. The spirotetronate class of polyketides, with more than 100 bioactive compounds described to date, has recently grown with the discovery of phocoenamicins, marine actinomycete derived compounds that possess different antibiotic activities and three compounds have initially been discovered, phocoenamicin, phocoenamicin B and C.

Exploring the MEDINA's strain collection for possible new phocoenamicins producers, 27 actinomycete strains were identified, including 3 marine-derived and 24 terrestrial strains, and their taxonomic identification by 16S rDNA sequencing showed that they all belong to the *Micromonospora* genus, suggesting that the biosynthesis of the phocoenamicins is restrained within this genus. Despite the close taxonomic relationship of the strains, the producers identified were isolated from very diverse ecosystems and a wide geographical distribution.

Using a One Strain Many Compounds (OSMAC) approach, these 27 strains were cultivated in 10 different media each, resulting in 270 fermentations, whose crude extracts were analyzed by LC-HRMS and tested against a panel of pathogens showing activity against methicillin-resistant *Staphylococcus aureus* (MRSA), *Mycobacterium tuberculosis* H37Ra and *Mycobacterium bovis*, revealing a rich antimicrobial potential within the 27 strains.

Metabolomics analysis showed that all 27 strains produced the three known phocoenamicins, in at least one of the culture media and the analysis of the production of these phocoenamicins determined the most suitable culture media. The influence of the different cultivation parameters in the chemical profile obtained was studied and only variations in the culture medium could explain the chemical variation and determine a significant change in the metabolic profile of the different *Micromonospora* strains.

The combination of the LC-UV-HRMS analysis, metabolomic profiling and molecular networking allowed the putative dereplication of the main compounds produced by the 27 strains in the different culture conditions, which were divided into three main groups, spirotetronates, siderophores and various other compounds. The spirotetronate maklamicin, structurally related to phocoenamicins, was also tentatively identified to be produced by all 27 strains and its coexistence

with the phocoenamicins in the extracts confirmed the obvious common biosynthetic origin of both families of compounds. Moreover, the analyses tentatively revealed the presence of several structurally related compounds not disclosed before and thus candidates for isolation and discovery of new bioactive compounds. This wide and chemically diverse metabolic profile of these strains highlighted the need for further research.

Combining these analyses proved to be a rapid and efficient way to prioritize strains. Although previous statements in the literature about phocoenamicins production only in unique marine environments were not confirmed, the marine-derived *Micromonospora* species were identified as the best producers of phocoenamicins in terms of both the abundance in their extracts of some of the major members, as well as the variety of molecular structures produced.

Exploring the growth of *Micromonospora* and the production of phocoenamicins, suggested the best growing conditions for the production of the three compounds. As a result, cultures of the three marine-derived *Micromonospora* strains (CA-214671, CA-214658 and CA-218877) were scaled up (3 and 5 L fermentations) and optimal chromatographic conditions for the purification of the phocoenamicins were established, leading to the isolation and structural elucidation of seven compounds, including two new phocoenamicins, phocoenamicins D and E, together with the known phocoenamicin, phocoenamicins B and C, as well as maklamicin and the new analog 29-deoxymaklamicin, reported for the first time as a natural product, and for which the name maklamicin B has been proposed. The two families of compounds shared multiple structural features, as well as common structural variations that were highlighted. Interestingly, one of the new phocoenamicins described bore the side chain of maklamicin, unique so far in this compound, indicating common structural features conserved within the two families.

All the compounds isolated were tested against a panel of bacterial human pathogens, including methicillin-resistant *S. aureus* (MRSA), *M. tuberculosis* H37Ra, *Enterococcus faecium*, *Enterococcus faecalis* and *Neisseria gonorrhoeae*. Similarly to other related spirotetronates, most of the compounds showed some antibacterial activity against Gram-positive bacteria and the antibacterial assays revealed some structure-activity relationships. Overall, the most active compounds were maklamicin B and maklamicin, followed by phocoenamicin and phocoenamicin B, being some of these activities reported for the first time.

The compounds demonstrated weak or no cytotoxicity against the human liver adenocarcinoma cell line (Hep G2). Finally, the toxicity of the three major compounds obtained, namely phocoenamicin, phocoenamicin B and maklamicin, was evaluated against zebrafish eleuthero embryos and no toxicity was displayed up to the highest concentration tested (25 μM). Maklamicin B resulted to be the most interesting compound, combining strong antimicrobial activity against MRSA, *M. tuberculosis* and *E. faecium* and no cytotoxicity.

The new analogues isolated highlighted the wide range of structural diversities of the spirotetronates and the possible structure-activity relationships recorded here, along with others reported before within the spirotetronate class, can be used as pieces in a puzzle to unveil the biosynthetic potential of these compounds.

Keywords: antibiotic discovery, antimicrobial activity, actinomycetes, spirotetronates, phocoenamicins, maklamicins

Resumen

Históricamente, los productos naturales (PN) han desempeñado un papel fundamental en el descubrimiento de antibióticos. Ofrecen características especiales en comparación con los compuestos sintéticos, lo que conlleva tanto ventajas como retos para el proceso de descubrimiento de fármacos. En los últimos años, los nuevos avances tecnológicos y científicos han reforzado el campo del descubrimiento de productos naturales y de nuevos antibióticos, con el objetivo de contribuir a la lucha contra la Resistencia Antimicrobiana (RAM). El medio marino alberga un tesoro de compuestos bioactivos y los actinomicetos marinos han demostrado ser uno de los productores más prolíficos. La clase de los policétidos espirotetronatos, con más de 100 compuestos bioactivos descritos hasta la fecha, ha crecido recientemente con el descubrimiento de las phocoenamicinas, compuestos derivados de actinomicetos marinos que poseen diferentes actividades antibióticas y de los que se han descubierto inicialmente tres compuestos, la phocoenamicina y las phocoenamicinas B y C.

Explorando la colección de cepas de MEDINA en busca de posibles nuevos productores de phocoenamicinas, se identificaron 27 cepas de actinomicetos, entre ellas 3 de origen marino y 24 terrestres, y su identificación taxonómica mediante secuenciación del ADNr 16S mostró que todas pertenecen al género *Micromonospora*, lo que sugiere que la biosíntesis de las phocoenamicinas está restringida a microorganismos de este género. A pesar de la estrecha relación taxonómica de las cepas, los productores identificados fueron aislados de ecosistemas muy diversos y de una amplia distribución geográfica.

Utilizando el método de "una cepa, muchos compuestos" (OSMAC por sus siglas en inglés), estas 27 cepas se cultivaron en 10 medios diferentes cada una, lo que dio lugar a 270 fermentaciones, cuyos extractos crudos se analizaron por LC-HRMS y se ensayaron contra un panel de patógenos y mostraron actividad contra *Staphylococcus aureus* resistente a la meticilina (MRSA), *Mycobacterium tuberculosis* H37Ra y *Mycobacterium bovis*, revelando un rico potencial antimicrobiano dentro de las 27 cepas.

El análisis metabolómico mostró que las 27 cepas producían las tres phocoenamicinas conocidas, en al menos uno de los medios de cultivo y el análisis de la producción de estas phocoenamicinas determinó los medios de cultivo más adecuados. Se estudió la influencia de los diferentes parámetros de cultivo en el perfil químico obtenido y sólo las variaciones en el medio de cultivo pudieron explicar la variación química y determinar un cambio significativo en el perfil metabólico de las diferentes cepas de *Micromonospora*.

La combinación del análisis LC-UV-HRMS, el perfil metabolómico y la creación de redes moleculares permitió la desreplicación putativa de los principales compuestos producidos por las

27 cepas en las diferentes condiciones de cultivo, que se dividieron en tres grupos principales, espirotetronatos, sideróforos y varios otros compuestos. También se identificó provisionalmente el espirotetronato maklamicina, estructuralmente relacionado con las phocoenamicinas, producido por las 27 cepas, y su coexistencia con las phocoenamicinas en los extractos confirmó el evidente origen biosintético común de ambas familias de compuestos. Además, los análisis revelaron provisionalmente la presencia de varios compuestos estructuralmente relacionados no revelados anteriormente y, por tanto, candidatos para el aislamiento y el descubrimiento de nuevos compuestos bioactivos. Este perfil metabólico amplio y químicamente diverso de estas cepas puso de manifiesto la necesidad de seguir investigando.

La combinación de estos análisis demostró ser una forma rápida y eficaz de priorizar las cepas. Aunque no se confirmaron las afirmaciones anteriores en la literatura sobre la producción de phocoenamicinas sólo en entornos marinos únicos, las especies de *Micromonospora* de origen marino fueron identificadas como las mejores productoras de phocoenamicinas, tanto por la abundancia en sus extractos de algunos de los principales miembros, como por la variedad de estructuras moleculares producidas.

La exploración del crecimiento de *Micromonospora* y la producción de phocoenamicinas, sugirió las mejores condiciones de cultivo para la producción de los tres compuestos. Como resultado, se escalaron los cultivos de las tres cepas de *Micromonospora* de origen marino (CA-214671, CA-214658 y CA-218877) (fermentaciones de 3 y 5 L) y se determinaron las condiciones cromatográficas óptimas para la purificación de las phocoenamicinas, lo que condujo al aislamiento y elucidación estructural de siete compuestos, entre ellos dos nuevas phocoenamicinas, las phocoenamicinas D y E, junto con las phocoenamicinas conocidas, las phocoenamicinas B y C, así como la maklamicina y el nuevo análogo 29-deoximaklamicina, descrito por primera vez como producto natural, y para el que se ha propuesto el nombre de maklamicina B. Las dos familias de compuestos compartían múltiples características estructurales, así como variaciones estructurales comunes que se pusieron de relieve. Curiosamente, una de las nuevas phocoenamicinas descritas presentaba la misma cadena lateral de la maklamicina, única hasta la fecha en este compuesto, lo que indicaba una funcionalidad conservada en las dos familias.

Todos los compuestos aislados se ensayaron contra un panel de patógenos humanos bacterianos, entre ellos *S. aureus* resistente a la meticilina (SARM), *M. tuberculosis* H37Ra, *Enterococcus faecium*, *Enterococcus faecalis* y *Neisseria gonorrhoeae*. Al igual que otros espirotetronatos relacionados, la mayoría de los compuestos mostraron cierta actividad antibacteriana frente a bacterias Gram-positivas y los ensayos antibacterianos revelaron algunas relaciones estructura-actividad. En general, los compuestos más activos fueron maklamicina B y

maklamicina, seguidos de phocoenamicina y phocoenamicina B, siendo algunas de estas actividades notificadas por primera vez.

Los compuestos demostraron una citotoxicidad débil o nula frente a la línea celular de adenocarcinoma hepático humano (Hep G2). Por último, se evaluó la toxicidad de los tres compuestos principales obtenidos, a saber, phocoenamicina, phocoenamicina B y maklamicina, frente a embriones de pez cebra eleuthero y no se observó toxicidad hasta la concentración más alta ensayada (25 μM). La maklamicina B resultó ser el compuesto más interesante, ya que combinaba una fuerte actividad antimicrobiana frente a MRSA, *M. tuberculosis* y *E. faecium* con la ausencia de citotoxicidad.

Los nuevos análogos aislados pusieron de manifiesto la amplia gama de diversidades estructurales de los espirotetronatos y las posibles relaciones estructura-actividad aquí registradas, junto con otras comunicadas anteriormente dentro de la clase de los espirotetronatos, pueden utilizarse como piezas de un rompecabezas para desvelar el potencial biosintético de estos compuestos.

Palabras clave: descubrimiento de fármacos, actividad antimicrobiana, actinomicetos, espirotetronatos, phocoenamicinas, maklamicinas

1. INTRODUCTION

1. Introduction

1.1 Antibiotic Discovery

Antibiotics have arguably changed modern medicine and their introduction into clinical use was the greatest medical breakthrough of the 20th century. Sulfonamides were the first broad spectrum antimicrobials and are still in use today, followed by the discovery of penicillin [1]. After penicillin, during the decades of 1940 and 1950, many new antibiotics have derived from microbial sources, such as streptomycin, erythromycin, cephalosporins, bacitracin, chloramphenicol, polymyxin, tetracycline, aminoglycosides, macrolides, vancomycin, and neomycin. These compounds were effective in the treatment of various infections, such as bacterial pneumonia (*Klebsiella pneumoniae* and others), syphilis (*Treponema pallidum*) and tuberculosis (*Mycobacterium tuberculosis*), among others. The two decades that followed, 1950-1970, were considered as the "golden age" of antibiotic discovery, but since the late 1980s until the present days, there has been a discovery void and very few new classes of antimicrobial compounds have reached the market [2].

Several types of antimicrobial agents exist such as antibiotics, disinfectants, and food preservatives that can be used against microorganisms. The antibiotics are classified in bactericidal drugs, which can induce cell death or bacteriostatic drugs that simply inhibit the cell growth. There are natural, semi-synthetic and synthetic agents having different mechanisms of action, including interference with cell wall synthesis, such as β-lactams, protein synthesis inhibition such as tetracyclines, metabolic pathway inhibition such as sulfonamides and interference with DNA replication and translation, such as fluoroquinolones [2],[3]. Most antimicrobial drugs are naturally produced by microorganisms, including environmental fungi and saprophytic bacteria or are synthetic derivatives of them, with only a few classes (e.g. sulfonamides and fluoroquinolones), being entirely synthetic [4].

1.1.1 Natural Products Antibiotics

Natural products (NPs) are small molecules, usually with a molecular weight below 3000 Da, and are secondary metabolites produced by living organisms, such as plants, animals or microorganisms. They have no primary role directly involved in the growth or reproduction of an organism but are generally used to control ecological relationships that involve defense, competition for space or food, communication between organisms, among other functions [5].

They offer a wide variety of biological activities, and have been the most promising sources of chemical inspiration [6] for drug discovery and development [7], resulting in the discovery of some of the most important molecules in recent history [8].

Historically, NPs have played a major role in the discovery of antimicrobials. They offer an exceptional chemical diversity and structural three-dimensional complexity that, having evolved over time [9], they often possess unique and highly selective biological activities based on the hypothesis that all natural products have some receptor-binding function [10].

NPs are structurally 'optimized' by evolution to serve particular biological functions, including the regulation of endogenous defense mechanisms and the interaction with other organisms, which explains their high relevance for infectious diseases and cancer [9].

They are an invaluable source of inspiration in drug design and development [11], compared to the lack of success of synthetic molecules which often lack the physiochemical properties to penetrate bacterial membranes [12]. Having evolved over several millennia to acquire specific ligand–protein binding motifs, NP structures cover a wide range of biologically relevant chemical space that cannot be efficiently explored by synthetic compounds [11]. Moreover, the structures of natural products can inspire the design and synthesis of analogues that may have improved properties [13].

More than 300,000 natural products have been discovered, that are classified according to their chemistry into terpenoids and steroids, fatty-acid-derived substances and polyketides, alkaloids, non-ribosomal peptides, and shikimate-derived compounds. They can exhibit different bioactivities, such as antibacterial, antifungal, and antiparasitic activities, with different mechanisms of action for killing pathogens [14].

They have provided the pharmacophores for most of the major classes of antibiotics, including the β-lactams, aminoglycosides, macrolides, tetracyclines, rifamycins, glycopeptides, streptogramins and lipopeptides [15]. In fact, according to Newman and Cragg's review analyzing the new drugs approved from 01/1981 to 09/2019, of all the new antibacterial drugs (vaccines excluded), 89 were natural products or natural product derivatives (68.5%), while only 36 were totally synthetic drugs (27.7%) [16].

1.2 Antimicrobial Resistance (AMR)

Antimicrobial resistance (AMR) occurs when microbes possess or develop the ability to survive the action of antimicrobial compounds [17]. As a result, these surviving microorganisms pass on their resistant features to succeeding generations and are spread more and more in the environment through natural selection. It can appear in different types of microbes including

bacteria, fungi, viruses, and some protozoa [18]. Infections caused by resistant pathogens are usually more difficult to treat, causing significant morbidity and mortality and are considered a major global health concern [19].

Microbes produce a plethora of molecules with antimicrobial activity that have been optimized throughout evolution, probably as a result of the competition for resources and struggle for existence in their microenvironment [19]. Likewise, there is broad evidence showing that resistance mechanisms against these compounds were developed by the producing organisms as self-immunity mechanisms, and have been in nature long before the use of antibiotics by humans [20]. Antimicrobial resistance genes, identified to be responsible for the resistance against antimicrobial natural products, have been found across the different bacterial lineages in nature and they determine the environmental resistome [19],[2]. The analysis of metagenomic DNA from 30,000-year-old permafrost sediments revealed that it contained several resistance genes for the *β*-lactam, carbapenem and vancomycin, natural products antibiotics and these genes were remarkably similar to their modern equivalents [8].

AMR has emerged as a significant challenge, marking an evolutionary battle between microbial adaptation and human medical advancements. Taking a short trip into the history of antibiotics and their resistances, Alexander Fleming discovered the existence of penicillin in 1928, after observing that the mold colonies of *Penicillium* inhibited the growth of *Staphylococcus* bacteria and extracting the active substance. It is only in the early 1940s, that Howard Florey and Ernst Chain purified penicillin which led to the massive production of penicillin G in 1943, changing medical history [2]. However, even before this massive production, in 1940, the first penicillin resistant *Staphylococcus* strains had already been described [19]. Furthermore, methicillin was introduced in 1959 in order to combat penicillin resistant strains and only a year later, the first methicillin resistant *Staphylococcus* strain was reported. Vancomycin was then introduced in 1954 for the treatment of methicillin-resistant *Staphylococcus* and in 1979, a first strain resistant to vancomycin was reported, and so on [19].

1.2.1 Antimicrobial Resistance Mechanisms

The origins of antibiotic resistance can be traced back to the natural environments where antibiotics are produced. Microbes use different types of mechanisms to overcome the effectiveness of the antimicrobial components. Antimicrobial resistance can be broadly classified in intrinsic, acquired, or adaptive [19].

Intrinsic is the resistance exhibited due to the inherent properties of the microorganism [19] and is related to the fact that a microorganism has no structures on which an antimicrobial compound can act or it initially produces enzymes that can inactivate it [20].

On the other hand, acquired resistance results from genome modification when a previously sensitive bacterium acquires a resistance mechanism by either mutation or acquiring new genetic material from an exogenous source (horizontal gene transfer), such as plasmids from other bacteria [19],[20]. Horizontal gene transfer is considered to be the most important factor [18] and can occur through three main mechanisms: transformation, transduction and conjugation [21].

Finally, adaptive is the resistance induced by a specific environmental signal (e.g., stress, growth state, pH, nutrient conditions). In contrast to intrinsic and acquired resistance, adaptive resistance is transient. It allows microbes to respond more rapidly to antimicrobial challenge and generally reverts to the original state once the inducing signal is removed, being therefore the result of epigenetic changes by modifying gene expression as a response to environmental changes [19],[22].

The different protective mechanisms by which bacteria can escape antibiotics include a) producing enzymes that inactivate the antimicrobial by chemically altering it, b) changing the target site of the antibiotic using various strategies (e.g. target replacement, target site mutations, target site enzymatic alterations, target site protection, target overproduction or target bypass), c) preventing the entry of (decreased permeability) or exporting the drug out of a bacterial cell before they can exert their effects by bacterial membrane efflux pumps and finally d) forming biofilms, syntrophic communities of microorganisms in which cells are in close association with each other and often also to a surface. These adherent cells become embedded within a slimy and hard-to-remove extracellular matrix that is composed of polysaccharides, proteins, and nucleic acids [19],[2],[3],[4],[23].

1.2.2 Resistant Pathogens

World Health Organization (WHO) and Centers for Disease Control and Prevention (CDC) have identified the most concerning antibiotic-resistant pathogens, commonly referred to as superbugs and classified them into three categories, namely urgent, serious, and concerning, based on their level of concern for human health, a list that is regularly updated [8],[3].

The ESKAPE pathogens, among others, are some of the highest priority pathogens due to their ability to "escape" the effects of antibacterial drugs and the development of resistance mechanisms against multiple antibiotics. They pose significant challenges to healthcare as they are common causes of life-threatening nosocomial infections amongst critically ill and

immunocompromised individuals [23]. ESKAPE is an acronym formed from the first letters of the genus names of each bacterium that is part of the group, including both Gram-positive and Gram-negative species. In particular, they are, in this order:

-*Enterococcus* species, are Gram-positive bacteria and their normal habitat is the gut of humans and animals. There are more than 20 *Enterococcus* species, although *E. faecium* and *E. faecalis* are the most clinically relevant. *E. faecium* has developed resistance to vancomycin through the acquisition of vanA and vanB genes.

-*Staphylococcus aureus* is a Gram-positive and is part of the normal skin flora of humans and animals. Reports of methicillin-resistant *S. aureus* (MRSA) emerged in the 1960s, and currently, MRSA isolates are estimated to account for 25% of *S. aureus* isolates. In the healthcare setting, MRSA can cause severe infections such as bloodstream infections, sepsis, pneumonia, and surgical site infections [24].

-*Klebsiella pneumoniae* is a member of the family Enterobacteriaceae. It is a non-fastidious, Gram-negative bacillus and species of this genus are the bacterial pathogens most often found associated with infections in healthcare settings and in recent years have acquired resistance against β-lactam antibiotics such as penicillins, cephalosporins, and carbapenems. It produces extended-spectrum beta-lactamases (ESBLs) and carbapenemases, enzymes that break down a wide range of beta-lactam antibiotics.

-*Acinetobacter baumannii*, is a Gram-negative that causes a variety of infections, including in the respiratory and urinary tracts, leading to high rates of cross contamination in nosocomial infections. It possesses an arsenal of resistance mechanisms, including efflux pumps, enzymatic degradation of drugs, and modifications of antibiotic targets.

-*Pseudomonas aeruginosa* is a Gram-negative, facultative anaerobe found in the normal gut flora and a relevant pathogen in healthcare environments. Many *P. aeruginosa* strains show an intrinsic reduced susceptibility to several antibacterial agents, as well as a tendency to develop resistance during therapy. It is inherently resistant to many antibiotics due to its low outer membrane permeability and can acquire additional resistance through mutations or horizontal gene transfer.

-*Enterobacter* species are non-fastidious Gram-negative rods, which can cause infections in immunocompromised patients, usually in healthcare environments and have demonstrated a wide range of antibiotic resistance mechanisms. They share similar resistance mechanisms to *K. pneumoniae*.

Finally, the emergence and spread of multidrug-resistant strains of *Mycobacterium tuberculosis* represents one of the most important challenges to disease control worldwide with high rates of mortality [24]. *M. tuberculosis* is the bacterium responsible for tuberculosis (TB), a

disease that primarily affects the lungs but can also impact other parts of the body. It has developed various mechanisms to resist antibiotic treatment, such as cell wall impermeability, target alteration and drug inactivation [25]. *Mycobacterium bovis*, closely related to *Mycobacterium tuberculosis*, is commonly known as the causative agent of bovine tuberculosis (TB) in cattle. However, it can also infect various other mammals, including humans, causing a zoonotic disease known as human tuberculosis. Bovine tuberculosis is a chronic infectious disease that primarily affects the respiratory system in cattle but can also affect other organs. It poses a significant economic burden on the livestock industry due to decreased productivity, trade restrictions, and control measures [26].

1.2.3 Emergence of AMR and Main Factors

Although AMR is an inevitable phenomenon which occurs naturally over time as a result of selective pressure, the human factor is accelerating this process, clearly driving the evolution of resistance. The widespread use, overuse and misuse of antimicrobials in humans, animals and the environment has accelerated the process and has led to the explosion of antimicrobial resistance [19],[2].

In a pristine ecosystem, free from external antimicrobial selection pressure, antimicrobial-resistant and non-resistant species coexist in a stable balance. Antimicrobial resistant bacteria have been found in every environment examined so far including sea, soil, drinking water and various food products. The human microbiota is no exception, and microorganism populations in human beings include species that are naturally resistant to some antimicrobials [4]. The increased exposure to environmental levels of antibiotics has disrupted this natural balance between microbes [27]. It is well documented that increased antibiotic use is correlated with higher resistance rates, as countries with high rates of antimicrobial resistance also report higher rates of antimicrobial consumption and vice versa. Hence, AMR needs to be viewed under a One-Health approach, as human health is inseparably linked to the health of animals and the viability of ecosystems [19].

Antimicrobials are among the most commonly prescribed drugs used in human medicine, and studies have shown that up to 50% of all antibiotics prescribed to people are considered unnecessary. However, various studies have shown that more antimicrobials are used in veterinary medicine, agriculture, animal and fish production than in humans and that antimicrobial resistance has in part emerged as a result of antimicrobial use outside of human medicine [4]. In fact, while about 1/3 of the total antibiotic use is in humans, 2/3 is in animals, primarily for growth promotion. Additionally, environment contamination with antimicrobials due to improper handling of human excreta, contaminated effluent from hospitals/pharmaceutical companies and use of biocides in

agriculture also contributes to the increase of AMR [18]. The majority of consumed antibiotics are excreted unchanged and are then introduced into the environment directly or through waste streams that are considered hotspots for the dissemination of AMR. Moreover, the antibiotic compounds are often not completely removed in treatment plants, from where they then disseminate further [24]-[27]. Finally, the above mentioned issues are more likely to appear in low-income and middle-income countries [4], as poverty is a major root factor of antimicrobial misuse in developing countries [28].

Antimicrobials are the pillars of modern medicine, and any medical advances depend on the ability to fight infections using antibiotics, including organ transplants, cancer therapy and treatment of chronic diseases. It is estimated that globally approximately 700,000 deaths are attributed to antimicrobial resistance every year, being this the second cause of death in the world which, according to CDC, could rise to 10 million deaths per year by 2050 [18]-[20], more than cancer and heart diseases together [2]. WHO published a report on the global shortage of novel antimicrobials in April 2021, concluding that the current antibiotic development pipelines and clinically approved antibiotics are insufficient to combat drug-resistant pathogens [8].

Therefore, this scenario can lead to a dark post-antibiotic era, when minor injuries and common infections could become the leading causes of death [3]. All evidence suggests that no single solution exists and several synergistic approaches are needed [4]. Together with limiting unnecessary antibiotic use, it is recognized that only novel chemical classes of antibiotics will bring novel mechanisms of action and will hopefully surpass known mechanisms of resistance [19].

1.3 Challenges and Advances in NP Drug Discovery Pipeline

The special characteristics of NPs in comparison with synthetic compounds carry both, advantages and challenges, for the drug discovery pathway [9].

Challenges in NP discovery include various shortfalls and technical barriers such as the inability to culture the majority of environmental microorganisms in the laboratory, the time consuming dereplication process, and the scale-up of the production to get the sufficient amount, considering the necessary efforts to isolate the active principles, elucidate their structures and perform biological assays [7]-[9].

Despite the urgency of the clinical need, from the 1990s onwards the large pharmaceutical companies have mostly abandoned antibiotic research and NP discovery efforts. The time required and the difficulties in the research and development, along with the short prescription duration of antibiotics and the existing broken antibiotic business model, have led to the withdrawal of the

pharmaceutical industry from antibiotic research and directed towards other clinical applications such as medicines of chronic diseases [12],[29]-[30]. Many of the pharmaceutical companies disbanded or sold their collections of screening extracts, leaving antibiotic discovery and development to academic, governmental institutions and small biotech companies [31]. As a result, there is a complete absence of new classes of antibiotics reaching the market. [24],[25].

In recent years, there has been a renewed great interest in natural products from unexplored microbial sources, especially microorganisms associated with plants, mammals and invertebrates from both marine and terrestrial habitats. [7],[12],[14]. The bioactive molecules produced by these microorganisms are often present in rather small amounts. Therefore, accessing sufficient biological material to isolate and characterize a bioactive NP are also challenges that need to be addressed [9]. Furthermore although natural resources are still considered as inexhaustible for novel chemicals, the rediscovery of previously reported NPs is frequent as they are commonly present in more than one genus, family or even phylum. The process of identifying known compounds responsible for the activity of an extract called dereplication is particularly important to accelerate the recognition of previously known compounds early on [31]. Finally, the toxicity and unfavourable pharmacokinetics (PKs) can limit the clinical potential of NPs and structural modification is often required. The structural complexity of NPs often makes the latter task highly challenging [11].

Over the past few years, several new technological and scientific advances have been developed, which have been economically sustainable and proven efficient in natural product discovery. Microbial culturing advances, genome mining and engineering strategies, improved analytical techniques and bioinformatic tools [14], are opening up new opportunities to explore new microbial sources and access new reservoirs of microorganisms, initiating a ‘new era’ and making NP drug discovery attractive again [7]-[9].

Different biotic and abiotic stress conditions can result in the production of distinct metabolites, suggesting that a deep understanding of the factors underlying metabolite production can also contribute toward the discovery of novel compounds. This has triggered microbial culturing advances, such as co-cultivation and *in situ* cultivation [14], mimicking the natural ecological conditions where microorganisms normally co-exist within complex microbial communities, as well as the development of well-established approaches in microbiology such as the “OSMAC” (One Strain Many Compounds) approach, modifying culture conditions and parameters such as temperature, pH, variations in media composition (nutrient levels, carbon and nitrogen sources), aeration, and incubation time that aim to stimulate the production of different and hopefully novel bioactive compounds, activating silent gene clusters and metabolic pathways. The rationale behind the OSMAC approach is that microorganisms possess the genetic potential to

produce a wide variety of secondary metabolites, but they may not express all of these compounds under standard laboratory conditions [9],[15].

Understanding the ecological and biological factors that affect metabolite production is crucial for the optimal exploitation of the producing microorganisms. Insight into NP biosynthetic pathways and advances in genome mining, searching for genes that are likely to govern biosynthesis of scaffold structures, has confirmed the plethora of biosynthetic gene clusters (BGCs) in the majority of microbial sources. Identifying and manipulating these BGCs are considered key drivers for modern NP-based drug discovery [9],[12],[32]. Furthermore, the supply problem of many novel and potent NPs that are found in small quantities as minor metabolites may be solved by overexpression of their biosynthetic gene clusters in cultivable organisms [15].

Metabolomics, the study of all small molecules in an organism at a specific time and under specific conditions, taking "snapshots" of biological systems, is considered as the last link in the biology chain and its coupling with other high-throughput technologies such as genomics, provides a bridge between molecular mechanisms and metabolite production [15][33]-[34]. Along with the OSMAC approach, metabolomics can be used to explore the variation of the organism's chemical diversity in response to different factors.

Enabled by technological developments in chromatography and spectrometry, metabolomics approaches are based on the simultaneous screening of large sets of metabolites, using different techniques such as LC-MS, GC-MS, and NMR spectroscopy, even if they are produced at low concentrations and the use of numerical analyses and databases to detect patterns and relevant metabolites. It is a scientific field at the interface of different disciplines (chemistry, bioinformatics, ecology, microbiology, and systems biology) and was developed as an approach in metabolic profiling, providing information on the metabolite composition in NP extracts, thus helping to prioritize NPs for isolation and accelerate dereplication [9],[32]-[33].

Raw data processing and curation can be done using several software such as R, MetGem, OpenMS and MZmine and online platforms such as MetaboAnalyst, Workflow4Metabolomics and XCMS Online, can be used to perform various analyses and generate conclusions over the data sets.

Over the last few years, molecular networking (MN) has gained a lot of attention in the field of natural products. MN is a bioinformatic tool that explores chemical diversity visualizing the entire metabolome detected in a dataset. It can organize thousands of sets of MS/MS data recorded from a given set of extracts and visualize the relationship of the metabolites as clusters of structurally related molecules, annotating unknown analogues and new NP scaffolds [9],[15]. It is based on the assumption that chemistry influences how the molecules will be fragmented by tandem mass spectrometry. Therefore, structurally related compounds will have a similar

fragmentation pattern and will be connected whereas the unrelated will be separated [35]. In a molecular network, each node represents a compound and the nodes with similar spectra are linked to form clusters or "molecular families". Moreover, these links provide valuable structural information. Compounds that belong to the same cluster usually share the same core structure but differ due to simple chemical modifications such as alkylation or oxidation. [36].

Molecular networking has led to the creation of the Global Natural Products Social Molecular Networking (GNPS), a web-based platform (http://gnps.ucsd.edu) developed by researchers at the University of California at San Diego. GNPS uses an algorithm to compare the MS/MS spectra and is based on various parameters like the cosine score. After the analysis, searching of the GNPS libraries, in-house databases, and other public spectral libraries can lead to the rapid annotation of known compounds, making GNPS an important dereplication tool [37]. GNPS offers two main workflows, the classical MN and feature-based molecular networking (FBMN). In classical MN, raw MS/MS spectra files are processed directly to generate a MN. This often leads to multiple nodes for the same compound when detected over a large retention time span and creates huge MNs that are not fully representative of the actual number of compounds in the dataset. In order to overcome this problem, FBMN uses a feature detection and alignment tool, such as MZmine 2, to preprocess the raw data and is used for advanced molecular networking analysis, enabling the relative quantification of the compounds and resolution of isomers [38].

Finally, over the last few years, various toxicity screening platforms have been developed to facilitate and accelerate the preclinical studies of novel antimicrobial compounds. One example is the use of zebrafish larvae. Zebrafish (*Danio rerio*) is a small tropical fish that lives in the freshwater rivers and lakes of South Asia and is characterized by the dark blue stripes covering its adult body [39]-[40]. Both, adults and embryos, are popular as laboratory models in biological research. Embryos and larvae are mostly used to evaluate the toxicity of compounds due to their high sensitivity and are particularly useful in the early stages of the preclinical studies [41]-[42]. They are legally not considered an animal during the first 5 days post fertilization (dpf) and therefore, their usage is in compliance with the 3R guiding principles that highlight the importance of replacing animals with non-animal systems. They can be considered as a step between *in vitro* cell-based models and *in vivo* mammalian experiments [42]. Their small size (1-5 mm) allows the performance of miniature *in vivo* experiments in multi-well plates and high throughput screening. As a result, the amounts of compounds required for these experiments are very low, making zebrafish attractive to NP drug discovery, where the amounts of NPs available are usually limited [43]. Moreover, in these early life stages, their body is transparent, enabling the direct observation using a simple stereo microscope [44].

These novel interdisciplinary approaches and methodologies have been economically sustainable and also proven efficient in NP discovery [30]. We are entering a New Golden Age of NP drug discovery [32], aiming to fully exploit the still untapped chemical diversity of microbial communities for the discovery of new antibiotics and improve the drug development pipeline [12].

1.4 Marine Natural Products (MNPs)

Marine natural products (MNPs) represent the secondary metabolites derived from organisms in the sea and other major water bodies and marine pharmacology focuses on the components with pharmacological properties produced by these organisms, marine species of plants, animals and microorganisms [45]. These metabolites are often chemically different from those in the terrestrial environment because of the distinct ecological pressures within the habitats. As in the case of terrestrial organisms, this diversity of bioactive compounds is considered to be part of the defense, survival and predatorial strategies employed. Thus, these organisms seem to be a great source for the discovery of novel bioactive molecules and the development of therapeutic agents [46]-[47].

The enormous marine resources have been exploited since ancient times and included the use of marine animals like fish and preparations from algae as sources of medicines [45], such as the red algae *Chondrus crispus* and *Mastocarpus stellatus*, whose beverage was popular as a folk cure for infections [31]. In 1950, the first two biologically active MNPs were officially reported by Bergmann, spongothymidine and spongouridine from the Caribbean marine sponge *Cryptotethya crypta*. Twenty years later they were synthetically optimized and would become the first clinically approved marine drugs, commercially known as cytarabine and vidarabine [48].

Since then, the exploration of the ocean has resulted in the discovery of thousands of structurally unique MNPs and the marine environment has become a promising source of molecules and drugs of therapeutic use, such as halogenated terpenes, polyketides and prostaglandins [46]. Up to date (March 2024), 41493 marine molecules have been described [49] and at least 3,000 of them have demonstrated bioactivity [45].

Many different bioactivities have been attributed to MNPs, including antibacterial against Gram-positive and Gram-negative bacteria, antifungal, antiviral, antiparasitic, antitumor, analgesic, anti-inflammatory, antioxidant and immunomodulatory activities [5],[33].

1.4.1 Marine Environment

Oceans cover more than 70% of the planet's surface [45], hosting approximately 87% of life on earth that includes a wide variety of plant, animal and microorganism species [5]. The remarkable ability of these organisms to survive in extreme habitats, such as extreme variations in temperature, pressure, salinity, light, oxygen concentration and nutrients availability, enables marine organisms to develop unique physiological and metabolic capabilities, along with a striking capacity to adapt in their environment [45]. This adaptation in extraordinary conditions has evolved over a long period of time [46] and due to these extreme variations in ecological pressure, including competition for space and predation, they contain a much more extensive phylogenetic diversity than that of the terrestrial environment [50].

The National Oceanic and Atmospheric Administration (NOAA) of the United States has estimated that 80% of the oceans remains unexplored [46] and their diversity seems to be infinite. For instance, coral reefs are particularly rich in different organisms and in some areas around 1000 species per m^2 can be found [51]. In late 1970, it was established that marine plants and animals are genetically and biochemically unique and having virgin areas of marine life, the prospect of yielding novel products from the sea was enormous [45].

Out of 33 animal phyla known to date, a total of 32 phyla are represented in the marine environment, while 15 of them are exclusively marine. Marine organisms include sponges, tunicates, fish, soft corals, nudibranchs, sea hares, opisthobranch molluscs, echinoderms, bryozoans, prawns, shells, sea slugs, and last but not least, marine microorganisms [45]. In the beginning, the research of marine wildlife focused on a small number of organisms which included sponges, molluscs, tunicates and macroalgae, which illustrated a very diverse range of unique molecular structures [46]. With the continuous exploitation of the marine environment, attention turned to microorganisms such as marine actinobacteria, proteobacteria cyanobacteria, fungi, and several other groups [45]-[46]. Marine microorganisms have proven to be great repositories of bioactive molecules and have yielded some of the most important active compounds known today. Furthermore, over time, it has been realized that many compounds previously isolated from marine macroorganisms, such as sponges and tunicates, are in fact products of associated microorganisms [5]. Finally, recently, marine actinomycetes were considered to be a promising resource for novel bioactive secondary metabolites and are widely distributed within the marine ecosystem, found in intertidal zones, seawater, animals, plants, sponges and ocean sediments [14].

This highly unexplored biodiversity makes the marine environment an extremely prolific source of novel and structurally unique compounds [33] leading to the production of metabolites which may not be found in terrestrial environments [5]. They present themselves as a hotspot for

the discovery of new drug leads with unique chemical structures and mechanisms of action [5],[33],[45].

1.4.2 Marine-derived Drugs

To date, eighteen marine-derived drugs have been clinically approved and reached the market for the treatment of various diseases, mostly different types of cancer, but also viral infections, hypertriglyceridemia and severe pain [6],[47]-[48],[52].

They are MNPs or synthetic derivatives inspired from a MNP. As shown in **Table 1**, most of the approvals occurred in the 21st century [6] and seven of them have only been approved during the years 2018-2021, showing a significant increase in the recent years. However, it is worth noting that none of these pharma drugs is an antibiotic.

Table 1. The clinically approved drugs deriving from MNPs [6],[47]-[48].

Compound name	Trademark	Year of Approval	Marine Organism	Disease Area	Pharmaceutical Company
cytarabine	Cytosar-U®, Depocyst®	1969	sponge	cancer	Pfizer
vidarabine	Vira-A®	1976	sponge	antiviral	Mochida Pharmaceutical Co.
ziconotide	Prialt®	2004	cone snail	severe chronic pain	Jazz Pharmaceuticals
ω-3-acid ethyl esters	Lovaza®	2004	fish	hypertriglyceridemia	GlaxoSmithKline
eicosapentanaenoic acid ethyl ester	Vascepa®	2012	fish	hypertriglyceridemia	Amarin
ω-3 carboxylic acid	Epanova®	2014	fish	hypertriglyceridemia	AstraZeneca
iota-carrageenan	Carragelose®	2006	red algae	antivirus	Marinomed Biotech AG
eribulin mesylate	Halaven®	2010	sponge	cancer	Eisai Inc.

E7389					
brentuximab vedotin	Adcetris®	2011	cyanobacterium	cancer	Seagen
trabectedin	Yondelis®	2007	tunicate	cancer	PharmaMar
panobinostat	Farydak®	2015-2022 (withdrawn)	sponge	cancer	Novartis
plitidepsin	Aplidin®	2018	tunicate	cancer	PharmaMar
polatuzumab vedotin	Polivy®	2019	cyanobacterium	cancer	Genetech/Roche
enfortumab vedotin	Padcev®	2019	cyanobacterium	cancer	Astellas Pharma & Seagen
lurbinectedin	Zepzelca®	2020	tunicate	cancer	PharmaMar
belantamab-mafodotin-blmf	Blenrep®	2017-2020 (withdrawn)	cyanobacterium	cancer	GlaxoSmithKline
disitamab vedotin	Aidix®	2021	cyanobacterium	cancer	Remegen Biosciences
tisotumab vedotin-tftv	Tivdak®	2021	cyanobacterium	cancer	Seagen

Trabectedin (Yondelis®), approved in 2007 and commercialized by PharmaMar was the first approved anticancer drug directly derived from a MNP and the first marine anticancer drug to be approved in the European Union. It is used for the treatment of soft tissue sarcoma and ovarian cancer. It was originally isolated in very low yields from the ascidian *Ecteinascidia turbinata* and the quantities required for advanced preclinical and clinical studies were obtained by very large-scale aquaculture in open ponds. Later on, its semisynthesis starting from cyanosafracin B was accomplished and established as the procedure to produce the drug substance [53].

Furthermore, two of these marine-derived medicines, plitidepsin (Aplidin®), approved in 2018 for the treatment of numerous cancer forms and iota-carrageenan (Carragelose®), an antiviral nasal spray, are currently under research for the treatment of COVID-19, as they have demonstrated antiviral activity against SARS-CoV-2 [48],[54].

Until now, many MNPs have been investigated as drug candidates in different phases of clinical trials and a plethora of drug leads are under preclinical development for various diseases. There are currently 6 drug candidates in phase III, 15 in phase II and 19 in clinical phase I [55].

Among them, salinosporamide A, a molecule isolated from a marine actinomycete of the genus *Salinospora* has demonstrated potent cytotoxic activity and is now in phase III clinical trials for the treatment of multiple myeloma [46] and newly diagnosed glioblastoma in combination with standard temozolomide-based radiochemotherapy under the brand name Marizomib [56].

1.5 Actinomycetes

Actinomycetes are filamenting bacteria belonging to the order of Actinomycetales, and the Actinobacteria phylum, one of the largest among the 30 major phyla currently attributed to the domain Bacteria. It is estimated that less than 1% of the actinomycetes have been identified and recorded to date [57]-[58].

Within the actinomycetes, *Streptomyces* is by far the best characterized genus, a strikingly diverse genus with around 600 species identified so far. Due to this wide distribution, the rest of the actinomycete genera are commonly called “rare actinomycetes”, even though it is nowadays known that they are not actually rare in the environment, just less frequently isolated than *Streptomyces* strains. In fact, only 11 rare actinomycetes genera had been reported by 1970, followed by 100 genera by 2005 and 220 genera by 2010 [58].

Actinomycetes are Gram-positive, facultative anaerobic filamentous bacteria [59]-[60] and are often distinguished by their mycelial growth morphology. Many members of this order have a complex life cycle with the ability to form spores upon differentiation, [61]. They generally have high guanine-cytosine (G + C) genomic DNA content, higher than 70% in various *Streptomyces* and *Frankia* species, and present either linear or circular chromosomes [57]. As in many bacteria, linear plasmids are common in actinomycete species, [61].

These bacteria are ubiquitous in soil environments, associated to plants and insects, as well as marine and fresh water ecosystems [60]. They have an important ecological role in the decomposition of organic material [60] and almost 90% of actinomycetes genera so far have been isolated from soil associated environments [59]. Besides free-living microbes, they are recognized as important interaction partners, living in symbiosis with plants, fungi, insects, and animals. These organisms profit from the actinomycetes for various ecological functions, such as for protection against pathogens, growth promotion or the degradation of complex natural polymers. At the same time, the actinomycetes benefit from the resources of the hosts they interact with [60]. Various

genes and regulatory sequences have been identified that are able to promote or inhibit the gene expression responding to specific environmental changes [57].

They exhibit great diversity in a variety of characteristics including pH, thermophilicity and moisture tolerance. This diversity is also reflected in the extreme and remote locations where actinomycetes have been found, with samples having been discovered in Mariana Trench and Antarctica [61]. The factors that influence the microorganisms' behavior are not well understood yet, but variations such as nutrient concentration and accessibility in them are surely a determining driver [57].

Representative major occurring genera of Actinomycetales include *Streptomyces*, *Kutzneria*, *Actinoplanes*, *Nocardia*, *Actinomadura*, *Micromonospora*, *Amycolatopsis*, *Nonomuraea*, *Nocardiopsis*, *Marinactinospora*, *Rhodococcus*, *Lentzea*, *Actinokineospora*, *Planomonospora*, *Streptomonospora*, *Microbacterium,* and *Thermoactinomyces* [62].

As mentioned, actinomycete species are primarily found in soils and were originally thought to be solely terrestrial. In fact, the first marine actinomycete was only discovered in 1984. Since then, many marine species have been discovered in aquatic systems worldwide. *Streptomyces*, *Micromonospora,* and *Actinomyces* have been found at depths as great as 500 m and it has been demonstrated that *Micromonospora* in particular may have greater relative abundance at 450 m depth in comparison with more shallow waters. They thrive in association with a variety of aquatic organisms, including invertebrates such as sponges, corals, and echinoderms, as well as vertebrates [61].

According to recent studies, these interactions involve signaling molecules that control the expression of BGCs and have played a major role in the evolution of the high chemical diversity of actinomycete-produced secondary metabolites in diverse environments [60]. In the past two decades, hundreds of actinomycete genomes have been sequenced and many of them have been fully annotated. The analysis of the sequences has demonstrated that a significant portion of the BGCs are associated with polyketide synthase (PKS) and nonribosomal peptide synthetase (NRPS) pathways, indicating that polyketides, nonribosomal peptides, and their hybrid compounds are the major secondary metabolites of actinomycetes [63]. Therefore, considering their extraordinary metabolism plasticity and their biosynthetic potential, actinomycetes can provide bioactive compounds never observed with unique structural moieties and complexity [57].

They have been described as microbial cell factories [64] and played a crucial role in drug discovery, yielding more than 10,000 bioactive compounds [60]. It is estimated that each actinomycete strain has the potential to produce between 10 to 20 families of secondary metabolites [61] and nearly three-quarters of all microbial bioactive compounds discovered so far

were produced by actinomycete bacteria [14], including antibiotics as well as many anticancer, antifungal, anthelmintic and immunosuppressive agents [60]-[61].

Since Selman Waksman discovered actinomycin from a strain of the genus of *Streptomyces*, the first antibiotic isolated from an actinomycete, these bacteria represent an inexhaustible source of antibiotics [65]. Most of the known antimicrobials today were originally isolated from actinomycetes between 1950 and 1970, especially from the genus *Streptomyces* [57]-[58],[65]. Over 80% of all antibiotics used in the medical field originate from Actinobacteria, with 50% of clinically relevant antibiotics originating from *Streptomyces* [61].

There are different antibiotic classes produced by actinomycetes, including *β*-lactams, aminoglycosides, glycopeptides, macrolides, tetracyclines, ansamycins, lincosamides, epoxides and aminocoumarins [57],[61],[65]. Some representative antibiotics derived from actinomycetes and used in the clinic today are neomycin, streptomycin, kanamycin, cephamycin, vancomycin, erythromycin, and tylosin [61], and a long list of therapeutically relevant semisynthetic analogs such as imipenem.

The antibiotics produced by actinomycetes possess diverse chemical structures with a wide range of biological activities. Their structure–activity relationship (SAR) has been extensively studied in order to develop new and more effective drugs. In this regard, apart from the wide variety of NPs isolated, the bioactive compounds from this class of bacteria remain an unexhausted source of new scaffolds and the inspiration for the discovery of semisynthetic and fully synthetic antibiotics [57],[66].

1.5.1 The genus *Micromonospora*

The genus *Micromonospora* has an increasingly important role in the discovery of a high number of new bioactive compounds [67] and is a member of the family Micromonosporaceae (order Actinomycetales), first described by Ørskov in 1923 [67]-[68]-[69]. To date (March 2024), the genus *Micromonospora* consists of 125 species with validly published and correct names (https://www.bacterio.net/genus/micromonospora).

Although *Micromonospora* exhibits significant physiological and biochemical diversity, the genus forms a well-defined group in terms of morphology, phylogeny, and chemotaxonomy [64]. Members of this genus are aerobic to microaerophilic, chemoorganotrophic, sensitive to pH below 5, with NaCl tolerance ranges from 1.5 % to 5 % (w/v) and have optimal growth temperatures of 20-40°C. As their name suggests, they produce single spores directly attached to substrate mycelium or carried on short sporophores [64],[67]-[68]-[69]. The spores are nonmotile, hydrophilic and spherical to oval in shape, with a diameter of 0.7–1.5 mm [70]. Compared to

Streptomyces, no aerial mycelia are produced [71]. They often produce carotenoid mycelial pigments, resulting in yellow, red, orange, brown, purple, blue-green or black colonies [68],[71].

The genus Micromonospora is widespread in nature, inhabiting diverse environments, such as soil, coastal, marine and freshwater sediments, peat swamp forests, plant rhizospheres and extreme habitats (e.g. hyper-arid deserts, deep-sea sediments and hypersaline lakes). Furthermore, some members of this genus are also known to form symbiotic relationships with plants and animals [64],[69]-[71]-[72]. About 83% of them reported so far are of terrestrial origin, including plants, endophytes and extreme habitats-derived strains, while the marine-derived species are frequently reported from both marine sediment and sponges [69]. Compared to *Streptomyces*, *Micromonospora* spores are more resistant, and viable spores have been recorded from sediments at least 100 years old [70].

Within the rare actinomycetes group, *Micromonospora* is the most prolific in producing metabolites, accounting for more than 700 compounds to date [72] and are of significant interest to drug discovery [67]. Since the discovery of micromonosporin, the first antibiotic isolated from *Micromonospora* in 1947 by Waksman, many antibiotics have been reported from this genus [68], including pharmaceutically important chemical molecules such as gentamicin and calicheamicin [67]. Overall, *Micromonospora* is a diverse genus of Actinobacteria with significant ecological, biotechnological, and pharmaceutical importance.

1.6 Spirotetronates

Polyketide natural products constitute an important group of secondary metabolites used in human/veterinary medicine and agriculture. Spirotetronates are a class of polyketides produced by a large diversity of actinomycetes, most of them belonging to the genera of *Streptomyces*, *Micromonospora* and *Actinomadura* but also to *Verrocosispora*, *Actinospica*, *Actinoallomurus*, *Saccharothrix*, *Amycolatopsis* and *Actinocrispum*, so far, nine different genera in total, all Gram-positive and generally aerobic bacteria [73],[74],[75],[76]. The producing microorganisms have been isolated from different sources, such as soil, plants, sea and marine sediments and organisms and are geographically distributed worldwide [73],[74],[75],[77].

The first spirotetronate discovered back in 1969 was chlorothricin, produced by a *Streptomyces* strain isolated from a soil sample in Argentina [74]. Since then, more than 100 compounds of this structural class have been discovered with the list being constantly expanded. (**Table 2**). An extensive bibliographic search revealed that 167 spirotetronates distributed in 28 families of compounds have been discovered to date (March 2024).

Table 2. Natural spirotetronates reported to date (March 2024), distributed into families of compounds, biological source, geography and ecology of their first isolation, bioactivity, classification and year of their discovery.

Name/Family Number of Compounds	Biological Source	Geography/ Ecology	Bioactivity	Class/ C_x	Year of Discovery	References
abyssomicins 40	*Verrucosispora* sp. *Streptomyces* sp.	Japan/marine	antibiotic antiviral antitumor	I/C_{11}	2004	[78],[79],[80], [81],[82],[83], [84],[85]
A88696 3	*Streptomyces* sp.	n.d.	antiulcer	I/C_{11}	1993	[86]
chrolactomycins 2	*Streptomyces* sp. *Actinospica* sp.	terrestrial	antibiotic antitumor	I/C_{13}	1999	[87],[76]
okilactomycins 5	*Streptomyces* sp.	Japan/ terrestrial	antibiotic antitumor	I/C_{13}	1987	[88],[89]
maklamicin 1	*Micromonospora* sp.	Thailand/ endophytic	antibiotic/ anticancer	II/C_{11}	2011	[90]
nomimicins 4	*Actinomadura* sp.	Japan/ compost	antibiotic	II/C_{11}	2012	[91],[92]
PA-46101 A and B 2	*Streptomyces* sp.	n.d.	antibiotic	II/C_{11}	1989	[93]
Phocoenamicins 3	*Micromonospora* sp.	marine	antibiotic	II/C_{11}	2017	[94],[77]
chlorothricins 3	*Streptomyces* sp.	Argentina/terrestrial	antibiotic	II/C_{13}	1969	[95],[96],[97]
pyrrolosporin A and B 2	*Micromonospora* sp.	Peru/terrestrial	antitumor antibiotic	II/C_{13}	1996	[98],[99]
NAI-414A and B 2	*Actinoallomurus* sp.	Italy/terrestrial	antibiotic antitumor	II/C_{13}	2012	[100]
decatromicins A-G 7	*Actinomadura* sp.	Japan/terrestrial	antibiotic	II/C_{13}	1999	[99],[101],[102]
kijanimicins 5	*Actinomadura* sp.	Kenya/terrestrial	antibiotic anticancer anti-inflammatory antiviral	II/C_{13}	1981	[103],[104]
tetrocarcins 20	*Micromonospora* sp.	Japan/terrestrial	antitumor/ antibiotic	II/C_{13}	1980	[104],[105],[106],[107],[108],[109]
BE-45722A, B and C 3	*Actinomadura* sp.	Japan/terrestrial	antibiotic antiviral	II/C_{13}	1997	[110],[111]
MM46115 1	*Actinomadura* sp.	Cameroon/ mycetoma	antiviral antibiotic	II/C_{13}	1990	[112]
JK-1 and 2 2	*Actinomadura* sp.	n.d.	antibiotic	II/C_{13}	2004	[113]
arisostatins A and B 2	*Micromonospora* sp.	Japan/marine	antitumor antibiotic	II/C_{13}	1999	[114]
AC6H 1	*Micromonospora* sp.	Japan/ terrestrial	antitumor antibiotic	II/C_{13}	1992	[115]
saccharocarcins	*Saccharothrix* sp.	U.S./terrestrial	antibiotic	II/C_{13}	1996	[116]

6						
lobophorins 18	*Streptomyces* sp.	marine	antibiotic anti-inflammatory anticancer	II/C_{13}	1999	[117],[118],[119],[120],[121],[122],[123],[124], [125]
microsporanates A-F 6	*Micromonospora* sp.	China/marine	antibiotic	II/C_{13}	2017	[104]
streptaspironates A–D 4	*Streptacidiphilus* sp.	The Netherlands/ decaying pine wood	-	I/C_{15}	2020	[126]
glenthmycins A−M 13	*Streptomyces* sp.	Australia/endophytic	antibiotic	II/C_{13}	2022	[127]
wychimicins A-D 4	*Actinocrispum* sp.	Japan/terrestrial	antibiotic	II/C_{13}	2022	[128]
versipelostatin 1	*Streptomyces* sp.	n.d.	anticancer CNS	II/C_{17}	2002	[129]
tetronothiodin 1	*Streptomyces* sp.	n.d.	antiulcer	I/C_{19}	1992	[130]
quatromicins 6	*Amycolatopsis* sp.	n.d.	antiviral	4 subunits	1991	[131],[132]

n.d. not detected

Structurally, the spirotetronates are tetronate compounds in which two ring structures are linked to each other by one spiroatom. In particular, they are characterized by a cyclohexene ring spiro-linked to a tetronic acid moiety and embedded in a macrocycle. The existence or not of a decalin unit groups them into class I (without) and class II (with the decalin unit). Further classification groups them based on the number of carbons of the macrocycle, in small (C_{11}), medium (C_{13}) and large spirotetronates ($\geq C_{15}$) (**Figure 1**). Finally, they often bear various oligosaccharide chains and/or other peripheral moieties attached to the decalin and/or the macrocycle and different side chains that enrich their structural variety. The decalin unit is linked either by a ketone group or more rarely by a carboxylic ester or an alcoholic group [73],[74],[75]. An exception to this classification are the quartromicins, unusual spirotetronate polyketides containing four spirotetronate subunits within one molecule [131].

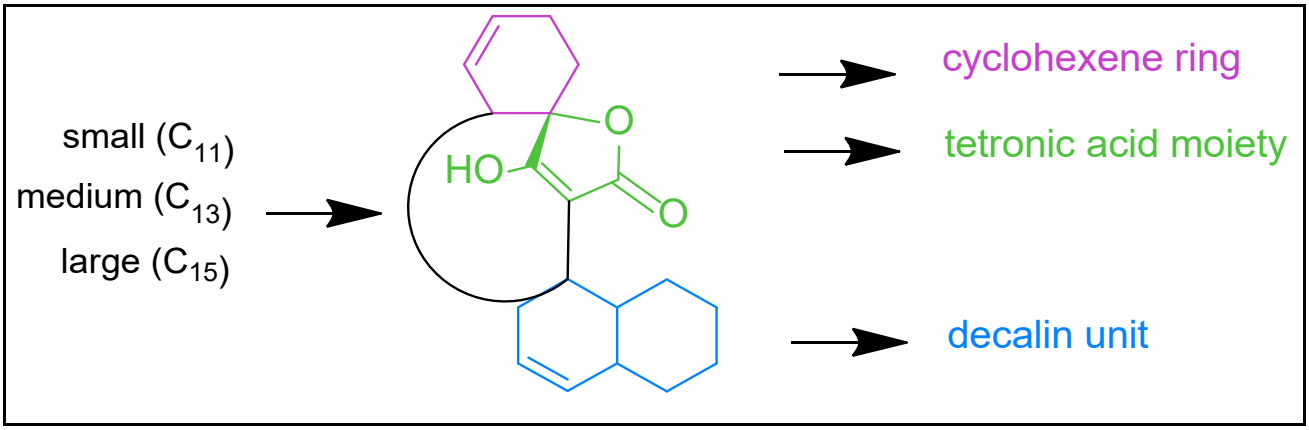

Figure 1. Structure and main moieties of spirotetronates.

Regarding their bioactivity, they have demonstrated a wide variety of biological activities, mostly antibiotic against Gram-positive bacteria and antitumor, but also antiviral, antiulcer, anti-inflammatory and active against CNS diseases [74]-[75] (**Table 2**). Along with their potent bioactivities, certain spirotetronates have been considered tools to elucidate a biological effect. For example, abyssomicin C was found to be the first natural product to block pABA biosynthesis. However, apart from some exceptions, there is no clear understanding of the role of the spirotetronate motif, the effect of the macrocyclic size, the oligosaccharide and side chains and the decalin system in the biological activities of the spirotetronates [73]. Despite their potent bioactivities, their structural complexity and the difficulties towards large-scale culturing, have been limiting their availability for further preclinical and clinical studies [75].

Recently, the spirotetronate class has grown with the discovery of the phocoenamicin family of compounds. Examination of intestinal contents from a marine mammal led to the identification of a *Micromonospora* strain, which afforded a new complex glycosylated polyketide, phocoenamicin, with potent activity against the intestinal pathogen *Clostridium difficile* [94]. Later on, phocoenamicins B and C, together with phocoenamicin, were isolated in our laboratory from cultures of *Micromonospora* sp. strain CA-214671, originally isolated from marine cave sediments collected near the Canary Islands and the compounds demonstrated antimicrobial activity against methicillin-resistant *Staphylococcus aureus* (MRSA) and *Mycobacterium tuberculosis* H37Ra [77]. The characteristic diol side chain unique in phocoenamicins and two 6-deoxyglucose moieties with an acetyl linkage to a chlorinated phenol are the highlighted structural features of phocoenamicins and remain unchanged throughout the family (**Figure 2**).

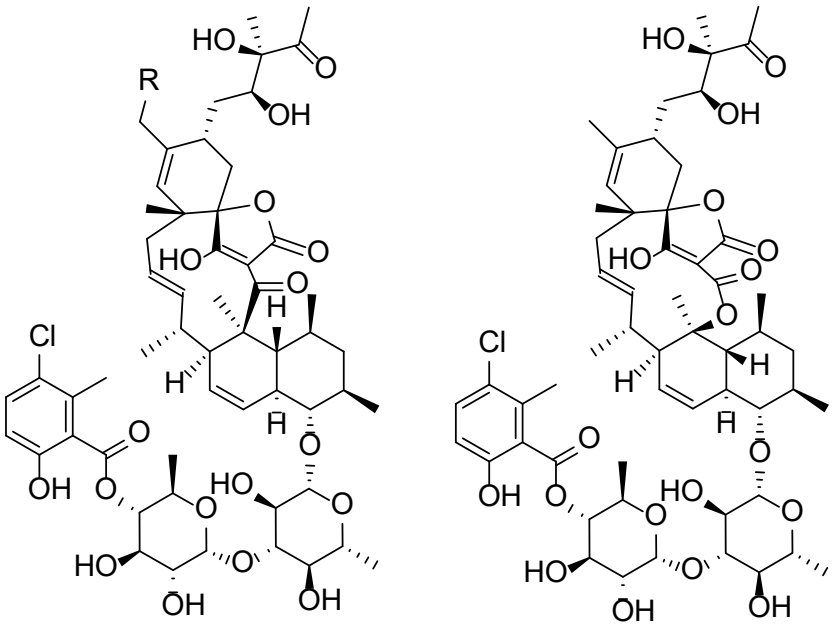

phocoenamicin R=H
phocoenamicin B R=OH

phocoenamicin C

Figure 2. Structure of phocoenamicin, phocoenamicin B and C.

2. OBJECTIVES

2. Objectives

1) Determination of the best conditions for the production of antimicrobial spirotetronates already identified from marine actinomycetes of MEDINA's collection.
2) Metabolic profiling of the producing strains and molecular networking of their production.
3) Scaling-up of fermentation and isolation of the compounds, as well as determination of the structure of related minor analogues also present in the fermentation broths.
4) Evaluation of the biological profile of the best hits against an extended panel of microbial pathogens.
5) Determination of possible structure–activity relationships of all the compounds isolated.
6) Evaluation of the safety of the isolated compounds by testing the cell viability against the human liver adenocarcinoma cell line (Hep G2) and the safety of the major compounds against zebrafish eleuthero embryos.

3. RESULTS

3. Results

3.1 Identification of the Producing Microorganisms

The microbial strains used in this work belong to the culture collection of Fundación MEDINA, which contains approximately 190,000 microbial strains and is one of the largest in the world. The producing strains were identified by searching an internal repository of LC/MS analyses of microbial extracts against an internal database of LC/UV/MS data of microbial natural products, which includes several members of the phocoenamicin family [133]. The high-performance liquid chromatography coupled to mass spectrometry (HPLC-UV-MS) profile of the phocoenamicins, including RT, UV spectrum and positive and negative mass spectra, was used for the search and led to the identification of 27 microbial strains belonging to the MEDINA culture collection that potentially biosynthesized at least one of the phocoenamicins.

Taxonomic identification of the 27 strains was based on sequencing of the 16S ribosomal gene with the universal primers fD1 and rP2. The sequences obtained were compared against the sequences of all prokaryotic species recognized as "type strains" with validly published names registered in the EzBioCloud database. The closest species identified, the (%) percentage of similarity, the geographic origin, and the ecological source of isolation of each strain are shown in **Table 3**.

Table 3. Closest species assignment using the EzBioCloud database, the (%) percentage of similarity, the source of isolation and the geographic origin of each strain.

Strain	*Micromonospora* species	Similarity (%)	Geographic Origin *	Ecology
CA-107814	*M. terminaliae*	99.48	Costa Rica (1)	soil-rice cultivation
CA-108000	*M. endophytica*	100	Costa Rica (1)	soil-rice cultivation
CA-184181	*M. siamensis*	99.32	Mexico (2)	soil
CA-214658	*M. endophytica*	99.63	Spain (3)	marine cave sediment
CA-214671	*M. chaiyaphumensis*	99.84	Spain (3)	marine cave sediment
CA-218877	*M. endophytica*	100	Spain (3)	marine invertebrate *Porifera* sp.
CA-238377	*M. terminaliae*	99.54	Georgia (4.a)	rhizosphere soil of *Pteridium tauricum*
CA-238397	*M. chalcea*	100	Georgia (4.a)	rhizosphere soil of *Pteridium tauricum*
CA-238398	*M. siamensis*	99.32	Georgia (4.a)	rhizosphere soil of *Pteridium tauricum*
CA-243027	*M. terminaliae*	100	Georgia (4.a)	rhizosphere soil of *Pteridium tauricum*
CA-243168	*M. endophytica*	100	Central African Republic (5)	forest organic humid soil
CA-244160	*M. terminaliae*	99.53	Union of the Comoros (6.a)	forest organic dry soil
CA-244161	*M. terminaliae*	99.47	Union of the Comoros (6.a)	forest organic dry soil
CA-244669	*M. terminaliae*	99.41	Union of the Comoros (6.b)	forest organic humid soil
CA-244673	*M. chalcea*	100	Union of the Comoros (6.b)	forest organic humid soil
CA-244674	*M. endophytica*	99.31	Union of the Comoros (6.b)	forest organic humid soil
CA-244675	*M. terminaliae*	99.49	Union of the Comoros (6.b)	forest organic humid soil
CA-246501	*M. terminaliae*	99.53	Georgia (4.a)	rhizosphere soil of *Pteridium tauricum*

CA-246506	*M. aurantiaca*	99.64	Georgia (4.a)	rhizosphere soil of *Pteridium tauricum*
CA-248285	*M. soli*	99.07	New Zealand (7)	swampy soil
CA-248314	*M. endophytica*	99.66	New Zealand (7)	swampy soil
CA-248649	*M. terminaliae*	100	Union of the Comoros (6.c)	forest organic soil
CA-249271	*M. endophytica*	99.38	Union of the Comoros (6.d)	forest organic soil
CA-249379	*M. terminaliae*	99.54	Union of the Comoros (6.a)	forest organic dry soil
CA-251294	*M. terminaliae*	99.51	Union of the Comoros (6.c)	forest organic soil
CA-253038	*M. siamensis*	99.29	Georgia (4.b)	rhizosphere soil of *Populus canescens*
CA-259211	*M. endolithica*	99.19	Georgia (4.c)	rhizosphere soil of *Ranunculus buhsei*

* Places and dates of collection indicated in brackets are specified in **Figure 3**.

All the strains identified as phocoenamicins producers belonged to the *Micromonospora* genus, indicating that the common pathway for the production of these molecules must be highly conserved within species of this genus. The closest type species determined were distributed into seven different species, with *M. terminaliae* and *M. endophytica* being the closest species in more than half of the strains (18 strains), followed by *M. siamensis, M. chalcea, M. solis, M. chaiyaphumensis* and *M. aurantiaca.* As all three of the known phocoenamicins were originally isolated from actinomycete strains of *Micromonospora* sp., and all strains identified as potentially producing them also belong to this genus, it can be proposed that the biosynthesis of this family of compounds might be confined to the *Micromonospora* species.

Despite the close taxonomic relationship of the strains, the ecological and geographical sources displayed great diversity. Although the phocoenamicins were originally isolated from marine-derived actinomycetes, the producers identified in this study were isolated from many different sources, as shown in **Table 3**. These sources included forest organic soil, either dry or humid, rhizosphere soil from various plants, rice cultivations, soil in swamp ecosystems, marine sediments and finally a strain isolated from a marine invertebrate. This demonstrated that the production of phocoenamicins cannot be associated exclusively to marine environments, as previously believed [134]-[135].

As far as their geographical origin, they were widely distributed throughout the planet, covering almost all continents, as shown in **Figure 3**. Overall, the 27 strains were isolated from various regions in Costa Rica, Mexico, Spain, Georgia, Central African Republic, Comoros Islands and New Zealand and their original isolation was performed between the years 1998 and 2006.

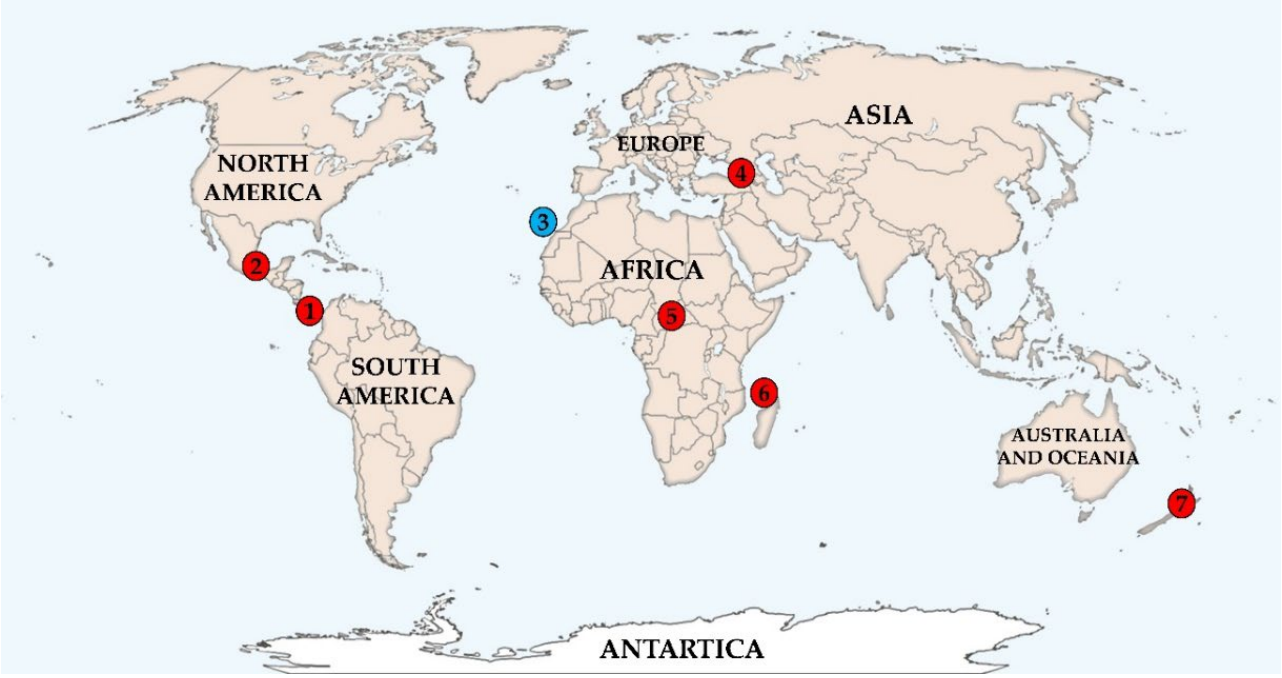

Figure 3. Geographic distribution of the 27 strains within the seven different countries worldwide. The blue colored circle corresponds to the three marine-derived strains and the red to the 24 terrestrial strains. Numbers correspond to the different countries, regions and year of collection: 1. Costa Rica (Guanacaste, 1998) 2. Mexico (Las Tuxtlas, Veracruz, 2001) 3. Spain (Gran Canaria, 2004) 4. Georgia, a. (Batumi, Adjara, 2004) b. (Poti, Samegrelo, 2005) c. (Khulo, Adjara, 2005) 5. Central African Republic (Damara/Sibut, 2005) 6. Union of the Comoros, a. (Mdji Diakagnoa, 2005) b. (Ouralé-Ouandaoé, 2005) c. (Tsinimouachongo, 2005) d. (Zikaledjou, 2005) 7. New Zealand (Pehitawa Forest Reserve, 2006).

3.2 OSMAC approach and Metabolomics Analysis of the Culture Broths

The 27 strains were cultured in 10 different media based on the OSMAC approach (One Strain Many Compounds) [136] to identify the best growth conditions and exploit their biosynthetic potential. The culture media selected covered a range of different carbon and nitrogen sources previously shown to enhance the production of secondary metabolites by members of this genus, and a fermentation time of 14 days was used in all cases, suitable for slow-growing bacteria such as *Micromonospora*. After fermentation, the culture broths were extracted with acetone for subsequent liquid chromatography coupled to high resolution mass spectrometry (LC-HRMS) analysis using electrospray positive ionization mode. 280 samples were injected in total, including 270 extracts from the fermentation broths and 10 extracts from the corresponding unseeded control media. Preliminarily, a study of the production of the three known phocoenamicins was carried out in each of the conditions analyzed.

All 27 strains were confirmed to produce the three known phcoenamicins in at least one of the culture media. For phocoenamicin, the (+)-HRESIMS data detected a peak displaying an

ammonium adduct ion at *m/z* 1088.4982 $[M + NH_4]^+$ at a retention time (RT) of 6.45 min, corresponding to the molecular formula $C_{56}H_{75}ClO_{18}$. For phocoenamicin B, a peak with an adduct ion at *m/z* 1104.4927 $[M + NH_4]^+$, in agreement with the molecular formula $C_{56}H_{75}ClO_{19}$ was detected at a RT of 5.62 min and for phocoenamicin C, a peak at a RT of 6.01 min with an adduct ion at *m/z* 1104.4933 $[M + NH_4]^+$, corresponding to the molecular formula $C_{56}H_{75}ClO_{19}$. The ESI-TOF spectra of the three phocoenamicins are displayed below (**Figure 4**). In all three cases, the characteristic UV spectrum of the phocoenamicins, as shown in **Figure 5**, was observed and all the data were in good agreement with those previously published for the three compounds [77]. As the three molecules were detected in multiple analytical runs, the values of *m/z* and retention time are representative for each compound.

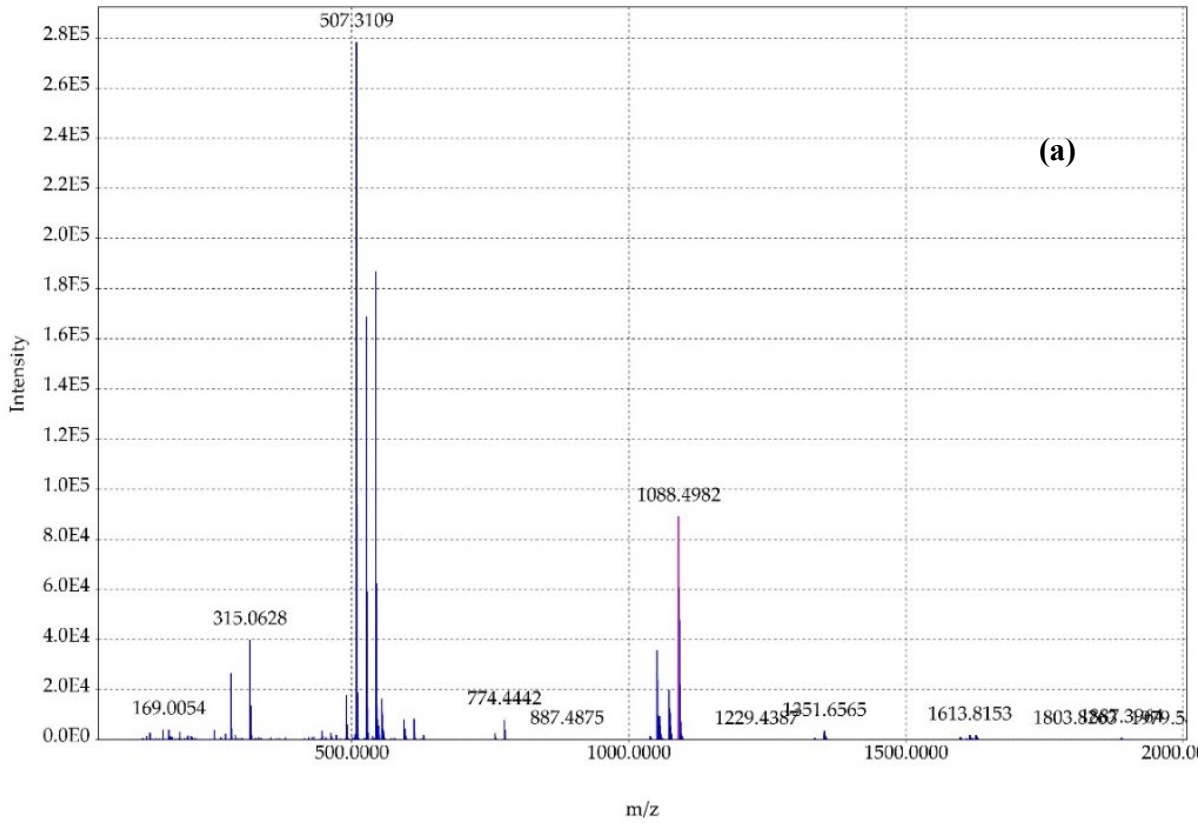

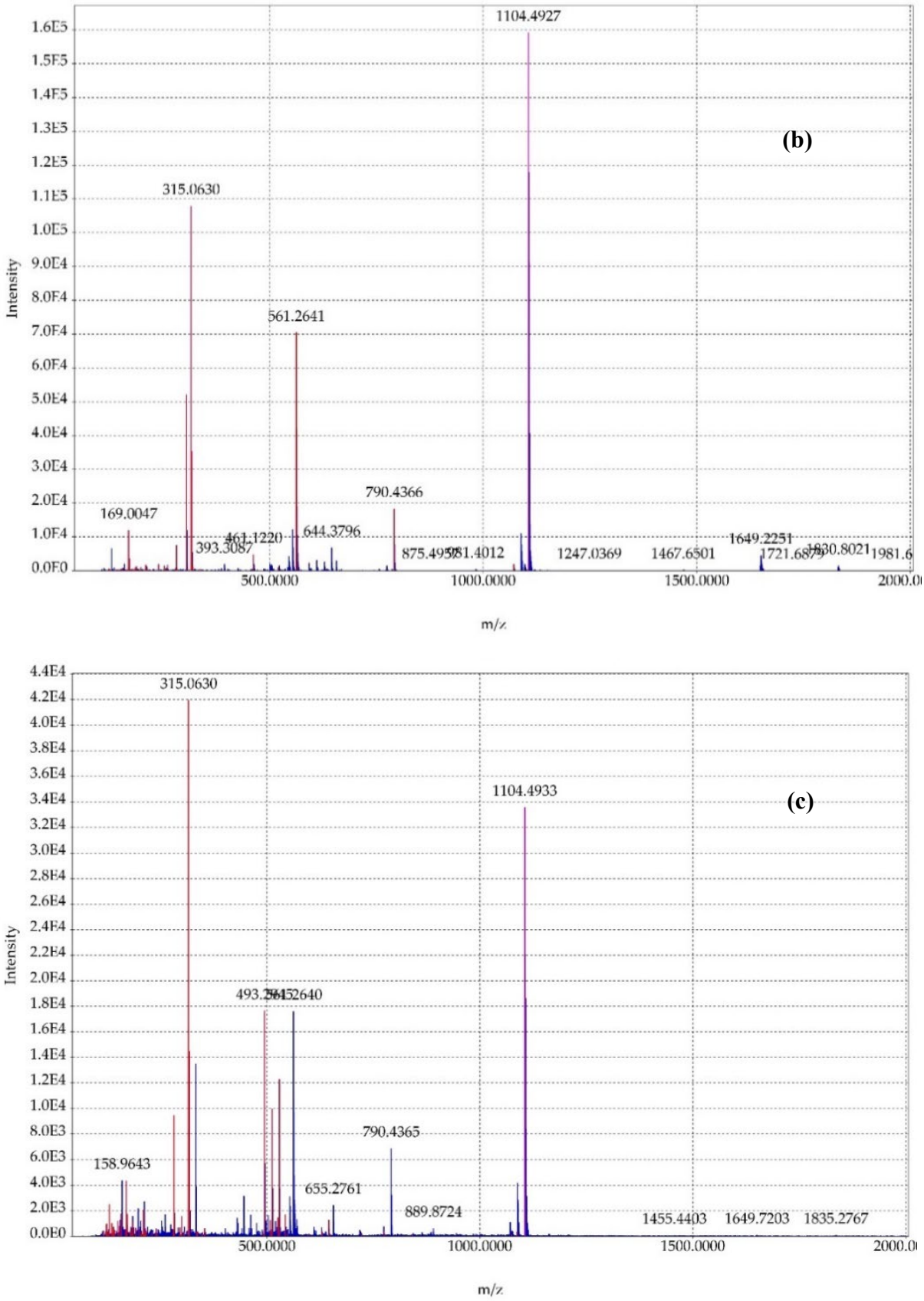

Figure 4. The ESI-TOF spectra of **(a)** phocoenamicin, **(b)** phocoenamicin B and **(c)** phocoenamicin C as detected within the crude extracts of the 27 strains.

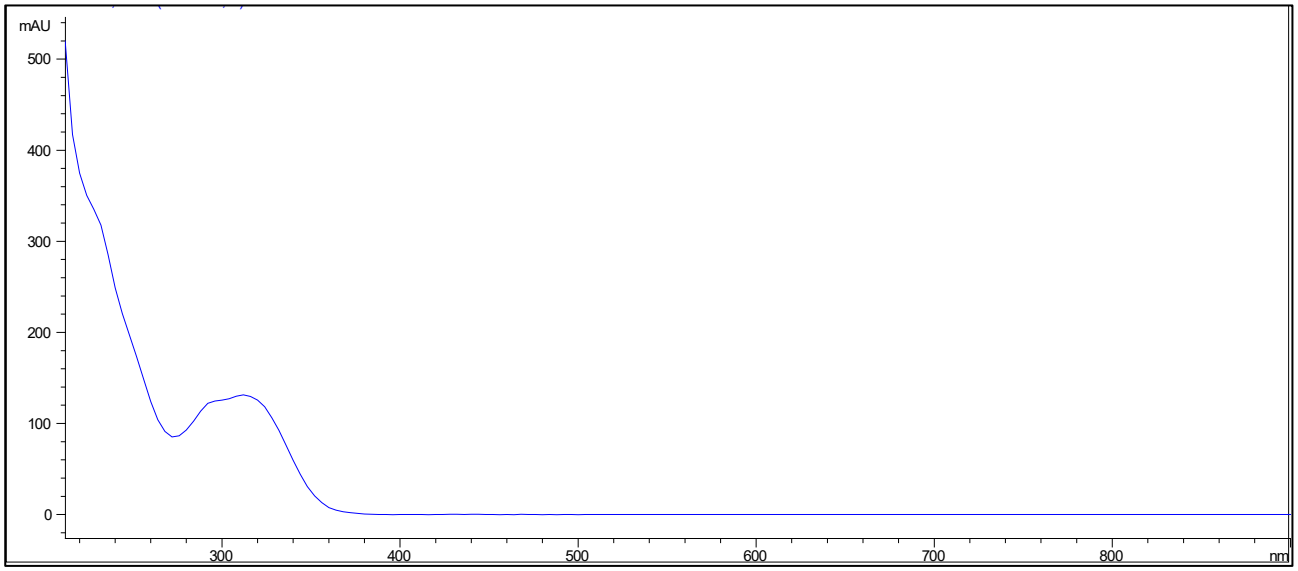

Figure 5. UV spectrum of phocoenamicin B, characteristic of all members of the family of phocoenamicins.

The manual exploration of the data suggested that phocoenamicin was the most abundant compound, detected in all strains and in almost every culture medium, with the exception of DEF-15, DEF-15S and DNPM for some of the strains. Phocoenamicin B was detected in lower amounts, but still significantly in all strains, and phocoenamicin C was the least produced metabolite and almost absent in extracts of some of the strains (CA-253038, CA-249379, CA-244669 and CA-108000).

Moreover, the qualitative study of the production of the three phocoenamicins suggested that, taken globally, the data for the 27 strains indicated that the most suitable culture media to obtain these compounds were RAM2-P V2, FR23, M016, and SAM-6. On the contrary, APM9, FPY-2 and FPY-12 exhibited significantly lower production levels, while in DEF-15, DEF-15S and DNPM the production was very low or non-existent.

Next, the metabolite profiles of the extracts were subjected to multivariate data analysis (MVDA) to explore the metabolite production profile of the strains in depth. The LC-MS raw data obtained from the analysis were preprocessed by MZmine 2 [137] (version 2.53). The treatment included mass detection, chromatogram building and deconvolution, noise reduction and data filtering, peak detection and integration, chromatographic alignment and gap filling [137], resulting in a data matrix of 6050 metabolite features.

The samples were classified in groups according to their taxonomy, geography, ecology, culture medium, and the different producing strains. The processed data were then converted into a suitable format (comma-separated values, CSV file) for each group and was uploaded to the MetaboAnalyst 5.0 platform [138] to carry out the statistical analysis. Missing values were

replaced, and further feature filtering based on interquantile range (IQR) reduced the data to 2500 features. The purpose of the data filtering was to identify and remove variables that were unlikely to be of use when modeling the data. Normalization was performed using Pareto scaling and log transformation to make individual features more comparable and transform the data matrix into a more Gaussian-type distribution, as shown in **Figure 6**.

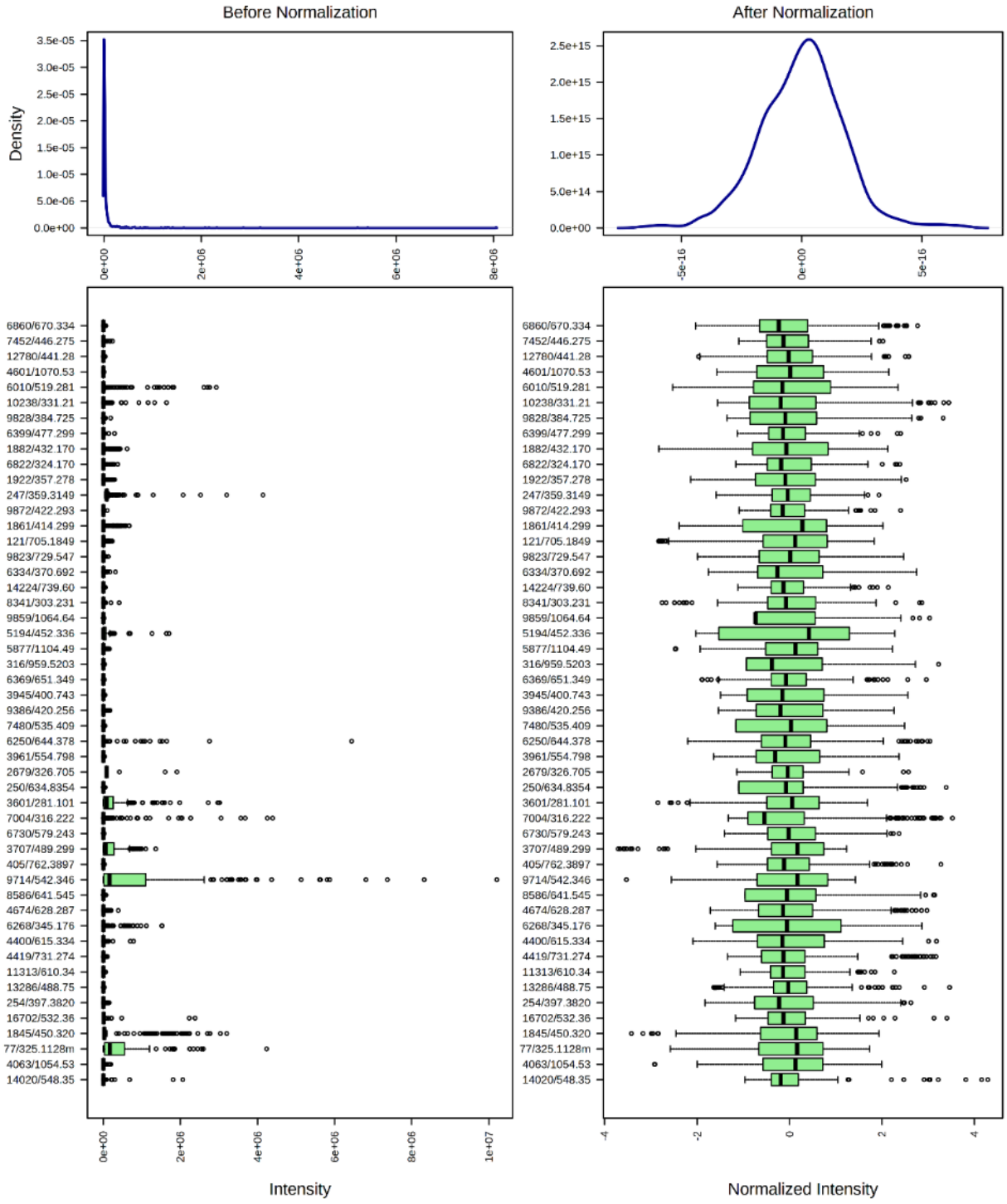

Figure 6. The boxplot and density plot showing the normalization result in MetaboAnalyst 5.0 after sample normalization, data transformation and scaling of the preprocessed LC-HRMS data obtained from the 270 extracts.

Principal Component Analysis (PCA) was used as an exploratory tool to reveal possible metabolite production patterns, trends, or outliers within the extracts. PCA reduces data by projecting them onto lower dimensions that are called principal components (PCs). As it is an unsupervised chemometric analysis, it ignores any information about the different groups of the samples and can only distinguish classes when the within-group variation is sufficiently lower than the between-group variation. The aim is to create the best summary of the data while using the least PCs possible [139]-[140]. The features included in the analysis were peaks defined by an *m/z* value and RT. The extracts that only contained the different media without bacterial cultivation were used as control samples. Five different parameters were studied as class labels, in particular the different strains, taxonomic species, culture media, source, and geography and PCA was generated for each one of them to explore if these parameters can be associated to a differential metabolite production.

As shown in **Figure 7**, PC1 and PC2 were capable of discriminating samples according to the culture medium (e), with a total variance explained of 42.4%. There was a close clustering of the control samples in all cases, demonstrating that the discrimination observed was mainly due to biological factors and not due to the media components. Furthermore, the extracts in media that were previously identified as poor producing, were clustered closer to the control media. Samples could not be grouped according to any of the other parameters (a)–(d). This suggested that such parameters did not contribute to a different chemical profile, since they did not influence the distribution of objects.

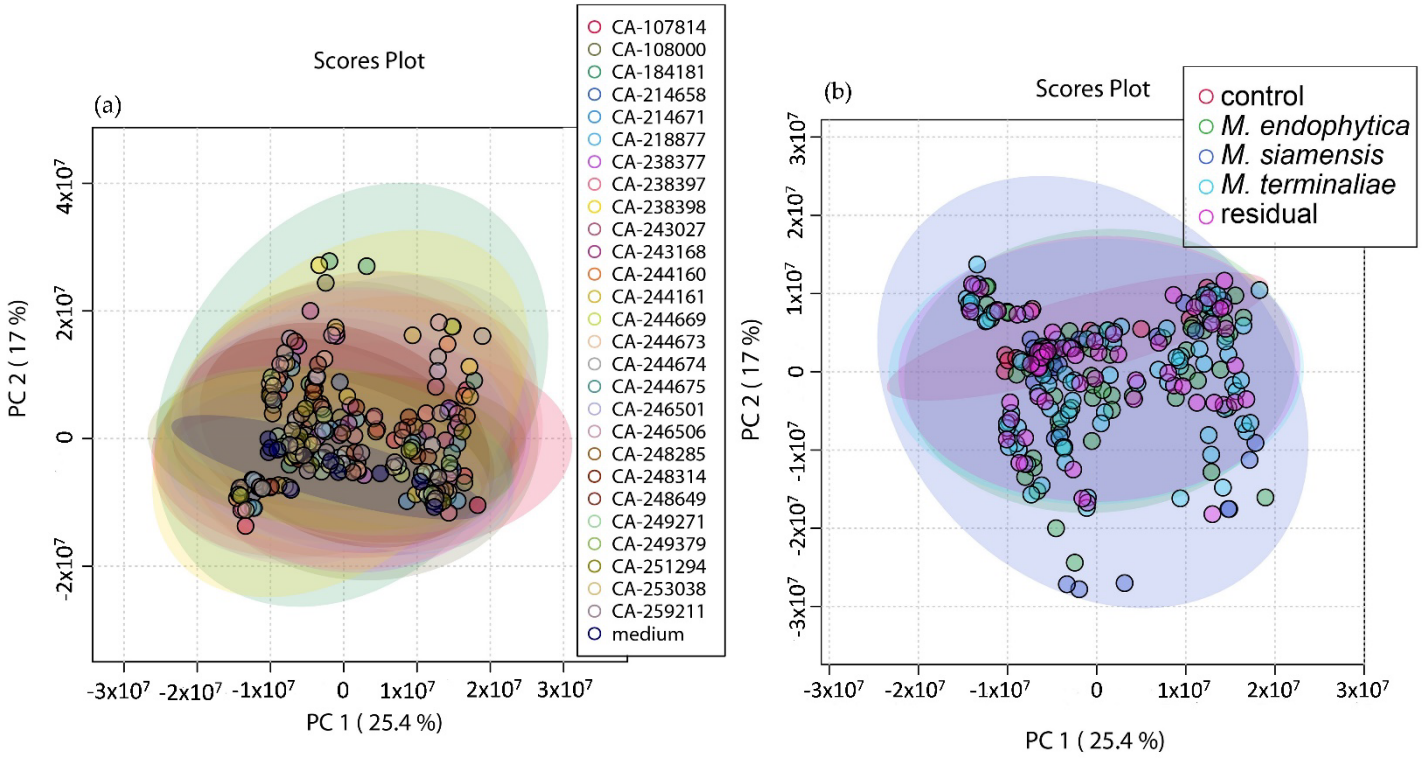

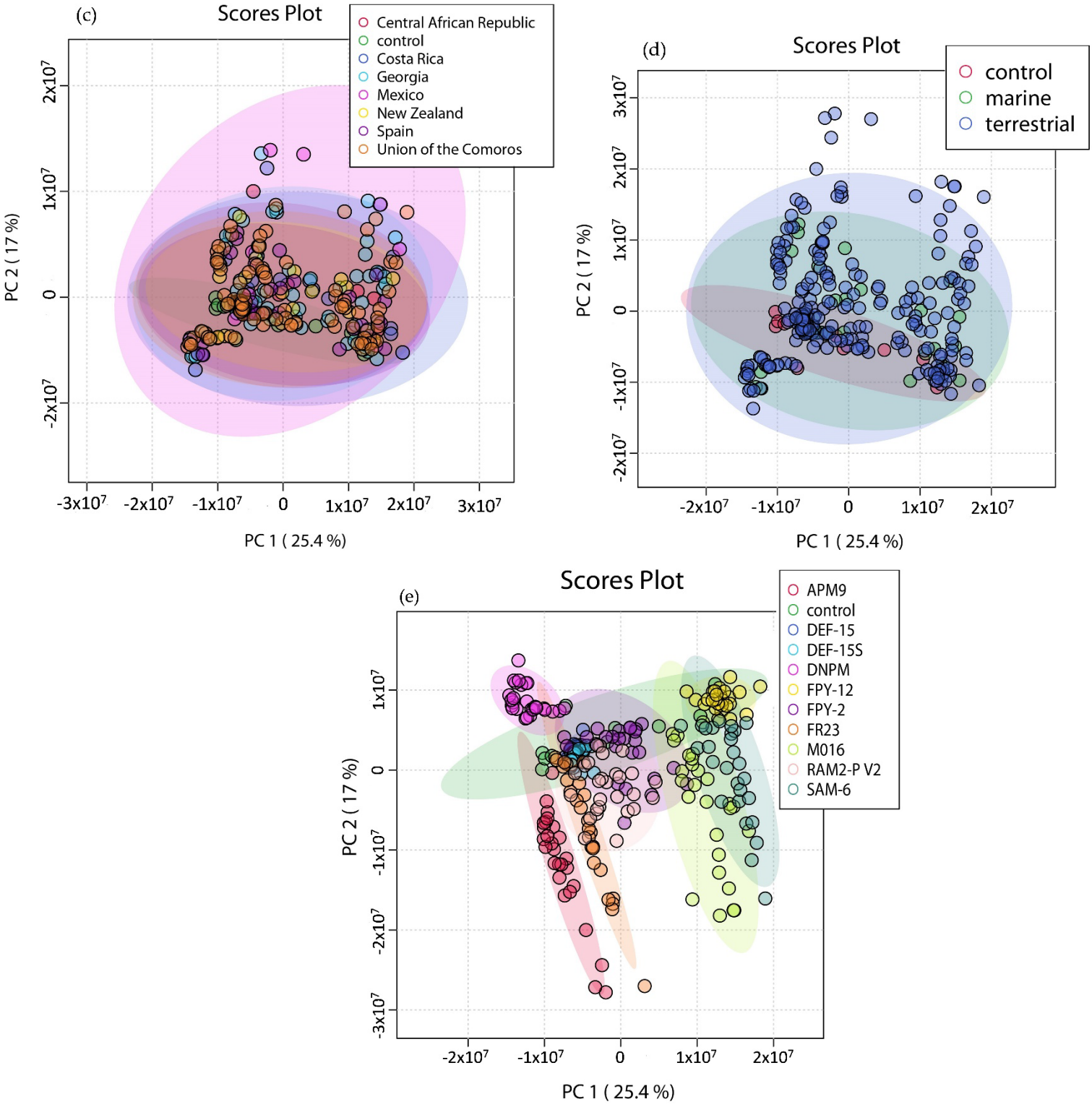

Figure 7. PCA 2D-Score plot of principal component 1 (PC1) (variance of 25.4%) and PC2 (variance of 17%), with a total variance of 42.4%. Five different models were examined, using the parameters: (**a**) different strains; (**b**) taxonomy species; (**c**) geographic origin; (**d**) ecology; and (**e**) culture medium. Only model (**e**) managed to discriminate the samples and distinguish them in groups according to the culture medium.

Next, partial least squares-discriminant analysis (PLS-DA) was used to validate the previous observation and explore in depth the chemical variation within the extracts. PLS-DA can be considered as a "supervised" view of PCA, taking into account the different groups within the samples and maximizing the covariance between the data matrix and the class label [141].

Cross-validation (CV) and permutation tests are necessary steps when using PLS-DA as it is prone to overfitting and may create clusters even in random data. A significantly important model shows R_2 (explained variance) and Q_2 (predicted variance) values > 0.7 on cross-validation and *p*-value < 0.05 on the permutation test [142].

Only the culture medium could be used to explain chemical variation with values of R_2 = 0.859 and Q_2 = 0.841 with 5 components and *p*-value < 0.01 on the permutation test (**Figure 8**). Indeed, all the other PLS-DA attempts of the different Y-class models (strain, taxonomy, geography, and ecology) apart from the absence of discrimination (see Supplementary Information, **Figure S1**), resulted in overfitting and lack of validation. (strain: R_2 = 0.393, Q_2 = 0.274, *p*-value = 0.62 taxonomy: R_2 = 0.325, Q_2 = 0.228, *p*-value = 0.44 geography: R_2 = 0.262, Q_2 = 0. 0.140, *p*-value = 0.12 and ecology: R_2 = 0.424, Q_2 = 0.278, *p*-value = 0.23)

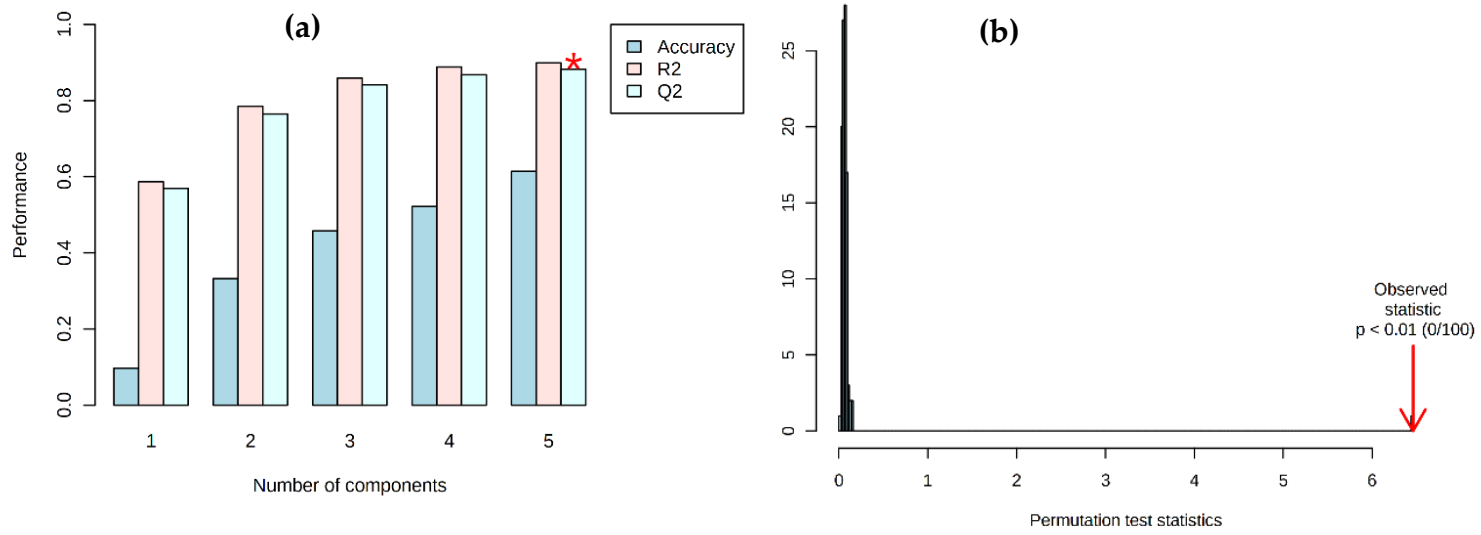

Figure 8. (a) Cross-validation test (CV) with values of R_2=0.859 and Q_2=0.841 and **(b)** permutation test with p-value < 0.01 of the PLS-DA analysis of the 270 extracts grouped by culture medium that validated its significance.

Consequently, the only parameter that could determine a significant difference in the metabolic profile of the different *Micromonospora* strains was the culture medium, as shown in **Figure 9a**. Regarding the media, the control extracts of the media that were identified as potent phocoenamicin producers were closely clustered together but the poor producing ones were

scattered and close to all the extracts of the same medium, reaffirming the significant influence of the culture medium in the metabolite production of these strains.

PLS-DA can also be used for the selection of the most important features that drive the separation between the groups [141]. Hence, the 3D loadings plot, as shown in **Figure 9b**, revealed the main components that were responsible for this separation. From the metabolites observed, only the ones that accounted for Variable Importance in Projection (VIP) higher than 1.5 were taken into account. The components that were further from the center of the plot contributed the most to the separation. Among them, the spirotetronate maklamicin was putatively identified via manual dereplication, as well as daidzein, genistein and the siderophores nocardamine and terragine B (see **Section 3.3**), confirming the chemical differences observed between the extracts cultivated in each medium.

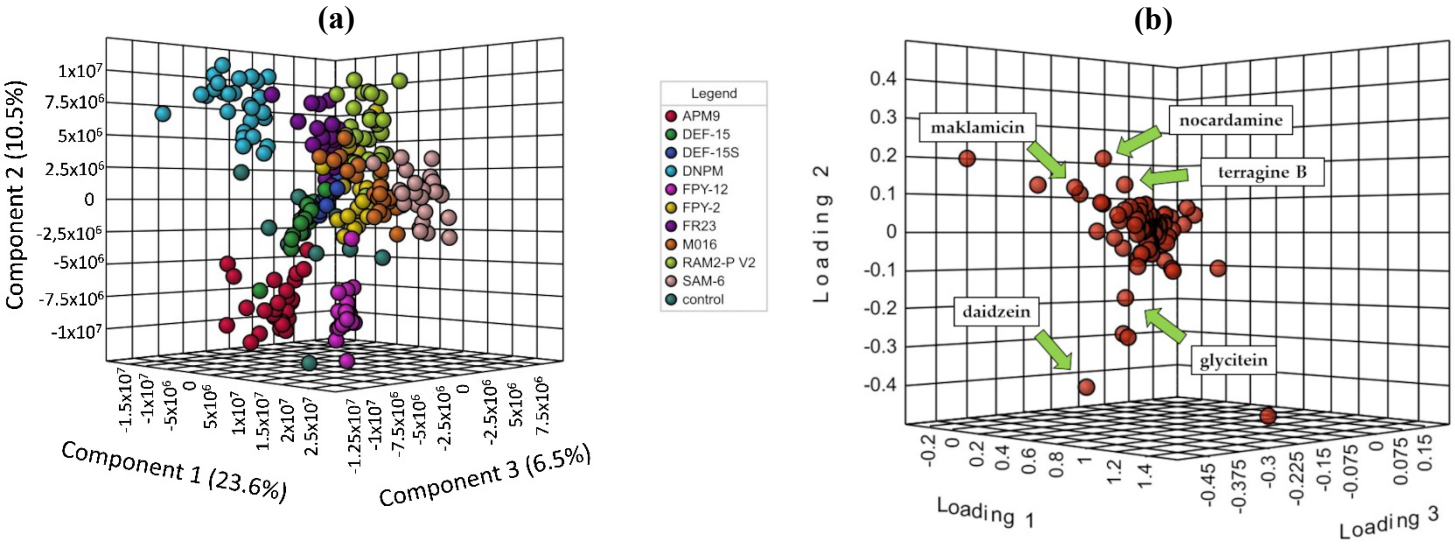

Figure 9. (a) PLS-DA 3D-Score plot of the 270 extracts grouped by culture medium and the 10 control extracts where the extracts are clustered according to the culture media; and **(b)** the main compounds that were responsible for the separation. The components that were further from the center of the plot contributed the most to the separation. Only the ones that accounted for Variable Importance in Projection (VIP) higher than 1.5 were considered.

The RAM2-P V2 medium was selected for further analysis by liquid chromatography coupled to tandem mass spectrometry (LC-MS/MS), given that it was identified as one of the culture media producing the richest metabolite profiles. The aim was to improve its resolving ability and explore more profoundly the metabolic potential of the strains. Following the previous procedure, the raw data obtained were processed with MZmine 2 and then analyzed using the MetaboAnalyst platform, where sample normalization, data transformation and scaling of the preprocessed LC-MS/MS data obtained was performed (Supplementary Information, **Figure S2**).

The data matrix contained 1287 features and the samples were distributed into two groups according to their ecology: marine-derived, and terrestrial strains.

Firstly, hierarchical clustering was performed by MetaboAnalyst 5.0 to build a hierarchy of clusters according to the metabolic profile of the 27 strains. Hierarchical cluster analysis (HCA) is an unsupervised quantitative method used to assess the chemical similarity of different samples [143]. Ward's clustering algorithm and Euclidean distance measure were used to create the dendrogram that is shown in **Figure 10**. The three marine-derived strains were closely clustered indicating that they had a similar chemical composition when cultured in the RAM2-P V2 medium.

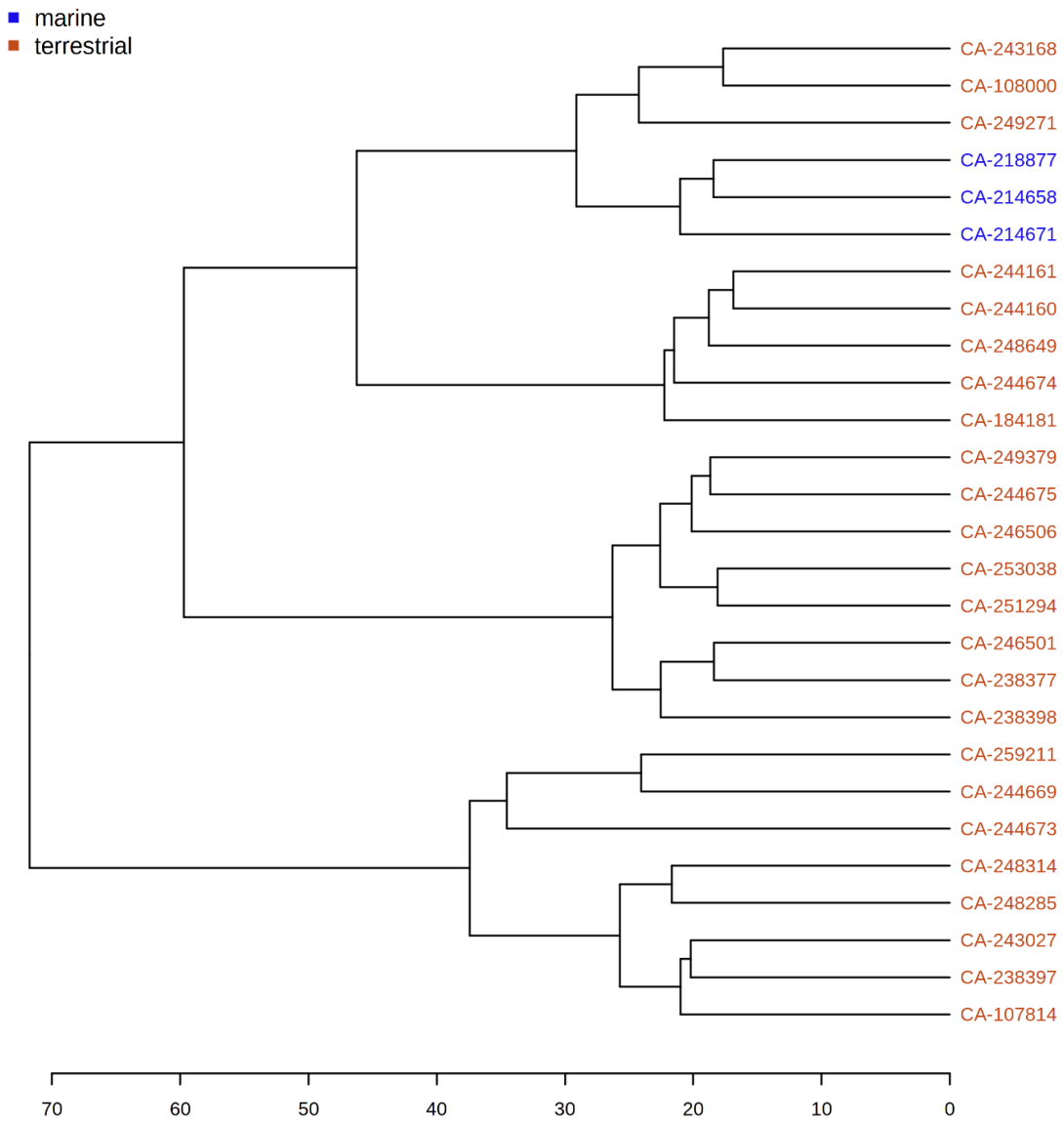

Figure 10. Dendrogram generated from the Hierarchical Cluster Analysis showing the close clustering of the three marine-derived strains (blue) compared to the terrestrial (brown).

Furthermore, the relative concentration of the three phocoenamicins was explored, comparing the peak intensities of the marine and terrestrial strains. As shown in **Figure 11**, phocoenamicin was produced more within the terrestrial strains, while phocoenamicins B and C within the marine.

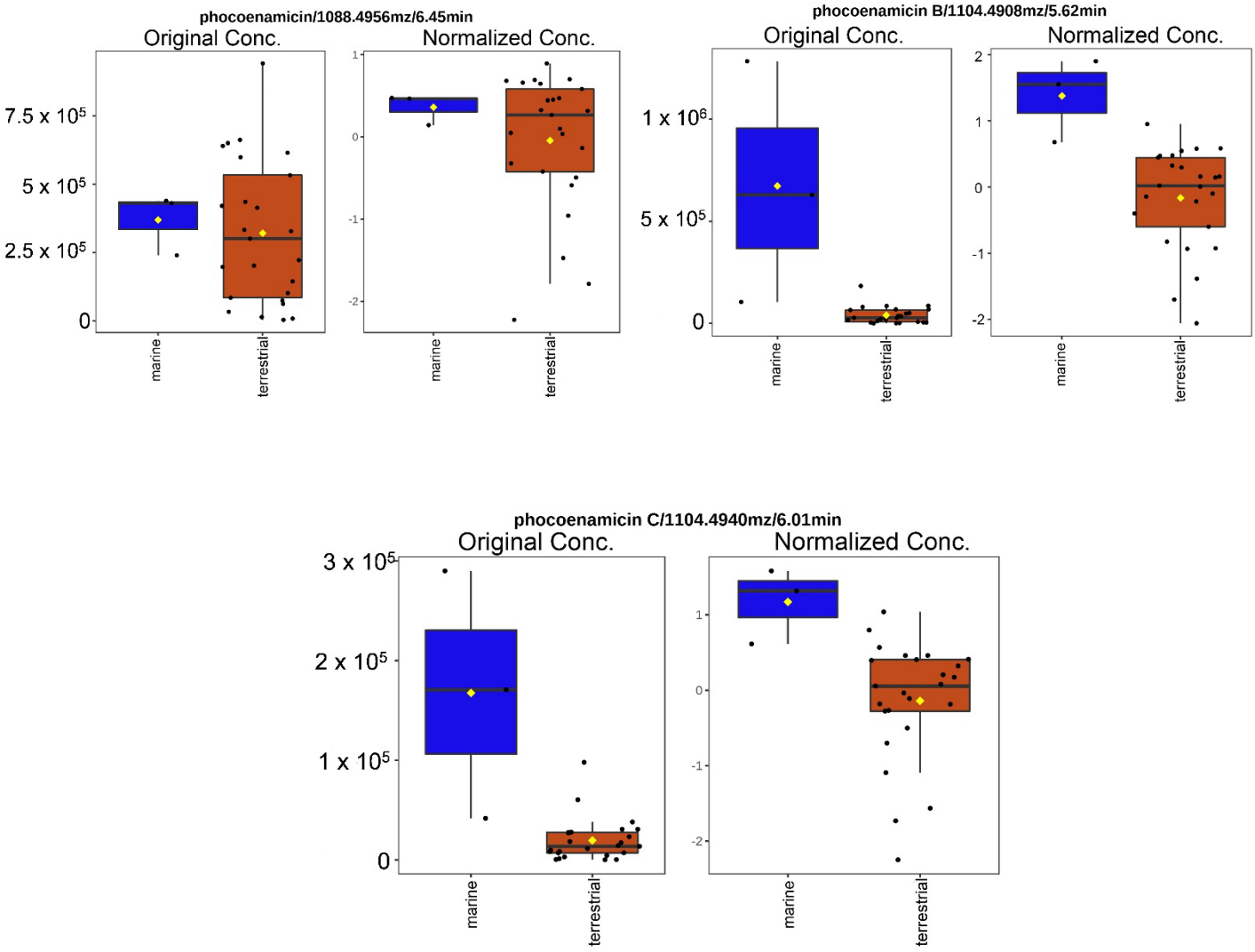

Figure 11. The relative concentration of the three phocoenamicins, before and after normalization techniques and based on their peak intensities and grouped by their source, marine (blue) and terrestrial strains (brown).

The peak intensity plot of the processed raw data generated by MZmine 2 (**Figure 12**) allowed us to identify tendencies based on the peak area, keeping in mind the limitation of using non-quantitative mass spectrometry data. The interpretation of the plot suggested that the maximum levels of phocoenamicin production in RAM2-P V2 medium were obtained in extracts of the terrestrial strains CA-184181 and CA-238649, and for phocoenamicins B and C in the

marine strain CA-214658, followed by the also marine CA-218877, reaffirming the previous results that phocoenamicin is produced more by the terrestrial strains while phocoenamicins B and C by the marine-derived ones.

Additionally, the putative phocoenamicin derivatives identified (see **Section 3.5**) were also studied and their production levels were compared within the 27 strains in RAM2-P V2 medium. Among them, the compound with an adduct ion at *m/z* 920.4935 produced by the strains CA-248649, CA-244161 and CA-251294 presented significant production levels and the compound with an adduct ion at *m/z* 774.4410 was produced in higher amounts by the strain CA-249379. Lastly, the marine strains CA-214658 and CA-218877 demonstrated the highest diversity in producing a wide array of minor unknown compounds (**Figure 12**), suggesting that they could be good candidates for the scale-up of the production and isolation of these putative minor analogues.

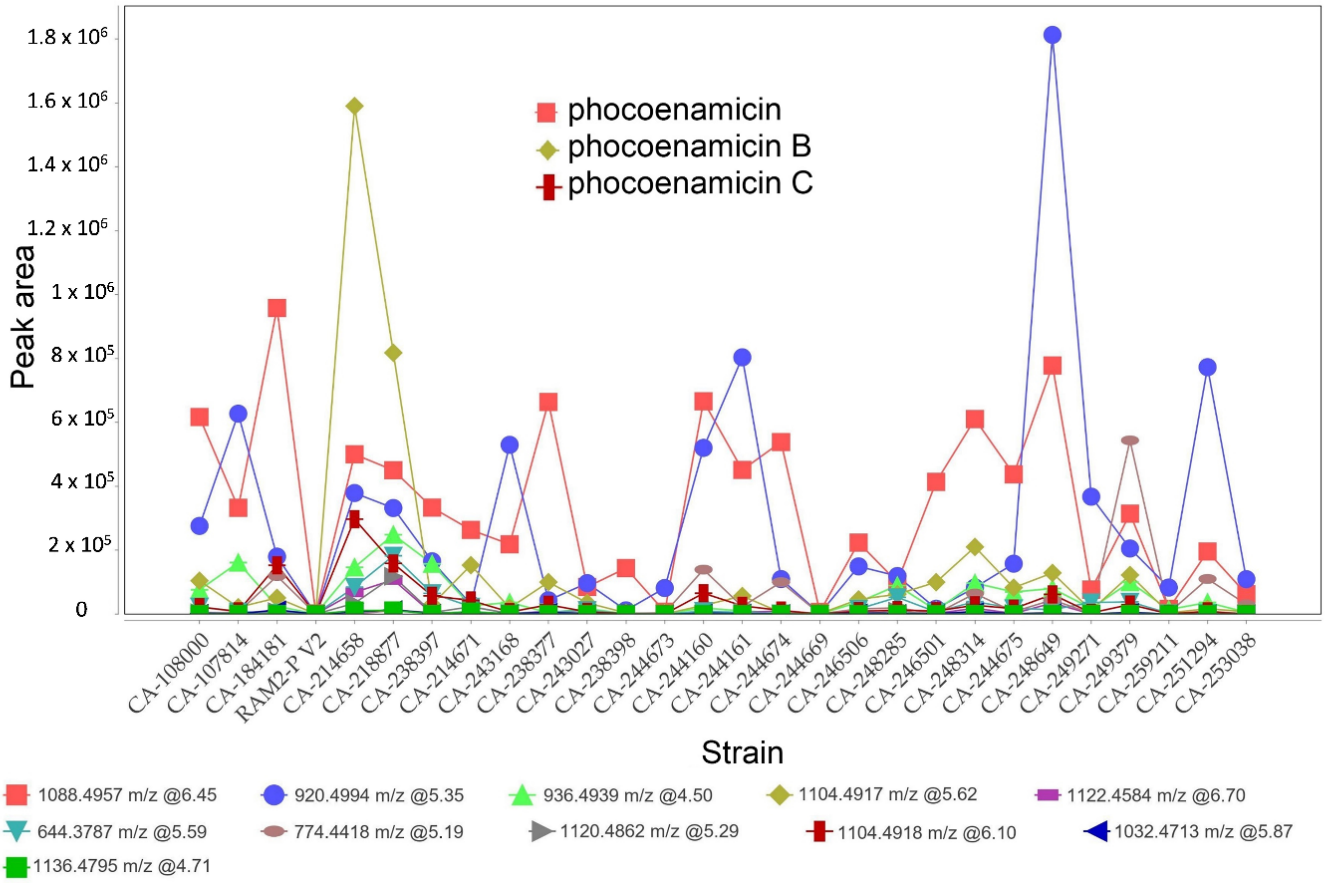

Figure 12. Peak intensity plot based on peak area generated by MZmine 2 for the three phocoenamicins along with the putative phocoenamicin analogues identified in RAM2-P V2 medium. The *m/z* values, RT and their corresponding colors-shapes are shown for each compound.

All in all, the marine-derived strain CA-214658 cultured in medium RAM2-P V2 was identified as the best production condition of this family of compounds. The Total Ion Chromatogram (TIC) of its crude extract displaying the ions detected is shown in **Figure 13**.

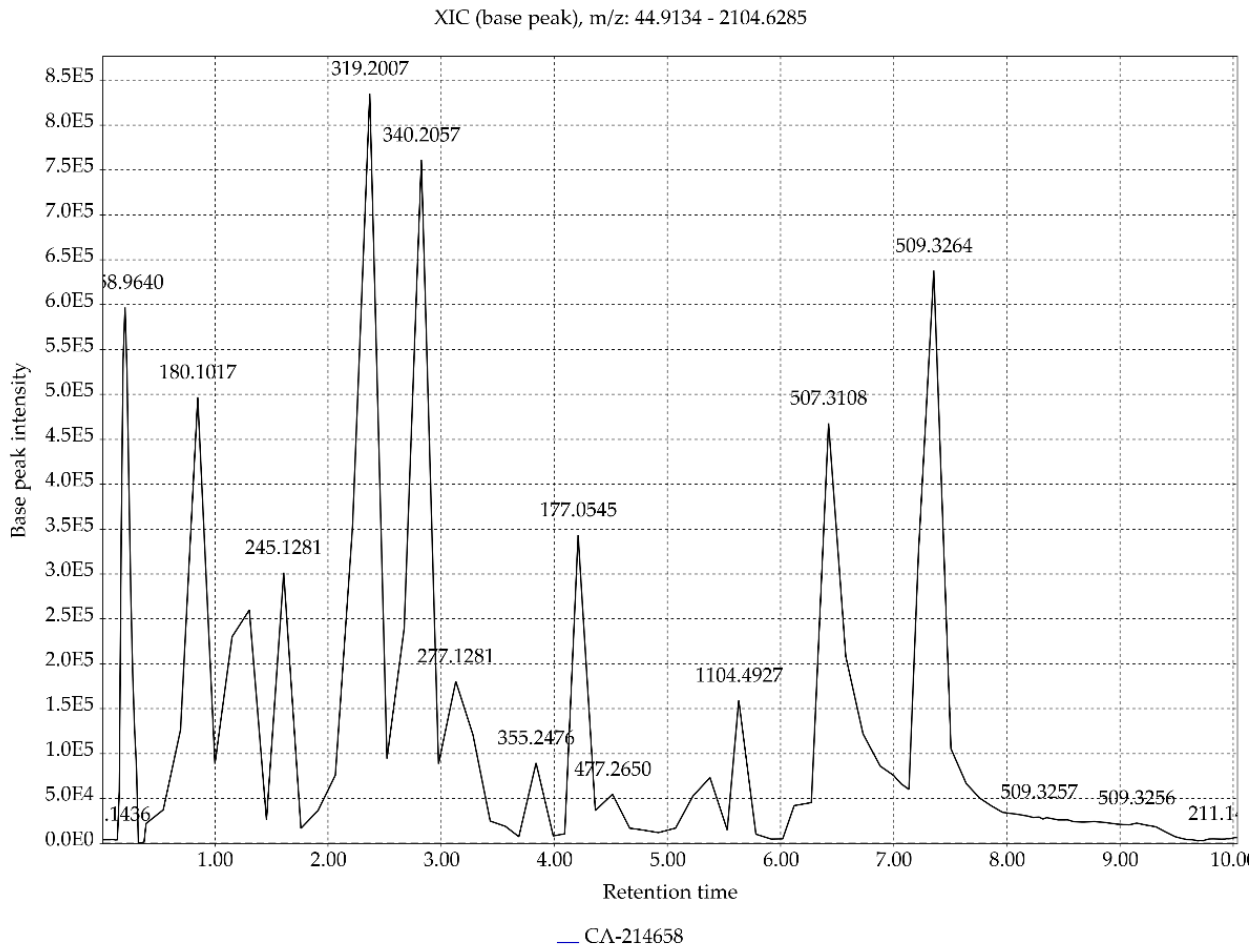

Figure 13. Total Ion Chromatogram (TIC) of the crude extract from the strain CA-214658 grown in RAM2-P V2 medium.

3.3 Dereplication of the Main Compounds Produced

The combination of the LC-UV-MS analyses and metabolomic profiling allowed the putative dereplication of the main compounds produced within the 27 strains in the different growing conditions, as shown in **Table 4**. The proposed dereplication was accomplished searching the molecular formulae determined for the compounds using HRMS data against various databases. In particular, the in-house MEDINA database, the Dictionary of Natural Products (DNP), the COlleCtion of Open Natural ProdUcTs (COCONUT), the Natural Product Activity & Species Source database (NPASS) and the ChemSpider database were used. The comparative analyses led to the tentative identification of multiple, chemically diverse, compounds. The *m/z* detected with the corresponding adduct ion, the theoretical mass of each adduct and its deviation in ppm, the molecular formulae, and the RT are shown for each compound. The molecules included in the table

were detected in multiple samples, therefore the values of *m/z* and retention time displayed are representative for each compound.

Table 4. Putatively dereplicated metabolites detected in the crude extracts of the fermentation broths.

Compound	*m/z* Detected, Adduction	Theoretical Mass (Δ ppm)	Molecular Formula	Retention Time
spirotetronates				
phocoenamicin	1088.4982, $[M + NH_4]^+$	1088.4980 (+0.2)	$C_{56}H_{75}ClO_{18}$	6.44
phocoenamicin B	1104.4927, $[M + NH_4]^+$	1104.4929 (−0.2)	$C_{56}H_{75}ClO_{19}$	5.53
phocoenamicin C	1104.4933, $[M + NH_4]^+$	1104.4929 (+0.4)	$C_{56}H_{75}ClO_{19}$	6.02
maklamicin	542.3478, $[M + NH_4]^+$	542.3476 (+0.4)	$C_{32}H_{44}O_6$	6.38
siderophores				
nocardamine	601.3551, $[M + H]^+$	601.3556 (−0.8)	$C_{27}H_{48}N_6O_9$	1.26
deoxynocardamine	585.3589, $[M + H]^+$	585.3606 (−2.9)	$C_{27}H_{48}N_6O_8$	1.02
demethylenenocardamine	587.3396, $[M + H]^+$	587.3399 (−0.5)	$C_{26}H_{46}N_6O_9$	0.95
terragine D	479.2848, $[M + H]^+$	479.2864 (−3.3)	$C_{24}H_{38}N_4O_6$	2.54
terragine B	319.1652, $[M + H]^+$	319.1652 (0.0)	$C_{17}H_{22}N_2O_4$	2.80
IC 202B	533.3275, $[M + H]^+$	533.3293 (−3.4)	$C_{23}H_{44}N_6O_8$	1.51
deferoxamine	561.3604, $[M + H]^+$	561.3606 (−0.4)	$C_{25}H_{48}N_6O_8$	0.70
proferrioxamine A1	547.3450, $[M + H]^+$	547.3450 (0.0)	$C_{24}H_{46}N_6O_8$	0.65
desferrioxamine D1	603.3695, $[M + H]^+$	603.3712 (−1.1)	$C_{27}H_{50}N_6O_9$	1.06
legonoxamine A	637.3914, $[M + H]^+$	637.3919 (−0.8)	$C_{31}H_{52}N_6O_8$	2.34
legonoxamine G	623.3763, $[M + H]^+$	623.3763 (0.0)	$C_{30}H_{50}N_6O_8$	2.21
legonoxamine H	665.3861, $[M + H]^+$	665.3869 (−1.2)	$C_{32}H_{52}N_6O_9$	2.47
microferrioxamine B	729.5473, $[M + H]^+$	729.5484 (−1.5)	$C_{37}H_{72}N_6O_8$	4.78
microferrioxamine C	743.5632, $[M + H]^+$	743.5641 (−1.2)	$C_{38}H_{74}N_6O_8$	4.97
microferrioxamine D	757.5792, $[M + H]^+$	757.5797 (−0.7)	$C_{39}H_{76}N_6O_8$	5.21
acyl ferrioxamine 2	679.4015, $[M + H]^+$	679.4025 (−1.4)	$C_{33}H_{54}N_6O_9$	2.78
various				
daidzein	255.0648, $[M + H]^+$	255.0652 (−1.6)	$C_{15}H_{10}O_4$	2.55
genistein	271.0594, $[M + H]^+$	271.0601 (−2.6)	$C_{15}H_{10}O_5$	3.20
glycitein	285.0754, $[M + H]^+$	285.0757 (−1.1)	$C_{16}H_{12}O_5$	2.67
antascomicin D	646.3946, $[M + H]^+$	646.3950 (−0.6)	$C_{36}H_{55}NO_9$	3.80
21-demethyl-leptomycin A	513.3208, $[M + H]^+$	513.3211 (−0.6)	$C_{31}H_{44}O_6$	5.07
indothiazinone-4-carboxylic acid	273.0327, $[M + H]^+$	273.0328 (−0.4)	$C_{13}H_8N_2O_3S$	2.98
anandin A	358.2743, $[M + H]^+$	358.2741 (+0.6)	$C_{23}H_{35}NO_2$	4.52
ganefromycin epsilon	644.3794, $[M + H]^+$	644.3793 (+0.2)	$C_{36}H_{53}NO_9$	4.70
actiphenol	276.1238, $[M + H]^+$	276.1230 (+2.9)	$C_{15}H_{17}NO_4$	2.48
N^b-Acetyltryptamine	203.1177, $[M + H]^+$	203.1179 (−1.0)	$C_{12}H_{14}N_2O$	2.41
N-Acetyltyramine	180.1023, $[M + H]^+$	180.1019 (+2.2)	$C_{10}H_{13}NO_2$	0.92
actiphenamide	294.1331, $[M + H]^+$	294.1336 (−1.7)	$C_{15}H_{19}NO_5$	2.48
antibiotic BE 54476	392.2429, $[M + H]^+$	392.2431 (−0.5)	$C_{22}H_{33}NO_5$	4.14

As already mentioned, the three phocoenamicins were putatively detected within all the extracts. Together with the phocoenamicins, maklamicin was also tentatively identified to be produced by all 27 strains. Maklamicin is also a spirotetronate originally found to be produced by an endophytic *Micromonospora* sp. collected in Thailand and has shown strong to modest antimicrobial activities against various Gram-positive bacteria [90]. As shown in **Figure 14**, structurally, maklamicin is closely related to the phocoenamicins, having 11 carbons on its macrocycle and a decalin unit, as phocoenamicins. The closest proximity is with phocoenamicin B, their major differences being the absence of the two 6-deoxyglucose moieties, the 3-chloro-6-hydroxy-2-methylbenzoate moiety, and the diol side chain, unique in the phocoenamicins [77],[94]. Within the 270 extracts of this study, the production of the two families was analogous in all cases. Furthermore, phocoenamicin and maklamicin co-eluted in the crude extracts of the fermentation broths and further purification would be needed for their separation. The co-production of the two families has not been reported before and indicates the existence of a common biosynthetic pathway in their production.

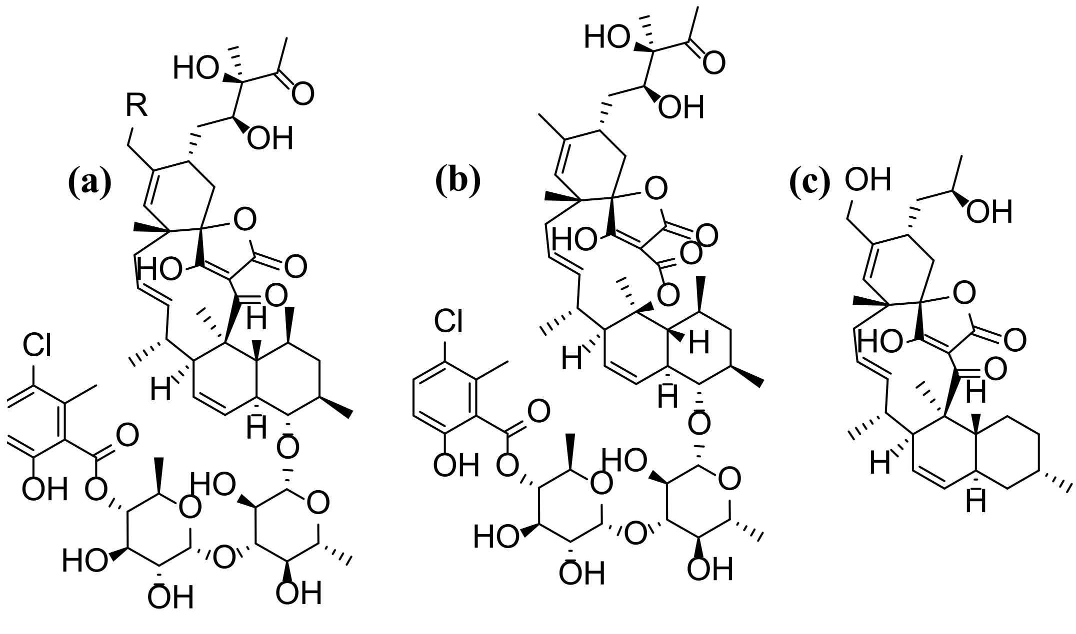

phocoenamicin R=H
phocoenamicin B R=OH

phocoenamicin C

maklamicin

Figure 14. Structures of: (**a**) phocoenamicin and phocoenamicin B; (**b**) phocoenamicin C; and (**c**) maklamicin.

Apart from the spirotetronates, the majority of the compounds putatively dereplicated belonged to the hydroxamate siderophores structural class, and in particular to the desferrioxamine family, with the most common being deferoxamine [144], nocardamine [145], terragine B [146] and IC 202B [147]. Finally, various other compounds were tentatively identified within the extracts. The most abundant were the isoflavones daidzein [148], genistein [149] and glycitein [150] for which antioxidant, anticancer and antimicrobial properties have been reported.

3.4 Molecular Networking (MN)

Molecular Networking (MN) explores chemical diversity visualizing the entire metabolome detected in a dataset and organizing it in clusters based in tandem mass spectrometry**.** Structurally related compounds are connected forming clusters whereas the unrelated are separated [35]. In a molecular network, each node represents a compound and the nodes with similar spectra are linked to form clusters or "molecular families" and these links provide valuable structural information [36]. Molecular networking has led to the creation of Global Natural Products Social Molecular Networking (GNPS), a web-based platform (http://gnps.ucsd.edu) developed by researchers at the University of California at San Diego.

GNPS was used to organize the MS/MS data obtained from the crude extracts of the 27 strains grown in RAM2-P V2 medium, whose extract was used as well as a control sample. It offers two main workflows, the classical MN and feature-based molecular networking (FBMN). In classical MN, raw MS/MS spectra files are processed directly to generate a MN. This often leads to multiple nodes for the same compound when detected over a large retention time span and creates huge MNs that are not fully representative of the actual number of compounds in the dataset. Classical MN led to the creation of a massive molecular network with 2514 nodes organized in 65 clusters (at least two nodes connected), difficult to interpret, even though an overview of the metabolites and their relationships could be observed, as shown in **Figure 15**, visualized using the Cytoscape software (version 3.8.2). The cluster formed by the phocoenamicins was identified, shown in a red circle in **Figure 15**.

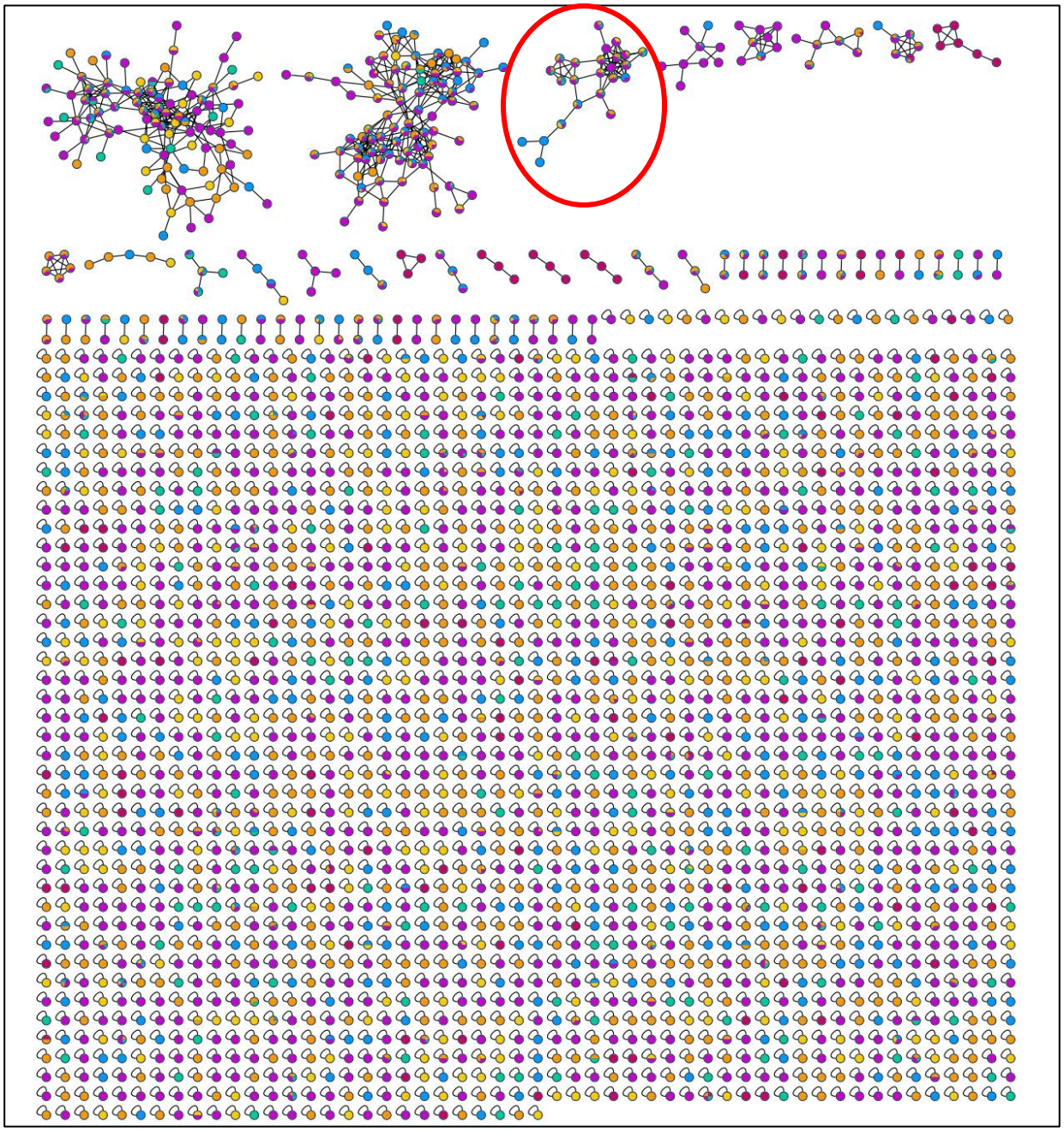

Figure 15. The classical molecular network (GNPS) generated from the extracts of the 27 strains cultured in RAM2-P V2 medium. The nodes are coloured according to the geographic origin of the 27 strains. In a red circle, the phocoenamicins cluster is shown.

In order to overcome this problem, FBMN uses a feature detection and alignment tool, such as MZmine 2, to preprocess the raw data and is used for advanced molecular networking analysis, enabling the relative quantification of the compounds and resolution of isomers [38]. FBMN workflow was chosen for further analysis of the dataset, leaving behind many nodes that were a replicate of the same compound and compounds that were only produced in traces within the extracts, therefore providing a more realistic view of the compounds produced by *Micromonospora*.

The raw data were preprocessed by MZmine 2 [137] and then uploaded to the GNPS platform to perform the analysis. A metadata file was also uploaded to describe the properties of each sample-strain (taxonomy, geography, ecology). The results were visualized using the Cytoscape software (version 3.8.2) and are shown in **Figure 16**.

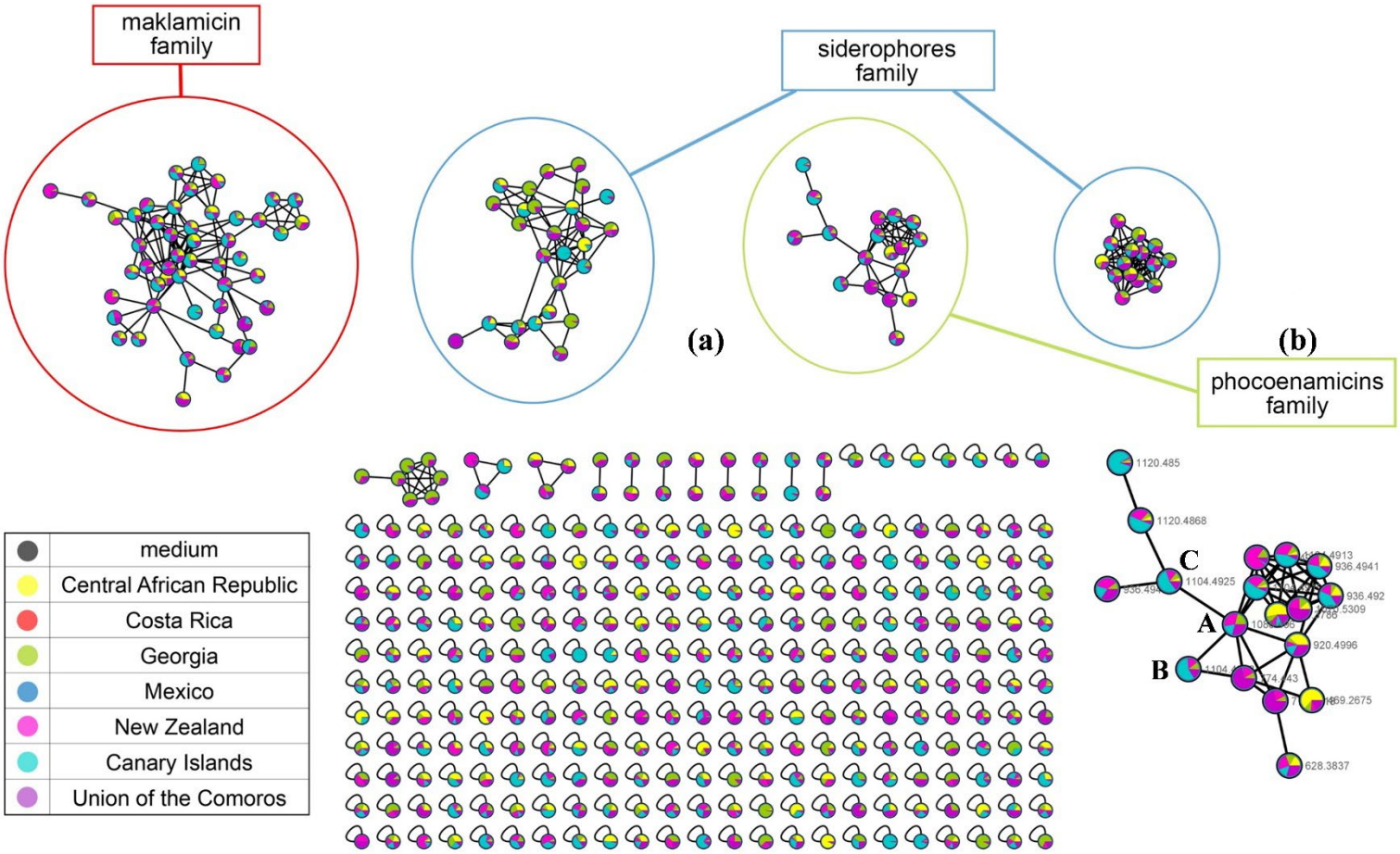

Figure 16. (**a**) The molecular network generated from the FBMN analysis of the 27 strains grown in the RAM2-P V2 medium. The medium was used as control to remove the compounds that were not produced by the strains. The nodes are colored according to the geographic distribution of the strains that produced them. Four main clusters were detected, two created by the siderophores, one by maklamicin and one more from the phocoenamicins; and (**b**) the phocoenamicins cluster revealed 18 nodes and the known phocoenamicins were putatively identified as phocoenamicin (A), phocoenamicin B (B) and phocoenamicin C (C). *m/z* values of new derivatives in the network are detailed in **Table 4**.

The FBMN analysis resulted in 447 nodes (parent ions) that were organized in 15 clusters (molecular families, at least two nodes connected). The four main clusters were putatively identified. Two of them corresponded to the siderophores, one by the phocoenamicins and one to maklamicin and related compounds (**Figure 16a**). Many of the nodes remained unannotated, highlighting the need for further study of the potential of these strains. Some of them that were

related to known compounds were tentatively characterized as new according to the manual dereplication process (see **Section 3.5**).

Focusing on the phocoenamicins cluster, the three phocoenamicins were putatively detected clustering together (A–C, **Figure 16b**). As shown in **Figure 16b**, the cluster was composed of 18 nodes in total. Some of the nodes represented adducts of the same molecule and this was taken into account upon their tentative identification, based on the RT span and the MS/MS fragments, resulting in 10 different compounds. The nodes are marked by experimental *m/z* values and colored according to the geographic distribution of the strains that produced them. As can be seen, they are widely distributed on almost all continents. Moreover, considering that the FBMN analysis additionally provides relative quantification, in the culture medium RAM2-P V2, phocoenamicins B and C were produced in higher amounts by the marine-derived strains, while phocoenamicin is produced more abundantly by the rest of the strains, in agreement with the previously mentioned observations. Furthermore, the compounds originating some of the nodes could not be identified, indicating that they could putatively represent new analogues of this family of compounds. For example, the parent ion with *m/z* 1120.4868 that was directly connected with phocoenamicin C showed a difference of 16 Da, indicating a possible oxygenation and the proposed molecular formula $C_{56}H_{75}ClO_{20}$ generated for the compound was in agreement with this fact (see **Section 3.5**).

3.5 Putative Identification of Possible New Compounds

The LC-UV-HRMS analysis, the molecular networking and the manual dereplication tentatively detected several peaks corresponding to compounds with molecular formulae that were not found within various databases and therefore are putatively new metabolites related to the phocoenamicins, the maklamicin or the siderophores.

In particular, the annotations were based on GNPS, searching the compounds that were in each molecular cluster and combining the manual putative dereplication of *m/z*, UV profile, RT and proposed molecular formula against the databases previously mentioned (DNP, COCONUT, NPASS and ChemSpider). In **Table 5**, the putatively unknown compounds are grouped by family. Their *m/z* values and adduct ions detected, theoretical masses and deviation in ppm, the predicted molecular formulae and the chromatographic retention time are shown. As in **Table 4**, due to the detection of these molecules in multiple analytical runs, representative values of *m/z* and retention times for each compound are displayed.

Table 5. Potential derivatives detected in the crude extracts of the fermentation broths.

Compound	*m/z* Detected, Adduction	Theoretical Mass (Δ ppm)	Molecular Formula Predicted	Retention Time
spirotetronates				
phocoenamicin derivative	1120.4862, $[M + NH_4]^+$	1120.4878 (−1.4)	$C_{56}H_{75}ClO_{20}$	5.29
phocoenamicin derivative	1032.4713, $[M + NH_4]^+$	1032.4718 (−0.5)	$C_{53}H_{71}ClO_{17}$	5.70
phocoenamicin derivative	1122.4584, $[M + NH_4]^+$	1122.4590 (−0.5)	$C_{56}H_{74}Cl_2O_{18}$	6.71
phocoenamicin derivative	1136.4795, $[M + NH_4]^+$	1136.4828 (−2.9)	$C_{56}H_{75}ClO_{21}$	4.54
phocoenamicin derivative	920.4994, $[M + NH_4]^+$	920.5002 (−0.9)	$C_{48}H_{70}O_{16}$	5.24
phocoenamicin derivative	936.4939, $[M + NH_4]^+$	936.4951 (−1.3)	$C_{48}H_{70}O_{17}$	4.46
phocoenamicin derivative	644.3787, $[M + NH_4]^+$	644.3793 (−0.9)	$C_{36}H_{50}O_9$	5.55
phocoenamicin derivative	774.4418, $[M + NH_4]^+$	744.4423 (−0.7)	$C_{42}H_{60}O_{12}$	5.19
maklamicin derivative	509.3250, $[M + H]^+$	509.3262 (−2.4)	$C_{32}H_{44}O_5$	7.30
maklamicin derivative	495.3091, $[M + H]^+$	495.3105 (−2.8)	$C_{31}H_{42}O_5$	7.09
maklamicin derivative	511.3060, $[M + H]^+$	511.3054 (+1.2)	$C_{31}H_{42}O_6$	6.12
maklamicin derivative	539.3350, $[M + H]^+$	539.3367 (−3.2)	$C_{33}H_{46}O_6$	6.60
maklamicin derivative	523.3049, $[M + H]^+$	523.3054 (−1.0)	$C_{32}H_{42}O_6$	6.91
siderophores				
nocardamine derivative	599.3379, $[M + H]^+$	599.3399 (−3.3)	$C_{27}H_{46}N_6O_9$	1.85
deferoxamine derivative	631.4384, $[M + H]^+$	631.4389 (−0.8)	$C_{30}H_{58}N_6O_8$	2.88
deferoxamine derivative	645.4531, $[M + H]^+$	645.4545 (−2.2)	$C_{31}H_{60}N_6O_8$	3.23
deferoxamine derivative	687.4638, $[M + H]^+$	687.4651 (−1.9)	$C_{33}H_{62}N_6O_9$	3.44
deferoxamine derivative	659.4342, $[M + H]^+$	659.4338 (+0.6)	$C_{31}H_{58}N_6O_9$	2.94
deferoxamine derivative	671.4694, $[M + H]^+$	671.4702 (−1.0)	$C_{33}H_{62}N_6O_8$	3.66

Several phocoenamicin derivatives were tentatively detected. Some of the molecular formulae predicted ($C_{48}H_{70}O_{16}$, $C_{48}H_{70}O_{17}$, $C_{36}H_{50}O_9$, $C_{42}H_{60}O_{12}$) proposed a possible change in the oligosaccharide motif of phocoenamicins that was not observed before within the family.

Maklamicin [151] is the only member of the family naturally produced so far. 29-deoxymaklamicin, that tentatively matched the accurate mass (508.3169) and the proposed

molecular formula ($C_{32}H_{44}O_5$) of one of these putatively new compounds, was also reported before, but as a product of a genetically engineered strain [152]. The GNPS analysis revealed five assumably new analogues of maklamicin in total. Likewise, various siderophore-related and putatively new compounds were detected in agreement with the literature, confirming that the fountain of actinomycetes producing new siderophores is infinite [153].

3.6 Further Exploration of the Culture Conditions for the Production of the Phocoenamicins

The marine-derived CA-214671 strain grown in FR23 medium, from which phocoenamicins B and C were originally isolated, was selected to explore the production conditions of the compounds. Seven small-volume fermentations of 150 mL, each from a different aliquot from the strain, so that reproducibility could be considered, were prepared to monitor the growth level of the microorganism, the pH of the fermentation and the production of the three phocoenamicins during 17 days of incubation. Seven days inocula of the strain CA-214671 were prepared in ATCC-2 inoculum medium and were used to seed Erlenmeyer flasks with FR23 medium.

The fermentation was followed up to 17 days and an aliquot of 2 mL was obtained every working day from each fermentation flask to measure the growth of the microorganisms as wet weight (**Figure 17**).

Table 6. The wet weight measurements (g) for each of the seven fermentations (days 0-17).

Aliquot/Day	0	2	3	6	7	8	9	10	13	14	15	16	17
CA-214671-a03	0.211	0.1782	0.2023	0.2365	0.2875	0.2825	0.2952	0.2936	0.3094	0.3065	0.3366	0.3436	0.3441
CA-214671-a04	0.1938	0.1978	0.1989	0.2772	0.3203	0.2909	0.2807	0.2987	0.3237	0.3314	0.352	0.3617	0.3791
CA-214671-a05	0.2108	0.1998	0.2311	0.2765	0.3014	0.3198	0.3116	0.3074	0.324	0.3276	0.3351	0.3569	0.3524
CA-214671-a06	0.2321	0.297	0.2411	0.2723	0.2998	0.3241	0.3249	0.3379	0.3034	0.3343	0.3389	0.3358	0.3458
CA-214671-a07	0.2269	0.2073	0.2054	0.2635	0.2856	0.3093	0.2937	0.2995	0.3205	0.3271	0.3324	0.3522	0.3163
CA-214671-a08	0.1959	0.1911	0.2102	0.2842	0.3158	0.2912	0.3146	0.3012	0.3279	0.2909	0.3278	0.3301	0.3359
CA-214671-a09	0.2401	0.1871	0.2058	0.2746	0.3141	0.3034	0.2999	0.2934	0.2795	0.2917	0.3075	0.3076	0.3512

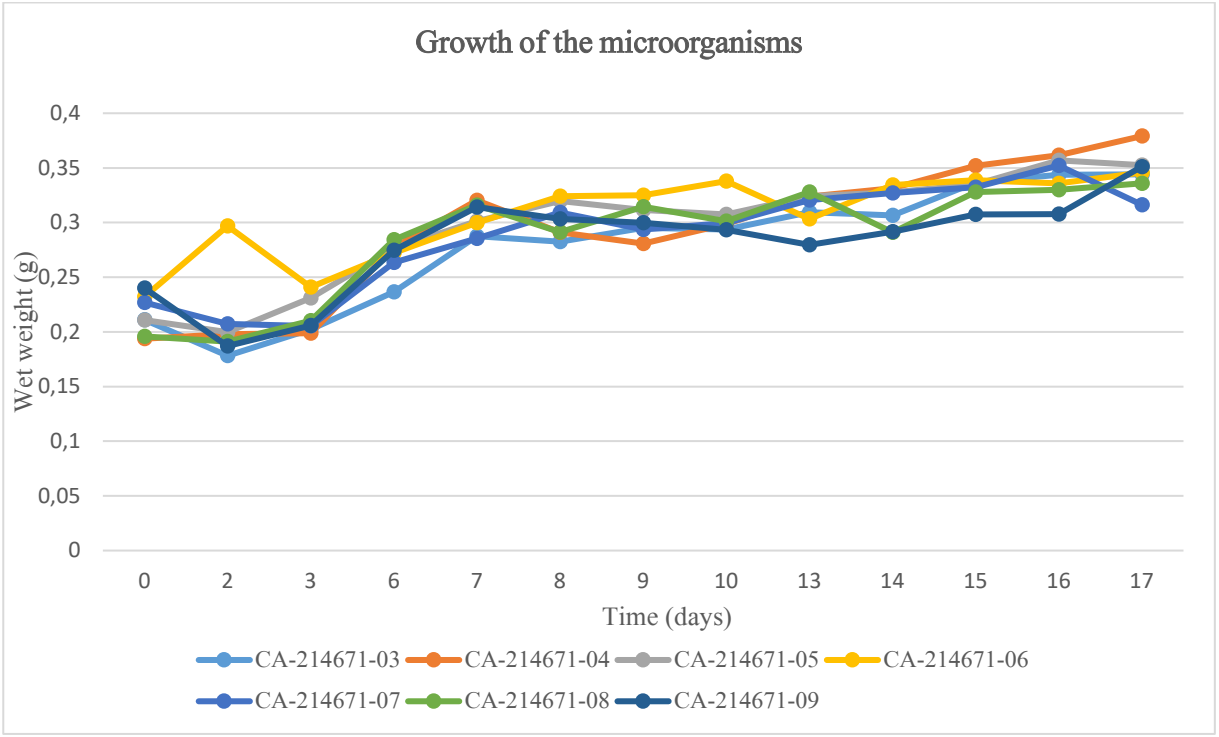

Figure 17. The growth curve for the seven fermentations (days 0-17).

The seven different aliquots presented a similar growing pattern during the 17 days, with maximum growth observed after 17 days. As shown in **Figure 18**, the growth followed an exponential pattern until day 7, reaching a more stationary phase with much lower growth increase after this time.

Additionally, the pH of each fermentation sample obtained at each time was also determined using a portable pH meter (**Table 7**) and a curve was generated (**Figure 18**).

Table 7. The pH measurements for each of the seven fermentations (days 2-17).

Aliquot/Day	2	3	6	7	8	9	10	13	14	15	16	17
CA-214671-a03	5.68	6.05	7.02	7.14	6.73	6.48	6.79	6.26	5.65	5.6	5.87	5.69
CA-214671-a04	5.86	6.1	7.26	7.21	7.09	6.91	6.82	5.78	5.62	5.53	5.51	5.57
CA-214671-a05	5.9	6.65	7	6.9	6.68	6.27	6.42	5.7	5.48	5.46	5.57	5.72
CA-214671-a06	6.43	6.81	5.9	5.74	5.67	5.8	5.78	5.4	5.36	5.36	5.46	5.43
CA-214671-a07	6.2	6.19	7.22	6.91	7.1	6.9	6.64	5.92	5.69	5.57	5.47	5.57
CA-214671-a08	5.91	6.57	6.88	6.64	6.52	5.97	6.01	5.59	5.68	5.68	5.42	5.66
CA-214671-a09	5.83	6.8	6.6	6	5.81	5.68	5.96	5.57	5.59	5.69	5.63	5.62

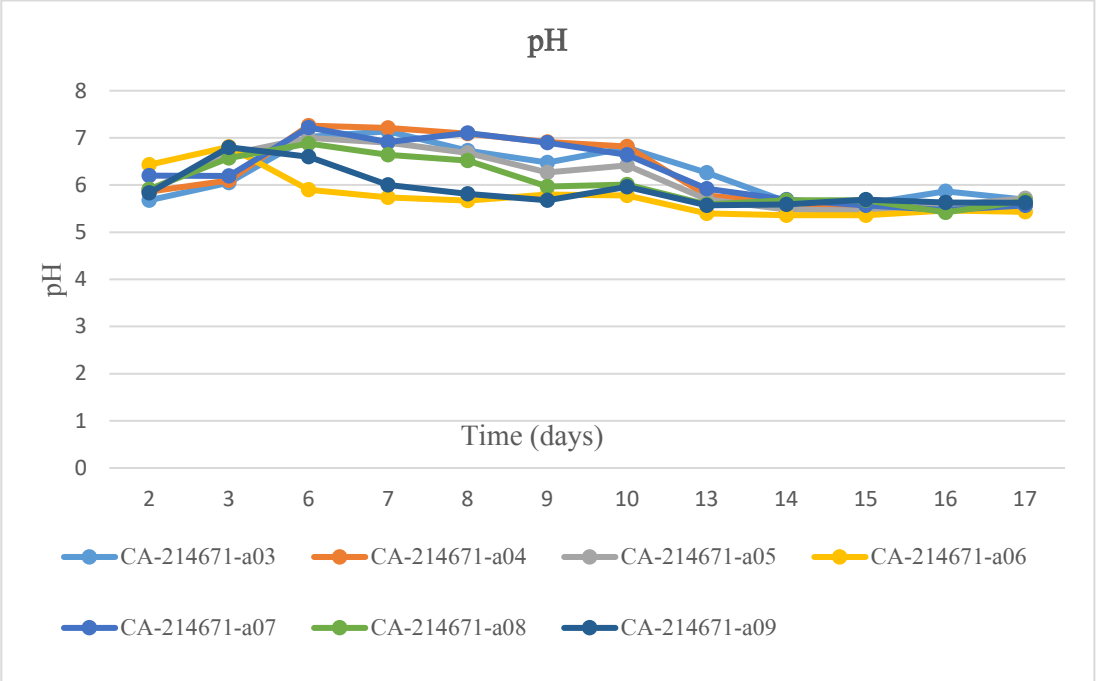

Figure 18. The pH curve for the seven fermentations (days 2-17).

The pH values reported presented a range of 5.36-7.26. The first three days of the fermentations, pH values around 6 were observed, followed by an increase to around 7 during the days 6-10 and again a decrease to pH around 5.5 during the last days of the fermentations (days 13-17), corresponding to the compounds produced in each phase by the actinomycetes.

Finally, a second aliquot of 2 mL was obtained every day and stored in -20ºC in falcon tubes in order to be analyzed by HPLC-MS at the end of the 17 days, look for the three phocoenamicins and estimate their production during the fermentation process. These aliquots were extracted with acetone (1:1) and the 84 extracts generated were analyzed by HPLC-MS.

The production curves were generated using negative ionization mode and based on the RT and the peak area of the ions $[M-H]^-$ detected for each compound (**Figure 19**). The LC-UV-MS data revealed that the three compounds were putatively detected in all the different inocula. Even though quantification based on peak intensities is relative and cannot be compared between the different aliquots, tendencies in the production of the three compounds were observed. In agreement with the previous observations, phocoenamicin was the most abundant compound, followed by phocoenamicin B and significantly less production of phocoenamicin C was observed.

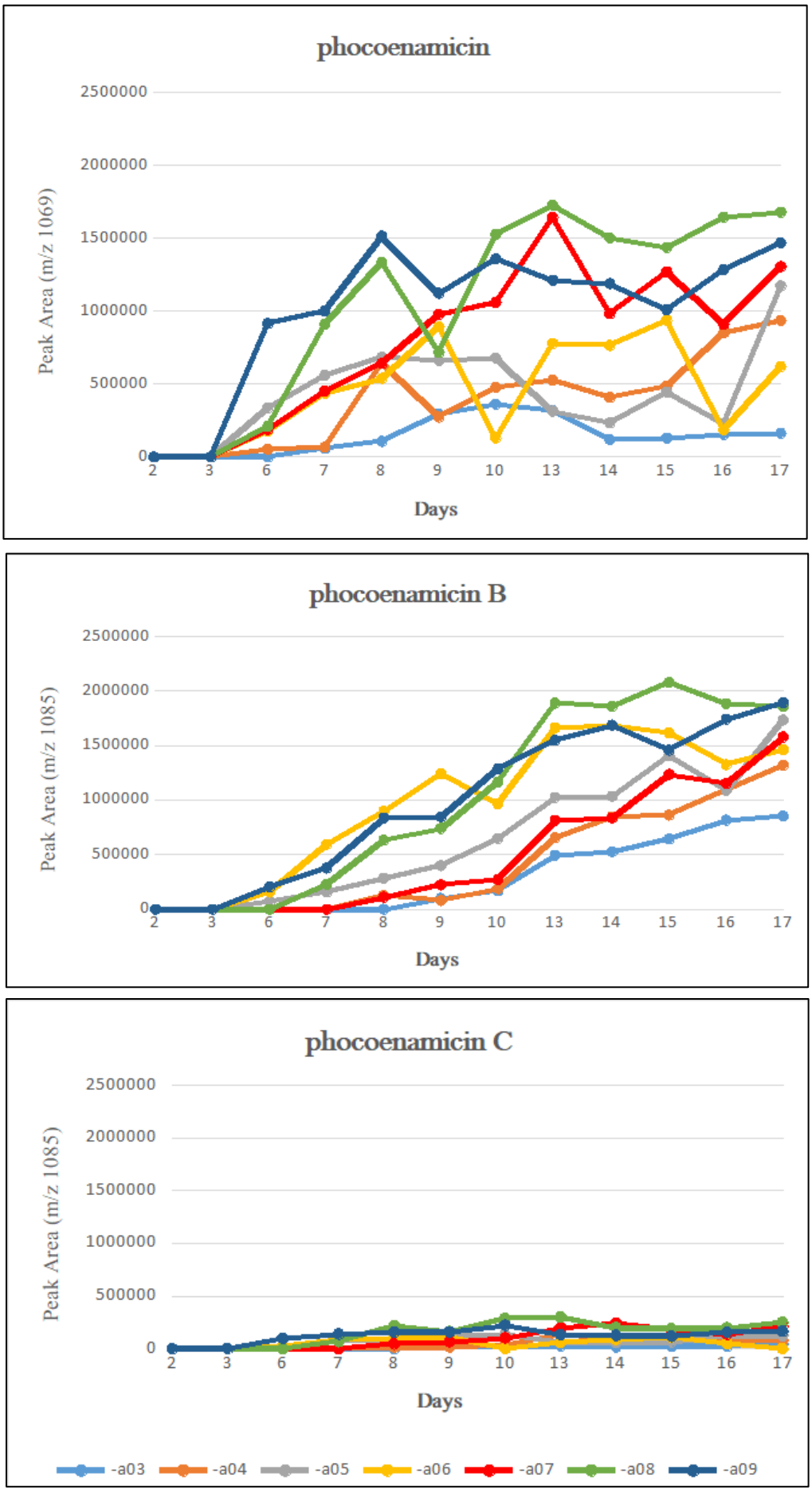

Figure 19. Production of the three known phocoenamicins during the 17 days of fermentation based on the RT and the peak area of the $[M-H]^-$ ions detected for each compound.

The production of the phocoenamicins began on the 6th day for the majority of the 7 fermentations. Moreover, a significant increase was observed between the 10th-13th day of the fermentations and a decrease between the 15th-16th day, suggesting that 14 days of fermentation is the optimal period for the production of the three compounds. In **Figure 20**, the chromatographic profiles obtained during the 17 days of fermentation, can be seen.

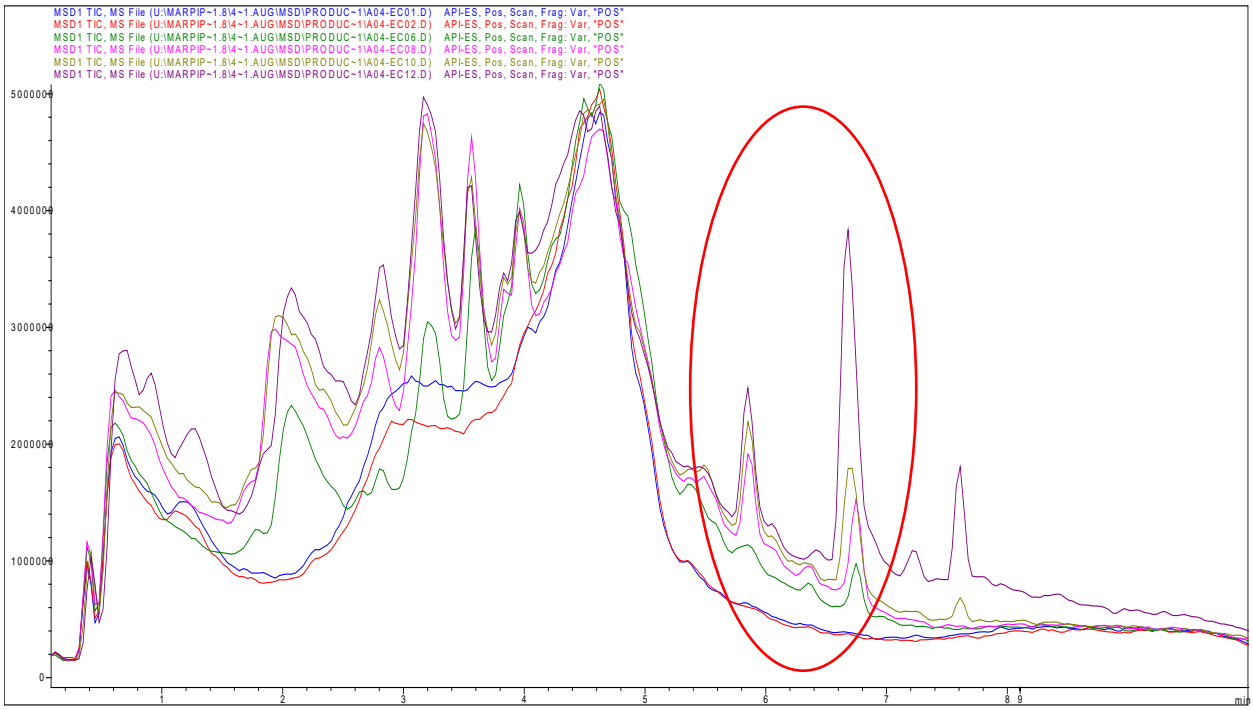

Figure 20. Comparison of the chromatographic profiles obtained by HPLC-MS for the samples of the fermentation from the aliquot -a09 during the 17 days of the fermentation. The peaks included in the red circle were tentatively identified as the three phocoenamicins based on the RT and the $[M-H]^-$ ions.

3.7 Scaled-up of the Production of the Three Marine-derived *Micromonospora* Strains

As mentioned above, the three marine-derived strains (CA-214671, CA-214658 and CA-218877) were identified as the most potent phocoenamicin producers and presented the highest diversity in producing minor phocoenamicin derivatives. Therefore, they were selected to scale-up the production of this family of compounds.

A total of 5 L (one hundred 500 mL flasks containing 50 mL of FR23 culture medium each) were prepared for strain CA-214671 and 3 L (sixty 500 mL flasks containing 50 mL of RAM2-P V2 medium each) were prepared for strains CA-214658 and CA-218877. The flasks were incubated during 14 days before harvesting, resulting in a 5 L fermentation broth for strain CA-214671, and 3 L for strains CA-214658 and CA-218877.

The mycelium of the fermentation broths was sedimented by centrifugation, followed by filtration and extraction with ethyl acetate, while the supernatant was subjected to liquid–liquid extraction with ethyl acetate to obtain the organic extracts. The combined ethyl acetate fractions were evaporated to afford the final crude organic extracts, which were fractionated through reversed phase C18 medium pressure liquid chromatography (MPLC), yielding 66 fractions for strain CA-214671, 39 for CA-214658 and 33 for CA-218877 strain.

LC-UV-MS analysis of these fractions revealed the presence of various spirotetronates and minor amounts of related compounds that suggested their novelty as natural products, confirming previous observations. The fractions obtained for each fermentation broth were combined into groups according to their LC-UV-MS profiles to be further purified by preparative and semi-preparative Reversed Phase HPLC and isolate the compounds of interest.

3.8 Determination of the Optimal Chromatographic Conditions for the Isolation of the Phocoenamicins

The extracts obtained from the 5 L fermentation of the CA-214671 strain grown in FR23 medium were further processed and used to determine the optimal chromatographic conditions for the isolation of phocoenamicin B by preparative and semi-preparative reversed-phase HPLC. As the three phocoenamicins present similar physicochemical properties, these conditions had to be fine-tuned for the isolation of the rest of the members of the family of compounds.

The solvents used were H_2O and CH_3CN of HPLC grade. The time of the analysis was set to 45 min, collecting the fractions between 2 min – 42 min each 0.5 min, resulting in 80 fraction zones collected. The gradient elution for the best separation of the initial groups of fraction extracts containing the phocoenamicins was 40-100% CH_3CN and the fractions of interest were further processed using an isocratic elution of 50% CH_3CN in water to achieve the optimal separation and isolation of the compounds. The sample CA-214671-a04-MR010-ET01-FR34-FH37-FH26, originated from fractionation of the 5 L fermentation, was used to compare the different chromatographic parameters, where the main peak was putatively identified as phocoenamicin B.

Next, the most suitable reversed-phase HPLC column for the separation of the phocoenamicins was explored. Initially, a C18 stationary phase semi-reparative and preparative column was used as it is considered a universal column for most HPLC separations. It resulted in a quite efficient separation but weak resolution, as shown in **Figures 21** and **22**.

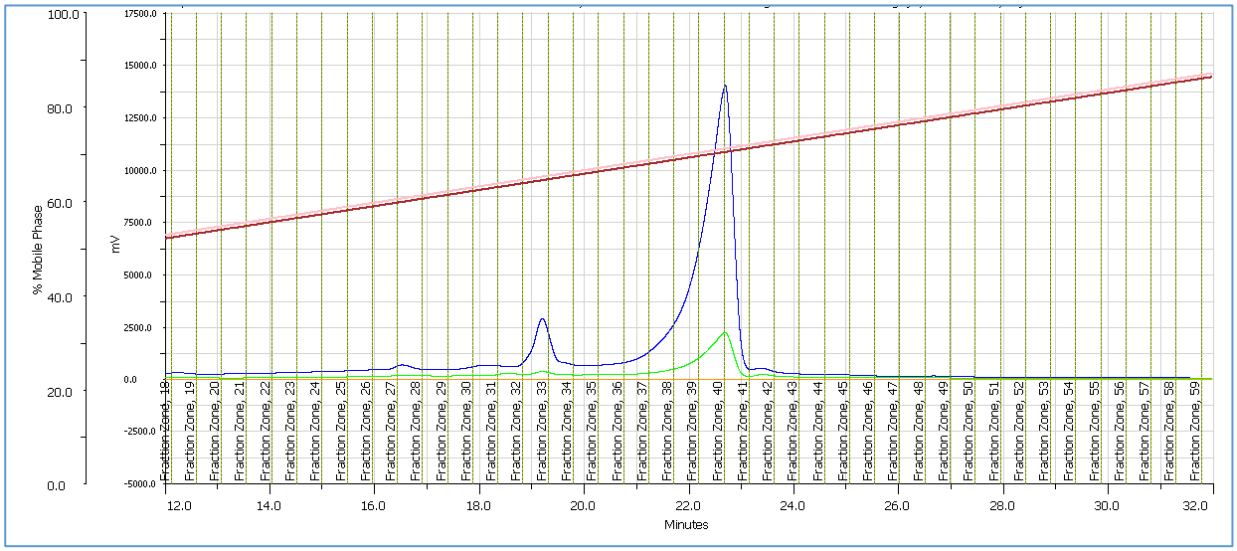

Figure 21. Chromatogram of the sample CA-214671-a04-MR010-ET01-FR34-40 with a solvent gradient of 40-100% CH_3CN and using a semi-preparative column XBridge Prep C18 5µm (10×150 mm).

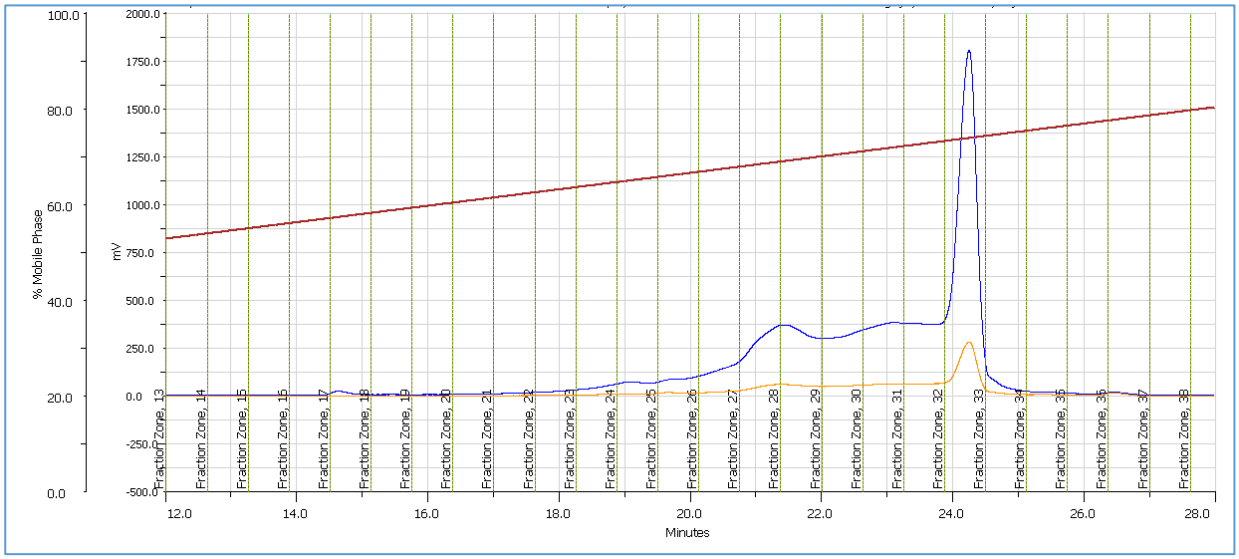

Figure 22. Chromatogram obtained with a solvent gradient of 40-100% CH_3CN and using the preparative column XBridge Prep C18 5µm (19×250 mm).

Since the introduction of the silica based reversed-phase HPLC columns, the stationary phases within these columns have mostly been some form of silica support modified with various aliphatic functional groups. Other functional groups, such as phenyl or amino have also been used, even though to a lesser extent, for their potential to improve peak shape with some classes of compounds. HPLC columns modified with phenyl ($-C_6H_5$) stationary phases offer additional molecular interactions between the column and the analyte, such as π–π interactions to influence the separation selectivity and obtain better chromatographic characteristics [154]-[155]. They are

used mainly for compounds with the presence of aromatic rings [156]-[157], as are the phocoenamicins.

Therefore, the semi-preparative column Phenyl (**Figure 23**) and the preparative column Pentafluorophenyl (PFP) (**Figure 24**) were used to compare the resolution in the chromatograms. The phenyl-based stationary phases resulted in sharper peaks with better resolution and were used to further process the rest of the sample.

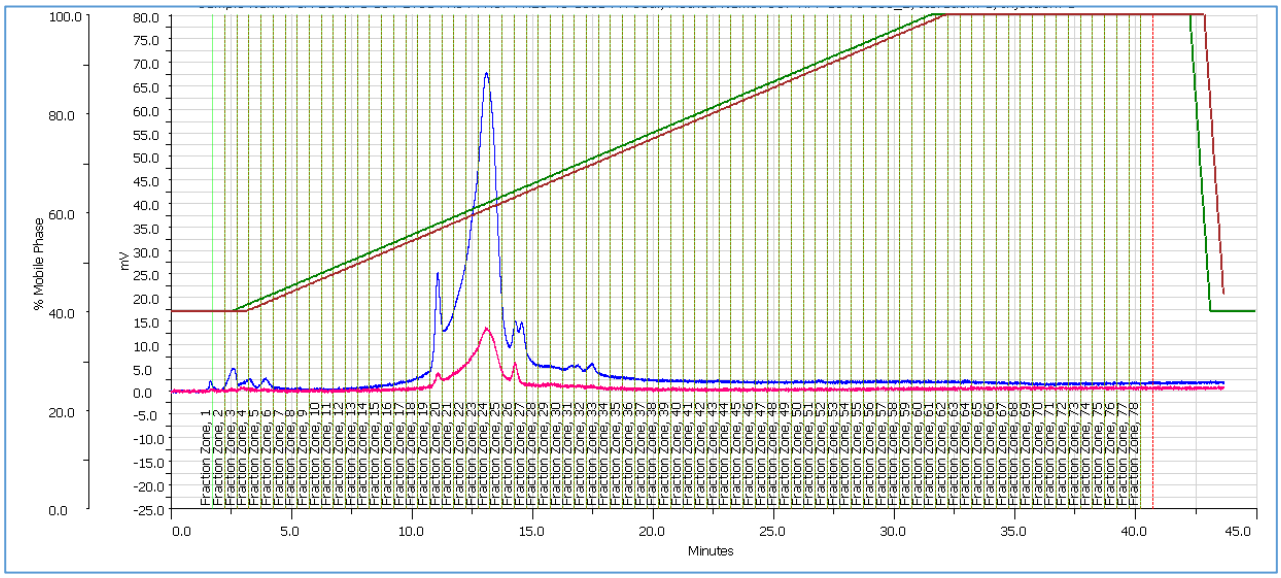

Figure 23. Chromatogram obtained with a solvent gradient of 40-100% CH_3CN and using the preparative column XBridge Prep Phenyl 5µm (10×150 mm).

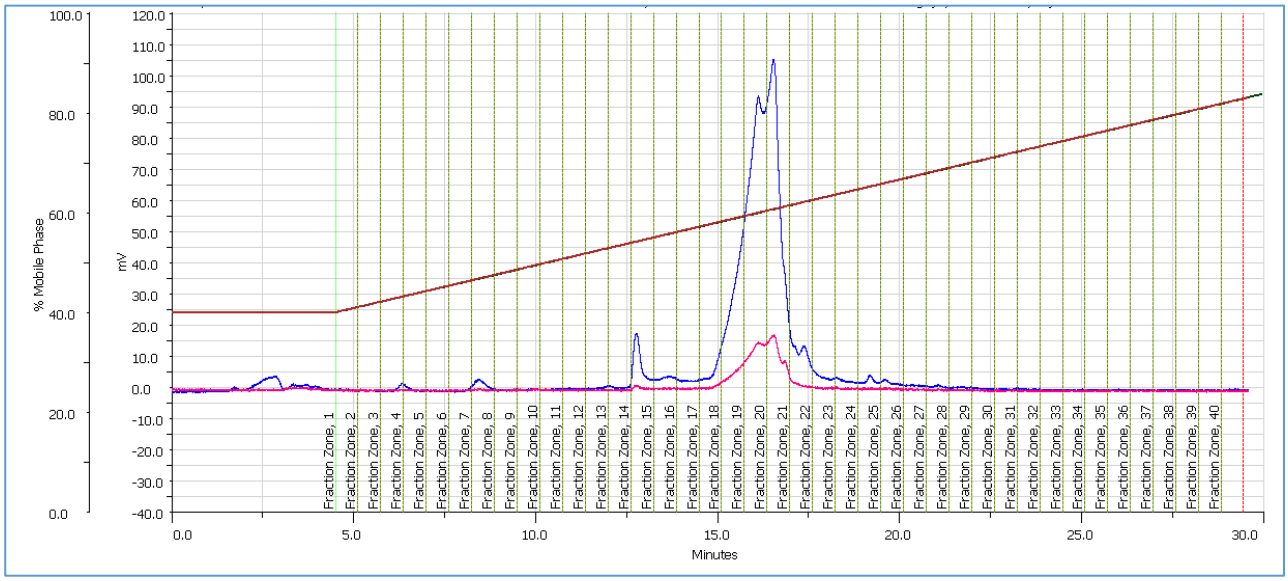

Figure 24. Chromatogram obtained with a solvent gradient of 40-100% CH_3CN and using the reversed-phase preparative column Kinetex® 5µm PFP (250 × 21.20 mm) (Pentafluorophenyl with TMS endcapping).

Trifluoroacetic acid (TFA) is commonly used as a mobile phase additive in HPLC separation and acts as a buffer to improve peak shape and resolution. The silica used in columns may have metal ion impurities, which can cause peak tailing and loss of resolution. TFA added to the mobile phase can "shield" the metal ion and help to maintain good peak shape. It is usually used in a concentration of 0.1% (v/v) in both A and B solvents. Due to its high volatility, TFA can easily be removed from the collected fractions by evaporation [158].

Analytical HPLC was used to check the improvement in the resolution of the peaks with the use of 0.1% TFA in the solvents in a 5-100% CH_3CN gradient and 30 min of analysis. The use of 0.1% TFA in the solvents resulted in a much better chromatographic profile (**Figure 25**) for the previously analyzed sample.

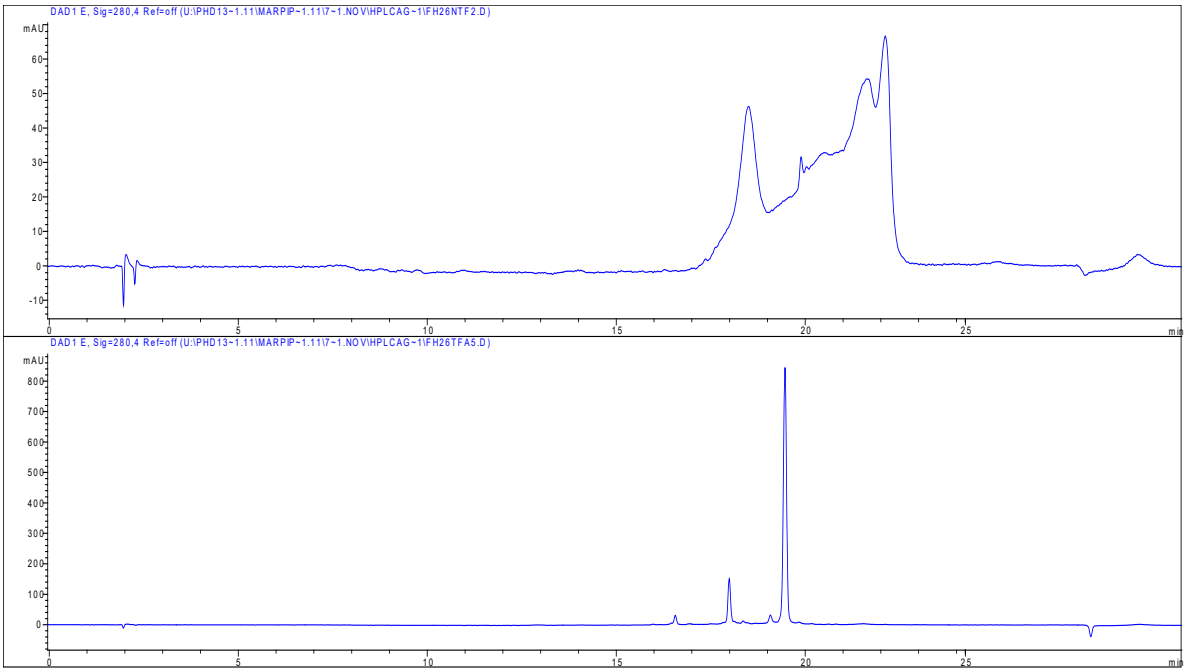

Figure 25. Comparison of the chromatographic profiles obtained by HPLC Agilent Series 1100 using solvents without (1st) and with (2nd) 0.1% TFA in the solvents, using the reversed-phase semi-preparative column Xbridge C18 5µm (4.6x150mm), gradient 5-100% CH_3CN.

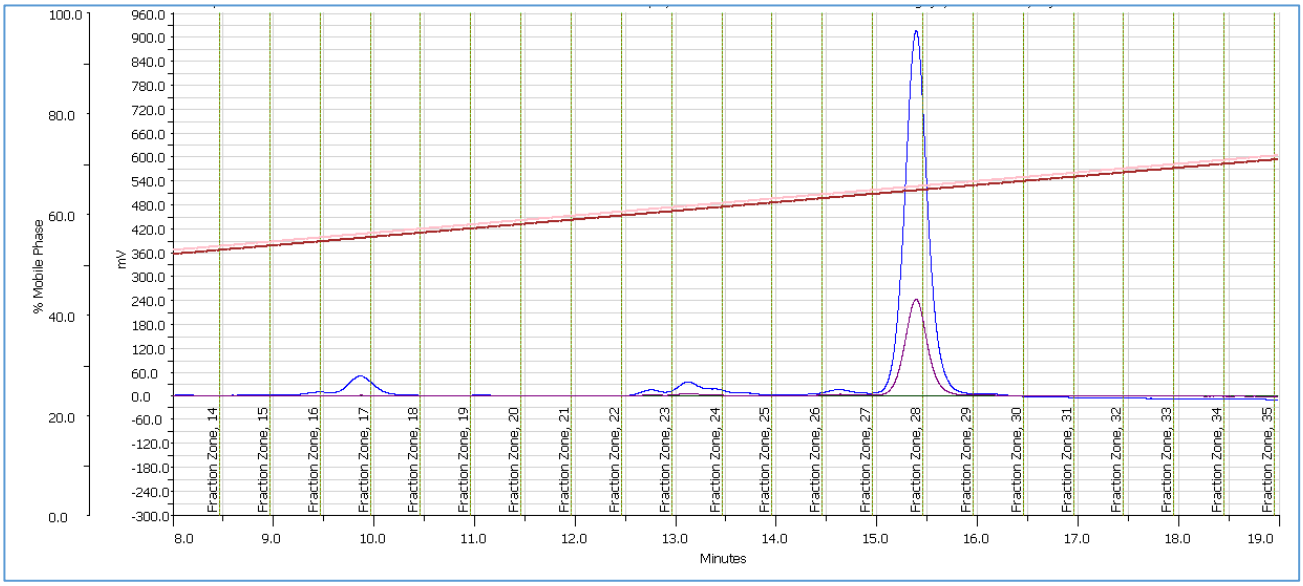

Figure 26. Chromatogram obtained for the sample CA-214671-a04-MR010-ET01- FR34-FH37-FH26 40-100% CH_3CN, 0.1% TFA, preparative reversed-phase HPLC column (Kinetex® 5 µm PFP 100Å AXIA Packed LC Column, 250 × 21.20 mm; 14 mL/min, UV detection at 210 and 280 nm).

Finally, the fraction zones of the main peak were evaporated in N_2 and dissolved in MeOH to check by LC-MS (**Figure 27**) the possible degradation of the molecule due to the use of TFA.

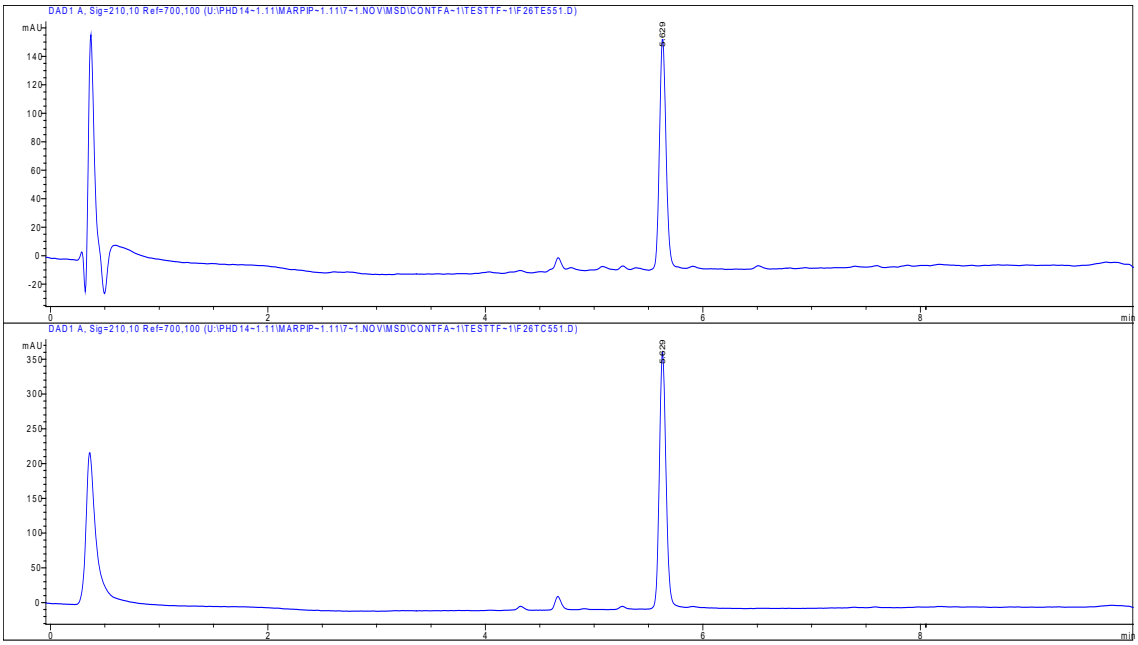

Figure 27. Chromatographic profiles obtained by LC-MS of the collected fraction zones, before and after evaporating the solvents 0.1% TFA, using a solvent gradient of 10-100% and a reversed-phase Zorbax SB-C8 column (2.1 × 30 mm, 5 µm).

No degradation was observed after the evaporation of the solvents, so 0.1% TFA was added in the HPLC solvents for the purification of the rest of the sample that putatively contains phocoenamicin B.

Using the above-mentioned parameters and an isocratic elution of 50-50% H_2O/CH_3CN 0.1 % TFA, 2.5 mg of the compound were isolated in total, corresponding to the main peak observed (fraction zones 28-30), as shown in **Figure 28**.

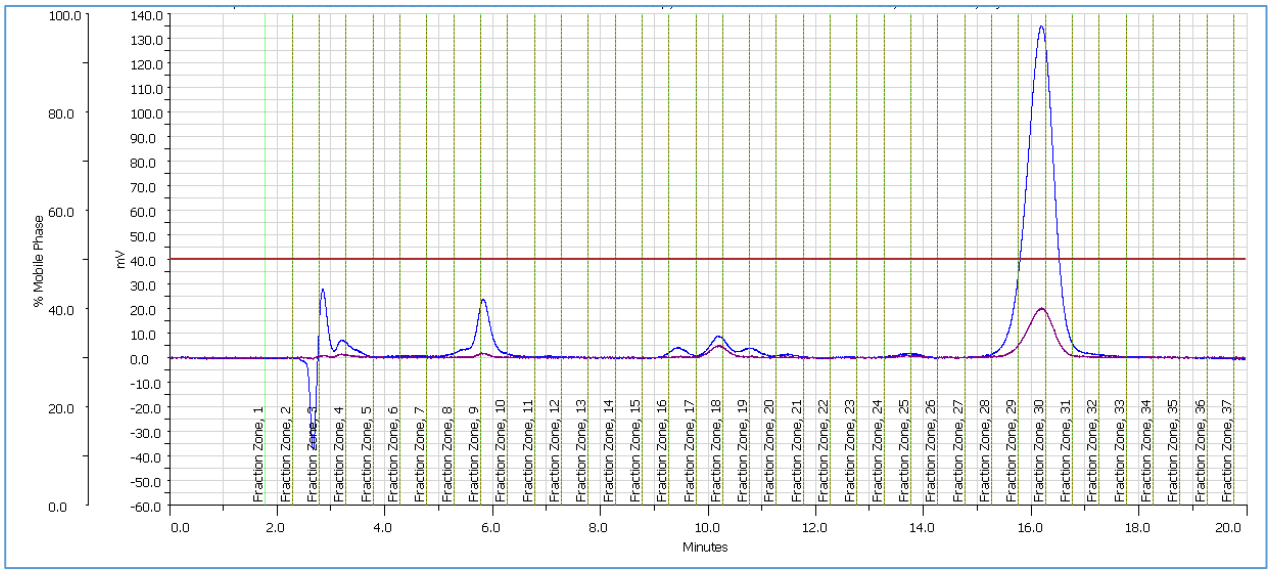

Figure 28. Chromatogram of the sample CA-214671-a04-ET1-FR34-FH37-FH26 50-50% H_2O/CH_3CN, 0.1% TFA, semi-preparative Reversed Phase HPLC column (XBridge prep Phenyl 5 µm, 10 ×150 mm; 3.6 mL/min, UV detection at 210 and 280 nm)

The purity of the compound in fraction zones 28-30 was evaluated by HPLC-MS, as shown in **Figure 29**.

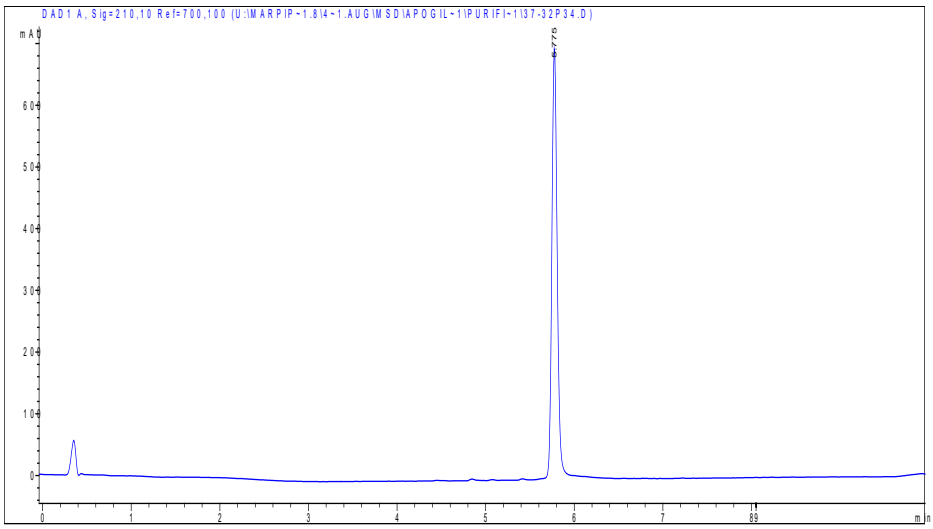

Figure 29. The chromatographic profile obtained by HPLC-MS (UV detection at 210 nm) of the sample obtained, fraction zones 28-30, using a solvent gradient of 10-100% and a reversed-phase Zorbax SB-C8 column (2.1 × 30 mm, 5 µm).

2.5 mg of the isolated sample were analyzed by NMR and the identification of phocoenamicin B was confirmed by the interpretation of the following NMR spectra: ^{1}H, ^{13}C, HSQC, HMBC, COSY, NOESY, TOCSY, ROESY.

3.9 Isolation of Seven Spirotetronates

As mentioned before, the mycelium of the three large-volume fermentation broths was separated from the supernatant by centrifugation, followed by filtration. Both phases were extracted with ethyl acetate, the mycelium using a magnetic stirrer (190 rpm, 2 h) and the supernatant by liquid–liquid extraction in a separatory funnel, to obtain the final organic extracts. Reversed Phase C-18 silica gel was mixed with each organic extract and loaded onto a C-18 column (ODS) that was eluted (MPLC) with a linear H_2O-CH_3CN gradient. LC-UV-MS analysis of the fractions revealed the presence of various spirotetronates and minor amounts of related compounds and allowed to group the fractions obtained according to their profiles.

HPLC of selected fractions of these MPLC chromatographies led to the isolation of seven compounds (**1**-**7**), including two new phocoenamicins (**1**-**2**), together with the known phocoenamicin, phocoenamicins B and C (**3**-**5**) and one maklamicin analogue (**6**), together with maklamicin (**7**), also belonging to the spirotetronate class of compounds **Figure 30**).

The fermentation broth from strain CA-214671 afforded 66 fractions that were combined into seven groups (Fractions A-G) according to their LC-UV-MS profiles:

Fraction A (127.8 mg) was chromatographed by preparative reversed-phase HPLC (Kinetex® 5 µm PFP 100Å AXIA Packed LC Column, 250 × 21.20 mm; 14 mL/min, UV detection at 210 and 280 nm) with a linear 1:1 H_2O-CH_3CN + 0.1% TFA isocratic elution in 40 min yielding **1** (1.1 mg. t_R 12 min) and **4** (6.1 mg, t_R 18 min).

Fraction C (39.4 mg) was chromatographed by semi-preparative Reversed Phase HPLC (XBridge prep Phenyl 5 µm, 10 ×150 mm; 3.6 mL/min, UV detection at 210 and 280 nm) with an isocratic elution of 50% CH_3CN/ 50% H_2O with 0.1% TFA over 40 min yielding **2** (1.0 mg, t_R 19 min).

The fermentation broth from strain CA-214658 afforded 39 fractions that were combined into five groups (Fractions A-E) according to their LC-UV-MS profiles:

Fraction A (285.9 mg) was chromatographed by semi-preparative Reversed Phase HPLC (XBridge prep Phenyl 5 µm, 10 × 150 mm; 3.6 mL/min, UV detection at 210 and 280 nm) with a linear H_2O-CH_3CN + 0.1% TFA gradient of 40-70% in 40 min yielding **6** (1.3 mg, t_R 32 min) and **7** (3.6 mg, t_R 22 min).

The fermentation broth from strain CA-218877 afforded 33 fractions that were combined into five groups (Fractions A-E) according to their LC-UV-MS profiles:

Fraction D (135.4 mg) was chromatographed by semi-preparative reversed-phase HPLC (XBridge prep Phenyl 5 μm, 10 × 150 mm; 3.6 mL/min, UV detection at 210 and 280 nm) with a linear H_2O-CH_3CN + 0.1% TFA gradient of 50-70% in 40 min yielding **3** (5.2 mg, t_R 26 min) and **5** (0.6 mg, t_R 18 min).

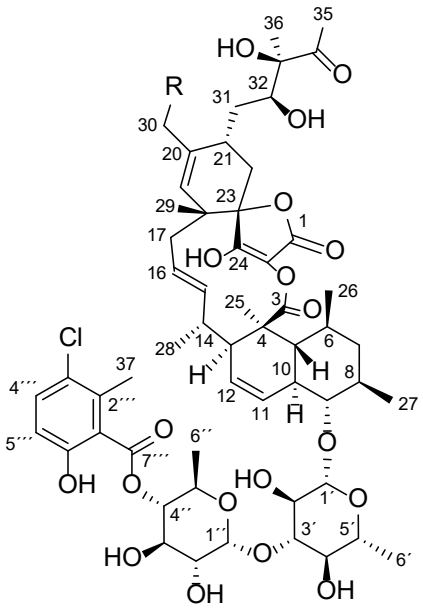

1 R=OH
5 R=H

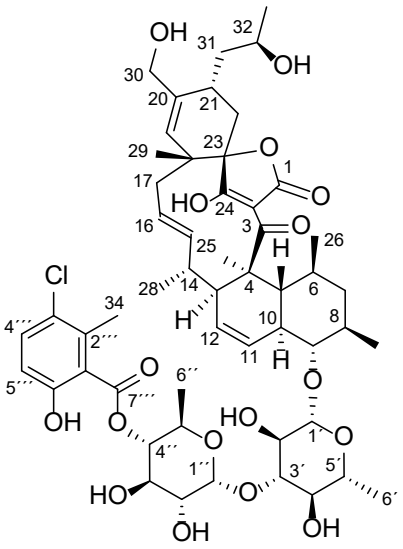

2

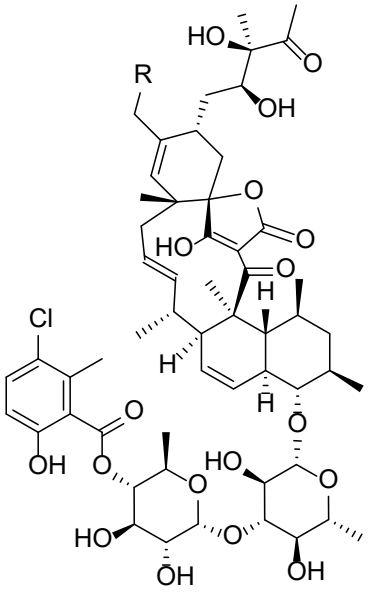

3 R=H
4 R=OH

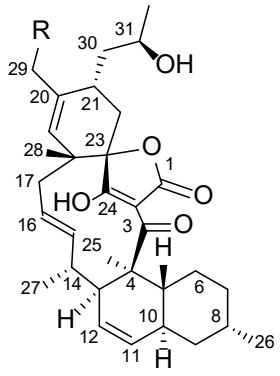

6 R=H
7 R=OH

Figure 30. Compounds **1**-**7** isolated from culture broths of *Micromonospora* sp. strains CA-214671, CA-214658 and CA-218877.

The compounds were characterized by measuring the specific Optical Rotation and analyzed by FT-IR, 1D and 2D NMR and LC-HRMS. The characterization data of the new natural spirotetronates isolated **1**, **2** and **6** are summarized below:

(**1**): white amorphous solid; $[\alpha]_D^{25}$ +1.1 (*c* 0.12, MeOH); UV (DAD) λ_{max} 230, sh 290, 320 nm; IR (ATR) ν_{max} 3376, 2934, 1676, 1445, 1381, 1296, 1203, 1139, 1070, 1025 cm^{-1}; for ^{1}H and ^{13}C NMR data see **Table 8**; (+)-ESI-TOFMS *m/z* 1120. 4884 $[M+NH_4]^+$ (calcd for $C_{56}H_{79}ClNO_{20}^+$, 1120.4878).

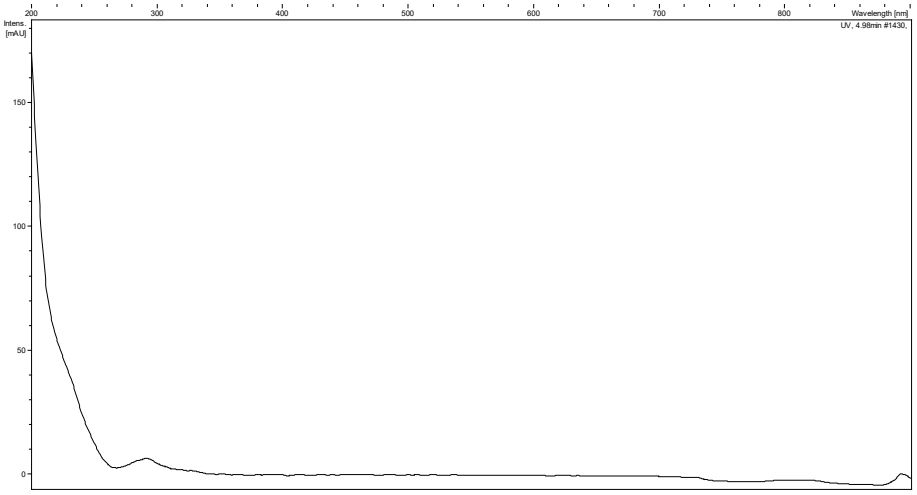

Figure 31. UV spectrum of compound **1**.

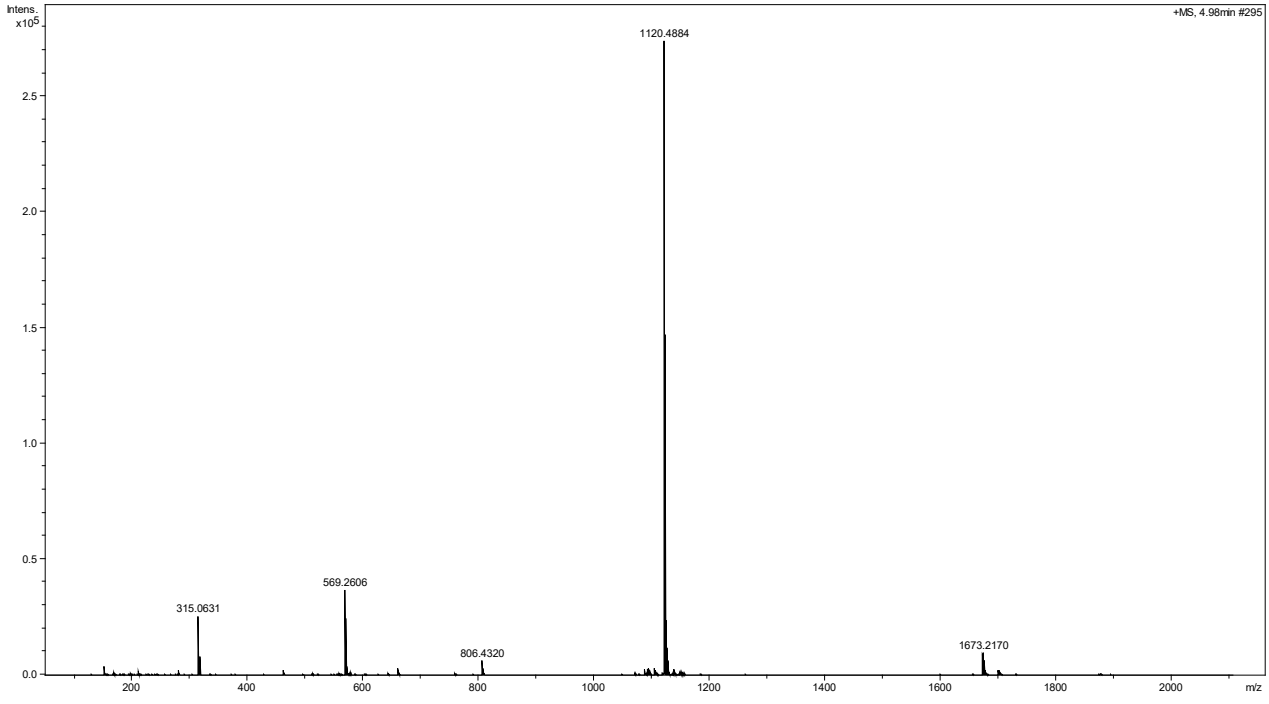

Figure 32. ESI-TOF spectrum of compound **1**.

(**2**): white amorphous solid; $[\alpha]_D^{25}$ +6.4 (*c* 0.12, MeOH); UV (DAD) λ_{max} 230, sh 290, 320 nm; IR (ATR) ν_{max} 3388, 2927, 1743, 1677, 1445, 1379, 1293, 1204, 1070, 1024 cm^{-1}; for ^{1}H and ^{13}C NMR data see **Table 8**; (+)-ESI-TOFMS *m/z* 1015.4462 $[M+H]^+$ (calcd for $C_{53}H_{72}ClO_{17}^+$, 1015.4453)

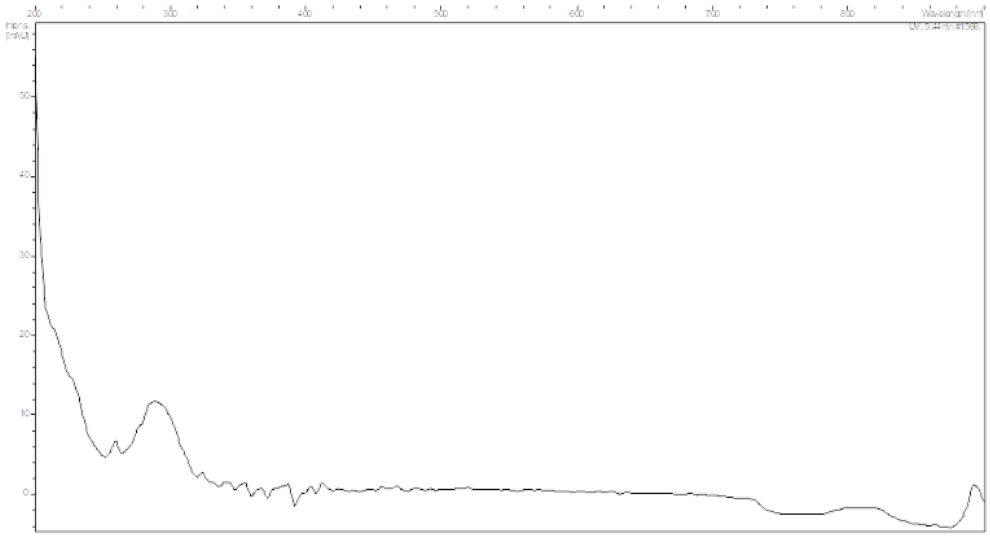

Figure 33. UV spectrum of compound **2**.

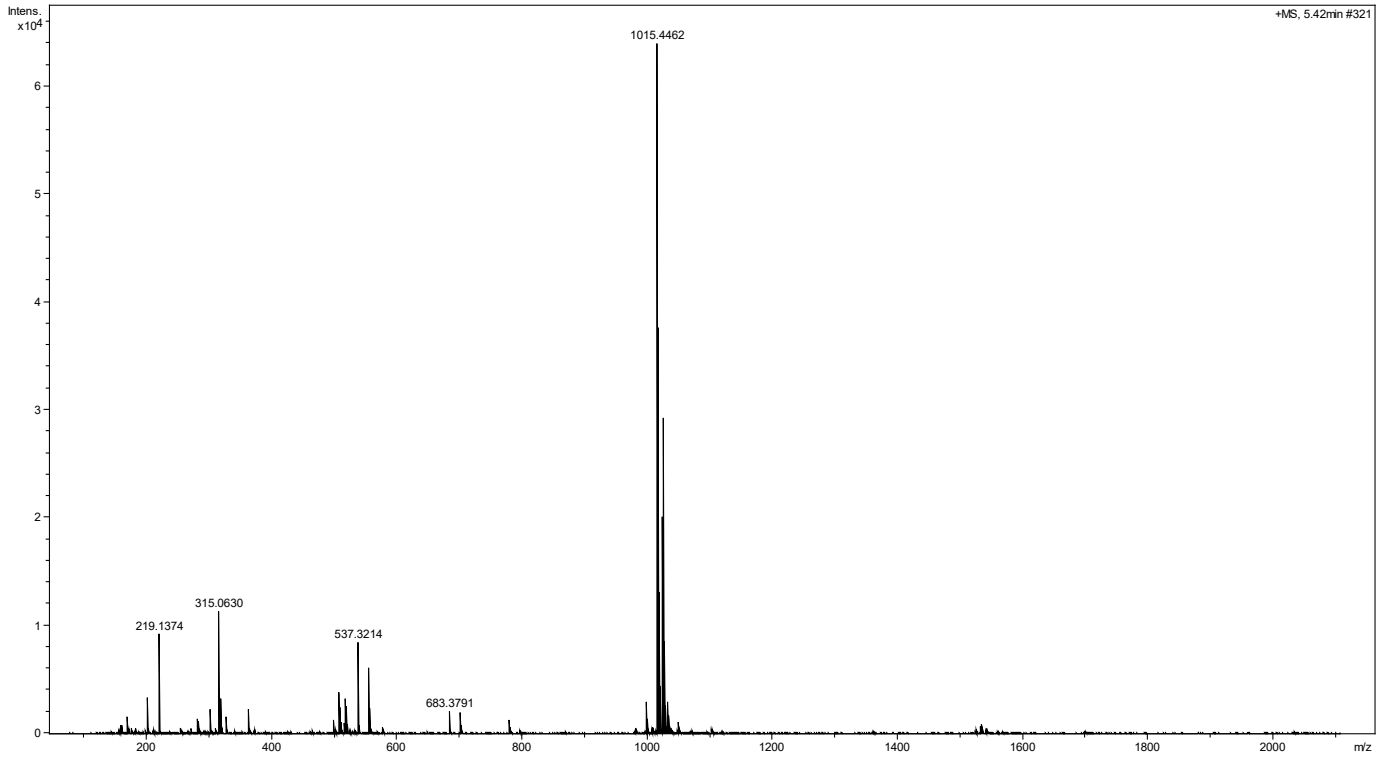

Figure 34. ESI-TOF spectrum of compound **2**.

(**6**): white amorphous solid; $[\alpha]_D^{25}$ –8.5 (*c* 0.12, MeOH); UV (DAD) λ_{max} 230, sh 310 nm IR (ATR) ν_{max} 3384, 2924, 1679, 1617, 1410, 1207, 1137 cm^{-1}; for ^1H and ^{13}C NMR data see **Table 9**; (+)-ESI-TOFMS *m/z* 509.3275 $[M+H]^+$ (calcd for $C_{32}H_{45}O_5^+$, 509.3262), 1017.6455 $[2M+H]^+$ (calcd for $C_{64}H_{89}O_{10}^+$, 1017.6450).

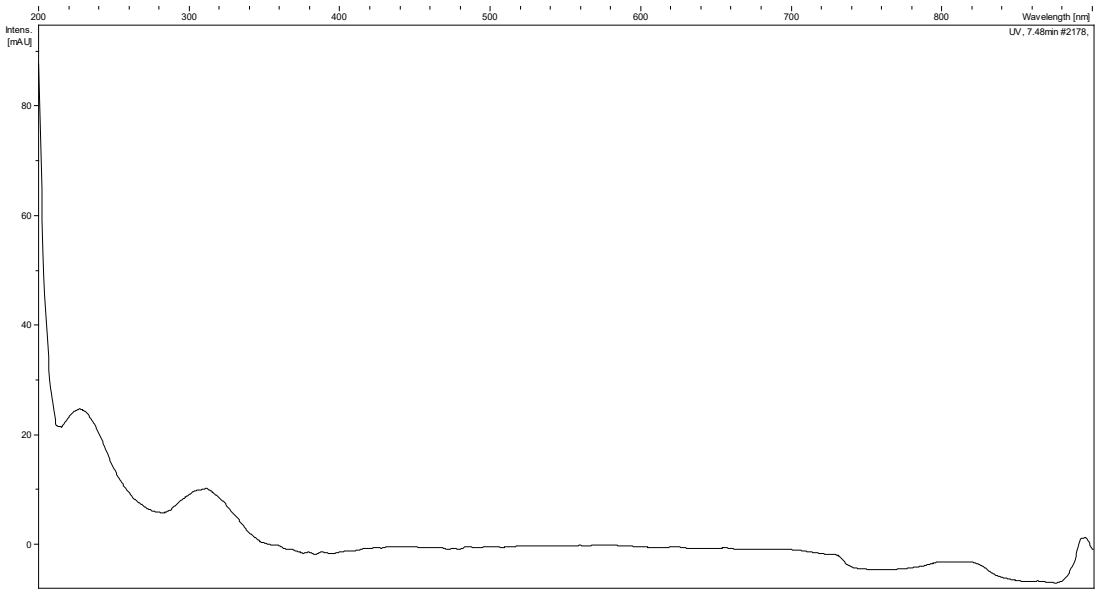

Figure 35. UV spectrum of compound **6**.

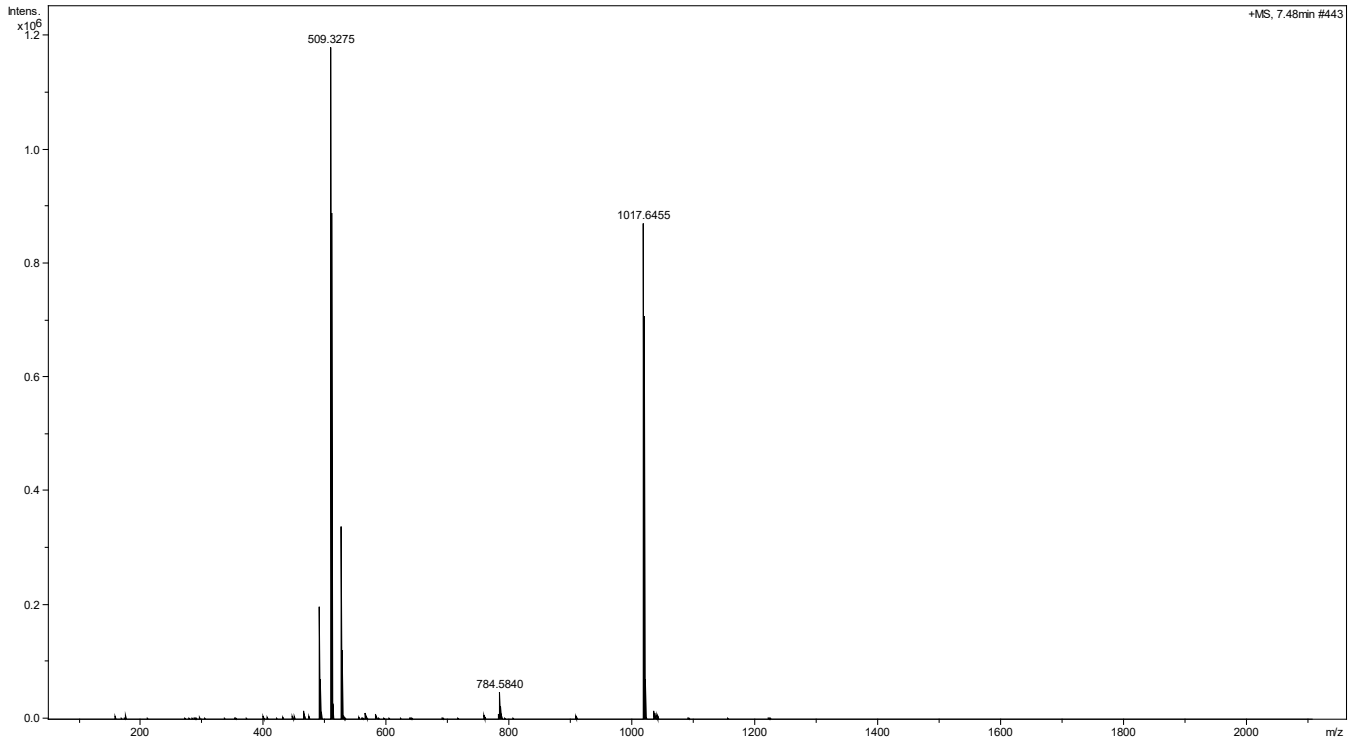

Figure 36. ESI-TOF spectrum of compound **6**.

3.10 Structure Elucidation

Compound **1** was isolated as a white amorphous solid. A molecular formula of $C_{56}H_{75}ClO_{20}$ was deduced from the (+)-ESI-TOF analysis that displayed an adduct ion at *m/z* 1120.4884 $[M + NH_4]^+$, accounting for 19 degrees of unsaturation. IR absorptions at 3376, 1776, 1676 and 1445 cm^{-1} were indicative of the presence of hydroxy, carbonyl, and olefinic groups. The molecular formula together with the characteristic UV absorption pattern with maxima at 230, 290 and 320 nm strongly suggested a phocoenamicin-related structure for the compound.

Its ^{13}C NMR spectrum revealed the presence of three carbonyl esters at δ_C 169.2, δ_C 175.6, 165.6 and one ketone at 215.4, together with five methylene sp^3 carbons, ten methyl groups and numerous methine and quaternary sp^2 and sp^3 carbons (**Table 8**). The ^1H NMR data, in combination with the HSQC spectrum, revealed that **1** contains a substituted benzoic acid moiety and two deoxysugar units, characteristic for this family of compounds (**Table 8**).

Table 8. NMR spectroscopic data (500 MHz, CD_3OD) for phocoenamicins **D** and **E**.

	Phocoenamicin D (1)		**Phocoenamicin E (2)**	
Position	**δ_C, type**	**δ_H, Mult. (J in Hz)**	**δ_C, type**	**δ_H, Mult. (J in Hz)**
1	165.6, C	-	186.3, C	-
2	*nd	-	99.7, C	-
3	175.6, C	-	201.5, C	-
4	47.7, C	-	50.5, C	-
5	43.9, CH	1.60, m	43.6, CH	1.81, m
6	38.4, CH	1.53, m	39.2, CH	1.57, m
7α	45.8, CH_2	1.78, m	45.2, CH_2	1.79, t (9.6)
7β		1.10, m		1.19, t (9.6)
8	40.7, CH	1.64, m	40.7, CH	1.65[a], s
9	87.9, CH	3.03, t (9.9)	87.8, CH	3.08, t (10.1)
10	48.1, CH	1.94, m	47.9, CH	2.02, m
11	126.8, CH	6.33, t (9.3)	126.9, CH	6.37, d (9.2)
12	127.1, CH	5.65, ddd (9.8, 5.9, 2.4)	125.8, CH	5.60, m
13	51.0, CH	1.99, m	43.9, CH	2.61, m
14	40.7, CH	2.17, m	40.2, CH	2.01, m
15	137.8, CH	4.90, ***w	145.9, CH	5.44, t (11.5)
16	128.5, CH	5.29, dd (14.6, 11.4)	122.2, CH	5.15, dd (14.0, 11.9)
17α	42.2, CH_2	2.28, m	43.5, CH_2	2.31, m
17β		1.88, m		1.99, m
18	44.9, C	-	41.0, C	-
19	132.7, CH	5.34, s	131.0, CH	5.34, s
20	139.1, C	-	138.7, C	-
21	30.1, CH	2.68, m	30.7, CH	2.68, m
22α	29.6, CH_2	1.87, m	30.6, CH_2	1.85, d (15.4)
22β		2.44, m		2.36[b], s

23	86.5, C	-	88.4, C	-
24	177.5, C	-	206.7, C	-
25	17.4, CH_3	1.33, **brs	17.2, CH_3	1.65[a], s
26	22.6, CH_3	0.91, **brs	23.2, CH_3	0.82, d (6.34)
27	19.9, CH_3	1.04, d (6.2)	19.9, CH_3	1.05, d (6.2)
28	22.5, CH_3	0.91, **brs	21.5, CH_3	0.87, d (6.8)
29	23.5, CH_3	1.33, **brs	24.1, CH_3	1.31, s
30α	65.1, CH_2	4.14, d (13.3)	65.0, CH_2	4.14, d (13.5)
30β		4.03, d (13.3)		4.03, d (13.5)
31α	33.8, CH_2	1.76, m	42.4, CH_2	1.63, **brs
31β		186, m		1.77, t (9.6)
32	74.0, CH	3.84, dd (11.6, 1.9)	66.0, CH	3.81, m
33	83.4, C	-	24.6, CH_3	1.18, d (6.1)
34	215.4, C	-	17.8, CH_3	2.36[b], s
35	25.8, CH_3	2.24, s	-	-
36	22.0, CH_3	1.19, s	-	-
1'	104.0, CH	4.35, d (5.4)	103.9, CH	4.36, d (6.8)
2'	75.3, CH	3.46, m	75.2[d], CH	3.46[c], m
3'	88.6, CH	3.48, m	88.5, CH	3.46[c], m
4'	75.6, CH	3.11, t (8.8)	75.5, CH	3.12, t (8.6)
5'	72.9, CH	3.25, m	72.7, CH	3.24, m
6'	18.3, CH_3	1.28, d (6.2)	18.3, CH_3	1.28, d (5.8)
1"	105.4, CH	4.61, d (7.7)	105.2, CH	4.61, d (7.8)
2"	76.0, CH	3.43, t (8.3)	75.9, CH	3.43, t (7.8)
3"	75.3, CH	3.65, t (9.4)	75.2[d], CH	3.64, t (9.2)
4"	77.8, CH	4.88, ***w	77.8, CH	4.90, ***w
5"	71.7, CH	3.69, m	71.6, CH	3.69, m
6"	18.0, CH_3	1.35, d (6.1)	18.0, CH_3	1.36, d (5.3)
1'''	124.4, C	-	124.3, C	-
2'''	135.6, C	-	135.4, C	-
3'''	126.0, C	-	125.9, C	-
4'''	132.4, CH	7.25, d (8.8)	132.3, CH	7.26, d (8.3)
5'''	115.9, CH	6.71, d (8.8)	115.9, CH	6.71, d (7.9)
6'''	155.3, C	-	155.1, C	-
7'''	169.2, C	-	169.3, C	-
37	17.9, CH_3	2.36, s	-	-

*nd = not detected; **brs = broad signal; ***w = obscured by the water peak; [a,b,c,d] overlapping signals

Compound **1** exhibited almost identical ^{13}C and ^{1}H NMR spectroscopic data than those described for phocoenamicin C (**5**) [77], the major difference between the ^{13}C NMR spectra of the two compounds being the presence of an oxygenated methylene carbon at δ_C 65.1 (C-30) in **1** (**Table 8**), instead of the methyl group at δ_C 22.4 observed in phocoenamicin C (**5**). This difference was confirmed in the HSQC and ^{1}H NMR spectra with the presence of two oxygenated methylene hydrogens at δ_H 4.03 and 4.14 in **1** that correlated to the carbon at δ_C 65.1 (**Table 8**) instead of the

methyl group at δ_H 1.73 ppm in phocoenamicin C (**5**). 2D HMBC correlations between H-19 and C-30, and between both H_2-30 and C-19, C-20 and C-21 confirmed that a hydroxymethyl group is located at C-20 (**Figure 37**). The same hydroxymethyl functionality at C-20 is observed in phocoenamicin B (**4**) [77], indicating a functional group conserved within the family. The difference was in agreement with the proposed molecular formula for compound **1**, having one oxygen more than **5**.

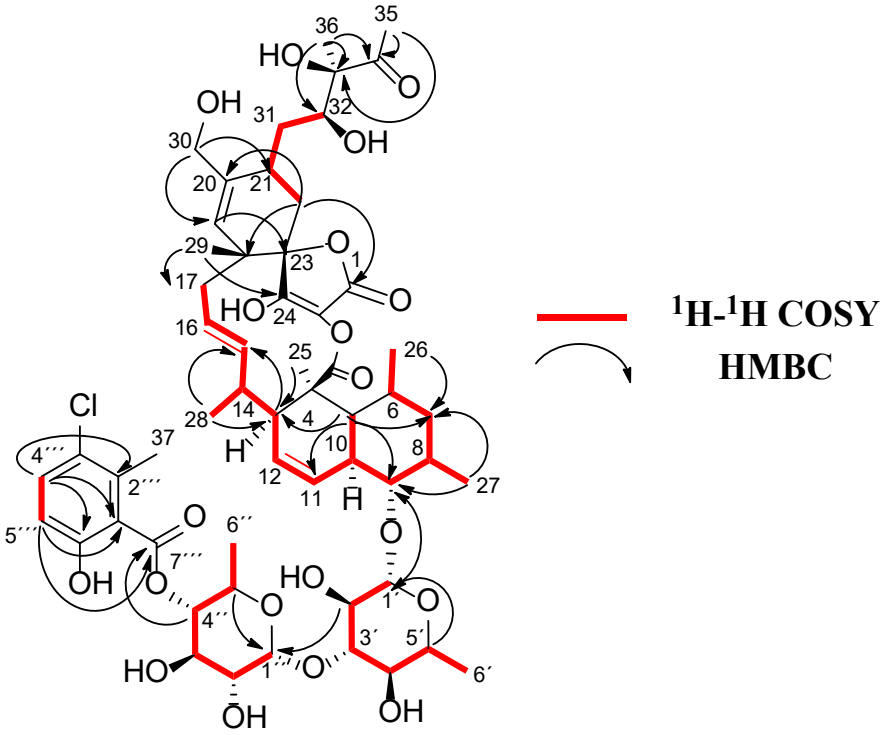

Figure 37. ^{1}H-^{1}H COSY and key HMBC correlations for **1**.

COSY and HMBC correlations (**Figure 37**) confirmed phocoenamicin D to have the same carbon skeleton as **5** and the linkages between the oxygenated C-9 of the *trans*-decalin substructure and C-1' of one of the deoxyglucose units, between C-3' of this deoxyglucose and C-1'' of a second deoxyglucose unit and finally between C-4'' of the latter and the carbonyl group (C-7''') of the 3-chloro-6-hydroxy-2-methylbenzoate moiety. Additionally, NOESY correlations confirmed the compound to have the same configuration in all its chiral centers as that was previously proposed for other members of the phocoenamicin family (**Figure 38**). Particularly, correlations between H-5, H-7β and H-9 and between H-6, H-8 and H-10 suggested a trans ring fusion of the decalin unit and further correlations between H-7α and H-26 and H-27 placed the methyl groups C-26 and C-27 at equatorial orientation. Additional NOEs between H-10 and H-25 placed the C-25 methyl group in the bottom face of the molecule. A series of NOESY correlations (H-13/H-15, H-14/H-16, H-15/H-17α, H-17β/H-19) determined a zigzag conformation of the C-13 to C-18 chain (**Figure 38**). Furthermore, the $^3J_{HH}$ coupling constants between H-11 and H-12 (9.3 Hz) and

between H-15 and H-16 (14.6 Hz) assigned the olefins as Z and E, respectively. NOE correlations from H-15 to H-28 placed the methyl group C-28 on the bottom face and from H-16 to H-29 placed C-29 on the top face of the molecule. The chair conformation of the cyclohexene ring was determined by NOEs between H-29, H-21 and H-22β that placed them on the same side of the ring (**Figure 38**). The configuration of the diol side chain and the tetronic acid could not be assigned due to extensive signal overlapping and was hypothesized to be identical with the rest of phocoenamicins, setting a configuration S*/R* at C-32 and C-33 carbons and an S* configuration for the tetronic acid stereogenic center, respectively [11,12]. Finally, NOESY correlations in the sugar units (**Figure 38**) established the axial orientation of all protons, confirming two units of β-6-deoxyglucopyranoside, whose absolute configuration is proposed as D in alignment with phocoenamicin (**3**) and other members of the family. [11,12]. The name phocoenamicin D was proposed for compound **1**.

Compound **2** was obtained as a white amorphous solid, whose (+)-ESI-TOF analysis identified a protonated adduct $[M + H]^+$ at *m/z* 1015.4462, thus giving a molecular formula of $C_{53}H_{71}ClO_{17}$, which indicated 18 degrees of unsaturation. IR absorptions at 3388, 1743, 1677 and 1445 cm^{-1} suggested again the presence of hydroxy, carbonyl and olefinic functionalities.

This molecular formula had three carbons, four hydrogens and three oxygen atoms less than that of **1**. The NMR data of **2** were very similar to those of **1** (**Table 8**). The major differences were observed in the side chain attached to C-21, where the signals of the quaternary oxygenated carbon C-33, the ketone C-34 and the methyl groups C-35 and C-36 in **1** were replaced by a doublet methyl signal (δ_C 1.18, δ_C 24.6) in **2**. Comparing with the NMR data obtained for **1**, the presence of a 2-hydroxy-1-propyl group attached to C-21 was further supported by the differences in the chemical shifts of carbons C-31 (δ_C 33.8 to 42.4), C-32 (δ_C 74.0 to 66.0) and the presence of a methyl group instead of a quaternary sp^3 carbon at C-33 (δ_C 83.4 to 24.6), as well as the COSY correlations from H-31 to H-32 and from H-32 to H-33, and the HMBC correlations from H-31 to C-22 and C-33. Furthermore, a ketone carbonyl signal was observed at C-3 (δ_C 201.5) in **2**, instead of the ester carbonyl carbon at δ_C 175.6 present in **1,** confirmed through an intense HMBC correlation to methyl C-25 (see Supplementary Material, **Figure S12**).

The rest of the NMR data were similar to those of **1,** confirming the presence of a spirotetronate with an eleven-membered macrocycle core, a *trans*-decalin unit and a disaccharide connected to a substituted benzoic acid moiety (**Figure 30**). Indeed, apart from a different side chain at C-21, the structure of the molecule is identical to that of phocoenamicin B (**4**), having a ketone group at C-3 and a hydroxymethyl group at C-20. The hydroxyethyl side chain at C-21 was previously reported as a structural element of maklamicin, a closely related spirotetronate [90].

Similarly to compound **1**, the relative configuration of the chiral centers of **2** was determined by a combination of NOESY correlations (see Supplementary Material **Figure S13**) and $^{3}J_{HH}$ coupling constants and was found to be identical to that of **1**. Regarding the hydroxyethyl side chain at C-31, and similarly to what is reported for maklamicin, NOESY correlations between H-22α/H-32 and H-31α/H-30 and a large $^{3}J_{HH}$ coupling constant between H-31α and H-32 (9.6 Hz) and between H-31β/H-21 (as indicated by an intense COSY crosspeak), set an anti-relationship between H-31α and H-32, as well as between H-31β and the 32-OH group and assigned an *R** configuration at C-32, the same configuration described for phocoenamicins and maklamicin [11,14]. Similar chemical shift values around this side chain in the NMR spectra of compounds **2**, **6** and **7** confirmed this stereochemical assignment. The name phocoenamicin E was proposed for the compound.

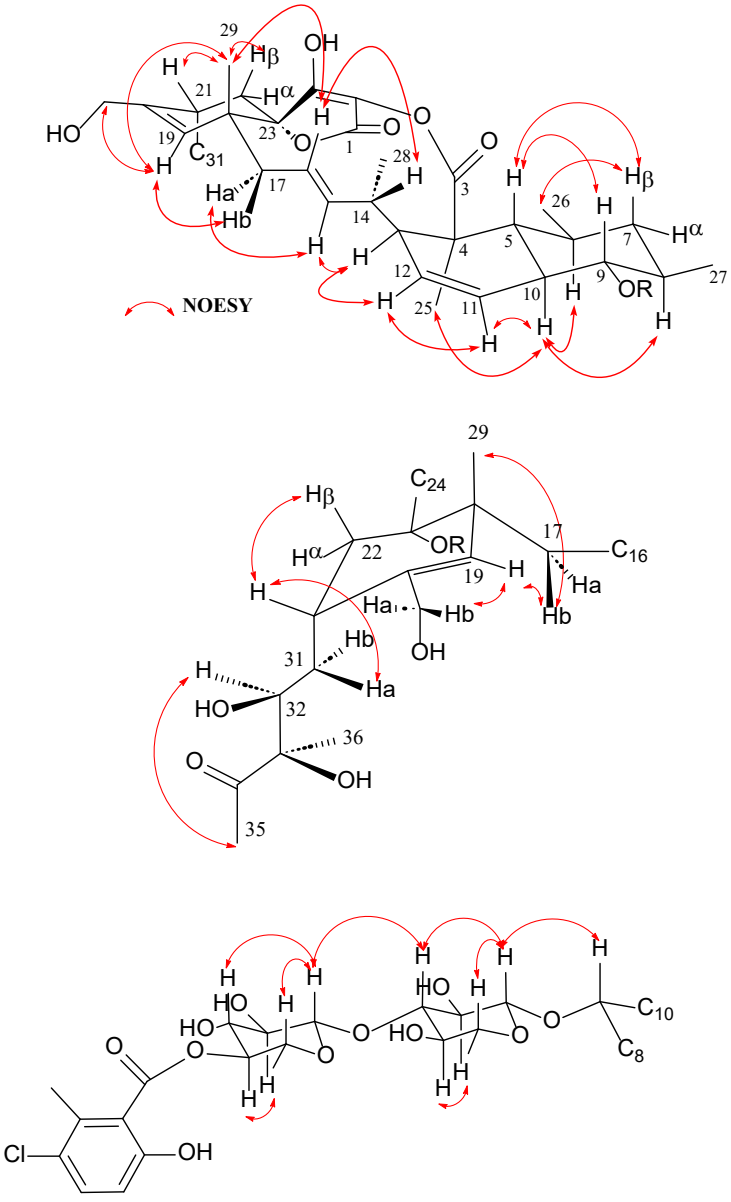

Figure 38. Key NOESY correlations observed in the structure of phocoenamicin D (**1**).

Compounds **6** and **7** were isolated as white amorphous solids. The (+)-ESI-TOF spectrum of **6** showed a protonated adduct at *m/z* 509.3275 $[M + H]^+$, accounting for a molecular formula of $C_{32}H_{44}O_5$, while the (+)-ESI-TOF spectrum of **7** showed ions at *m/z* 525.321 $[M + H]^+$ and 542.3486 $[M + NH_4]+$ assigning a molecular formula of $C_{32}H_{44}O_6$, thus revealing a difference of one oxygen atom between them.

Their UV, IR and NMR spectroscopic data were almost identical and shared common features. The UV absorption pattern (λ_{max} 230 and 310 nm), the IR spectrum of both (broad absorption bands for multiple hydroxy, carbonyl and olefinic groups), along with their molecular formulae suggested that these compounds were related to the spirotetronate maklamicin, with compound **7** sharing the same molecular formula and spectroscopic data, confirming its identity as maklamicin, and **6** lacking one oxygen atom.

Analysis of the ^1H NMR and ^{13}C NMR spectra of **6** (**Table 9**) identified the presence of 32 carbons, corresponding to three oxygen-bearing quaternary sp^2 carbons (δ_C 205.0, 202.4 and 177.5), three quaternary sp^3 carbons, seven sp^2 carbons, six sp^3 methylenes, seven sp^3 methines and six methyl groups.

Table 9. NMR spectroscopic data (500 MHz, CD_3OD) for maklamicin B (**6**) and maklamicin (**7**).

	maklamicin B (6)		**maklamicin (7)**	
Position	**δ_C, type**	**δ_H, mult. (*J* in Hz)**	**δ_C, type**	**δ_H, mult. (*J* in Hz)**
1	*nd	-	169.5, C	-
2	100.2, C	-	100.2, C	-
3	202.4, C	-	202.5, C	-
4	52.1, C	-	52.1, C	-
5	43.9, CH	1.50, dd (8.3, 12.5)	43.9, CH	1.51, dd (8.3, 10.3)
6α	24.4, CH_2	1.24, **brs	24.4, CH_2	1.29, **brs
6β		2.08, m		2.08, m
7α	34.1, CH_2	1.57, **brs	34.0, CH_2	1.60, m
7β		1.75, m		1.77, m
8	29.2, CH	2.07, m	29.3, CH	2.07, m
9α	40.9, CH_2	1.62, m	40.8, CH_2	1.64, **brs
9β		1.42, d (4.8)		1.43, d (4.9)
10	34.3, CH	2.04, m	34.3, CH	2.05, m
11	131.3, CH	5.41, d (9.3)	131.9, CH	5.40, d (10.0)
12	126.3, CH	5.48, ddd (9.9, 6.2, 2.4)	126.2, CH	5.49, ddd (10.0, 6.3, 2.3)
13	42.5, CH	2.85, m	42.6, CH	2.84, m
14	41.2, CH	1.88, m	41.3, CH	1.89, m
15	144.9, CH	5.43, m	145.2, CH	5.46, m
16	122.9, CH	5.07, ddd (13.6, 11.8, 2.5)	122.7, CH	5.09, ddd (13.9, 11.6, 2.7)
17α	43.7, CH_2	2.30, dd (14.3, 10.9)	43.4, CH_2	2.33, dd (14.7, 8.0)

17β		1.95, d (14.5)		2.02, d (14.5)
18	40.6, C	-	40.5, C	-
19	130.9, CH	5.03, s	131.1, CH	5.33, s
20	135.0, C	-	138.9, C	-
21	34.5, CH	2.42, br dd (8.8, 7.2)	30.5, CH	2.67, br dd (7.7, 7.4)
22α	30.9, CH_2	1.77, **brs	31.0, CH_2	1.83, d (15.6)
22β		2.33, dd (14.3, 7.2)		2.33, dd (14.7, 8.0)
23	87.9, C	-	88.2, C	-
24	205.0, C	-	204.9, C	-
25	16.3, CH_3	1.56, s	16.4, CH_3	1.58, s
26	19.5, CH_3	1.06, d (7.2)	19.4, CH_3	1.07, d (7.7)
27	21.3, CH_3	0.87, d (7.1)	21.2, CH_3	0.88, d (7.5)
28	24.4, CH_3	1.24, s	24.1, CH_3	1.29, s
29α	22.3, CH_3	1.75, s	65.1, CH_2	4.16, d (13.5)
29β				4.01, d (13.5)
30α	42.6, CH_2	1.63, dd (14.0, 11.1)	42.7, CH_2	1.62, **brs
30β		1.75, m		1.79, **brs
31	65.9, CH	3.78, dq (9.3, 6.6)	66.1, CH	3.79, dq (9.6, 6.7)
32	24.6, CH_3	1.17, d (6.2)	24.6, CH_3	1.17, d (6.3)

*nd = not detected; **brs = broad signal

Interpretation of 1D and 2D NMR spectroscopic data gave the full planar structure of **6** (Figure 1). HSQC and COSY spectra constructed the different fragments of the compound and then HMBC cross-peaks linked the fragments together, confirming a maklamicin-related compound (**Figure 39**).

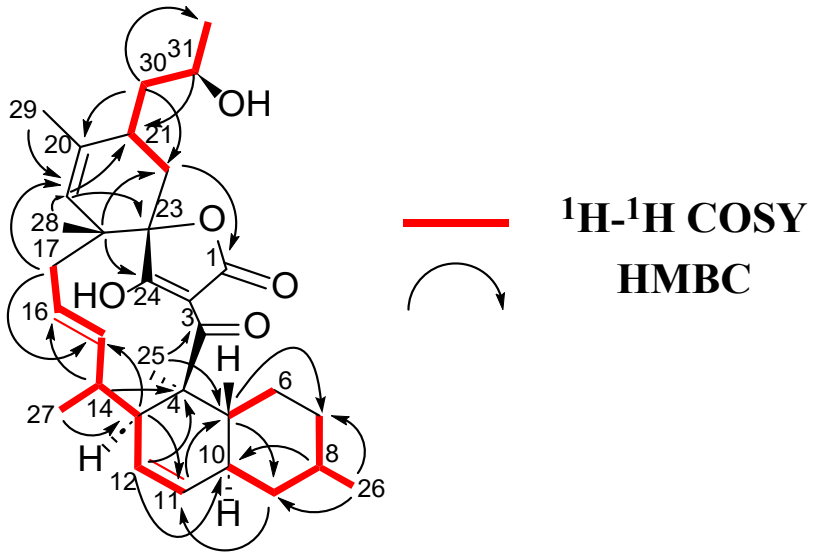

Figure 39. ^{1}H-^{1}H COSY and key HMBC correlations for **6**.

Firstly, a decalin unit was established through COSY (H-5/H-6, H-7/H-8/H-9/H-10, H/11/H-12/H-13) and plenty of HMBC correlations (C-4/H-12/H-13/H-25,C-5/H-9/H-11/H-25, C-7/H-5/H-26 and C-9/H-8/H-10/H-11/H-26), containing two methyl groups at C-4 and C-8 and a double bond at C-11/C-12 (**Figure 39**). The chain was extended through sequential COSY cross-peaks from H-13 to H-17 with a methyl group at C-14 and a double bond at C-15/C-16. Then a cyclohexene ring was determined through HMBC correlations (C-18/H-17/H-22 and C-23/H-17/H-19/H-21), containing two methyl groups at C-18 and C-20, as well as a side chain at C-21 (**Figure 39**). The ^{13}C NMR spectrum showed characteristic of tetronic acid carbons resonances, connected to a ketone group at C-3, which completed the structure. A HMBC correlation from H-17 to C-23 confirmed the presence of a spirocenter in the tetronic acid (C-23). Finally, the structure of the side chain was elucidated as a 2-hydroxypropyl unit attached to C-21, similar to that found in phocoenamicin E and maklamicin. Sequential COSY cross peaks (H-21/H-30/H-31/H-32), as well as HMBC correlations from H-30 to C-22 and C-32 and from H-31 to C-21 confirmed this proposal (**Figure 39**).

The major difference between compounds **6** and **7**, based on their NMR spectra, was the presence of a methyl group at δ_C 22.3 and δ_H 1.75 in **6**, instead of a hydroxymethyl group at δ_C 65.1 and δ_H 4.16, 4.01 observed in **7**. HMBC cross-peaks between the carbon of this methyl group and H-19, H-22 and H-30 and between its methyl protons and C-19, confirmed that the methyl group was located at C-20. Furthermore, the chemical shifts of C-20 and C-21 of **6** were slightly shifted to 135.0 and 34.5 ppm compared to 138.9 and 30.5 ppm in **7**, respectively (**Table 9**).

Finally, the relative configuration of **6** was elucidated by ROESY experiments (see Supporting Information **Figure S20**) and $^3J_{HH}$ coupling constants and determined to be the same as that of maklamicin. The latter was supported by the almost coincident NMR chemical shift values determined for most of the hydrogens and carbons of the molecule, except those around C-29, where the major difference between both compounds was found. Particularly, in the case of the side chain at C-21 and in line with previous findings in maklamicin, ROESY correlations observed between H-22α/H-31 and H-30β/H-29 (**Figure 40**) together with the large $^3J_{HH}$ coupling constants between H-21/H30β) and H-30α/H-31 set an anti-relationship between H-30α and H-31, as well as between H-30β and the 31-OH group and assigned an *R** configuration at C-31, the same configuration found in **2** and maklamicin [90]. Finally, the configuration for the tetronic acid chiral center was tentatively assigned as *S** in agreement with that of the previously reported spirotetronate antibiotics [73].

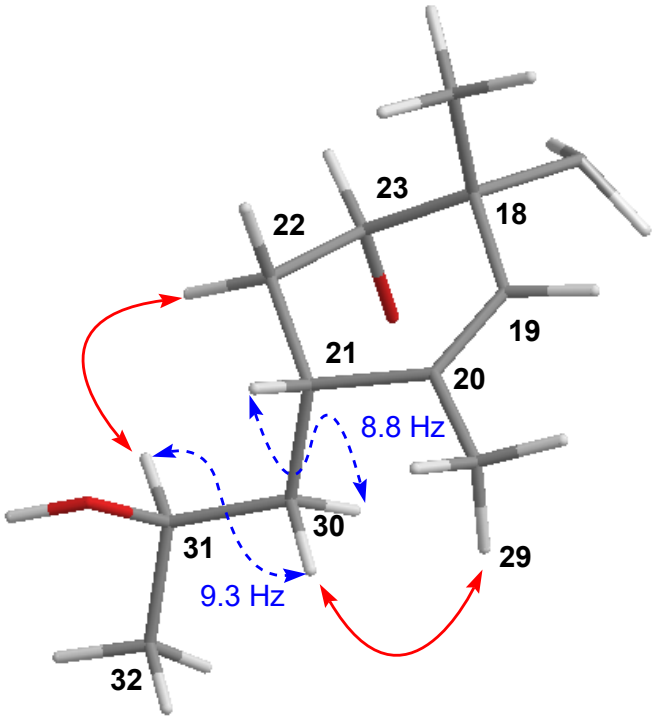

Figure 40. Key coupling constants (blue dashed) and ROESY (red) correlations establishing the configuration at C-31 for **6**.

Compound **6** was previously reported as a result of gene deletion (*makC2*) in a genetically engineered strain and an intermediate in the biosynthetic pathway of maklamicin [90]. Herein, it is reported for the first time as a natural product, therefore proposing the name maklamicin B.

3.11 Bioactivity assays

3.11.1 Antibacterial Activity of the Crude Extracts

The crude extracts were tested for their antimicrobial activity to evaluate the capacity of the strains to produce bioactive metabolites with potential therapeutic interest [159]. The crude extracts of the 270 fermentations, as well as the 10 extracts from the control media, were subjected to screening against MRSA MB5393, *M. bovis* BCG and *M. tuberculosis* H37Ra to evaluate their antimicrobial activity and to study if the antimicrobial activity could be associated to phocoenamicins production, as phocoenamicins had been initially tested against these three pathogens. The 10 extracts from the control media did not show any activity against the microorganisms tested, confirming that the bioactivity observed in the crude extracts can be exclusively attributed to the compounds produced by the *Micromonospora* strains and not to the fermentation media components. **Figure 41** shows how the bioactivity was influenced by the

growth in the different fermentation media. The graph represents the average of the percentages of inhibition (%) obtained from each of the extracts from the 27 strains versus the different media in which they had been grown. The average % inhibition of each of the 270 extracts against the three pathogens can be found in Supplementary Information (**Table S1**).

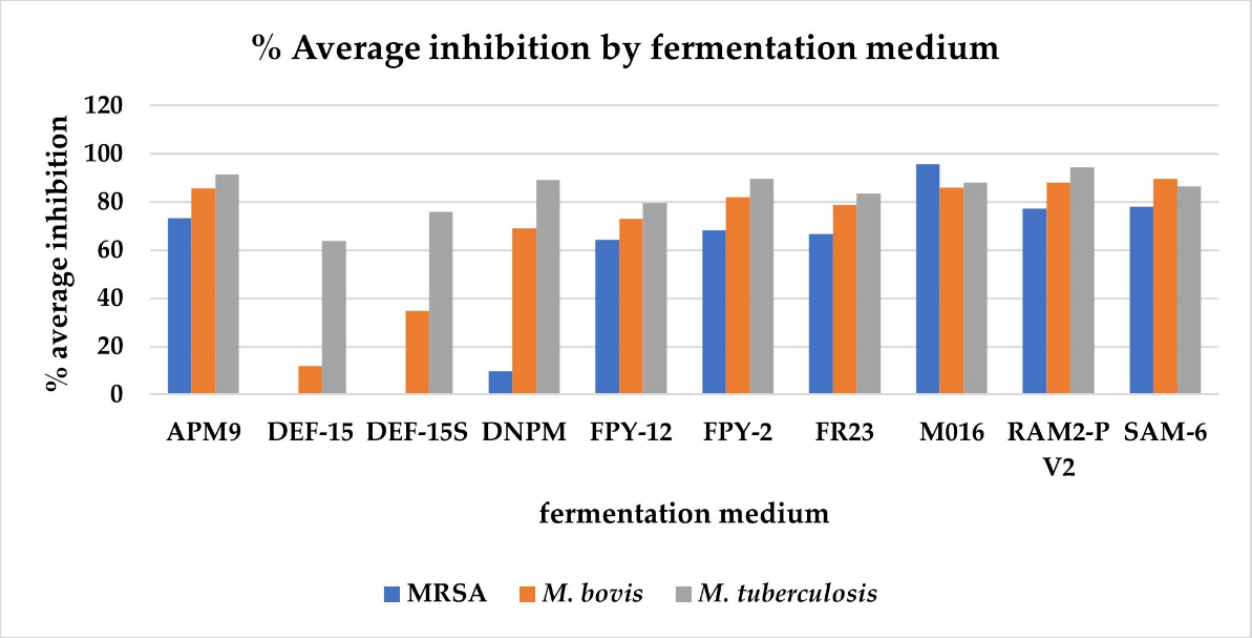

Figure 41. The average of the percentages of inhibition (%) obtained against methicillin-resistant *Staphylococcus aureus* (MRSA) MB5393, *Mycobacterium bovis* BCG and *Mycobacterium tuberculosis* H37Ra from each of the extracts from the 27 strains versus the different media in which they were grown. Extracts were tested at a concentration of 0.2 × WBE.

Extracts from all 27 strains exhibited some type of antimicrobial activity in some of the conditions and several trends were observed. The highest activity was detected against *M. tuberculosis* and then *M. bovis* and MRSA. Even though there were some differences between the strains, it was observed that the culture medium in which the *Micromonospora* strains were grown was clearly a more determining factor in the activity (% inhibition) of the extracts, than the different strains themselves. So, the highest inhibition (%) against the three pathogens was observed in the extracts from the fermentation medium M016, followed by the fermentation media RAM2-P V2, SAM-6 and APM9. On the contrary, the lowest inhibition was demonstrated in the extracts from fermentation media DEF-15, DEF-15S and DNPM. However, the same correlation was not observed when comparing other fermentation media, where significant differences in phocoenamicins production, as in the case of FPY-12 and FR23 media, did not translate into significant differences in inhibition. Finally, these results revealed a rich antimicrobial potential within the 27 strains and more assays should be performed against more pathogens in order to discover new antimicrobial activities and determine the responsible bioactive compound(s) in each case.

3.11.2 Antimicrobial Activity of Phocoenamicin B

The antimicrobial activity of phocoenamicin B, initially isolated from the 5 L fermentation of the CA-214671 strain grown in FR23 medium, was explored against a broader panel of pathogens, including methicillin-resistant *Staphylococcus aureus* (MRSA), methicillin-sensitive *Staphylococcus aureus* (MSSA), vancomycin-resistant (VR) *Enterococcus faecium*, vancomycin-sensitive (VS) *Enterococcus faecium*, vancomycin-sensitive (VS) *Enterococcus faecalis*, *Mycobacterium tuberculosis* H37Ra, *Mycobacterium bovis* and *Candida albicans*.

Gram-positive bacteria and *Mycobacterium* species were selected because phocoenamicins had previously showed activity against them, while *Candida albicans* was selected to test for antifungal activity.

For the preparation of the samples, the compound was serially diluted in dimethyl sulfoxide (DMSO) with a dilution factor of 2 to provide 10 concentrations starting at 128 μg/mL. The growth of the pathogens and the inoculum medium were used as negative controls, and a known antibiotic, depending on the pathogen for each assay, was used as a positive control. All bioassays were performed in duplicate. The results are presented in the following table:

Table 10. Antibacterial activity of phocoenamicin B.

		MIC (μg/mL)	
Compound		**phocoenamicin B**	**Control***
Pathogen	**Strain**		
MRSA	MB5393	8-16	1-2 (V)
MSSA	ATCC 29213	64-128	1-2 (V)
M. tuberculosis	(H37Ra) ATCC 25177	16-32	0.78-1.5 (S)
M. bovis	ATCC 35734	>128	1.5 (S)
E. faecalis	VANS 144492	>64	1-2 (V)
E. faecium	VR MBB5571	>128	>128 (V)
E. faecium	VS 144754	>128	2-4 (V)
C. albicans	ATCC 64124	>128	2-4 (A)

* (V) vancomycin, (S) streptomycin, (A) amphotericin B

The results revealed that phocoenamicin B demonstrated significant activity against MRSA and *M. tuberculosis* H37Ra, while weak activity against MSSA, *E. faecium* VS and *E. faecalis* VS and finally no activity against *E. faecium* VR, *M. bovis* and *C. albicans* at the highest concentration tested (128 μg/mL). The results for each pathogen are presented in **Supplementary Material, Tables S2-S4**.

3.11.3 Antimicrobial and Cytotoxic Activity of the Isolated Compounds

The seven compounds isolated were tested in parallel against a panel of human pathogens, including methicillin-resistant *S. aureus* (MRSA) MB5393, *M. tuberculosis* H37Ra (ATCC25177), *E. faecium* (VANS 144754), *E. faecalis* (VANS 144492) and *N. gonorrhoeae* (ATCC49226). The pathogens were selected based on the previous antimicrobial assays performed in our laboratory, as well as exploring previous reports in the literature. Overall, the seven spirotetronates exhibited strong to negligible activities, depending on the compound and the pathogenic bacterium, as shown in **Table 11**, expressed as minimum inhibitory concentration (MIC) values. Additionally, their cytotoxicity was evaluated *in vitro* against the human liver adenocarcinoma cell line (Hep G2) and demonstrated no cytotoxicity in most cases, except for the three compounds, phocoenamicin E (**2**), phocoenamicin B (**4**) and maklamicin (**7**) that presented weak activity (**Table 11**). The bioassays were performed in triplicate and the results for each of them are presented in **Supplementary Material, Table S5**.

Table 11. Antimicrobial bioassay results (MIC, μg/mL) against MRSA, *M. tuberculosis* H37Ra, *E. faecalis*, *E. faecium* and *N. gonorrhoeae* and cytotoxic activities (IC_{50}, μg/mL) against the Hep G2 cell line of the 7 spirotetronates isolated.

		MIC (μg/mL)							
Compounds		**(1)**	**(2)**	**(3)**	**(4)**	**(5)**	**(6)**	**(7)**	**Control***
Pathogen	**Strain**								
MRSA	MB5393	64	32-64	4	8	32	1	<0.25	2 (V)
M. tuberculosis	(H37Ra) ATCC 25177	64	32-64	8	16	32-64	1	32	1.6-3.125 (S)
E. faecalis	VANS 144492	>64	>64	8	>64	>64	32	1	2 (V)
E. faecium	VANS 144754	≥128	>64	4-8	≥64	>64	0.5	0.5	2 (V)
N. gonorrhoeae	ATCC 49226	>128	>128	>128	>128	>64	>128	>128	2 (P)
		IC_{50} (μg/mL)							
Hep G2 (liver) cell line		-	21.37	-	19.16	-	-	21.01	-

* (V) vancomycin, (S) streptomycin, (P) penicillin

The compounds tested had, in many cases, small structural differences when compared to each other, therefore the antibacterial assays revealed structural features that may influence the bioactivity and provided some structure–activity relationship findings.

Maklamicin (**7**) and maklamicin B (**6**) strongly inhibited the growth of MRSA with MIC values of <0.25 and 1 μg/mL respectively comparable to those of vancomycin (2 μg/mL), followed by phocoenamicin (**3**) and phocoenamicin B (**4**) (4 and 8 μg/mL, recpectively). The carboxylic ester instead of a ketone group in the macrocycle core (C-3) (**Figure 30**) observed in phocoenamicin C (**5**) and D (**1**) seem to weaken the activity against MRSA, as previously reported [77].

Interestingly, the most active compound against *M. tuberculosis* H37Ra was maklamicin B (**6**), followed by phocoenamicin (**3**) , which showed significant activities with MIC values of 1 and 8 μg/mL, respectively, while moderate to weak activity was detected in phocoenamicin B (**4**) and maklamicin (**7**) (16 and 32 μg/mL, respectively), indicating that the methyl group instead of the hydroxymethyl group in the side chain (C-20), as being the only difference in their structure (between compounds **6** and **7** and then between **3** and **4**), (**Figure 30**) probably increased the activity against this pathogen. The activity of maklamicin (**7**) and maklamicin B (**6**) against *M. tuberculosis* H37Ra was not studied before.

On the contrary, the bioactivity assay against *E. faecalis* showed that the presence of the hydroxymethyl group may enhance the bioactivity of maklamicin (**7**) (1 μg/mL) in comparison to maklamicin B (**6**) (32 μg/mL). The bioactivity of phocoenamicins against this pathogen was not studied before and showed that phocoenamicin (**3**) exhibits significant activity with a MIC value of 8 μg/mL, while the rest of the phocoenamicins demonstrated weak or no activity at the highest concentration tested. Next, maklamicin B (**6**) and maklamicin (**7**) demonstrated strong activity against *E. faecium* with MIC values of 0.5 μg/mL for both compounds, not reported before and lower than that of vancomycin (2 μg/mL), followed by phocoenamicin (**3**) (4-8 μg/mL). Finally, none of the compounds inhibited the growth of the Gram-negative *N. gonorrhoeae* at the highest concentration tested.

Furthermore, the MTT toxicity assays demonstrated that only phocoenamicin B (**4**), phocoenamicin E (**2**) and maklamicin (**7**) presented weak cytotoxicity against the Hep G2 cell line, with 50% inhibitory concentration (IC_{50}) values of 21.37, 19.16 and 21.01 μg/mL, respectively, while the rest of the compounds displayed no cytotoxicity at the highest concentration tested, making the most active of them potential candidates for further research and development.

3.12 Zebrafish Eleuthero Embryos Toxicity Assay

The small tropical fish Zebrafish (*Danio rerio*) is popular as a laboratory model in biological research and its embryos and larvae are mostly used to evaluate the toxicity of compounds due to their high sensitivity [18-19]. Their small size (1-5 mm) allows the performance of miniature *in vivo* experiments in multi-well plates and high throughput screening and the transparency of their body enables direct observation using a simple stereo microscope [44].

The toxicity of the three major compounds isolated, phocoenamicin (**3**), phocoenamicin B (**4**) and maklamicin (**7**) was evaluated using zebrafish eleuthero embryos using the immersion method,

as suggested for lipophilic compounds that have logD > 1 and thus are better absorbed by the zebrafish larvae [22-23].

The compounds were dissolved in dimethyl sulfoxide (DMSO) and then diluted in the fish medium (Danieau) in which the 3 days post fertilization (dpf) zebrafish larvae were swimming for 48h. Vehicle-treated Control eleuthero embryos (VHC) were also used and treated with the same concentration of DMSO (0.5%) in fish medium to compare the possible effects of the compounds. The concentrations tested were 1.6, 3.13, 6.25, 12.5 and 25 μM for each of the three compounds.

After the 48h exposure, corresponding to 5 dpf larvae, the possible mortality, touch-stimulation response, and developmental abnormalities were examined using a dissecting microscope coupled with a digital color camera and pictures were captured. Then, the score for the sub-lethal toxicity and lethality was determined for each fish and condition and the mean score was calculated. The assays were independently replicated three times, using 10 embryos for each condition and compound in each assay, and thus the total number of zebrafish embryos used was 480.

The results demonstrated that the mean score of toxicity was low for all three compounds and did not differ significantly from the control group ($p < 0.05$) (**Figure 42**). Therefore, the three spirotetronates were considered not toxic in a wide range of doses (1.6-25 μM), indicating the developing embryo's ability to process and eliminate them. In **Figure 43**, representative zebrafish larvae with no developmental abnormalities observed are shown for every compound after the exposure at the highest concentration of 25 μM, as well as for the control group (VHC).

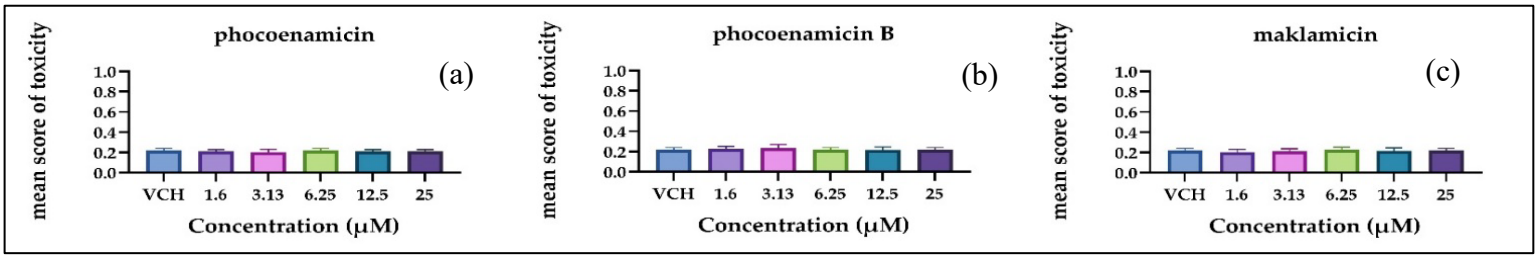

Figure 42. Mean scores of toxicity of the 5 dpf zebrafish eleuthero embryos after their exposure with (a) phocoenamicin, (b) phocoenamicin B and (c) maklamicin in five different concentrations (1.6-25 μM) and the control group (VHC). Three independent experiments were performed, the data were pooled and the mean ± SD was calculated. For the statistical analysis, the mean score of each concentration was compared with the mean scores of every other by using one-way ANOVA with Tukey's multiple comparison test, $p < 0.05$.

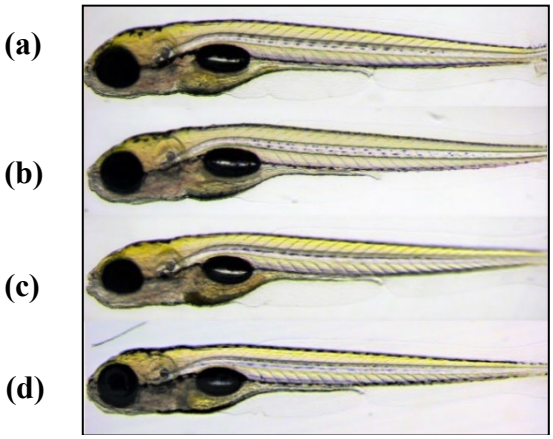

Figure 43. Lateral view of 5 dpf eleuthero-embryos with no developmental abnormalities, after 48h exposure, (**a**) with 25 μM of phocoenamicin (**b**) with 25 μM of phocoenamicin B, (**c**) with 25 μM of maklamicin and (**d**) Vehicle-treated Control eleuthero embryo (VHC).

Finally, the highest concentration tested (25 μM) was translated to MIC and IC_{50} values (μg/mL) in order to correlate the results with the antimicrobial and cytotoxicity assays (**section 3.11.3**). Phocoenamicin with molecular weight (MW) of 1071.64 corresponded to 26.79 μg/mL, phocoenamicin B with MW of 1087.64 g/mol corresponded to 27.19 μg/mL and maklamicin with MW of 524.69 corresponded to 13.12 μg/mL. In all cases, these concentrations were higher than the concentrations where the three compounds were found to display moderate or strong activities. Furthermore, for maklamicin and phocoenamicin B, which demonstrated moderate cytotoxicity, the cytotoxic concentrations are comparable (**4**) or higher (**7**) than those used in the zebrafish embryos toxicity assay, suggesting no broad-spectrum toxicity at the highest concentration tested.

4. DISCUSSION

4. Discussion

The microbial strains explored in this study as phocoenamicins producers belong to seven species of the *Micromonospora* genus, representing *M. terminaliae* and *M. endophytica* more than half of all the producing strains and it can be proposed that the biosynthesis of the phocoenamicins is restrained to the genus *Micromonospora*. Despite the close taxonomic relationship of the strains, they displayed great ecological and geographical diversity. Even though the phocoenamicins were originally isolated from marine actinomycetes, the producers identified in this study were isolated from very diverse ecosystems, resulting in 24 terrestrial strains and only 3 marine-derived strains. Regarding their geographical origin, they were widely distributed throughout the planet, covering almost all continents, confirming the hypothesis that this family of compounds is highly conserved within the *Micromonospora* community.

Using an OSMAC approach, the 27 strains were cultivated in 10 different media each, resulting in 270 fermentations, whose crude extracts were analyzed by LC-HRMS and explored by metabolomics analysis. All 27 strains produced the three known phocoenamicins in at least one of the fermentation conditions. The manual exploration of the data suggested that phocoenamicin was the most abundant compound, followed by phocoenamicins B and C. Furthermore, the analysis of the production of the three phocoenamicins suggested that, in general for all the 27 strains, the most suitable culture media were RAM2-P V2, FR23, M016 and SAM-6. The influence of the different strains, taxonomic species, culture media, ecological source and geography was studied and the only parameter that could determine a significant change in the metabolic profile was the culture medium.

The productive RAM2-P V2 medium was selected for further analysis by LC-MS/MS and molecular networking**.** The three marine-derived strains had a similar metabolite profile in the medium in comparison to the terrestrial ones. As a result, the relative peak intensities of the three phocoenamicins were analyzed comparing the marine and terrestrial strains. Phocoenamicin was produced more by the terrestrial strains (maximum levels from the strains CA-184181 and CA-238377), while phocoenamicins B and C within the marine strains (CA-214658 and CA-218877). All in all, the best production conditions for this family of compounds were observed with the marine-derived strain CA-214658 grown in the RAM2-P V2 culture medium.

The crude extracts of the 270 fermentations were tested against methicillin-resistant *S. aureus* (MRSA) MB5393, *M. bovis* BCG and *M. tuberculosis* H37Ra to evaluate the antimicrobial potential of the strains. All 27 strains exhibited some type of antimicrobial activity under some of the conditions and it was observed that the medium in which the *Micromonospora* strains were

grown influenced the inhibition (%) more than the different strains themselves. The results revealed rich antimicrobial activities within the 27 strains suggesting further research.

The combination of the LC-UV-HRMS analysis, metabolomic profiling and molecular networking allowed the putative dereplication of the main compounds produced within the 27 strains in the different growing conditions. The comparative analyses led to the tentative identification of multiple, chemically diverse compounds that were divided into three main groups, the spirotetronates, the siderophores and various other compounds.

The spirotetronate maklamicin, structurally related to phocoenamicins, was also tentatively identified to be produced by all 27 strains. Maklamicin was originally isolated from a *Micromonospora* species as well [90]. Within the 270 extracts of this study, the production of maklamicin conditioned the production of the phocoenamicins in all cases. The coexistence of maklamicin and the phocoenamicins in the extracts analyzed suggested a common biosynthetic origin of both families of compounds.

Apart from the spirotetronates, the majority of the compounds putatively dereplicated belonged to the hydroxamate siderophores, and in particular to the desferrioxamine family, with the most common being deferoxamine [144], nocardamine [145], terragine B [146] and IC 202B [147]. The hydroxamate siderophores have therapeutic and diagnostic importance and have demonstrated antimicrobial and antitumor activities. Furthermore, antibiotics linked to siderophores, natural conjugates named sideromycins, have shown a higher antibacterial efficacy compared to normal antibiotics due to an enhanced uptake using the siderophore-mediated iron active transport and their use has been explored in a “Trojan horse” approach to overcome bacterial resistance to antibiotics [34,35]. As metal chelators, Desferal, the brand name of desferrioxamine B, was the first pharma drug used to remove excess iron in patients suffering from iron toxicity or overload, such as in the case of *β*-thalassemia patients that depend on blood transfusions [164].

Finally, various other compounds were tentatively identified within the extracts. The most abundant were the isoflavones daidzein [148], genistein [149] and glycitein [150] that have antioxidant, anticancer and antimicrobial properties and several more metabolites with antibiotic properties, such as 21-demethyl-leptomycin A [165], that could explain the differences observed between the antimicrobial activity and the production levels of phocoenamicins in some of the extracts. The wide and diverse metabolic profile of these strains highlighted their metabolic potential and the need for further investigation.

Furthermore, the analyses tentatively revealed the presence of various peaks of compounds with predicted molecular formulae that were not found in the literature, putatively new metabolites related to the phocoenamicins (8 analogues), the maklamicin (5 analogues) or siderophores (6 analogues) and thus candidates for isolation and discovery of new bioactive compounds. Some of

the molecular formulae predicted ($C_{48}H_{70}O_{16}$, $C_{48}H_{70}O_{17}$, $C_{36}H_{50}O_9$, $C_{42}H_{60}O_{12}$) as phocoenamicin derivatives suggested a possible change in the oligosaccharide motif of their structure that was not observed before within the family. Spirotetronates have exhibited a huge structural variety and it has been demonstrated that even a small change in the structure of a spirotetronate can result in changing its bioactivity [95]. Therefore, large-scale fermentation should be performed in order to isolate these compounds, elucidate their structure and evaluate their potential bioactivity.

In this study, it was clearly demonstrated that combining manual exploration, metabolomics analysis and molecular networking can be a rapid and efficient way to prioritize strains. Additionally, a wide geographical distribution of phocoenamicin producing microbial strains, including both marine and terrestrial strains, opposed to initial statements about phocoenamicin production only in unique marine environments. The three marine-derived *Micromonospora* species have been identified as the best producers of phocoenamicins in terms of both the abundance in their extracts of some major members of the structural class and in the variety of molecular structures produced. Exploring the growth of *Micromonospora* and the production of the phocoenamicins, a significant increase was observed between the 10^{th} and the 13^{th} day of the fermentations and a decrease between the 15^{th} and the 16^{th} day, suggesting that 14 days of fermentation is the optimum period for the production of the three compounds.

Therefore, the production of the three marine derived strains isolated from Gran Canaria, Spain, was scaled-up and the optimal chromatographic conditions were determined. The gradient elution for the best separation of the initial groups of fraction extracts containing the phocoenamicins was 40-100% CH_3CN and the further processed fractions were purified by an isocratic elution of 50% CH_3CN to achieve the optimal separation and isolation of the compounds. Moreover, phenyl-based stationary phases resulted in sharper peaks with better resolution and the use of 0.1%TFA in the solvents resulted in a much better separation and chromatographic profile.

The fractionation of extracts from scaled-up cultures of the marine-derived strains led to the isolation of seven compounds (**1**-**7**), including two new phocoenamicins, phocoenamicins D and E (**1**-**2**), together with the known phocoenamicin, and phocoenamicins B and C (**3**-**5**). Furthermore, maklamicin (**7**) and 29-deoxymaklamicin (**6**), also belonging to the spirotetronate class of compounds, were isolated. 29-deoxymaklamicin (**6**) was previously reported as a result of gene deletion (*makC2*) in a genetically engineered strain [152], and herein it is reported as a natural product for the first time.

The two families of compounds share many common structural features as they contain a tetronic acid spiro-linked to a cyclohexene ring, embedded in an eleven-carbon macrocycle and connected to a *trans*-decalin moiety. Their major differences are the presence (phocoenamicins) or not (maklamicins) of the disaccharide linked to a chlorinated hydroxybenzoate moiety, as well as

the characteristic diol side chain unique in phocoenamicins. Interestingly, phocoenamicin E (**2**) bore, instead of the latter diol chain, the side chain of maklamicin (**7**) at C-21, not reported before in the phocoenamicin family and this finding reinforced the existence of a common biosynthetic pathway in the production of compounds of the two families.

Common structural variations shared by both families are the, hydroxymethyl group (phocoenamicin B, D, E and maklamicin) or methyl group (phocoenamicin, phocoenamicin C, maklamicin B) located at C-20, the diol side chain (phocoenamicin, phocoenamicins B, C and D) or hydroxyethyl group (phocoenamicin E and maklamicins) located at C-21, the ketone group (phocoenamicin, phocoenamicin B and E, maklamicins) or ester group (phocoenamicins C and D) located at C-3 and attached to the tetronic acid, indicating functional groups conserved within the two families. Among other structurally related spirotetronates, the hydroxymethyl or methyl group at C-20 can also be found in the nomimicin [91], lobophorin [121] and kijanimicin [166] families of compounds and the ester group at C-3 in chlorothricins [95] and PA-46101 A and B [93].

The bioactivity of the seven compounds isolated was evaluated against a panel of human pathogens, including methicillin-resistant *S. aureus* (MRSA), *M. tuberculosis* H37Ra, *E. faecium*, *E. faecalis* and *N. gonorrhoeae*. Similarly to other related spirotetronates, most of the compounds showed antibacterial activity against Gram-positive bacteria. Overall, the seven spirotetronates exhibited strong to negligible antibacterial activities, depending on the compound and the pathogen. As mentioned above, the compounds had small structural differences when compared to each other, therefore the antibacterial assays revealed some structure-activity relationships.

The growth of MRSA was strongly inhibited by maklamicin (**7**) (MIC <0.25 μg/mL) and maklamicin B (**6**) (1 μg/mL), followed by phocoenamicin (**3**) (4 μg/mL) and phocoenamicin B (**4**) (8 μg/mL). The ester instead of a ketone group located at C-3, which was present in phocoenamicin C (**5**) and D (**1**) seemed to reduce the activity against MRSA, as previously reported [77]. Other structurally related families of spirotetronates that have demonstrated strong activities against MRSA are decatromicins [102], the compounds JK [113], as well as the recently discovered glenthmycins [127].

The most active compound against *M. tuberculosis* H37Ra was maklamicin B (**6**) (1 μg/mL), followed by phocoenamicin (**3**) (8 μg/mL), while moderate to weak in phocoenamicin B (**4**) (16 μg/mL) and maklamicin (**7**) (32 μg/mL), suggesting that the methyl instead of hydroxymethyl group in the side chain (C-20), strengthened the activity against the pathogen. Streptomycin showed weaker activity (1.6-3.125 μg/mL) than maklamicin B (**6**). The activity of maklamicin (**7**) and maklamicin B (**6**) against *M. tuberculosis* H37Ra was not studied before. Other related families of spirotetronate polyketides that have exhibited strong activities against *M. tuberculosis* are lobophorins [167], and the above mentioned glenthmycins [127].

On the contrary, in the case of *E. faecalis*, the presence of the hydroxymethyl group may have enhanced the activity against it, as shown by maklamicin (**7**) (1 μg/mL), higher than vancomycin (2 μg/mL), in comparison to maklamicin B (**6**) (32 μg/mL). The bioactivity of phocoenamicins against this pathogen was not studied before and showed that phocoenamicin (**3**) exhibited significant activity (8 μg/mL), while the rest of the phocoenamicins demonstrated weak or no activity at the highest concentration tested. The spirotetronate MM46115 [112] and two of the glenthmycins [127] have been reported to exhibit bioactivity against *E. faecalis* comparable to maklamicin (**7**). Furthermore, both maklamicin B (**6**) and maklamicin (**7**) exhibited strong activity against *E. faecium* (0.5 μg/mL), and higher than vancomycin (2 μg/mL), an activity not previously reported, followed by phocoenamicin (**3**) (4-8 μg/mL), expanding the panel of antimicrobial properties of these compounds. Finally, none of the compounds inhibited the growth of the Gram-negative *N. gonorrhoeae* at the highest concentration tested.

Phocoenamicins C, D and E demonstrated weak to negligible activity against the pathogenic bacteria tested. All of them had either the hydroxymethyl group in the side chain (C-20) (compound **2**) or the carboxylic ester in the macrocycle core (C-3) (compound **5**) or both of these structural features (compound **1**) that, as mentioned above, based on the structure–activity relationship findings, may affect the bioactivity against these pathogens. More antimicrobial assays should be performed studying the activity against other pathogens, based on the hypothesis that all natural products have some receptor-binding function [10], like in the case of phocoenamicin against *Clostridium difficile*, where the chlorosalicyclic ester seems to play an essential role [94].

Furthermore, the cytotoxicity of the compounds was evaluated *in vitro* against the human liver adenocarcinoma cell line (HepG2) and demonstrated no cytotoxicity, except for the compounds **2** (21.37 μg/mL), **4 (**19.16 μg/mL) and **7 (**21.01 μg/mL) that presented weak activity, making the most active of the compounds potential candidates for further research and development. All in all, maklamicin B (**6**) resulted to be the most interesting compound, combining strong antimicrobial activity against MRSA, *M. tuberculosis* and *E. faecium* and no cytotoxicity.

Finally, zebrafish eleuthero embryos were used to evaluate the toxicity of the three major compounds, phocoenamicin (**3**), phocoenamicin B (**4**) and maklamicin (**7**). The three spirotetronates were considered not toxic in a wide range of doses (1.6-25 μM) and the highest concentration tested (25 μM) on zebrafish larvae was translated to μg/mL in order to correlate the results with the antimicrobial and cytotoxicity assays. In all cases, the testing concentrations were higher than the concentrations where the three compounds were found to display strong or moderate bioactivities against the pathogenic bacteria. Moreover, for maklamicin and phocoenamicin B, which demonstrated moderate cytotoxicity, the cytotoxic concentrations were comparable (**4**) or higher (**7**) than those used in the zebrafish embryos toxicity assay, suggesting no

broad-spectrum toxicity at the highest concentration tested. To the best of our knowledge, this is the first toxicity assay using zebrafish eleuthero embryos on spirotetronates.

The new analogues isolated highlight the wide range of structural possibilities of the spirotetronates that could unveil new biologic activities. The possible structure-activity relationships recorded here, along with other mentioned before within the spirotetronate class, can be used to unveil new biological activities.

5. MATERIALS AND METHODS

5. Materials and Methods

5.1 Taxonomical Identification of the Strains

Genomic DNA from each of the strains was isolated as follows: Each strain was grown in ATCC-2 medium (potato starch 2 g/L, dextrose 1 g/L, NZ Amine Type E 5 g/L, meat extract 3 g/L, peptone 5 g/L, yeast extract 5 g/L, calcium carbonate 1 g/L, pH 7) for 96 h. Each broth (1.5 mL) was centrifuged (15 min, 13,000 rpm, 4 ºC) in an eppendorf tube. The supernatant was discarded, and the pellet was re-suspended in 800 µL of extraction buffer (0.2% SDS, 50 mM EDTA, pH 8.5) and heated at 70 ºC for 30 min. The resulting mixture was centrifuged again under the same conditions (15 min, 13,000 rpm, 4 ºC). Next, the supernatant was transferred to an Eppendorf tube containing 60 µL of sodium acetate (3 M, pH 5.2) and the mixture was incubated at 4 ºC for 2 h and centrifuged again under the same conditions. 500 µL of the supernatant were transferred to an Eppendorf tube containing 1 mL of *i*-PrOH and the mixture was incubated at 4 ºC overnight. The next day, the content was centrifuged (15 min, 13,000 rpm, 4 ºC), the supernatant was discarded, and the pellet was washed with 200 µL of 70% ethanol. The washed pellet was centrifuged under the same conditions, the supernatant was discarded, and the pellet was dried for several hours at room temperature. Finally, the pellet (genomic DNA) was re-suspended in 100 µL of sterile water.

The 16S rRNA gene was PCR-amplified employing the universal eubacterial primers fD1 (50-AGAGTTTGATCCTGGCTCAG-30) and rP2 (50-ACGGCTACCTTGTTACGACTT-30). PCR reactions were carried out in a final volume of 50 µL containing 2 µL of dNTPs (10 mM each), 2 µL of each of the primers (10 µM), 2 µL of the DNA dilution, 5 µL of PCR buffer (10×), and 0.4 µL of Taq Polymerase (5 U/µL). Amplifications were performed on an iCycler iQ^{TM} Real-Time PCR Detection System (Bio-Rad Laboratories, Inc, Hercules, California, USA).

The PCR products were purified and sequenced at Secugen S. L. (Madrid, Spain). For each product the two strands were sequenced employing the primers mentioned above. The resulting DNA sequence lectures were aligned and visually inspected with Bionumerics 6.6 (Applied Maths, Sint-Martens-Latem, Belgium). The identification of the closest match 16S rRNA gene sequences was performed against the database of type strains with validly published prokaryotic names which was implemented at the EzTaxon server (http://ezbiocloud.net) through similarity searches and homology analysis.

5.2 Cultivation of the Producing Microorganisms

5.2.1 OSMAC Approach

The strains were cultured in 10 different media each based on the OSMAC approach (One Strain Many Compounds) [136] to determine the best growing conditions and maximize their production.

The strain fermentations were performed as follows: a seed culture of the strain was obtained by inoculating a 25 × 150 mm tube containing 10 mL of ATCC-2 medium (soluble starch 20 g/L, glucose 10 g/L, NZ Amine Type E 5 g/L, meat extract 3 g/L, peptone 5 g/L, yeast extract 5 g/L, calcium carbonate 1 g/L, pH 7) with 0.5 mL of a freshly thawed inoculum stock of the producing strain. The tubes were incubated in a rotary shaker (Kühner incubator model ISF-4-V, Adolf Kühner AG, Brisfelden, Switzerland) for 7 days (220 rpm, 28°C, 70% relative humidity).

Then, the fresh inoculum generated was mixed and employed to inoculate (5% v/v) EPA vials (28 × 90 mm glass tubes) each containing 10 mL of culture medium. The 10 culture media used were: APM9, DEF-15, DEF-15S, DNPM, FPY-12, FPY-2, FR23, M016, RAM2-P V2 and SAM-6 and their composition is indicated below (**Table 11**). All EPA vials were incubated in a rotary shaker for 14 days before harvesting (220 rpm, 28°C, 70% relative humidity). In parallel, a negative control of 10 uninoculated culture media was incubated to be used as controls in the experiments.

Table 11. Composition of the 10 culture media used in the OSMAC approach.

Culture medium	Carbon source	Nitrogen source	Trace elements and additional components
APM9	Glucose (SIGMA G8270)	Soybean Flour (SIGMA S9633)	$CoCl_2 \cdot 6H_2O$ (SIGMA C8661)
	Soluble starch from potato (PANREAC 121096)	-	$CaCO_3$ (ACROS ORGANICS 450680010)
DEF-15	Sucrose (FISHER S8600/70)	NH_4Cl (PANREAC 141121)	Na_2SO_4 (MERCK 1.06649)
	-	-	K_2HPO_4 (MERCK 5101)
	-	-	$MgCl_2 \cdot 6H_2O$ (MERCK 5833)
	-	-	NaCl (MERCK 1.06404)
	-	-	$CaCO_3$ (ACROS ORGANICS 450680010)
	-	-	$MnCl_2 \cdot 4H_2O$; $ZnCl_2$; $FeCl_2 \cdot 4H_2O$; NaCl

DEF-15-S	Sucrose (FISHER S8600/70)	NH_4Cl (PANREAC 141121)	Na_2SO_4 (MERCK 1.06649)
	Soluble starch from potato (PANREAC 121096)	-	K_2HPO_4 (MERCK 5101)
	-	-	$MgCl_2 \cdot 6H_2O$ (MERCK 5833)
	-	-	NaCl (MERCK 1.06404)
	-	-	$CaCO_3$ (ACROS ORGANICS 450680010)
	-	-	$MnCl_2 \cdot 4H_2O$; $ZnCl_2$; $FeCl_2 \cdot 4H_2O$; NaCl
DNPM	Dextrin from corn Type I (SIGMA D2006)	N-Z Soy BL (SIGMA P6713)	MOPS (FISHER BP 308)
	-	Bacto yeast extract (DIFCO 212750)	-
FPY-12	Fructose (PANREAC 142728)	Bacto peptone (DIFCO 211677)	$FeSO_4 \cdot 7H_2O$; $ZnSO_4 \cdot 7H_2O$;
	Glucose (SIGMA G8270)	Amicase (SIGMA A2427)	$MnSO_4 \cdot H_2O$; $CuSO_4 \cdot 5H_2O$; $CoCl_2 \cdot 6\ H_2O$
	Maltose (MERCK 1.05910)	-	-
FPY-2	Fructose (PANREAC 142728)	Bacto peptone (DIFCO 211677)	$FeSO_4 \cdot 7H_2O$; $ZnSO_4 \cdot 7H_2O$
	Sucrose (FISHER S8600/70)	Bacto yeast extract (DIFCO 212750)	$MnSO_4 \cdot H_2O$; $CuSO_4 \cdot 5H_2O$; $CoCl_2 \cdot 6\ H_2O$
	Maltose (MERCK 1.05910)	-	-
FR23	Glucose (SIGMA G8270)	Cottonseed flour (FLUKA C4898)	-
	Soluble starch from potato (PANREAC 121096)	-	-
	Cane molasses (Mercadona)	-	-
M016	Glucose (SIGMA G8270)	Bacto yeast extract (DIFCO 212750)	KH_2PO_4 (MERCK 1.04871)
	Soluble starch from potato (PANREAC 121096)	Bacto soytone (DIFCO 243620)	K_2HPO_4 (MERCK 5101)
	Maltose (MERCK 1.05910)	Bacto tryptone (DIFCO 211705)	$MgSO_4 \cdot 7H_2O$ (MERCK 5886)
	-	-	NaCl (MERCK 1.06404)
	-	-	$CaCl_2 \cdot 2H_2O$ (MERCK 1.02382)
	-	-	$SnCl_2 \cdot 2H_2O$; H_3BO_3; $Na_2MoO_4 \cdot 2H_2O$; $CuSO_4$;
	-	-	$CoCl_2 \cdot 6H_2O$; KCl; $ZnCl_2$; $MnSO_4 \cdot 4H_2O$; $FeCl_3$; HCl
RAM2-P V2	Glucose (SIGMA G8270)	Corn meal yellow (SIGMA C6304)	-
	Maltose (MERCK 1.05910)	Bacto yeast extract (DIFCO 212750)	-
	-	Proteose peptone (SIGMA P0431)	-
SAM-6	Glucose (SIGMA G8270)	Bacto yeast extract (DIFCO 212750)	$CoCl_2 \cdot 6H_2O$ (SIGMA C8661)

	Soluble starch from potato (PANREAC 121096)	NZ Amine type E (EKC) (SIGMA N4767)	$CaCO_3$ (ACROS ORGANICS 450680010)

5.2.2 Study of the Growing Conditions

Seven small-volume fermentations copies were generated to monitor the growth of the microorganism, the pH of the fermentation and the production of the three phocoenamicins during a period of 17 days. For that, the marine-derived CA-214671 strain was grown in the FR23 medium.

Each aliquot (0.7 mL) was inoculated in colony tubes in 14 mL of ATCC-2 inoculum medium (5% v/v) and incubated in a shaker incubator (Kühner incubator model ISF-4-V, Adolf Kühner AG, Brisfelden, Switzerland) for 7 days (220 rpm, 28ºC, 70% humidity). Next, the colony tubes of the aliquots were inoculated (3.75 mL) in Erlenmeyer flasks in 150 mL of FR23 medium (2.5% v/v) and again incubated in a Kühner incubator shaker under the same conditions for 17 days.

A 2 mL sample was obtained every working day from each fermentation flask to measure the growth of the microorganisms and create a growth curve (wet weight) during the 17 days of fermentation. Each sample was centrifuged (3500 rpm, 10 min), the supernatant was removed, and samples were weighed out (g). In parallel, the pH of the supernatant was determined using a portable pH meter (GLP21, Crison Instruments, HACH LANGE SPAIN, S.L.U., Barcelona, Spain). Finally, a second 2 mL sample was obtained every day and stored at -20ºC in 15 mL falcon tubes in order to be analyzed by HPLC-MS (as described in **section 5.8.3**) at the end of the 17 days period, determine the presence in the culture of the three phocoenamicins and estimate their production during the fermentation process.

5.2.3 Scale-up of the Fermentation

Each 3 or 5 L large scale fermentation was generated as follows: a fresh seed culture of the strain was obtained inoculating a 25 × 150 mm tube containing 16 mL of ATCC-2 medium with a freshly thawed inoculum stock of the strain. The tube was incubated for 7 days in an orbital Kühner shaker (220 rpm, 28°C, 70% relative humidity). The grown culture was then used to inoculate two flasks, each containing 50 mL of ATCC-2-M medium (5% v/v). The flasks were again incubated for 7 days in an orbital shaker under the same conditions.

The content of both flasks was then mixed, and the mixture was used to inoculate 100 flasks (500 mL), each containing 50 mL of FR23 fermentation medium (2.5% v/v) for strain CA-214671

or 60 flasks (500 mL) with 50 mL of RAM2-P V2 medium (2.5% v/v) for strains CA-214658 and CA-218877. The flasks were incubated during 14 days before harvesting, resulting in a 5 L fermentation broth for strain CA-214671, and 3 L fermentation broths for strains CA-214658 and CA-218877.

5.3 Extraction of the Fermentation Broths and Processing of the Samples

5.3.1 Extraction of the 270 Small Scale Fermentations and Processing

The fermentation broths were extracted by adding 10 mL of acetone to each 10 mL fermentation (1:1), including the negative control media. The mixtures were then vortexed and shaken in an orbital shaker incubator (Künher ISF-1-W incubator, Adolf Kühner AG, Brisfelden, Switzerland) (220 rpm, 28°C, 1 h), centrifuged (3500 rpm, 10 min) for the separation of the mycelium, and 12 mL of the supernatant were transferred to 16 mm TurboVap® tubes (Biotage, Uppsala, Sweden) to which 600 µL of dimethyl sulfoxide (DMSO) were added. Finally, evaporation of the samples was carried out in a hot nitrogen flow cabinet, until a final volume of 3.0 mL to reach a final concentration of 2 × WBE (Whole Broth Equivalent, that is, the natural concentration of each metabolite in the culture broth) in 20% DMSO in water. The contents of the tubes were transferred to 0.8 mL 96-Well Deep Well plates (Abgene™, Portsmouth, USA) using the MultiPROBE® II HT robotic liquid handling system (Packard Bioscience Co, Meriden, Connecticut, USA), transferring 540 µL to each well in the plate. 280 samples were obtained in total, 270 extracts from the fermentation broths and 10 extracts from the corresponding control media without the presence of the actinomycetes.

5.3.2 Extraction and Processing of the 84 samples for the Exploration of the Growing Conditions

After the 17 days of fermentation, the falcon tubes stored each day were defrosted and extracted with 2 mL of acetone (1:1), centrifuged (3500 rpm, 10 min) and 84 samples were obtained in total. 100 µL of the supernatant from each falcon tube were added in 96-well filtration MultiScreen® HTS, GV Sterile plates 0.22 µm Hydrophilic Low Protein Binding, Durapore® Membrane. The plates were filtered and centrifuged (2500 rpm, 5 min) to be analyzed by HPLC-MS (**see section 5.4.1**).

5.3.3 L-L Extraction of the Large-scale Fermentations and Processing

The large-scale fermentation broths from the three marine-derived strains were extracted as follows: First, the separation of the mycelium was separated from the supernatant by centrifugation at 9000 rpm for 10 min, followed by filtration under vacuum. The supernatant was subjected to EtOAc liquid-liquid extraction in a separatory funnel in a ratio 1:1 and rotary evaporated until dry. The mycelium was extracted with 700 mL EtOAc in a magnetic stirrer (190 rpm, 2 h), filtered in a Büchner funnel and evaporated until dry. The extraction procedure was repeated in triplicate to obtain the final organic crude extracts.

Reversed Phase C-18 silica gel was mixed with a solution of the final organic extracts in a 2:1 ratio, the solvent was evaporated under vacuum and the resulting material loaded onto a C-18 column (ODS) (200 × 35 mm) that was eluted (MPLC) with a linear H_2O-CH_3CN gradient (10 mL/min; 5–100% CH_3CN in 60 min; UV detection at 210 nm and 280 nm). (5% to 100% CH_3CN in 35 min + 100% CH_3CN in 25 min, 10 mL/min). Medium pressure liquid chromatography (MPLC) was performed on semiautomatic flash chromatography (CombiFlash Teledyne ISCO Rf400x). As a result, the crude extracts were fractionated through reversed phase C18 MPLC, giving 65 fractions for strain CA-214671, 39 for CA-214658 and 33 for CA-218877 strain.

The fractions obtained from each extract were analyzed and combined into groups according to their LC-UV-MS profiles, resulting in seven groups deriving from the CA-214671 fermentation and five from each of the CA-214658 and CA-218877 fermentations, which were evaporated to dryness in a centrifugal evaporator. Fractions containing compounds of interest from this chromatography were further purified by preparative and semi-preparative reversed-phase HPLC to isolate the compounds.

5.4 Isolation and Purification of the Compounds

As mentioned above (see **section 5.3.3**), the fractions from the large-scale fermentations obtained by MPLC were combined into groups according to their LC-UV-MS profiles and further separated by preparative and semi-preparative reversed-phase HPLC to isolate the compounds of interest. The analysis resulted in seven groups deriving from the CA-214671 fermentation and five from each of the CA-214658 and CA-218877 fermentations.

HPLC separations were performed on a Gilson GX-281 322H2 (Gilson Technologies, USA) using a semi-preparative reversed-phase column (Xbridge prep Phenyl 5 µm, 10 × 150 mm) and a flow rate of 3.6 mL/min or a preparative (Kinetex® 5µm PFP 100Å AXIA Packed LC Column, 250 × 21.20 mm) reversed-phase column with a flow rate of 14 mL/min. The solvents used were

H_2O 0.1 % trifluoroacetic acid (TFA) and CH_3CN 0.1 % TFA and were of HPLC grade. The time of the analysis was set to 45 min, collecting the fractions between 2 min – 42 min and resulting in 80 fraction zones collected. The gradient elution for the best separation of the initial groups of fraction extracts containing the phocoenamicins was 40-100% ACN and the fractions of interest were further processed to obtain an isocratic elution or a shorter gradient and isolate the compounds.

5.5 Characterization of the Isolated Compounds

5.5.1 Optical Rotation (OR)

Optical rotations of the isolated compounds were measured on a Jasco P-2000 polarimeter (JASCO Corporation, Tokyo, Japan). The measurement information and parameters were as follows:

Measurement Information:
Instrument Name: Polarímeter
Model Name: P-2000
Polarizer Dichrom Faraday Cell Flint Glass
Accessory RSC-200
Path Length: 100 mm
Light Source: Na
Monitor wavelength: 589 nm
D.I.T.: 5 sec
No. of cycle: 4
Cycle interval: 10 sec
Aperture(S): 3.0mm
Aperture(L): Auto
Mode: Specific O.R.
Path Length: 10 mm
Concentration: 0.45 w/v%

5.5.2 Fourier-Transform Infrared Spectroscopy (FT-IR)

IR spectra of the isolated compounds were recorded with a JASCO FT/IR-4100 spectrometer (JASCO Corporation) equipped with a PIKE MIRacle^{TM} single reflection ATR accessory. The measurement information and parameters were as follows:

Concentration of the samples: 6 mg/mL

Dissolvent: MeOH
Volume: 5 μL
Model name: FT/IR-4100 type A
Method: ATR
Start: 349.053 cm^{-1}
End: 7800.65 cm^{-1}
Resolution: 4 cm^{-1}

5.5.3 LC/UV/MS Analysis

LC-UV-MS analysis was performed on an Agilent 1100 (Agilent Technologies, Santa Clara, CA, USA) single quadrupole LC-MS system, using a Zorbax SB-C8 column (2.1 × 30 mm, 5 μm), maintained at 40°C and with a flow rate of 300 μL min^{-1} and a standard 10-min reversed-phase gradient chromatographic run, as follows:
Chromatographic conditions are described in section 5.6.1. Full diode array UV scans from 100 to 900 nm were collected in 4 nm steps at 0.25 s/scan. The eluting solvent was ionized using the standard Agilent 1100 electrospray ionization source adjusted to a drying gas flow of 11 L/min at 325 °C and a nebulizer pressure of 40 psig. The capillary voltage was set to 3500 V. Mass spectra were collected as full scans from 150 m/z to 1500 m/z, with one scan every 0.77 s, in both positive and negative modes.

ESI-TOF and MS/MS spectra were acquired using a Bruker maXis QTOF (Bruker Daltonik GmbH, Bremen, Germany) mass spectrometer coupled to an Agilent 1200 LC (Agilent Technologies, Waldbronn, Germany) with the same standard 10-min reversed-phase gradient chromatographic run, as described above (see **section 5.6.1**)

5.5.4 Nuclear Magnetic Resonance (NMR)

1D- and 2D-NMR spectra were recorded on a Bruker Avance III spectrometer (500 and 125 MHz for ^{1}H and ^{13}C NMR, respectively) equipped with a 1.7 mm TCI MicroCryoProbe™ (Bruker Biospin, Fällanden, Switzerland). Chemical shifts were reported in ppm using the signals of the residual solvents as internal reference (δ_H 3.31 and δ_C 49.15 for CD_3OD).

Prior to analysis, each sample was left overnight in the lyophilizer, its weight was measured and the NMR tube was prepared adding 40-60 μL of CD_3OD, depending on the quantity of each sample.

The following 1D and 2D NMR spectra were acquired, depending on the quantity of the compound available: 1H, 13C, HSQC, HMBC, COSY, NOESY, TOCSY, ROESY.

Finally, for stereochemical analysis, molecular models were generated using Chem&Bio Draw 12.0 (CambridgeSoft, PerkinElmer Informatics, Waltham, MA, USA).

5.6 Multivariate Data Analysis (MVDA) with MZmine 2 and MetaboAnalyst 5.0

5.6.1 Analysis by LC-HRMS

The 280 extracts obtained (270 extracts from the fermentation broths and 10 extracts from the corresponding control media) from the OSMAC approach were subjected to liquid chromatography-high resolution mass spectrometry (LC-HRMS) and additional analysis by tandem mass spectrometry was performed for the extracts obtained from the RAM2-P V2 medium, using positive ionization mode. ESI-TOF and MS/MS spectra were acquired using a Bruker maXis QTOF (Bruker Daltonik GmbH, Bremen, Germany) mass spectrometer coupled to an Agilent 1200 LC (Agilent Technologies, Waldbronn, Germany) with a standard 10-min reversed-phase gradient chromatographic run, as follows: Solvent A consisted of 10% CH_3CN and 90% H_2O with 1.3 mM TFA and ammonium formate, and solvent B was 90% CH_3CN and 10% water with 1.3 mM TFA and ammonium formate and were of HPLC grade. The gradient started at 10% B and went to 100% B in 6 min, was kept at 100% B for 2 min, and returned to 10% B for 2 min to initialize the system. Full diode array UV scans from 100 to 900 nm were collected in 4 nm steps at 0.25 s/scan. The mass spectrometer was operated in positive ESI mode. The instrumental parameters were 4 kV capillary voltage, drying gas flow of 11 L/min at 200 °C, and nebulizer pressure of 2.8 bar. TFA-Na cluster ions were used for mass calibration of the instrument prior to sample injection. Pre-run calibration was by infusion with the same TFA-Na calibrant. Mass spectra were collected as full scans from 150 m/z to 1500 m/z, with one scan every 0.77 s.

5.6.2 MZmine 2

The LC-MS raw data were initially converted into mzXML files using MSConvert (ProteoWizard, http://proteowizard.sourceforge.net).. The converted datasets were imported into MZmine v2.53, a bioinformatics tool for differential analysis of mass spectrometry data [137]. Peak detection was achieved by noise removal, chromatogram construction, and peak deconvolution. Firstly, the mass values were detected using the centroid mode in each spectrum and the noise level of the peaks was set to 100. Then, chromatograms were constructed for each of the mass values using the ADAP chromatogram builder [168], where group intensity threshold and minimum highest intensity were set to 300 and *m/z* tolerance to 20 ppm. Next, the “local minimum search” deconvolution algorithm was applied to each constructed chromatogram of each mass ion

to detect the individual peaks. For this algorithm, the chromatographic threshold was set to 10%, the search minimum in RT range to 0.2 min, the minimum relative height to 10%, the minimum absolute height to 100 and the minimum ratio of peak top/edge to 2. The separated peaks were then deisotoped using the function of isotopic peaks grouper in which *m/z* tolerance was set to 20 ppm, RT tolerance to 0.5 absolute (min), maximum charge of 3 and representative isotope as the most intense. The remaining peaks in different samples were aligned based on the mass and RT of each peak, creating a peak list. The ion *m/z* tolerance for alignment was set to 20 ppm, while RT to 0.5 min, and weight for *m/z* and RT were 80 and 20, respectively. Finally, the resulting peak list was gap-filled with missing peaks using intensity tolerance of 10%, *m/z* tolerance of 20 ppm and RT tolerance of 0.5 min.

At the same time, using the MZmine's setting of sample parameters, samples were organized in groups, according to their taxonomy, geography, ecology, culture medium and the different strains. Finally, the resulting data were converted into a MetaboAnalyst-CSV (comma-separated values) file, a text file that allows data to be saved in a table-structured format, taking into account the grouping parameters. As a result, five .csv files were generated, one for each of the grouping parameters to study their influence in the metabolic profile obtained. Each of these files was uploaded to the MetaboAnalyst 5.0 platform [138] to carry out the statistical analysis.

The LC-MS/MS raw data of the 27 strains cultured in the RAM2-P V2 medium were also processed by MZmine 2, employing the same parameters and noise level of 50 for the MS2 level. The processed data were used to visualize the production of the phocoenamicins by the peak intensities plot generated by MZmine 2.

5.6.3 MetaboAnalyst

As mentioned above, the CSV files for each group were uploaded to the MetaboAnalyst 5.0 platform [138] to carry out the statistical analysis.

The MetaboAnalyst module of the One Factor-Statistical Analysis was used, and each file was uploaded as peak intensities data type and samples in columns (unpaired) format. Missing values were replaced by 1/5 of minimum positive values of their corresponding values and further feature filtering based on interquantile range (IQR) reduced the dataset to 2500 features. Normalization was performed using total area sums, Pareto scaling, and log transformation to transform the data matrix into a more Gaussian-type distribution and make individual features more comparable. Using the above parameters, PCA and PLS-DA analyses were generated to explore the metabolomics production, using the MetaboAnalyst's commands. Within the PLS-DA analysis, the variables importance in projection (VIP) were studied, and cross validation and

permutation test (separation distance (B/W), 100 permutation numbers) were performed using the platform's commands. Finally, for the processed data of the 27 strains cultured in the RAM2-P V2 medium, using the ecology of the strains as the grouping parameter, the HCA dendrogram was generated.

5.7 Molecular Networking

5.7.1 Classical Molecular Networking

The LC-MS/MS raw data were converted into mzXML files using MSConvert (ProteoWizard, proteowizard.sourceforge.net), uploaded to the Global Natural Products Social Molecular Networking (http://gnps.ucsd.edu) platform using WinSCP (https://winscp.net/eng/index.php) and then processed by GNPS to generate a MS/MS molecular network. The molecular network was created using the online workflow (https://ccms-ucsd.github.io/GNPSDocumentation/) on the GNPS website (http://gnps.ucsd.edu) [169]. The parameters are publicly available at: https://gnps.ucsd.edu/ProteoSAFe/result.jsp?task=37e734c22f5f43cab7f8983d5121cea6&view=written_description. The molecular network generated was analyzed and visualized using Cytoscape software (version 3.8.2) [170]. The number of nodes and edges, as well as the average number of neighbors were generated using the Network Analyzer in Cytoscape software.

5.7.2 Preprocessing by MZmine 2 and Feature-Based Molecular Networking

The data files previously converted to mzXML format were imported to MZmine v2.53 for preprocessing [137]. For each sample, the mass detection was set to a noise level of 100 for the MS1 level and 50 for MS2 levels. The chromatograms were built using the ADAP chromatogram builder [168] with a minimum group size set to 5 scans, group intensity threshold and minimum highest intensity set to 300 and *m/z* tolerance to 20 ppm. The chromatograms were deconvoluted with the local minimum search algorithm (chromatographic threshold of 10%, search minimum in RT range of 0.1 min, minimum relative height of 10% and minimum absolute height of 100). Deisotoping of the chromatograms was achieved by the isotope peak grouper algorithm with *m/z* tolerance set to 20 ppm and RT tolerance to 0.5 min. All samples were combined in a peak list using the join aligner algorithm. The data were filtered in order to keep only peaks with minimum 2 peaks in a row and minimum 2 peaks in an isotope pattern. Lastly, the peak list was gap-filled

with an intensity tolerance of 10%, *m/z* tolerance of 20 ppm and RT tolerance of 0.5 min. The final peak list was exported in two different format files (.csv and .mgf).

The resulting files were uploaded to GNPS for feature-based molecular networking (FBMN) analysis. A metadata file was also created and uploaded as a text file, describing the properties of each sample-strain (taxonomy, geography, ecology). A molecular network was created with the feature-based molecular networking (FBMN) workflow [38] on GNPS (https://gnps.ucsd.edu [169]) with the following parameters: The data were filtered by removing all MS/MS fragment ions within +/− 17 Da of the precursor *m/z* and the MS/MS spectra were window filtered by choosing only the top 6 fragment ions in the +/− 50 Da window throughout the spectrum. The precursor ion mass tolerance was set to 1 Da and the MS/MS fragment ion tolerance to 0.5 Da. In the molecular network, the edges had a cosine score above 0.6 and more than 6 matched peaks. Edges between two nodes were kept only if each of the nodes appeared in each other's respective top 10 most similar nodes and the maximum size of a molecular family was set to 100. Then, the spectra in the network were searched against GNPS spectral libraries [169]-[171] and the library spectra were filtered in the same manner as the data results. The molecular network generated was analyzed and visualized using Cytoscape software (version 3.8.2) [170]. The number of nodes and edges, as well as the average number of neighbors were generated using the Network Analyzer in Cytoscape software.

5.8 Dereplication Process and Identification of Putative New Analogues

The LC-UV-HRMS analyses were carried out as previously described (see **section 5.6.1**). The major peaks in each chromatogram were initially searched manually against the in-house MEDINA's LC-HRMS library. The DAD (UV−vis) spectra, retention time, and mass spectra of the samples were compared to the corresponding LC-UV-MS data of known microbial metabolites stored in the proprietary database, containing annotated metabolite data obtained under identical conditions to those for the samples under analysis.

Then, the proposed molecular formula, the accurate mass and the UV profile were searched against the Dictionary of Natural Products (DNP), the COlleCtion of Open Natural ProdUcTs (COCONUT), the Natural Product Activity & Species Source database (NPASS) and the ChemSpider database. Additional information was taken into account, such as the biological source and the structure of the compound, where available within these databases. The combination of this manual comparative search along with the metabolomic profiling and molecular networking allowed the putative dereplication of the main compounds produced within the 27 strains in the different growing conditions.

Furthermore, this manual dereplication tentatively detected various peaks of compounds with molecular formulae that were not found within the above-mentioned databases, therefore are putatively new metabolites related to the phocoenamicins, maklamicin or siderophores. These annotations were also based on GNPS, searching the compounds that were in each molecular cluster and combining all the data obtained.

5.9 Bioactivity assays

5.9.1 High-Throughput Screening Assay of the 270 Fermentation Extracts

The following strains were used for the determination of the antimicrobial activities: methicillin-resistant *S. aureus* (MRSA) MB5393, *M. tuberculosis* H37Ra and *M. bovis* BCG. The preparation of the inocula and the HTS assays, followed the methodologies described below [172]-[173].

For the antibacterial tests against the Gram-positive bacterium methicillin resistant *Staphylococcus aureus* (MB5393) (MRSA), thawed stock inocula suspensions from cryovials were streaked onto Luria-Bertani agar plates (LBA, 40 g/L) and incubated at 37 °C overnight to obtain isolated colonies. Single colonies were inoculated into 10 mL of Luria-Bertani broth medium (LB, 25 g/L in 250 mL Erlenmeyer flasks) and incubated overnight at 37 °C with shaking at 220 rpm and then diluted in order to obtain assay inocula of approximately 1.1×10^6 CFU/mL.

M. tuberculosis H37Ra ATCC 25177 and *M. bovis* ATCC 35734 were grown for 15–21 days in Middlebrook 7H9 broth (Becton Dickinson ref 271310) supplemented with 10% ADC enrichment (Becton Dickinson ref. 211887) containing albumin, dextrose, and catalase; 0.5% glycerol as a carbon source; and 0.25% Tween 20 to prevent clumping. Suspensions were prepared, and the turbidity was adjusted to 0.5 OD at 600 nm. Then, further dilutions were made to reach the final bacterial suspension concentration of 5×10^5 CFU/mL for the assay.

90 µL/well of the diluted inocula were mixed with 10 µL/well of extracts (final concentration of 0.2 × WBE of each extract in the assay). A dose–response curve of a reference standard compound (vancomycin for MRSA assay and streptomycin for both *Mycobacterium* assays) was included as internal assay plate control. The assays were performed in duplicate for each microorganism.

For MRSA assay, absorbance at OD 612 nm was measured at T_0 (zero time) and immediately after that, plates were statically incubated at 37 °C for 20 h. After this period, the assay plates were shaken using the DPC Micromix-5 and once more the absorbance at OD 612 nm was measured at Tf (final time).

For *Mycobacterium* assays, plates were incubated for 7 days at 5% CO_2 and 95% humidity and 37°C. After this incubation, 30 µL of 0.02% resazurin and 15 µL of Tween 20 were added to each well, incubated 24 h and assessed for color development. A change from blue to pink indicated reduction of resazurin and therefore bacterial growth. For the Resazurin Solution, Resazurin sodium salt (R7017, Sigma-Aldrich) stock solution of 0.02 g was dissolved in 100 mL of sterile distilled water and sterilized by filtration. The wells were read for color change and the data were quantified by measuring fluorescence (excitation 570 nm, emission 615 nm). Both readouts absorbance and fluorescence were measured using an EnVision® multimode plate reader (Perkin Elmer, Waltham, MA, USA).

In order to process and analyze the data and calculate the RZ' factor (which predicts the robustness of an assay), the Genedata Screener software (Genedata, Inc., Basel, Switzerland) was employed. For an assay to be accepted, the RZ' factor must be close to 1 [174]. An extract was considered active when the percentage of inhibition was greater than 50%. In all experiments performed in this work, the RZ' factor obtained was between 0.85 and 0.95.

5.9.2 Antibacterial Activity and Cytotoxicity Assay of the Isolated Compounds

The antimicrobial activity of phocoenamicin B was initially explored against a wide panel of pathogens, including methicillin-resistant *Staphylococcus aureus* (MRSA), methicillin-sensitive *Staphylococcus aureus* (MSSA), vancomycin-resistant (VR) *Enterococcus faecium*, vancomycin-sensitive (VS) *Enterococcus faecium*, vancomycin-sensitive (VS) *Enterococcus faecalis*, *Mycobacterium tuberculosis* H37Ra, *Mycobacterium bovis* and *Candida albicans*. Furthermore, after the isolation of compounds **1**–**7**, all of them were tested again against the growth of Gram-positive bacteria methicillin-resistant *Staphylococcus aureus* (MRSA) MB5393, *Enterococcus faecalis* VANS 144492 and *Enterococcus faecium* VANS 144754, bacterium *Mycobacterium tuberculosis* (H37Ra) ATCC 25177, and Gram-negative bacterium *Neisseria gonorrhoeae* ATCC 49226. For the preparation of the inocula and the HTS assays of Gram-positive bacteria, as well the bacterium *Mycobacterium tuberculosis* H37Ra, the methodologies described above (**section 5.9.1**) were followed.

For *Candida albicans* assay, frozen stocks of the microorganism were used to inoculate Sabouraud Dextrose Agar (SDA) plates for confluent growth. Plates were incubated for 24 h, at 35 °C. The grown colonies were harvested from the SDA plates and suspended in RPMI-1640 modified medium. Modified RPMI-1640 medium was prepared as follows: 20.8 g of RPMI powder (Sigma) were poured into a 2 L flask, together with 13.4 g of YNB, 1.8 L of milliQ water, 80 mL of Hepes 1 M and 72 mL of glucose 50%. The volume was adjusted to 2 L and filtered. The OD_{660}

was adjusted to 0.25 using RPMI-1640 modified as diluent and blank. This inoculum was diluted 1:10 and kept on ice until used to inoculate 96-well microtiter plates. After dispensing the inoculums, the samples and the controls, the assay plates were read in a Tecan Ultraevolution spectrophotometer at 612 nm for *T*0 (zero time). Then, the plates were statically incubated at 37 °C for 20 h. After incubation, the plates were shaken in a DPC Micromix-5 and read again for *Tf* (final time) [172].

For all assays, the growth of the pathogens and the inoculum medium were used as negative controls, and a known antibiotic, depending on the pathogen for every assay, was used as a positive control.

Moreover, the cytotoxicity against the human liver adenocarcinoma cell line (Hep G2) of the seven isolated compounds was evaluated, where the *in vitro* cell viability was studied based on the MTT (3-(4,5-dimethylthiazol-2-yl)-2,5-diphenyltetrazolium bromide) colorimetric assay [175]. Hep G2 cells (human liver carcinoma, CCL-8065) were obtained from the American Type Culture Collection (ATCC, Manassas, VA, USA) and were grown in ATCC-formulated Eagle's M essential medium (MEM) with 10% qualified FBS, 2 mM L-glutamine, 1 mM sodium pyruvate, and 100 μM MEM non-essential amino acids. Cells were maintained at 37°C under a humidified atmosphere of 5% CO_2. MTT reduction rate is an indicator of the functional integrity of the mitochondria and, hence, of cellular viability. For the assay, the number of cells seeded per culture well was 100.000 cells/mL. After 72 h treatment, MTT reduction was estimated by measuring absorbance at 590 nm [172].

For the preparation of the samples, each compound was serially diluted in dimethyl sulfoxide (DMSO) with a dilution factor of 2 to provide 10 concentrations starting at 128 μg/mL except for compound **5**, where the highest concentration tested was 64 μg/mL. All assays were performed in triplicate for the seven isolated compounds and in duplicate for the initial sample isolated of phocoenamicin B. For the antimicrobial assays, the MIC was defined as the lowest concentration of compound resulting in a 90% growth inhibition of microorganism, while for the cytotoxicity, the IC_{50} was determined as the concentration that decreases 50% of the cell viability. The Genedata Screener software (Genedata, Inc., Basel, Switzerland) was used to process and analyze the data, as well as calculate the RZ' factor, which predicted the robustness of the assays [174].

5.10 Zebrafish Eleuthero Embryos Toxicity Assay

5.10.1 Zebrafish Care and Maintenance

Adult zebrafish (*Danio rerio*) stocks of AB strain (Zebrafish International Resource Center, Eugene, OR) were maintained in a UV-sterilized rack recirculating system equipped with a mechanical and biological filtration unit and kept under a 14/10 h light/dark cycle at the temperature of 27–28°C and pH of 6.8–7.5. Water quality was monitored daily for pH, temperature and conductivity, and weekly for ammonia and nitrite (SL1000 Portable Parallel Analyzer, Hach Instruments, Loveland, CO, USA) and nitrate levels (Tetra, Melle, Germany). Zebrafish were fed three times per day, twice with flake food (TetraMin, Tetra, Melle, Germany) and once with *Artemia* (brine shrimp).

Fertilized eggs of good quality (fertilized, clear cytoplasm and symmetric cleavage), collected from wild type AB zebrafish progenitors, were selected for the experiments and kept in Petri dishes containing Danieau's solution (1.5 mM HEPES, 17.4 mM NaCl, 0.21 mM KCl, 0.12 mM $MgSO_4$, 0.18 mM $Ca(NO_3)_2$, and 0.6 μM methylene blue) [176] at 28°C until compound exposure. All eleuthero embryos were derived from the same spawn of eggs for the comparison between the control and treated groups. Mortality in untreated groups of embryos was <10%. All further experimental work was done using Danieau's solution as incubation medium.

All procedures were carried out according to the Declaration of Helsinki and conducted following the ARRIVE guidelines [177] and the guidelines of the European Community Council Directive 2010/63/EU, implemented in 2020 by the Commission Implementing Decision (EU) 2020/569 and all the relevant ethical regulations from the Ethics Committee of the University of Leuven (Ethische Commissie van de KU Leuven, approval number ECD 027/2019) and from the Belgian Federal Department of Public Health, Food Safety and Environment (Federale Overheidsdienst Volksgezondheid, Veiligheid van de Voedselketen en Leefmilieu, approval number LA1210261).

5.10.2 Compounds Preparation and Toxicity Evaluation

Each of the three compounds (**3**, **4**, and **7**) was dissolved in 100% dimethyl sulfoxide (DMSO, spectroscopy grade) and diluted in Danieau's medium to a final concentration of 25 μM (0.5% DMSO), followed by ½ serial dilutions to provide five testing concentrations (1.6, 3.13, 6.25, 12.5 and 25 μM).

Next, 3 dpf zebrafish eleuthero embryos randomly selected were immersed in a 24-well plate containing the three compounds at the different testing concentrations (n=10 larvae per well). At

the same time, 10 Vehicle-treated Control eleuthero embryos (VHC) were also treated with 0.5% DMSO, in accordance with the final solvent concentration of testing compounds to compare the possible effects of the compounds. The eleuthero embryos were incubated under a 14/10 hour light/dark cycle at 27–28°C.

After the 48h exposure, at 5 dpf, the lethality (cardiac rhythm and degraded body were used as clinical criteria) and touch-stimulation response were assessed using non-anesthetized eleuthero embryos, while the possible morphological defects were evaluated after anesthetizing the eleuthero embryos in 0.5 mM tricaine. All observations were performed using a M80 stereo microscope (Leica Microsystems, Danaher Co., Germany) and pictures were captured with a Leica DFC310 FX digital color camera (Leica Microsystems, Danaher Co., Germany) and stored.

Mean score of lethality and sub-lethal toxicity per condition was calculated as follows: To each adverse effect observed (impaired motility, bad development, body curvature and swim bladder defects) a score of 1 was given (maximum 4 per larva), and a score of 6 to each dead embryo. The mean score was then calculated for all eleuthero embryos (pooled results) examined per condition.

5.10.3 Statistical Analysis

The results were obtained from three independent experiments, using ten larvae for each test concentration and compound. Statistical analysis was performed by using GraphPad Prism version 9.0 (GraphPad Software Inc., San Diego, CA, USA) and one-way analysis of variance (ANOVA) followed by Tukey's multiple comparison test. The criterion for statistical significance was $p < 0.05$.

6. CONCLUSIONS

6. Conclusions

I. Exploring the MEDINA's strain collection, 27 actinomycete strains were identified as possible phocoenamicins producers and they all belonged to the *Micromonospora* genus, suggesting that the biosynthesis of the phocoenamicins can be confined to *Micromonospora* species.

II. The phocoenamicin producing microbial strains were isolated from very diverse terrestrial and marine ecosystems, distributed throughout the planet, in contrast to initial descriptions of phocoenamicin production only from marine environments.

III. The culture media in which the *Micromonospora* strains were grown were identified as the most determining factor that influenced their metabolic profile, as well as the bioactivity profile against methicillin-resistant *S. aureus* (MRSA), *M. bovis* and *M. tuberculosis* H37Ra.

IV. The best producing strains, growth and chromatographic conditions for the production and isolation of the phocoenamicins were determined.

V. The compounds produced by the 27 strains in the different growth conditions were tentatively identified and were divided into three main groups, the spirotetronates, the siderophores and various other compounds, as well as several putatively new metabolites, structurally related to them.

VI. The spirotetronate maklamicin, structurally related to phocoenamicins, was also tentatively identified to be produced by all 27 strains and their coexistence in the extracts analyzed suggested a common biosynthetic origin of both families of compounds.

VII. The combination of the LC-UV-HRMS analysis, metabolomics analysis and molecular networking proved to be a fast and efficient way to prioritize strains and exploit their biosynthetic potential.

VIII. Three marine-derived *Micromonospora* species were identified as the best producers of phocoenamicins both in terms of the abundance in their extracts of some of the major compounds and the diversity of molecular structures produced.

IX. The cultivation of the three marine-derived strains led to the isolation and structural elucidation of two new phocoenamicins, phocoenamicins D and E, along with the three known phocoenamicins, as well as maklamicin and 29-deoxymaklamicin, reported for the first time as a natural product and for which the name maklamicin B is proposed.

X. The two families of compounds share many structural features, as well as common structural variations that were highlighted. One of the new phocoenamicins described bore the side chain of maklamicin, unique so far in this compound, indicating a functional group conserved within the two families.

XI. The bioactivity of the seven compounds isolated was evaluated against a panel of human pathogens and overall, the most active compounds were maklamicin B and maklamicin, followed by phocoenamicin and phocoenamicin B against MRSA, *M. tuberculosis* H37Ra, *E. faecalis* and *E. faecium*. Many of these activities were reported for the first time and were in some cases higher than the antibiotic used as positive control.

XII. As the compounds had small structural differences when compared to each other, the antibacterial assays revealed some structure-activity relationships.

XIII. The cytotoxicity of all the compounds and the toxicity against zebrafish eleuthero embryos of the three major compounds were evaluated and no broad-spectrum toxicity was detected at the highest concentration tested, making the most active of the compounds potential candidates for further research and development.

XIV. Maklamicin B was identified as the most interesting compound, combining strong antimicrobial activity against MRSA, *M. tuberculosis* and *E. faecium* and no cytotoxicity.

XV. The new analogues isolated highlighted the wide range of structural possibilities of the spirotetronates and the possible structure-activity relationships recorded can be used to unveil new biological activities.

---

7. SUPPLEMENTARY INFORMATION

7. Supplementary Information

Figure S1. PLS-DA 2D Score plots of the 270 *Micromonospora* extracts for the parameters (a) different strains, (b) taxonomy species, (c) geographic origin and (d) ecology. All four models resulted in overfitting and lack of validation.

Figure S2. The boxplot and density plot showing the normalization result in MetaboAnalyst 5.0 after sample normalization, data transformation and scaling of the preprocessed LC-HRMS data obtained from the 27 *Micromonospora* extracts in RAM2-P V2 medium.

Figure S3. Chromatographic profile obtained by MPLC/UV (Combiflash® Rf) from the crude extract of the 5 L fermentation of the CA-214671 strain grown in FR23 medium, absorbance: 210 nm (red) and 280 nm (purple).

Figure S4. Chromatographic profile obtained by MPLC/UV (Combiflash® Rf) from the crude extract of the 3 L fermentation of the CA-214658 strain grown in RAM2-P V2 medium, absorbance: 210 nm (red) and 280 nm (purple).

Figure S5. Chromatographic profile obtained by MPLC/UV (Combiflash® Rf) from the crude extract of the 3 L fermentation of the CA-218877 strain grown in RAM2-P V2 medium, absorbance: 210 nm (red) and 280 nm (purple).

Figure S6. ^{1}H NMR (methanol-d_4, 500 MHz) spectrum of compound **1**.

Figure S7. ^{13}C NMR (methanol-d_4, 125 MHz) spectrum of compound **1**.

Figure S8. HSQC spectrum of compound **1**.

Figure S9. COSY spectrum of compound **1**.

Figure S10. HMBC spectrum of compound **1**.

Figure S11. NOESY spectrum of compound **1**.

Figure S12. ^{1}H-^{1}H COSY and key HMBC correlations for compound **2**.

Figure S13. Key NOESY correlations for compound **2**.

Figure S14. ^{1}H NMR (methanol-d_4, 500 MHz) spectrum of compound **2**.

Figure S15. ^{13}C NMR (methanol-d_4, 125 MHz) spectrum of compound **2**.

Figure S16. HSQC spectrum of compound **2**.

Figure S17. COSY spectrum of compound **2**.

Figure S18. HMBC spectrum of compound **2**.

Figure S19. NOESY spectrum of compound **2**.

Figure S20. Key ROESY correlations for compound **6**.

Figure S21. ^{1}H NMR (methanol-d_4, 500 MHz) spectrum of compound **6**.

Figure S22. ^{13}C NMR (methanol-d_4, 125 MHz) spectrum of compound **6**.

Figure S23. HSQC spectrum of compound **6**.

Figure S24. COSY spectrum of compound **6**.

Figure S25. HMBC spectrum of compound **6**.

Figure S26. ROESY spectrum of compound **6**.

Table S1. Average % inhibition of the 270 *Micromonospora* extracts against MRSA MB5393, *M. bovis* BCG and *M. tuberculosis* H37Ra.

Table S2. Inhibition (%) of phocoenamicin B against MRSA (MB5973) and MSSA (ATCC29213).

Table S3. Inhibition (%) of phocoenamicin B against *M. tuberculosis* H37Ra and *M. bovis.*

Table S4. Inhibition (%) of phocoenamicin B against *E. faecium* VR (MBB5571), *E. faecium* (VS144754) and *E. faecalis* (VS144492).

Table S5. % inhibition of the seven spirotetronates against MRSA MB5393, *M. tuberculosis* H37Ra, *E. faecalis* VANS144492 and *E. faecium* VANS144754.

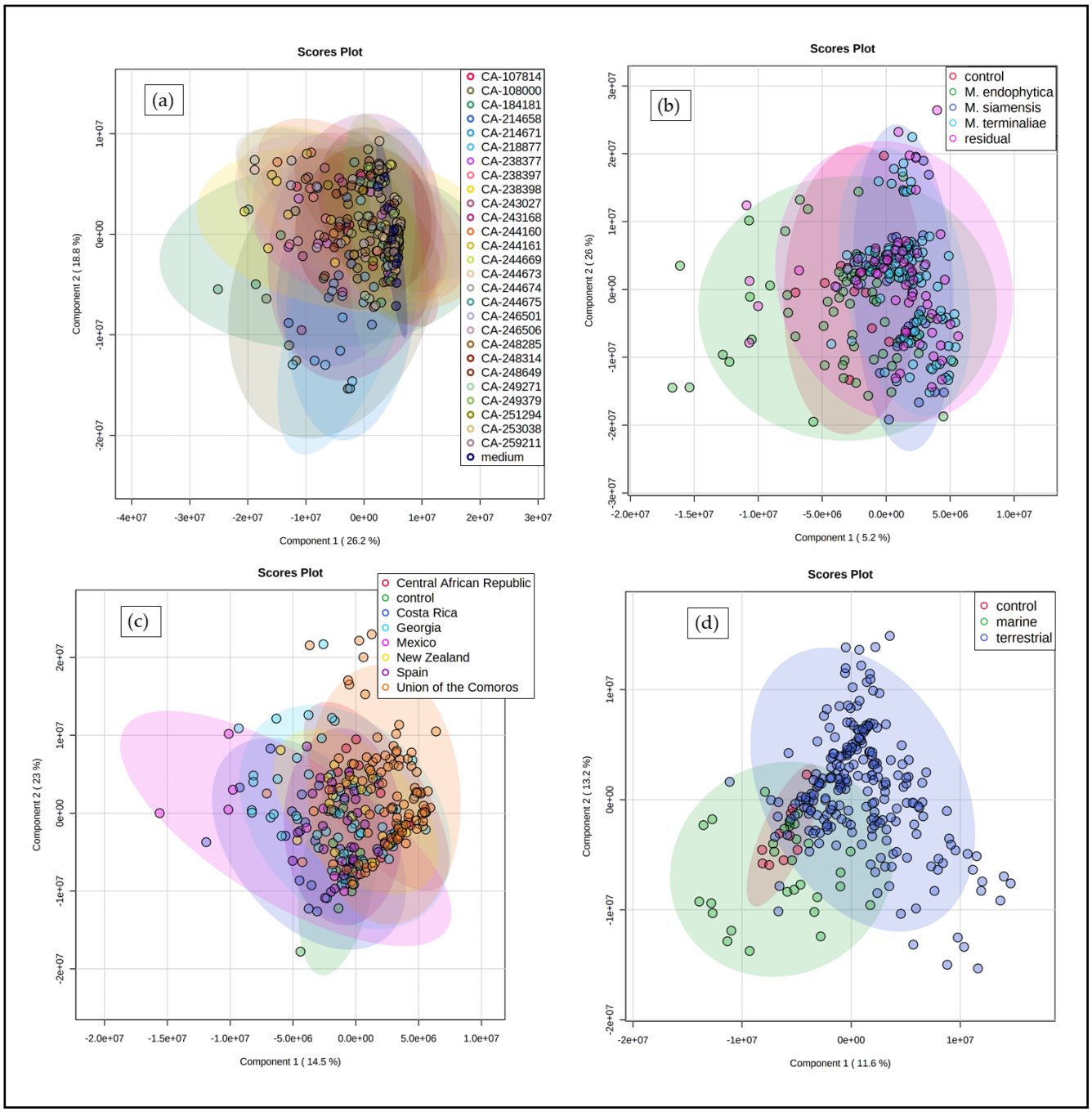

Figure S1. PLS-DA 2D Score plots of the 270 *Micromonospora* extracts for the parameters (a) different strains, (b) taxonomy species, (c) geographic origin and (d) ecology. All four models resulted in overfitting and lack of validation.

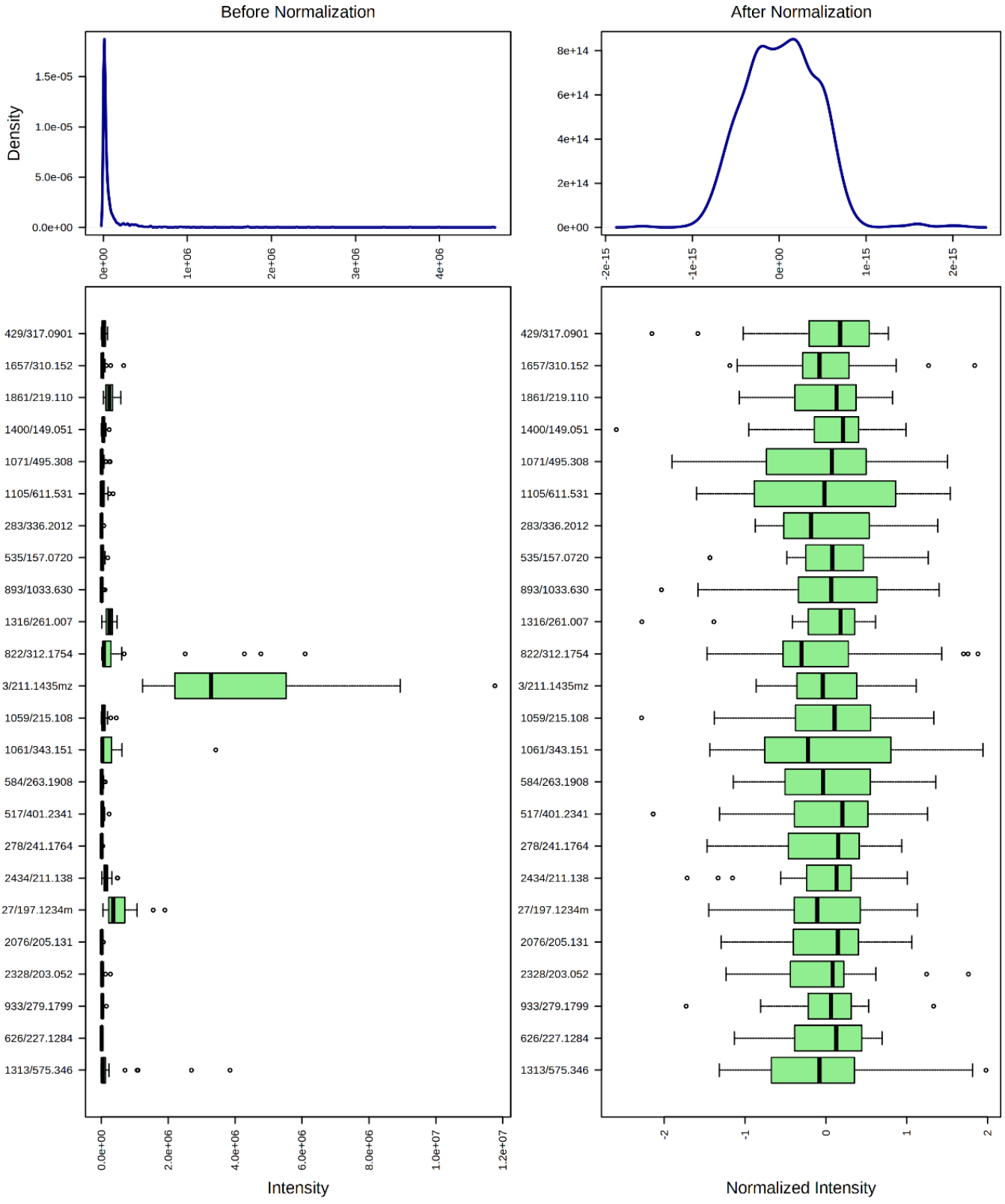

Figure S2. The boxplot and density plot showing the normalization result in MetaboAnalyst 5.0 after sample normalization, data transformation and scaling of the preprocessed LC-HRMS data obtained from the 27 *Micromonospora* extracts in RAM2-P V2 medium.

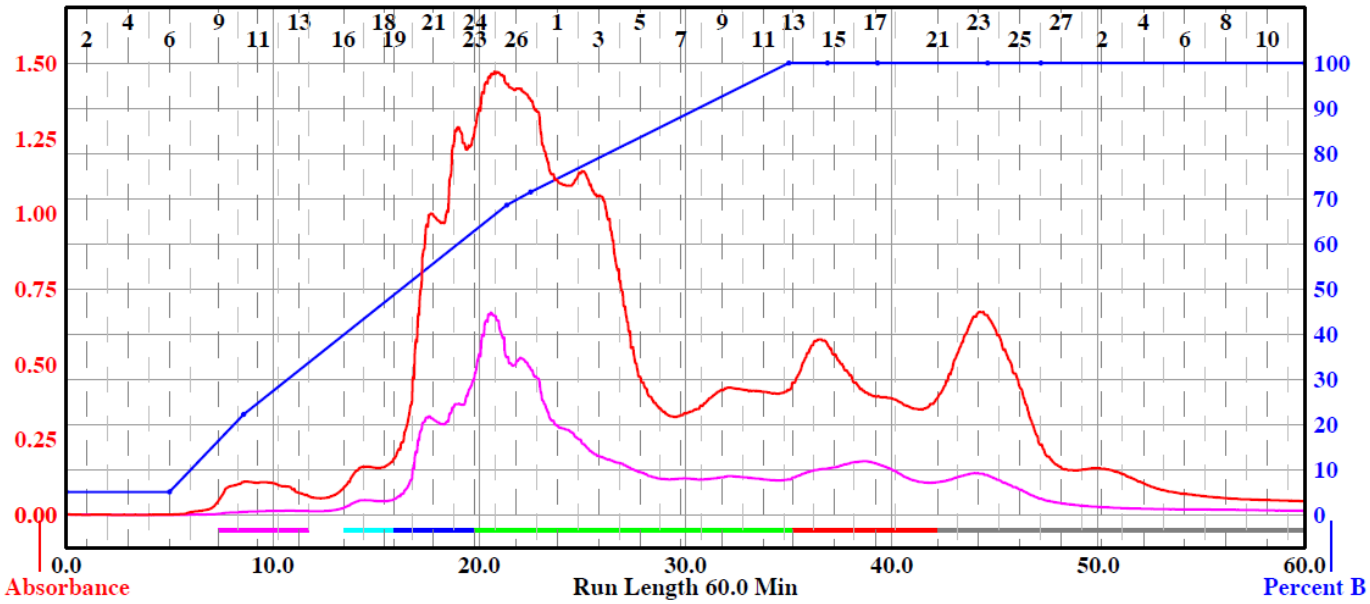

Figure S3. Chromatographic profile obtained by MPLC/UV (Combiflash® Rf) from the crude extract of the 5 L fermentation of the CA-214671 strain grown in FR23 medium, absorbance: 210 nm (red) and 280 nm (purple).

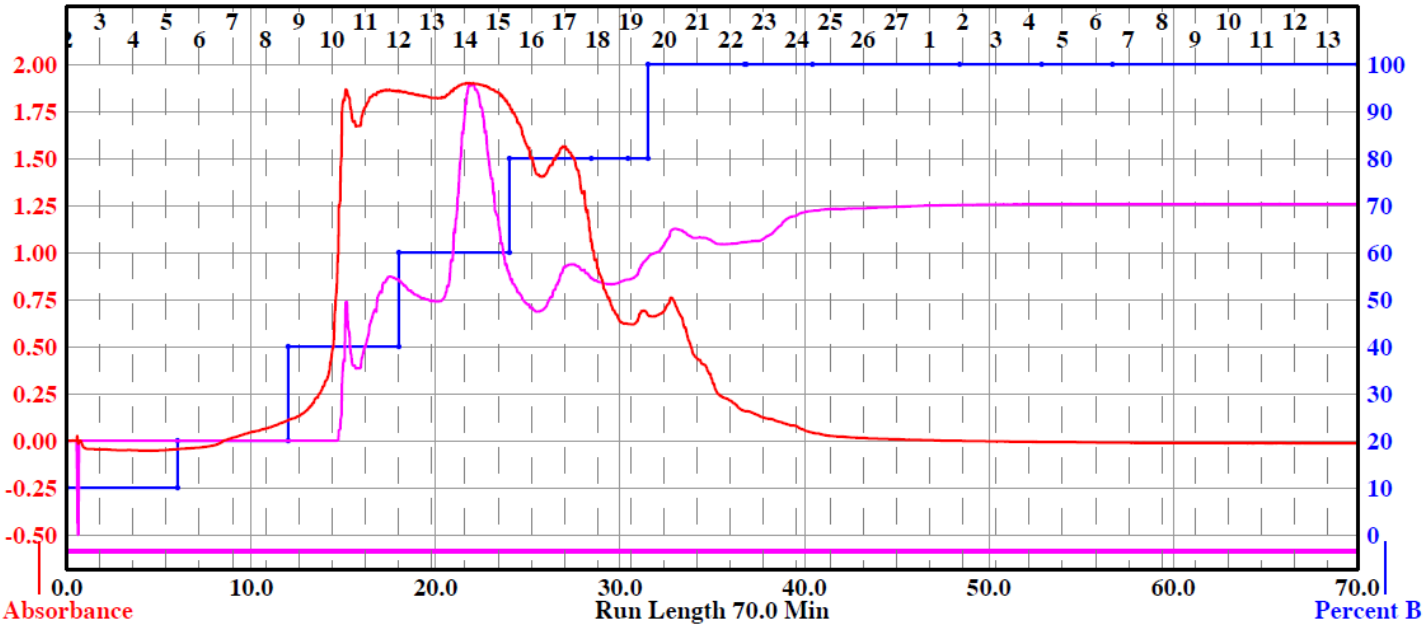

Figure S4. Chromatographic profile obtained by MPLC/UV (Combiflash® Rf) from the crude extract of the 3 L fermentation of the CA-214658 strain grown in RAM2-P V2 medium, absorbance: 210 nm (red) and 280 nm (purple).

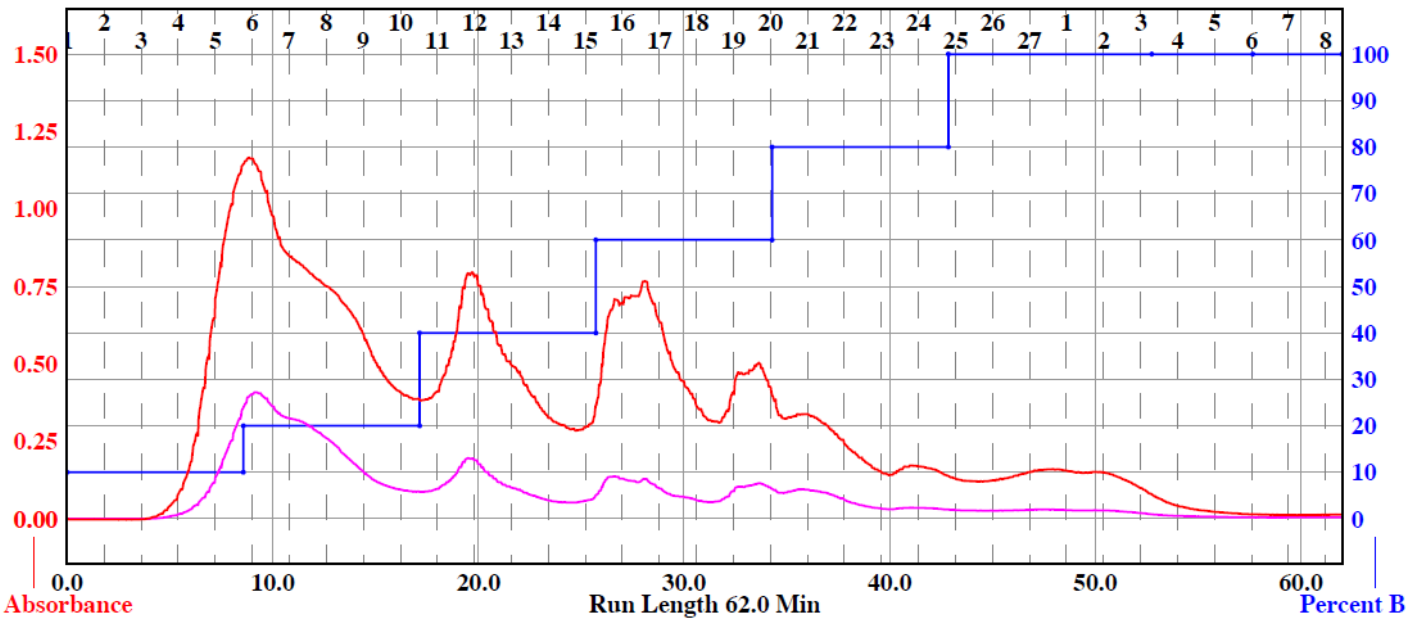

Figure S5. Chromatographic profile obtained by MPLC/UV (Combiflash® Rf) from the crude extract of the 3 L fermentation of the CA-218877 strain grown in RAM2-P V2 medium, absorbance: 210 nm (red) and 280 nm (purple).

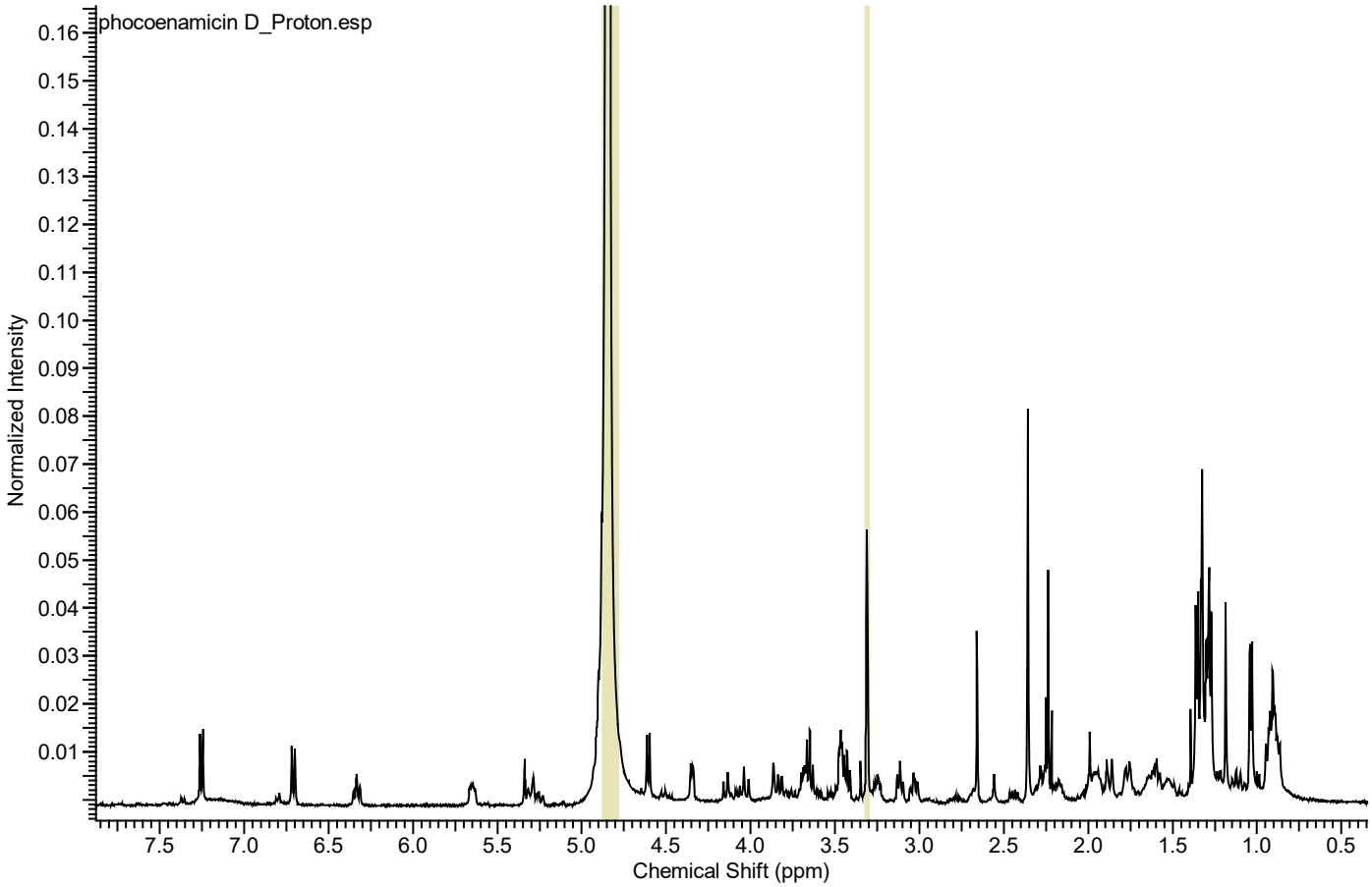

Figure S6. ^{1}H NMR (methanol-d_4, 500 MHz) spectrum of compound **1**.

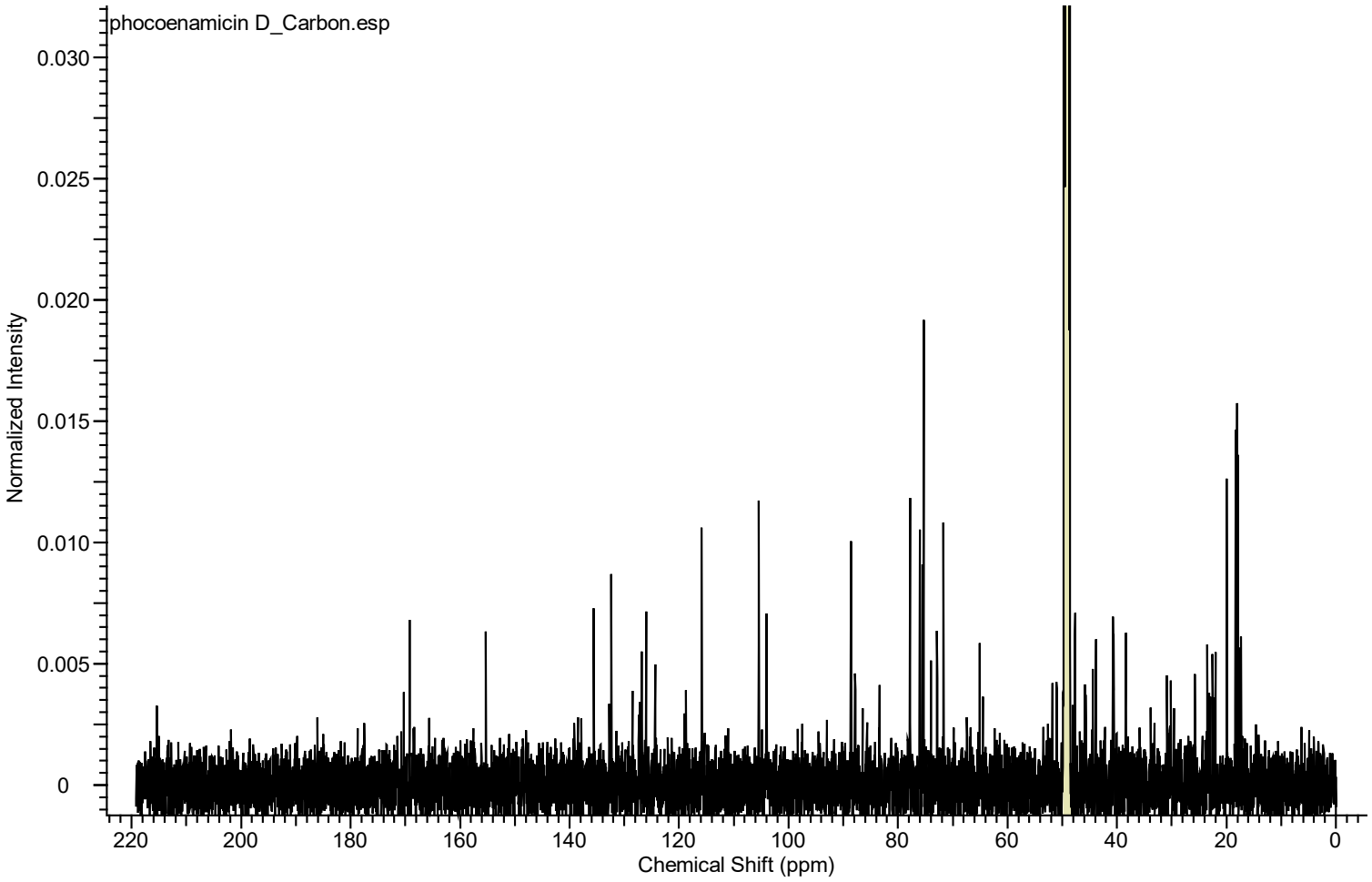

Figure S7. ^{13}C NMR (methanol-d_4, 125 MHz) spectrum of compound **1**.

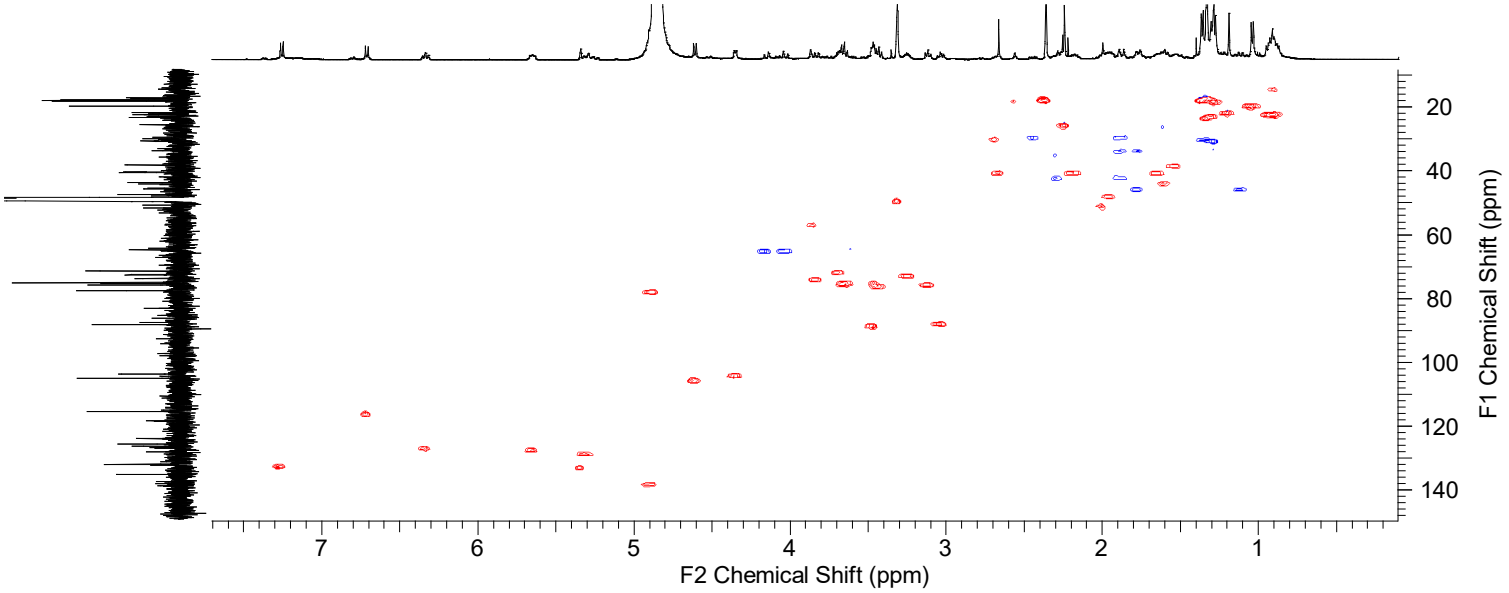

Figure S8. HSQC spectrum of compound **1**.

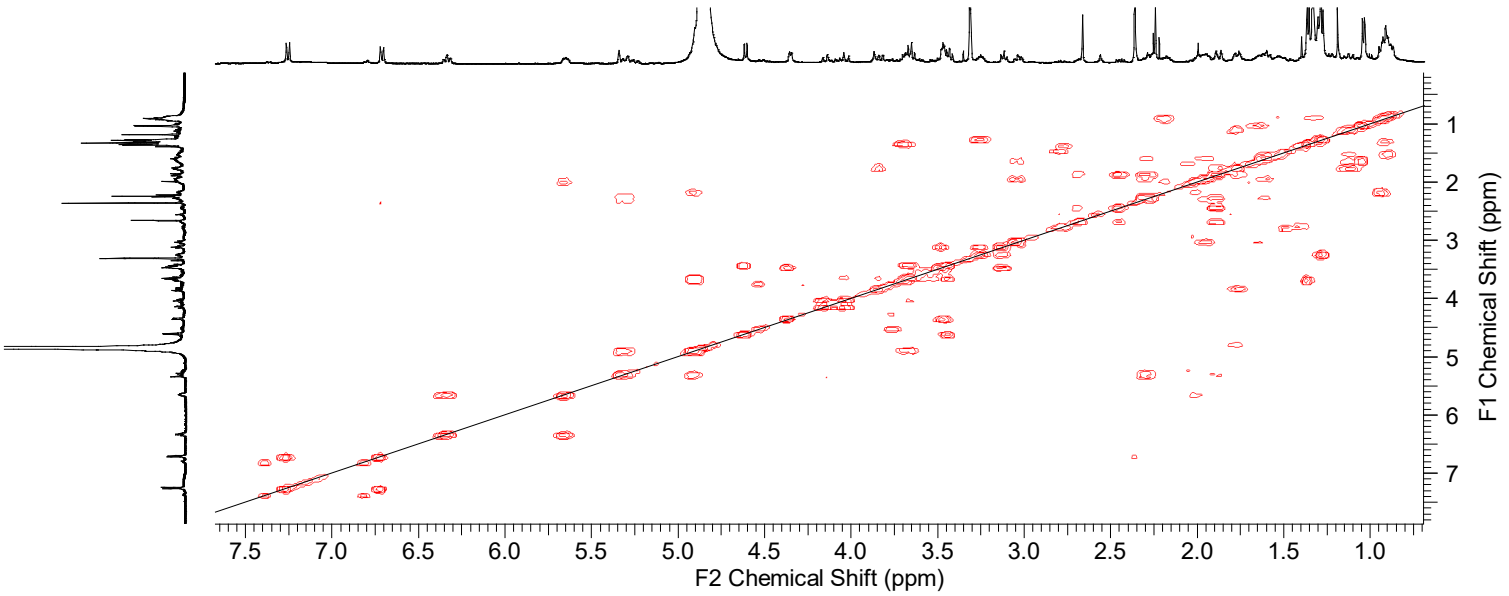

Figure S9. COSY spectrum of compound **1**.

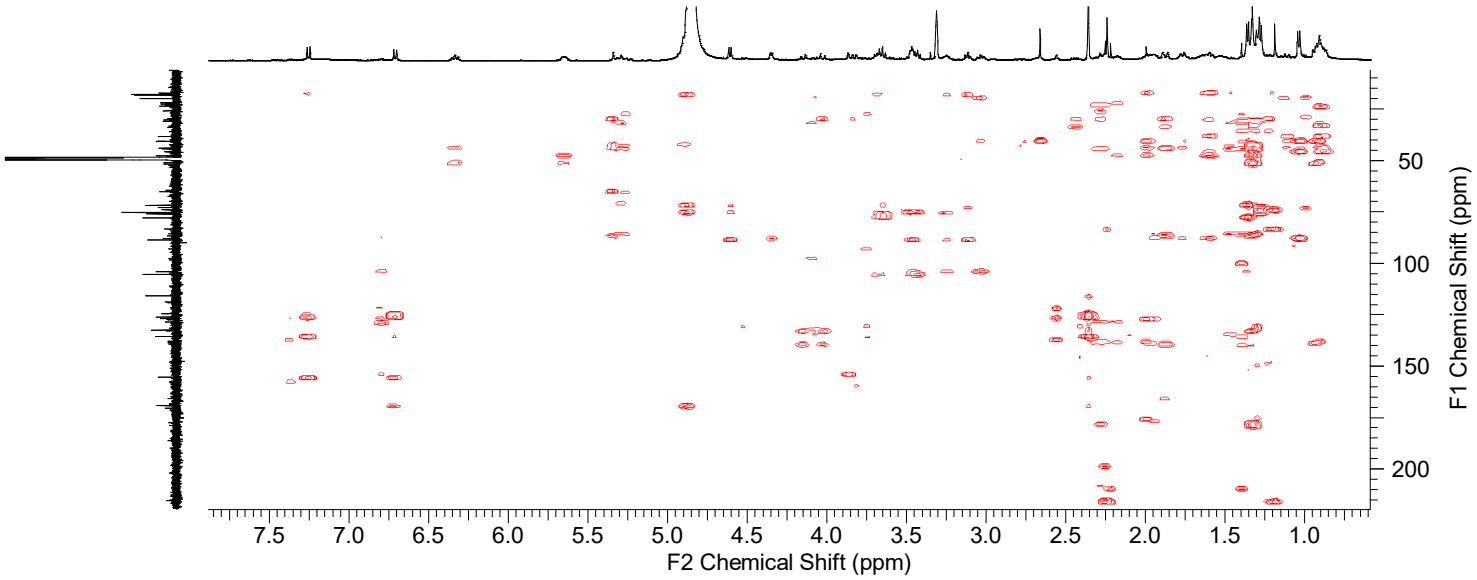

Figure S10. HMBC spectrum of compound **1**.

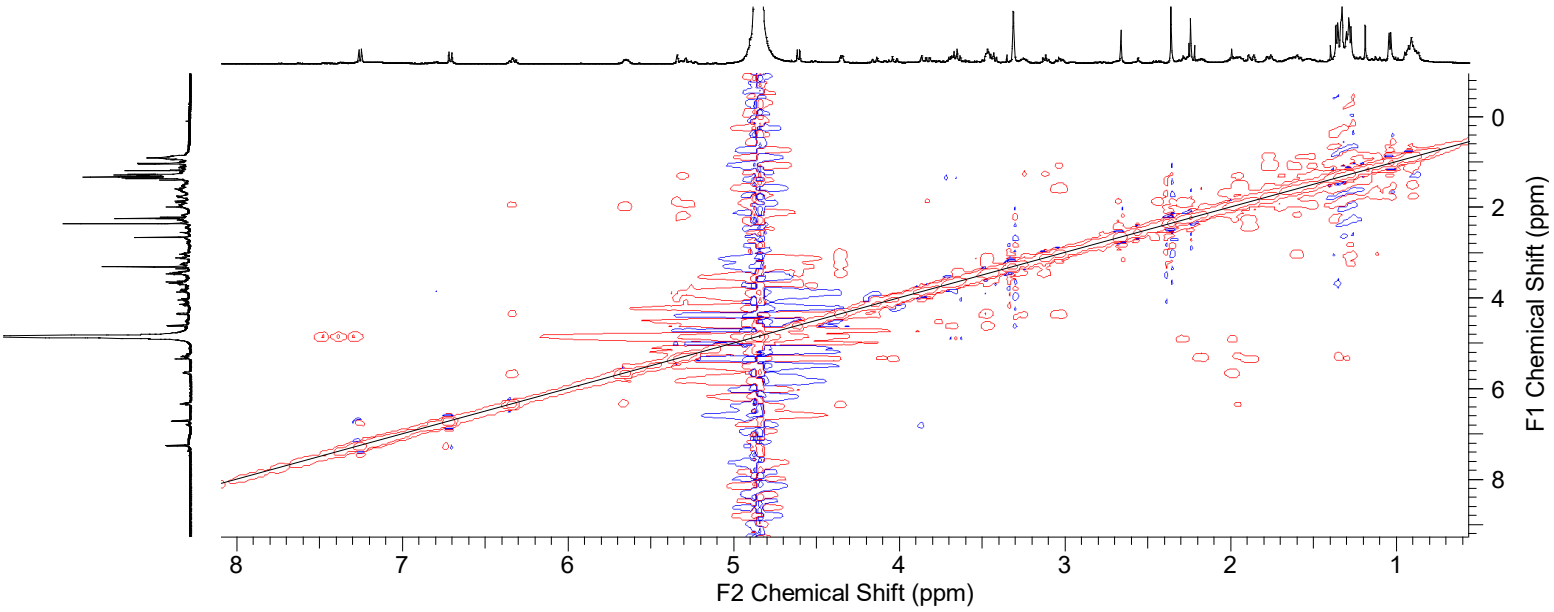

Figure S11. NOESY spectrum of compound **1**.

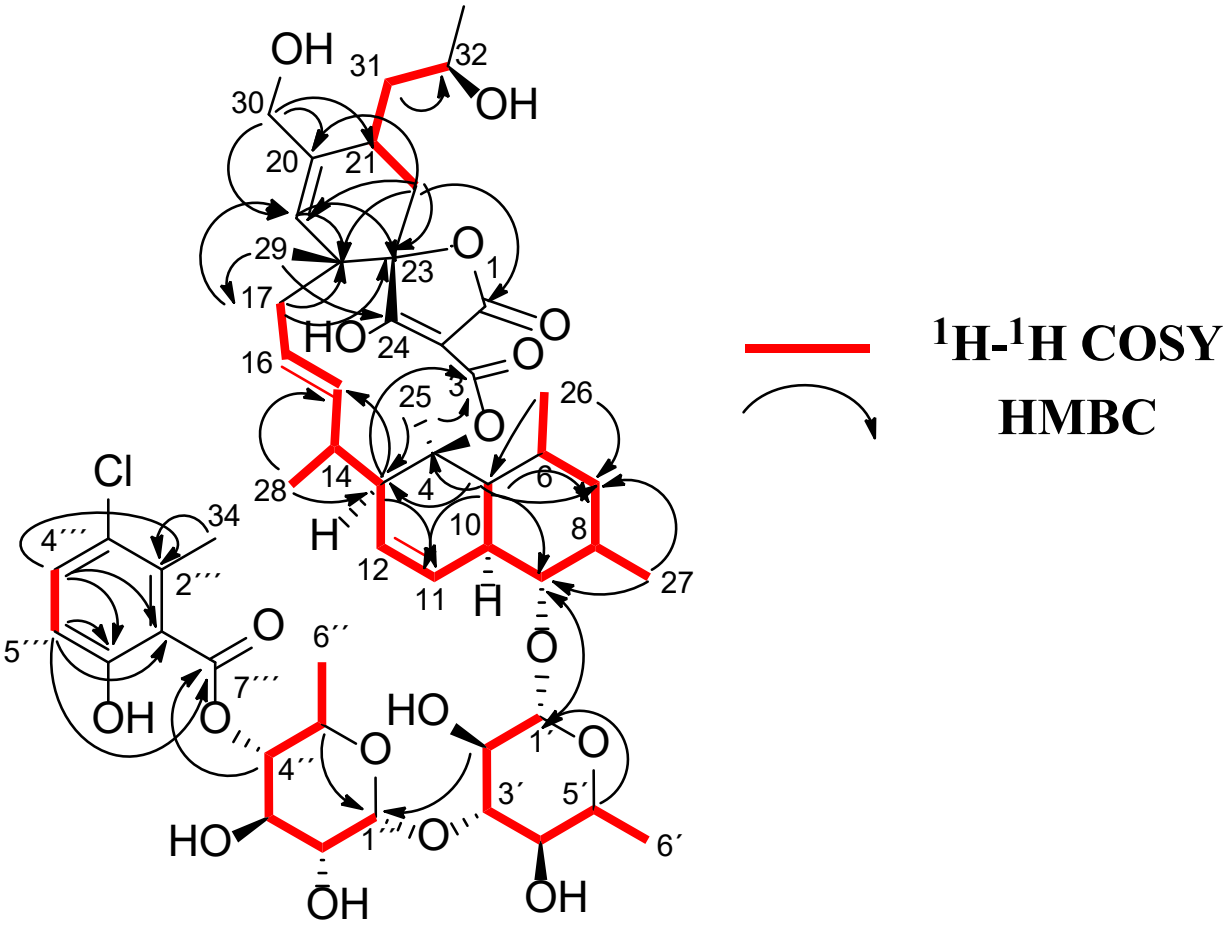

Figure S12. ^{1}H-^{1}H COSY and key HMBC correlations for compound **2**.

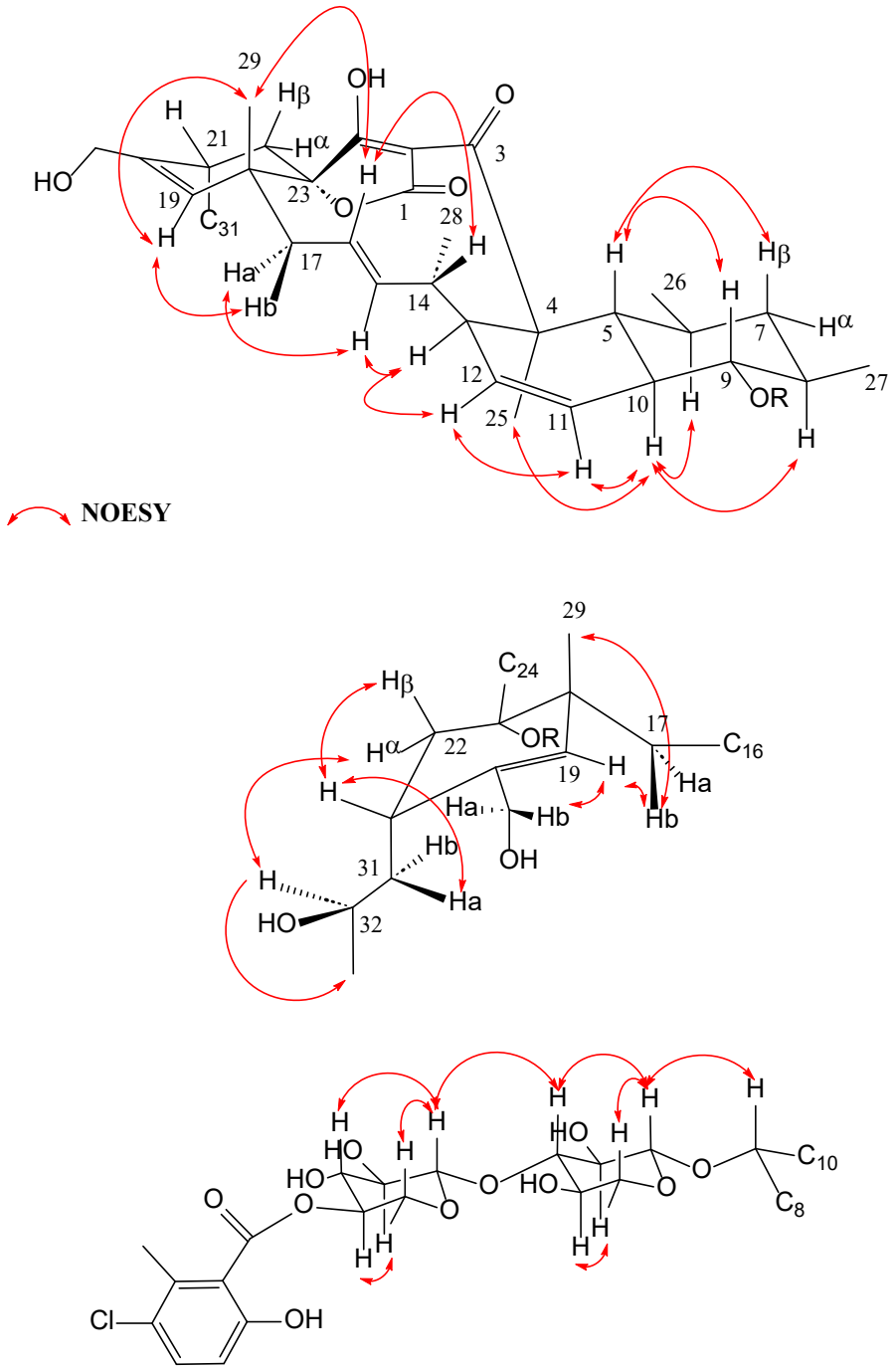

Figure S13. Key NOESY correlations for compound **2**.

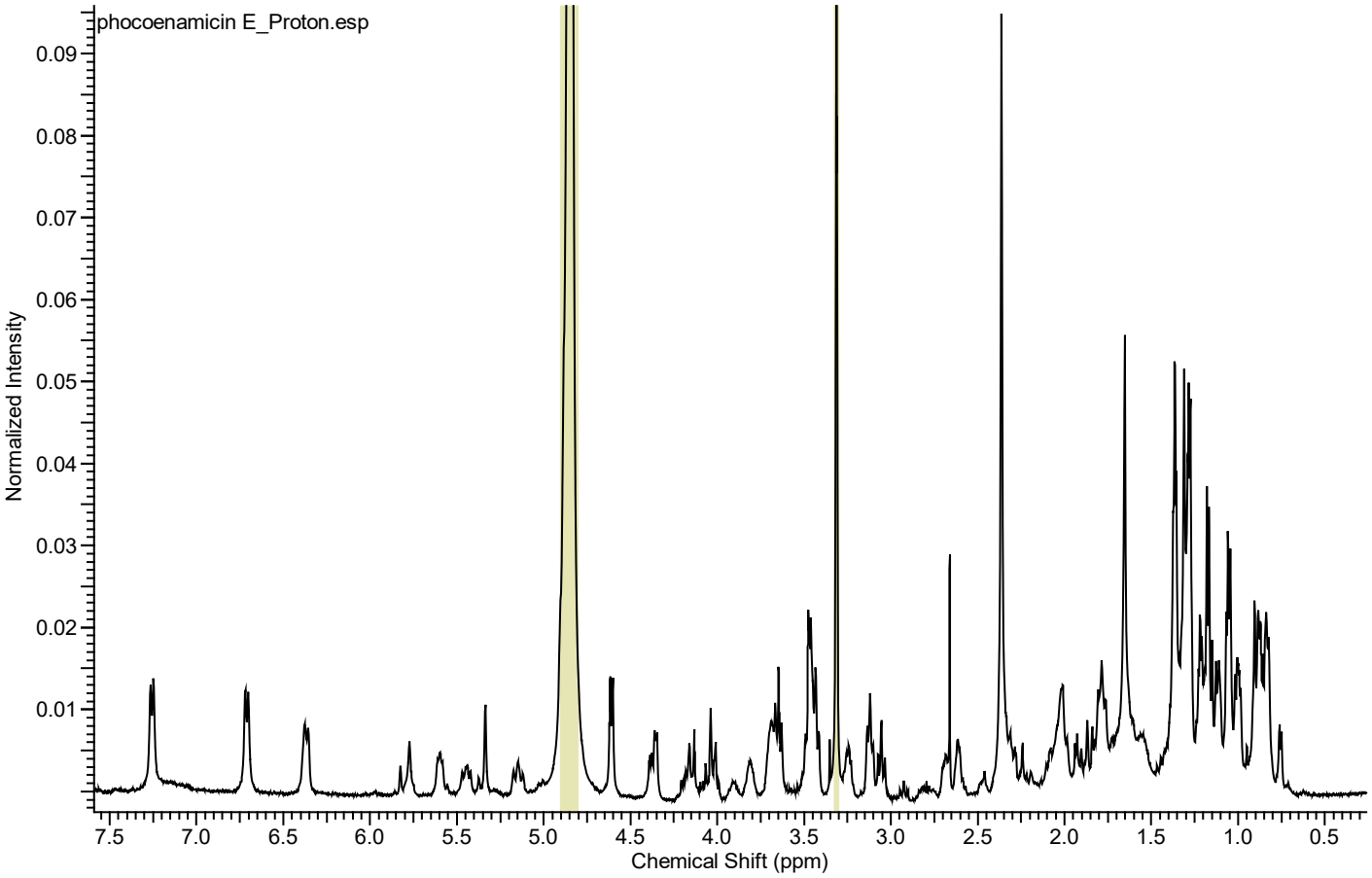

Figure S14. ^{1}H NMR (methanol-d_4, 500 MHz) spectrum of compound **2**.

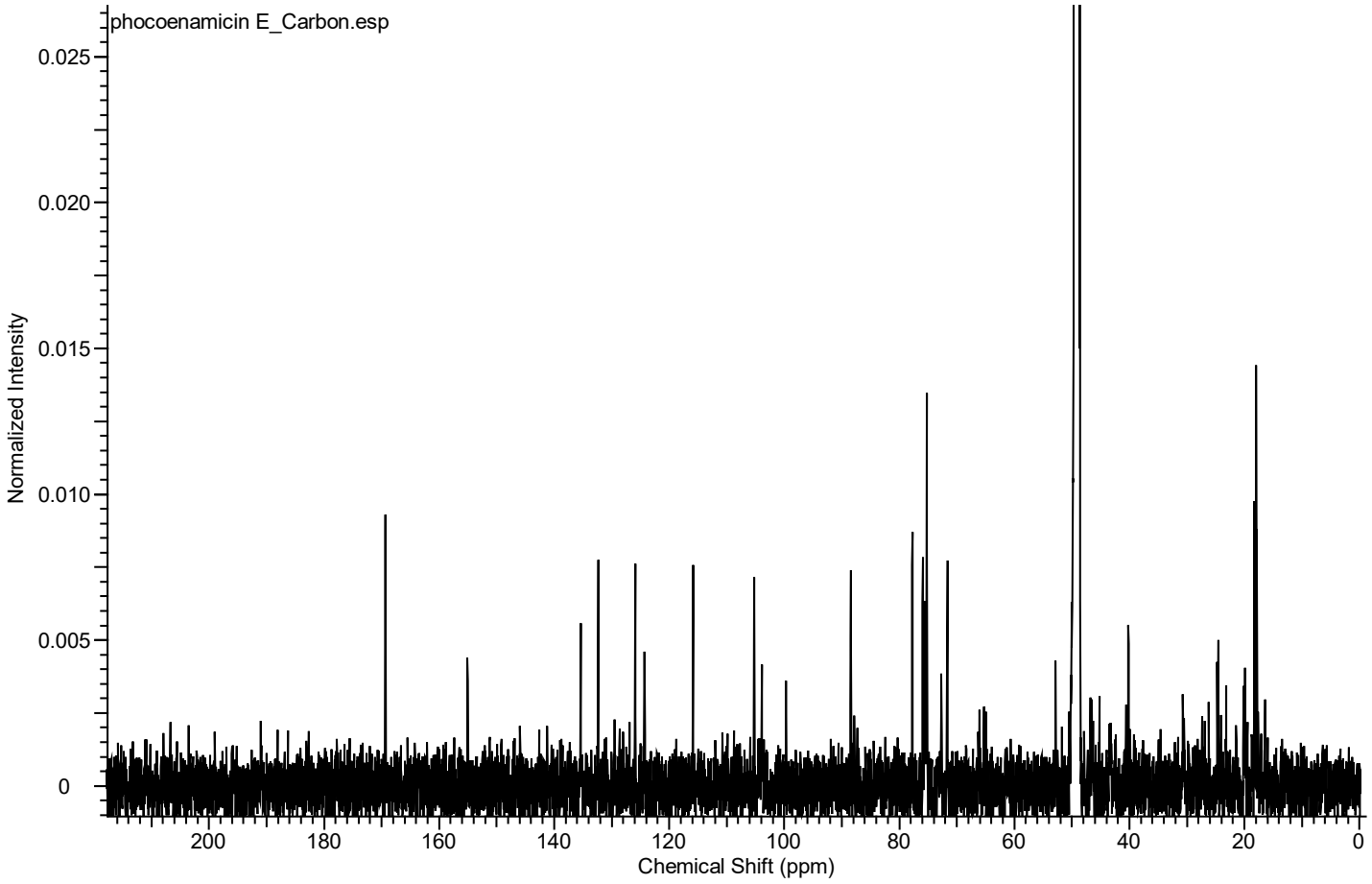

Figure S15. ^{13}C NMR (methanol-d_4, 125 MHz) spectrum of compound **2**.

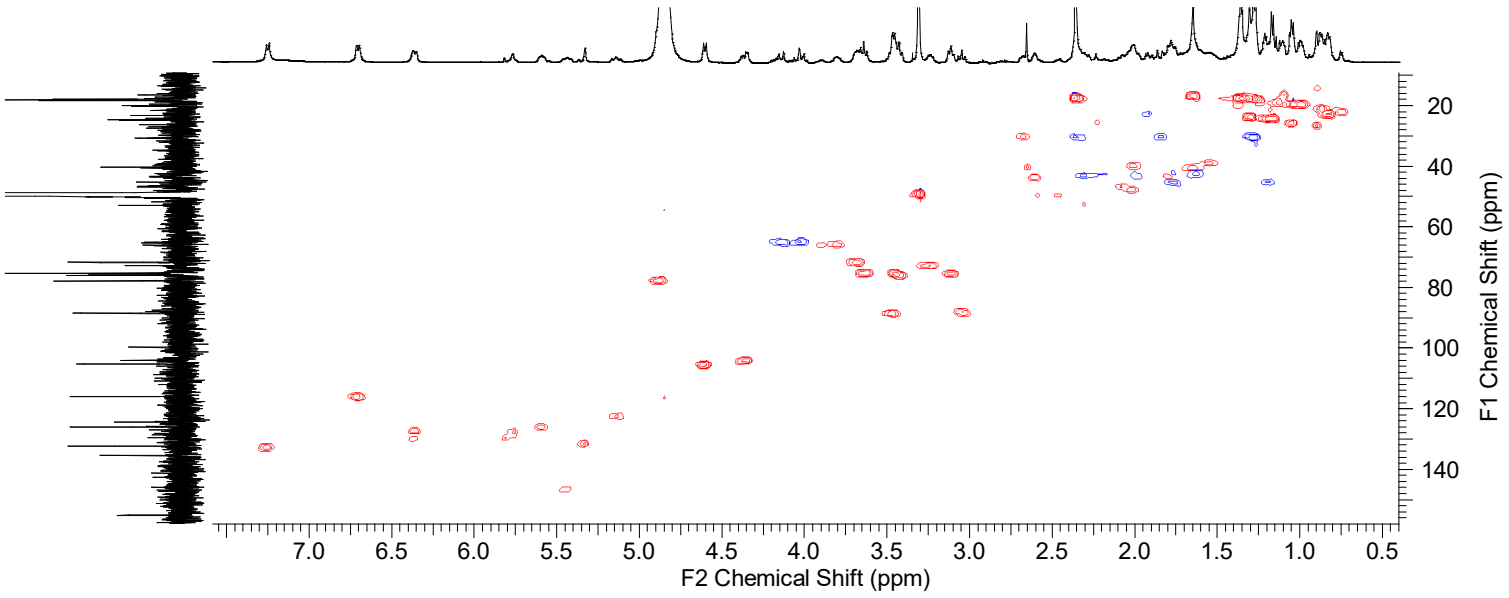

Figure S16. HSQC spectrum of compound **2**.

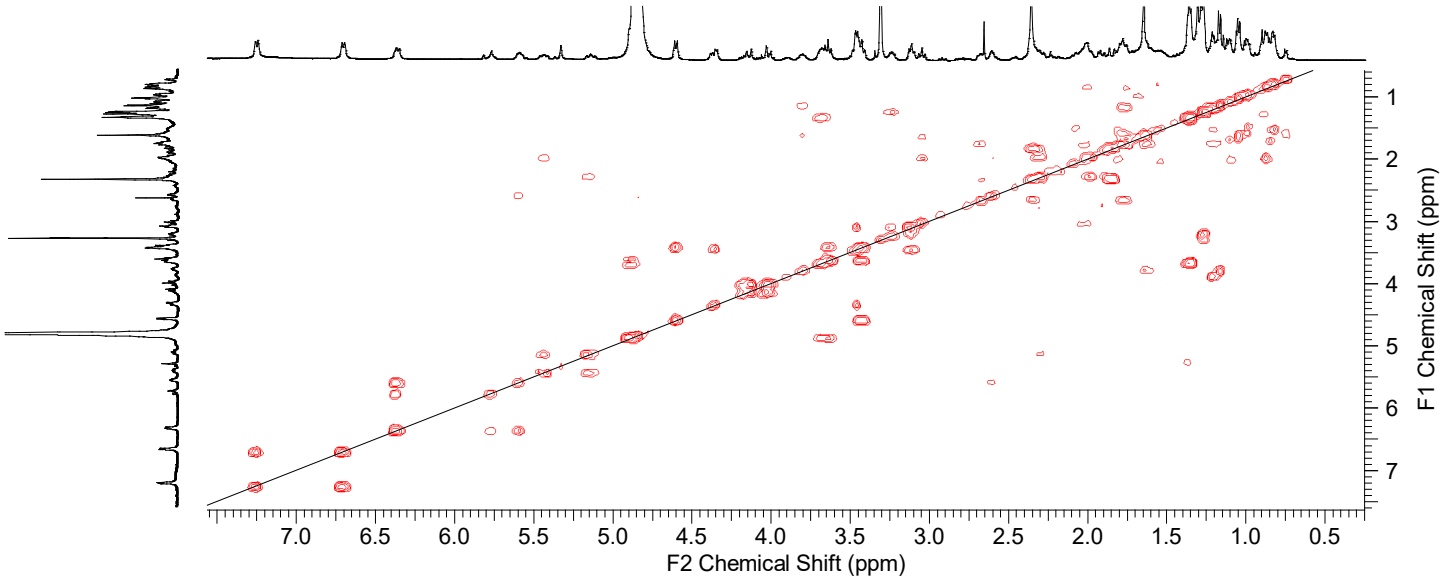

Figure S17. COSY spectrum of compound **2**.

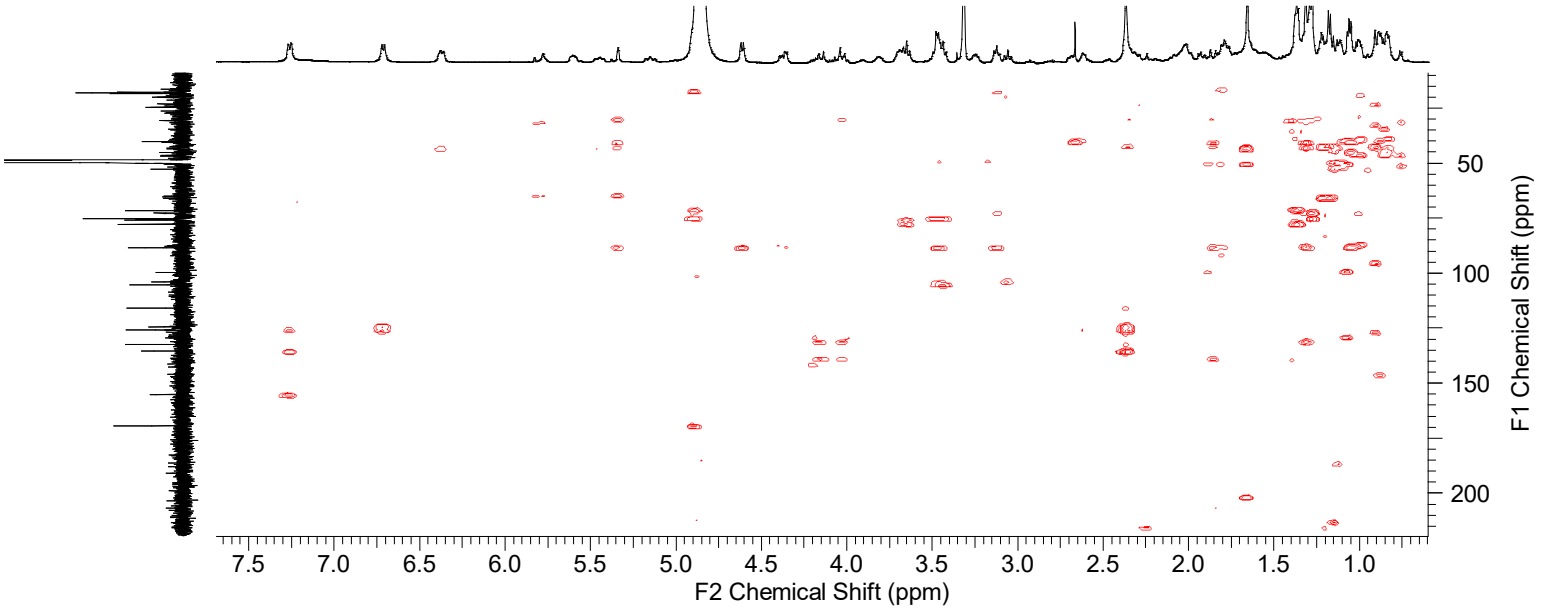

Figure S18. HMBC spectrum of compound **2**.

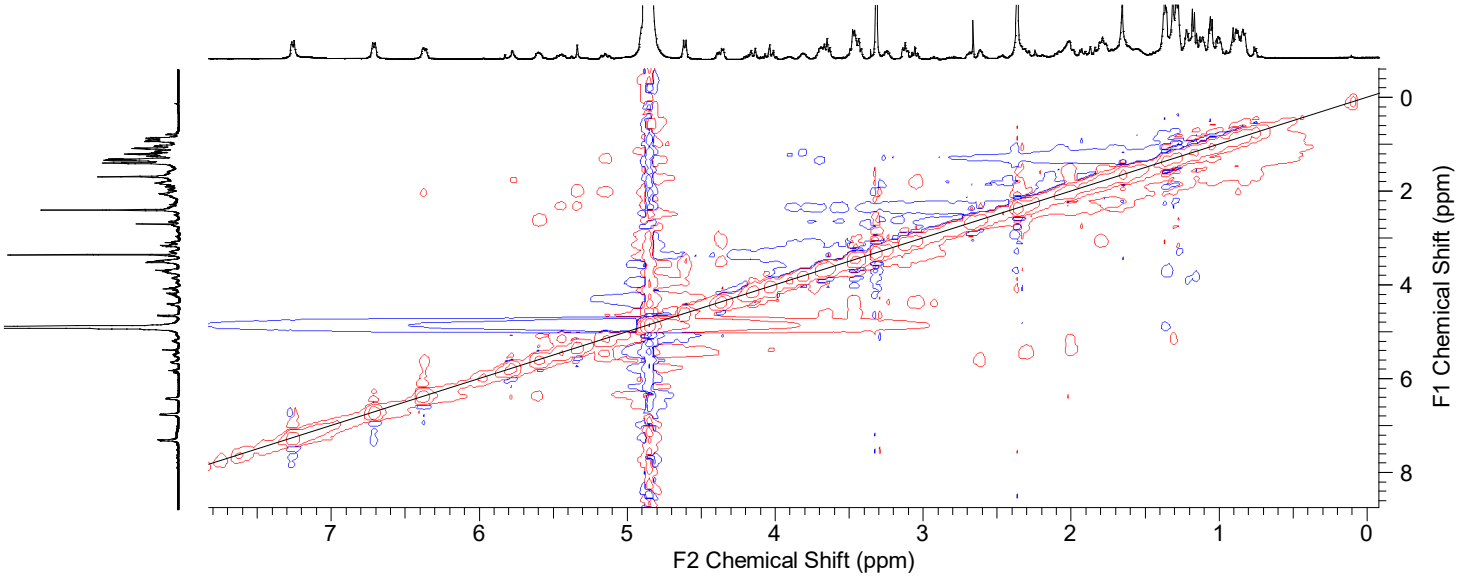

Figure S19. NOESY spectrum of compound **2**.

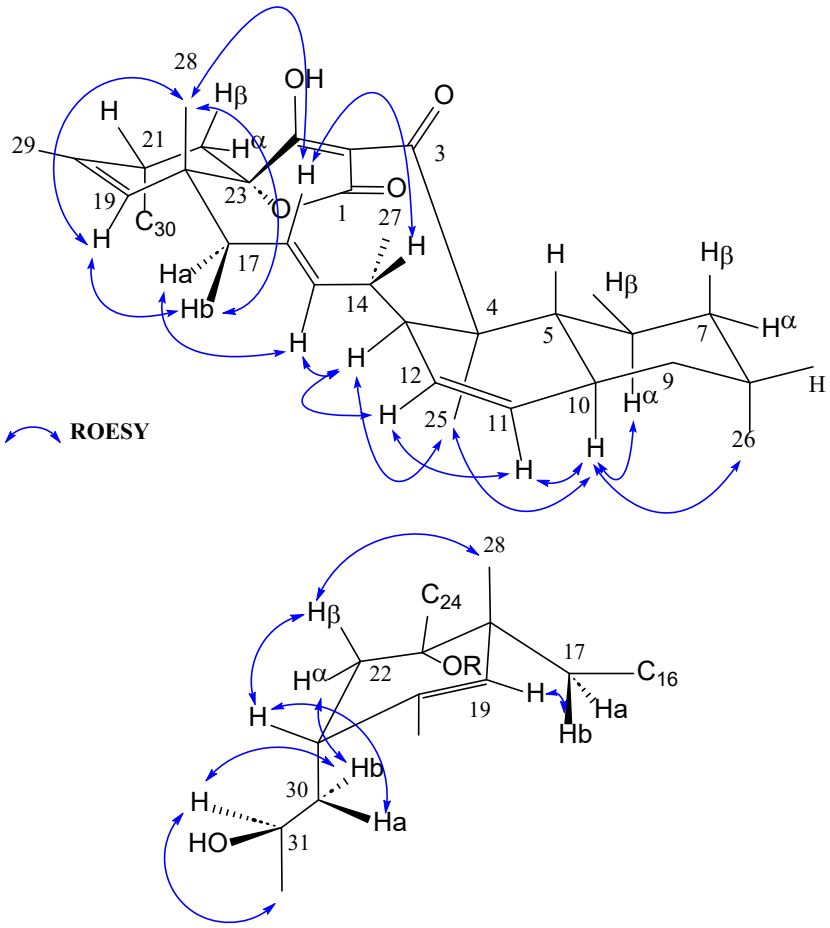

Figure S20. Key ROESY correlations for compound **6**.

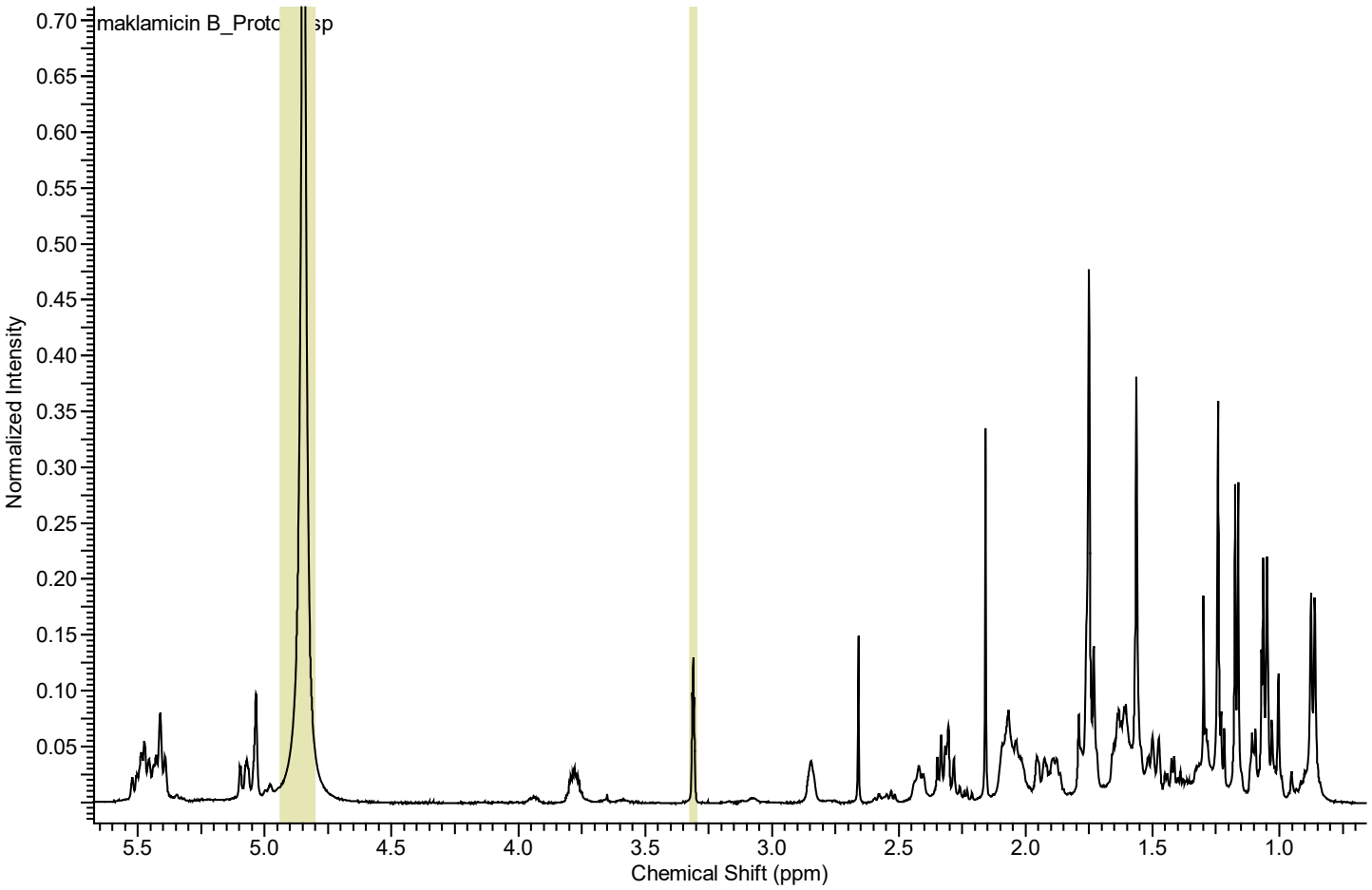

Figure S21. ^{1}H NMR (methanol-d_4, 500 MHz) spectrum of compound **6**.

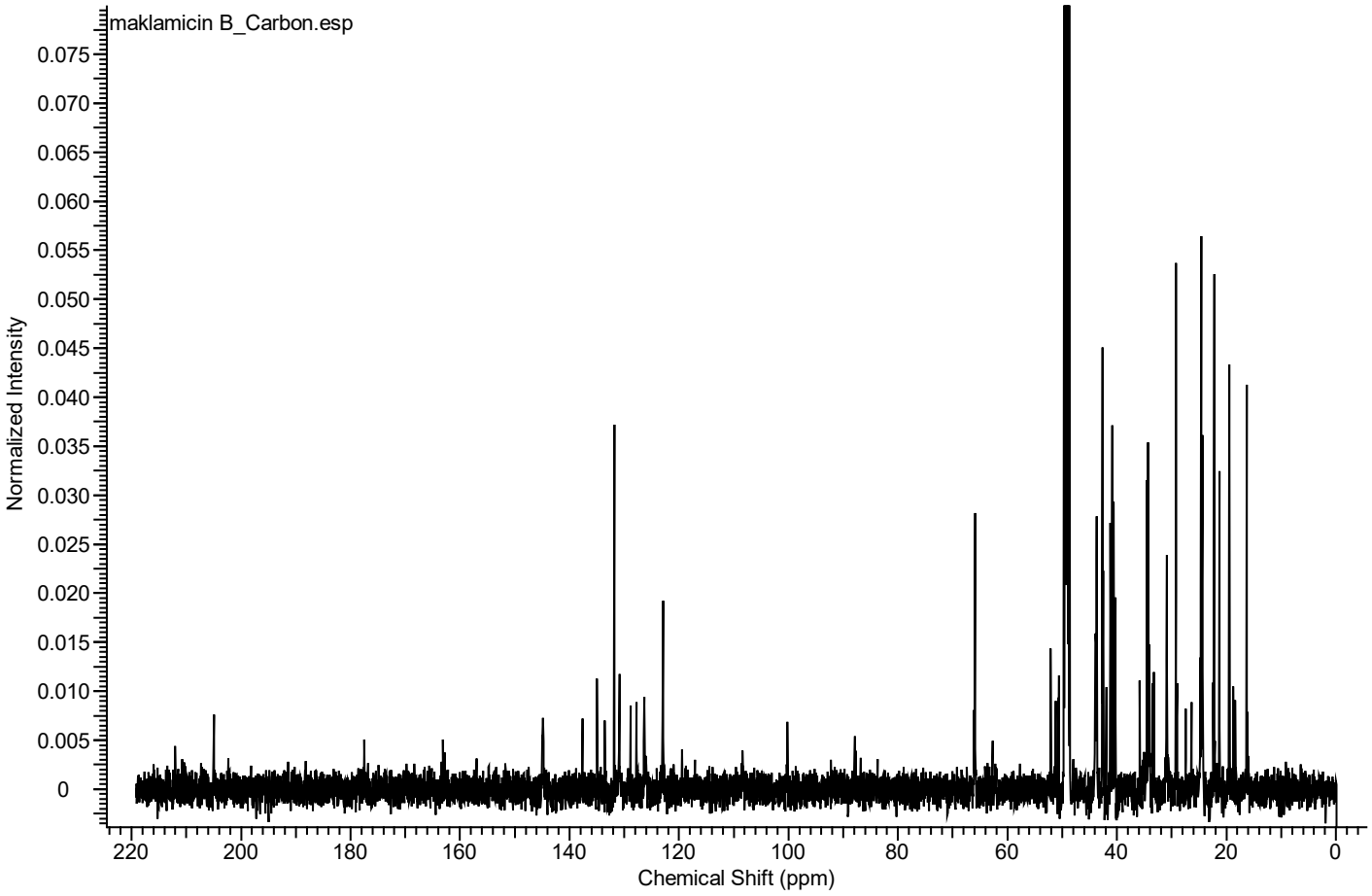

Figure S22. ^{13}C NMR (methanol-d_4, 125 MHz) spectrum of compound **6**.

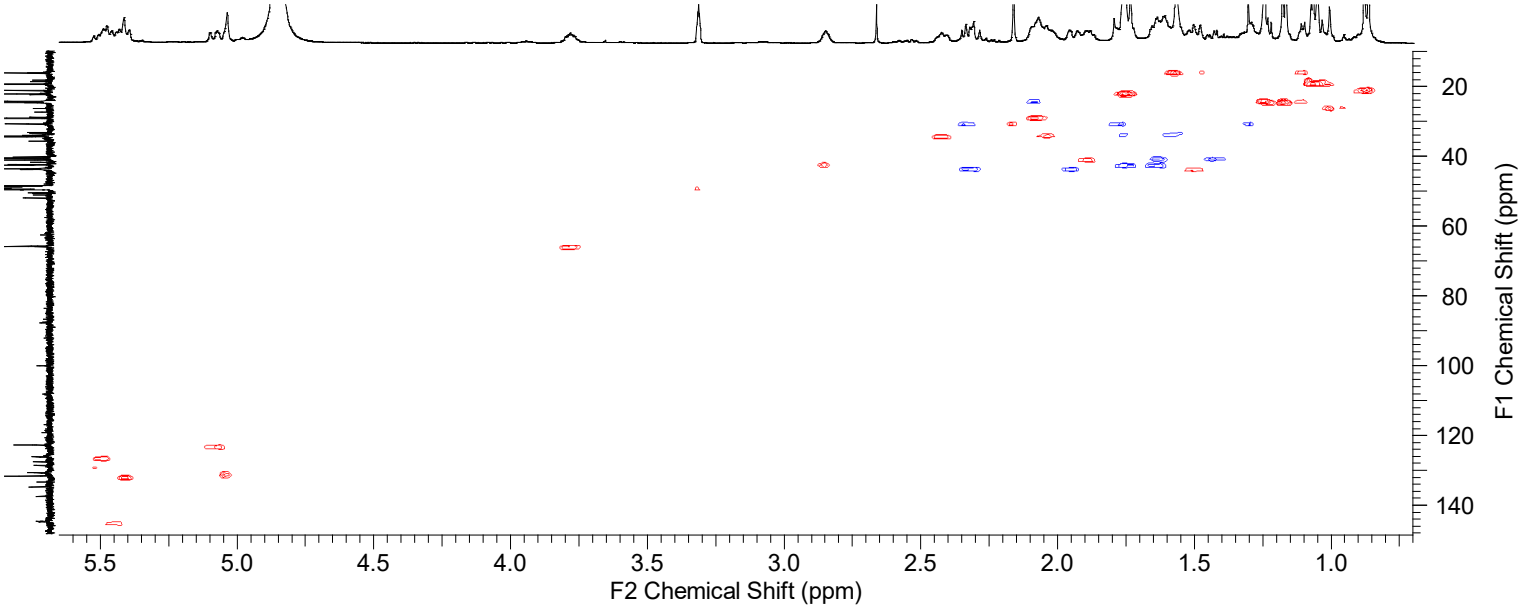

Figure S23. HSQC spectrum of compound **6**.

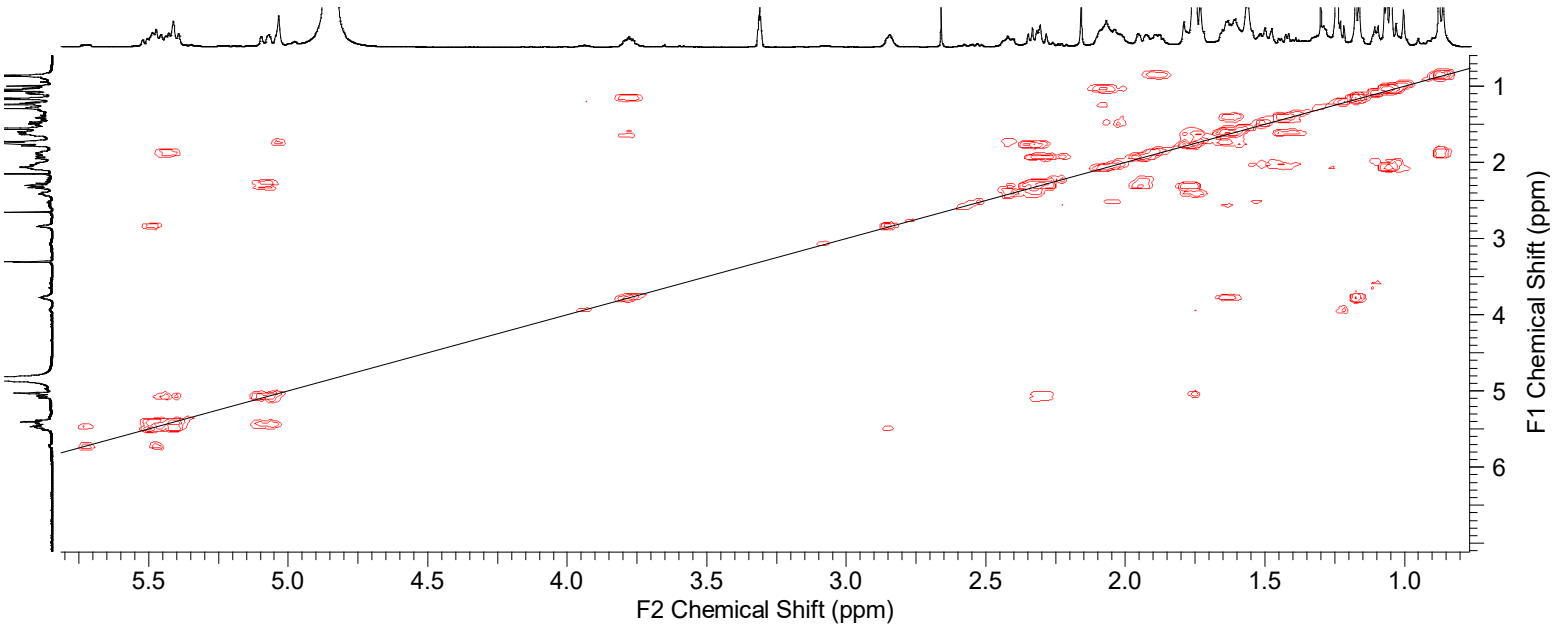

Figure S24. COSY spectrum of compound **6**.

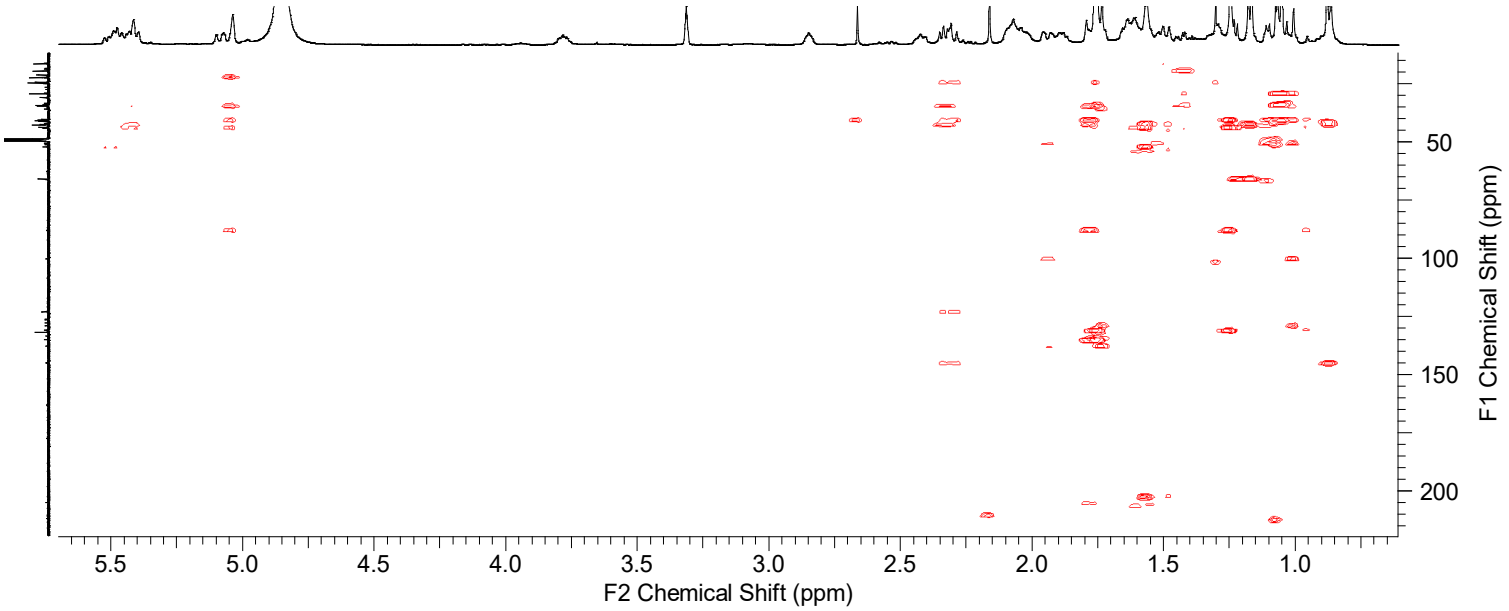

Figure S25. HMBC spectrum of compound **6**.

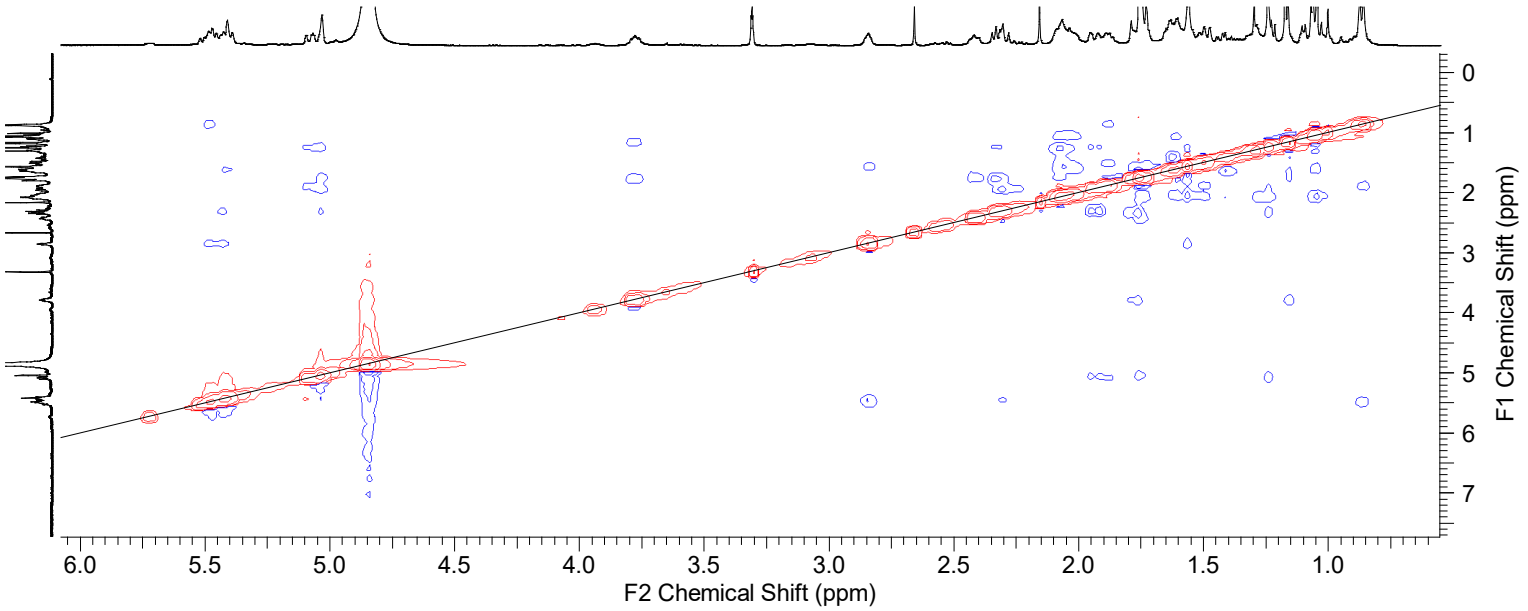

Figure S26. ROESY spectrum of compound **6**.

Table S1. Average % inhibition of the 270 *Micromonospora* extracts against MRSA MB5393, *M. bovis* BCG and *M. tuberculosis* H37Ra.

		Average % Inhibition		
STRAIN	**CULTURE MEDIUM**	**MRSA MB5393**	***M. tuberculosis* H37Ra**	***M. bovis* BCG**
CA-107814	APM9	-47,2	-89,7	-88,5
CA-107814	DEF-15	36,6	-38,9	-7,9
CA-107814	DEF-15S	25,8	-50,7	-10,2
CA-107814	DNPM	5,5	-96,8	-93,9
CA-107814	FPY-12	4,1	-86,9	-78,9
CA-107814	FPY-2	-99,1	-90,5	-89,1
CA-107814	FR23	-51,8	-93,8	-91,7
CA-107814	M016	-5,5	-90,5	-89,7
CA-107814	RAM2-P V2	-94,7	-92,1	-92,2
CA-107814	SAM-6	-4,5	-95,8	-93,5
CA-108000	APM9	-99,8	-90,0	-88,3
CA-108000	DEF-15	37,5	-75,6	-9,9
CA-108000	DEF-15S	28,2	-91,8	-11,7
CA-108000	DNPM	20,4	-97,0	-94,1
CA-108000	FPY-12	-97,0	-88,1	-88,1
CA-108000	FPY-2	-99,4	-90,6	-88,7
CA-108000	FR23	-38,1	-93,4	-90,7
CA-108000	M016	-99,5	-93,2	-91,8
CA-108000	RAM2-P V2	-90,4	-96,8	-94,5

CA-108000	SAM-6	-63,5	-95,2	-93,1
CA-184181	APM9	-94,7	-94,1	-92,2
CA-184181	DEF-15	23,8	-95,6	-9,8
CA-184181	DEF-15S	4,2	-60,6	-90,1
CA-184181	DNPM	25,1	-96,9	-91,4
CA-184181	FPY-12	-79,6	-87,7	-87,6
CA-184181	FPY-2	-101,7	-93,4	-91,6
CA-184181	FR23	-98,9	-96,9	-94,0
CA-184181	M016	-98,7	-97,3	-94,5
CA-184181	RAM2-P V2	-72,2	-97,1	-94,7
CA-184181	SAM-6	-100,9	-96,0	-93,2
CA-214658	APM9	-75,7	-91,7	-89,8
CA-214658	DEF-15	40,3	-35,5	-7,3
CA-214658	DEF-15S	27,2	-90,0	-23,4
CA-214658	DNPM	25,1	-96,5	-92,5
CA-214658	FPY-12	-36,3	-89,3	-88,3
CA-214658	FPY-2	-100,0	-93,0	-90,7
CA-214658	FR23	-65,7	-95,5	-91,7
CA-214658	M016	-101,9	-92,9	-91,5
CA-214658	RAM2-P V2	-67,6	-94,4	-92,5
CA-214658	SAM-6	5,9	-95,0	-90,5
CA-214671	APM9	-101,0	-89,4	-88,0
CA-214671	DEF-15	37,3	-62,5	-6,7
CA-214671	DEF-15S	26,5	-94,6	-50,9
CA-214671	DNPM	-16,0	-97,1	-93,5
CA-214671	FPY-12	-92,4	-92,2	-90,1
CA-214671	FPY-2	-92,3	-93,8	-91,7
CA-214671	FR23	16,8	-93,4	-28,7
CA-214671	M016	-90,0	-92,3	-89,6
CA-214671	RAM2-P V2	-68,8	-94,6	-91,9
CA-214671	SAM-6	-21,4	-57,9	-92,0
CA-218877	APM9	-97,0	-90,7	-86,5
CA-218877	DEF-15	39,2	-96,5	-11,5
CA-218877	DEF-15S	28,0	-88,9	-23,8
CA-218877	DNPM	-46,6	-96,5	-93,6
CA-218877	FPY-12	12,1	-88,3	-60,5
CA-218877	FPY-2	-86,7	-92,8	-90,7
CA-218877	FR23	9,8	-77,5	-84,8
CA-218877	M016	-101,5	-65,8	-15,1
CA-218877	RAM2-P V2	-77,3	-96,1	-93,0
CA-218877	SAM-6	15,8	-97,0	-93,0
CA-238377	APM9	-92,5	-92,9	-90,6
CA-238377	DEF-15	37,8	-26,7	-5,6
CA-238377	DEF-15S	5,8	-61,6	-32,1
CA-238377	DNPM	-98,0	-66,0	-94,1

CA-238377	FPY-12	-100,5	-89,6	-88,1
CA-238377	FPY-2	-94,0	-91,8	-88,6
CA-238377	FR23	-97,4	-31,4	-94,2
CA-238377	M016	-99,9	-97,0	-94,7
CA-238377	RAM2-P V2	-91,2	-96,5	-92,9
CA-238377	SAM-6	-99,7	-28,7	-72,2
CA-238397	APM9	-99,7	-91,8	-90,4
CA-238397	DEF-15	40,4	-69,5	-6,3
CA-238397	DEF-15S	23,2	-11,7	-7,0
CA-238397	DNPM	28,9	-94,4	-15,9
CA-238397	FPY-12	31,3	-6,0	-18,5
CA-238397	FPY-2	-98,8	-89,2	-88,7
CA-238397	FR23	-149,1	-34,0	-58,2
CA-238397	M016	-96,0	-72,0	-92,7
CA-238397	RAM2-P V2	-95,5	-92,9	-90,0
CA-238397	SAM-6	-100,2	-2,3	-60,8
CA-238398	APM9	-38,4	-92,4	-86,7
CA-238398	DEF-15	39,9	-7,5	-5,0
CA-238398	DEF-15S	27,0	-4,6	-5,0
CA-238398	DNPM	-3,1	-97,2	-41,5
CA-238398	FPY-12	-44,9	-10,0	-13,4
CA-238398	FPY-2	-55,0	-94,6	-52,7
CA-238398	FR23	-62,1	-95,2	-91,8
CA-238398	M016	-99,8	-93,5	-89,9
CA-238398	RAM2-P V2	0,1	-95,6	-68,3
CA-238398	SAM-6	-101,1	-95,8	-92,6
CA-243027	APM9	-88,9	-92,8	-89,7
CA-243027	DEF-15	38,7	-90,1	-10,1
CA-243027	DEF-15S	28,3	-11,1	-10,8
CA-243027	DNPM	33,7	-96,3	-93,2
CA-243027	FPY-12	28,3	-6,1	-9,4
CA-243027	FPY-2	-49,4	-90,4	-88,3
CA-243027	FR23	-97,1	-92,1	-93,8
CA-243027	M016	-79,7	-97,1	-94,8
CA-243027	RAM2-P V2	-62,6	-93,6	-89,3
CA-243027	SAM-6	-64,4	-95,4	-92,4
CA-243168	APM9	-79,9	-87,2	-89,8
CA-243168	DEF-15	41,6	-35,3	-7,2
CA-243168	DEF-15S	30,1	-97,6	-14,6
CA-243168	DNPM	14,5	-96,3	-86,1
CA-243168	FPY-12	-99,9	-87,7	-87,2
CA-243168	FPY-2	-89,7	-91,4	-89,1
CA-243168	FR23	38,8	-94,5	-39,4
CA-243168	M016	-97,1	-94,7	-92,4
CA-243168	RAM2-P V2	-100,4	-95,5	-91,9

CA-243168	SAM-6	-59,4	-96,2	-92,5
CA-244160	APM9	-95,7	-90,5	-88,5
CA-244160	DEF-15	40,2	4,3	-2,2
CA-244160	DEF-15S	4,8	-94,8	-84,7
CA-244160	DNPM	29,1	-98,7	-92,1
CA-244160	FPY-12	-115,7	-89,1	-86,5
CA-244160	FPY-2	-35,3	-91,9	-90,1
CA-244160	FR23	-54,8	-96,4	-92,5
CA-244160	M016	-100,2	-95,7	-94,0
CA-244160	RAM2-P V2	-53,9	-95,2	-92,4
CA-244160	SAM-6	-102,4	-93,6	-91,8
CA-244161	APM9	-87,9	-89,9	-89,1
CA-244161	DEF-15	37,5	-97,7	-22,6
CA-244161	DEF-15S	5,2	-97,9	-21,4
CA-244161	DNPM	18,1	-98,8	-92,4
CA-244161	FPY-12	-94,6	-89,4	-88,2
CA-244161	FPY-2	-95,2	-90,3	-89,7
CA-244161	FR23	-18,7	-96,9	-95,4
CA-244161	M016	-99,8	-94,9	-91,8
CA-244161	RAM2-P V2	-98,6	-96,3	-92,9
CA-244161	SAM-6	-100,4	-95,0	-92,3
CA-244669	APM9	-9,7	-90,5	-73,1
CA-244669	DEF-15	-7,1	-10,2	-4,6
CA-244669	DEF-15S	-23,1	-6,4	-5,2
CA-244669	DNPM	20,6	4,9	-10,3
CA-244669	FPY-12	-48,1	-88,3	-15,8
CA-244669	FPY-2	31,9	-62,7	-6,3
CA-244669	FR23	-99,4	-95,7	-91,1
CA-244669	M016	-99,9	-94,9	-90,6
CA-244669	RAM2-P V2	6,4	-78,4	-14,1
CA-244669	SAM-6	-99,5	-74,3	-92,7
CA-244673	APM9	-82,0	-94,0	-91,0
CA-244673	DEF-15	29,5	-98,8	-55,8
CA-244673	DEF-15S	24,1	-82,8	-69,4
CA-244673	DNPM	24,4	-17,4	-8,9
CA-244673	FPY-12	-82,8	-88,0	-86,5
CA-244673	FPY-2	24,2	-91,5	-88,4
CA-244673	FR23	-94,5	-96,2	-92,0
CA-244673	M016	-157,3	-33,7	-57,6
CA-244673	RAM2-P V2	34,8	-93,5	-86,7
CA-244673	SAM-6	-99,4	-94,9	-90,4
CA-244674	APM9	-90,4	-91,1	-89,7
CA-244674	DEF-15	36,6	2,5	-0,4
CA-244674	DEF-15S	10,7	-97,4	-65,7
CA-244674	DNPM	15,7	-97,5	-13,8

CA-244674	FPY-12	-90,6	-89,6	-87,9
CA-244674	FPY-2	37,9	-61,7	-9,1
CA-244674	FR23	-86,6	-42,6	-83,4
CA-244674	M016	-87,0	-84,6	-96,0
CA-244674	RAM2-P V2	-99,0	-95,7	-93,3
CA-244674	SAM-6	-85,0	-94,3	-90,3
CA-244675	APM9	-90,0	-90,4	-88,0
CA-244675	DEF-15	22,3	-96,7	-4,7
CA-244675	DEF-15S	-3,8	-98,0	-62,1
CA-244675	DNPM	-98,6	-92,2	-93,9
CA-244675	FPY-12	-98,0	-88,7	-87,7
CA-244675	FPY-2	-81,5	-92,2	-90,5
CA-244675	FR23	-126,8	-81,8	-92,7
CA-244675	M016	-99,5	-96,0	-91,9
CA-244675	RAM2-P V2	-99,3	-94,4	-90,8
CA-244675	SAM-6	-98,9	-95,4	-84,8
CA-246501	APM9	-91,9	-94,1	-91,1
CA-246501	DEF-15	42,0	-0,7	-2,6
CA-246501	DEF-15S	8,6	-62,3	-81,3
CA-246501	DNPM	-41,9	-98,0	-93,8
CA-246501	FPY-12	-139,0	-89,4	-88,4
CA-246501	FPY-2	-91,5	-91,5	-88,5
CA-246501	FR23	-95,6	-97,1	-76,1
CA-246501	M016	-98,6	-96,4	-91,6
CA-246501	RAM2-P V2	-103,9	-95,2	-92,4
CA-246501	SAM-6	-100,3	-96,4	-92,9
CA-246506	APM9	-99,5	-94,8	-92,0
CA-246506	DEF-15	18,6	-96,3	-8,6
CA-246506	DEF-15S	7,1	-96,8	-73,5
CA-246506	DNPM	-1,3	-95,0	-25,9
CA-246506	FPY-12	-57,3	-90,0	-82,0
CA-246506	FPY-2	-85,8	-92,8	-89,8
CA-246506	FR23	-98,1	-96,9	-93,0
CA-246506	M016	-99,3	-96,4	-93,7
CA-246506	RAM2-P V2	-88,7	-96,8	-93,8
CA-246506	SAM-6	-103,3	-95,8	-92,9
CA-248285	APM9	37,1	-93,1	-82,0
CA-248285	DEF-15	39,1	-97,0	-37,3
CA-248285	DEF-15S	18,5	-95,5	-5,5
CA-248285	DNPM	5,9	-97,7	-92,9
CA-248285	FPY-12	-74,5	-87,0	-86,3
CA-248285	FPY-2	-99,5	-88,2	-87,1
CA-248285	FR23	-108,3	-45,9	-47,4
CA-248285	M016	-98,2	-99,3	-96,0
CA-248285	RAM2-P V2	-98,5	-94,3	-91,1

CA-248285	SAM-6	-132,8	-93,6	-91,1
CA-248314	APM9	-94,6	-90,6	-86,7
CA-248314	DEF-15	43,6	-94,2	-11,5
CA-248314	DEF-15S	33,6	-93,9	-20,6
CA-248314	DNPM	44,7	-97,3	-92,5
CA-248314	FPY-12	-45,1	-87,8	-77,1
CA-248314	FPY-2	-97,3	-89,0	-88,6
CA-248314	FR23	-86,5	-93,9	-90,7
CA-248314	M016	-116,9	-93,0	-90,3
CA-248314	RAM2-P V2	-85,5	-93,4	-91,1
CA-248314	SAM-6	-12,3	-94,7	-92,5
CA-248649	APM9	-95,8	-87,5	-63,7
CA-248649	DEF-15	24,6	-46,2	-3,3
CA-248649	DEF-15S	4,2	-98,7	-25,0
CA-248649	DNPM	24,7	-98,2	-13,9
CA-248649	FPY-12	-98,8	-89,4	-86,5
CA-248649	FPY-2	-81,3	-90,2	-87,7
CA-248649	FR23	-83,1	-98,5	-77,3
CA-248649	M016	-101,0	-95,2	-90,1
CA-248649	RAM2-P V2	-100,1	-92,1	-90,8
CA-248649	SAM-6	-99,7	-95,5	-92,0
CA-249271	APM9	24,9	-91,2	-40,5
CA-249271	DEF-15	44,1	-95,3	-9,4
CA-249271	DEF-15S	26,5	-98,6	-24,1
CA-249271	DNPM	25,1	-96,5	-80,2
CA-249271	FPY-12	-98,8	-89,7	-85,6
CA-249271	FPY-2	-68,4	-93,7	-91,1
CA-249271	FR23	33,4	-94,9	-33,8
CA-249271	M016	-100,2	-94,1	-90,9
CA-249271	RAM2-P V2	-84,4	-95,4	-92,4
CA-249271	SAM-6	-82,5	-95,8	-89,4
CA-249379	APM9	-80,5	-93,2	-90,4
CA-249379	DEF-15	42,9	-75,0	-3,1
CA-249379	DEF-15S	15,9	-99,0	-49,8
CA-249379	DNPM	-99,7	-98,1	-93,1
CA-249379	FPY-12	-59,8	-89,8	-76,1
CA-249379	FPY-2	13,9	-92,8	-90,8
CA-249379	FR23	-32,3	-94,3	-90,4
CA-249379	M016	-99,6	-98,1	-94,5
CA-249379	RAM2-P V2	-97,9	-94,3	-88,5
CA-249379	SAM-6	-85,6	-84,8	-90,6
CA-251294	APM9	-76,9	-93,6	-90,5
CA-251294	DEF-15	23,3	-93,6	-22,1
CA-251294	DEF-15S	2,3	-96,9	-28,6
CA-251294	DNPM	-79,1	-97,8	-93,5

CA-251294	FPY-12	-99,9	-87,5	-87,0
CA-251294	FPY-2	-149,5	-94,4	-90,9
CA-251294	FR23	-53,5	-97,8	-91,3
CA-251294	M016	-89,9	-95,2	-91,8
CA-251294	RAM2-P V2	-98,4	-96,1	-90,6
CA-251294	SAM-6	-99,1	-95,1	-91,6
CA-253038	APM9	-89,1	-93,8	-90,3
CA-253038	DEF-15	27,1	-98,0	-30,9
CA-253038	DEF-15S	7,6	-70,9	-5,1
CA-253038	DNPM	-38,0	-99,0	-76,6
CA-253038	FPY-12	-95,9	-90,0	-86,6
CA-253038	FPY-2	1,7	-94,9	-87,0
CA-253038	FR23	-118,0	-34,4	-29,4
CA-253038	M016	-72,1	-27,7	-31,4
CA-253038	RAM2-P V2	-94,7	-99,0	-94,9
CA-253038	SAM-6	-100,2	-89,0	-89,7
CA-259211	APM9	-41,6	-91,9	-88,8
CA-259211	DEF-15	41,2	-93,7	-14,2
CA-259211	DEF-15S	42,3	-97,3	-35,1
CA-259211	DNPM	-101,3	-96,1	-4,5
CA-259211	FPY-12	36,9	-87,2	-55,4
CA-259211	FPY-2	-100,8	-92,0	-87,7
CA-259211	FR23	-84,7	-98,5	-96,2
CA-259211	M016	-98,8	-97,5	-94,4
CA-259211	RAM2-P V2	-100,8	-94,5	-90,7
CA-259211	SAM-6	-109,0	-94,9	-92,6

Table S2. Inhibition (%) of phocoenamicin B against MRSA (MB5973) and MSSA (ATCC29213).

	MRSA_MB5973			*MSSA ATCC29213*		
Conc. [ug/ml]	**% INH_1:**	**% INH_2:**	**MIC (ug/mL)**	**% INH: MSSA**	**% INH: MSSA**	**MIC (ug/mL)**
128	-100	-101	8-16	-93	-85	64-128
64	-100	-100		-84	-75	
32	-101	-100		-74	-54	
16	-100	-97		-52	1	
8	-6	-11		22	17	
4	-1	-6		21	10	
2	4	-2		0	-2	
1	4	-1		6	15	
0.5	5	3		21	-6	
0.25	10	2		13	11	

Table S3. Inhibition (%) of phocoenamicin B against *M. tuberculosis* H37Ra and *M. bovis*.

M. tuberculosis H37Ra					*M. bovis*				
Conc. [ug/ml]	% INH_1:	% INH_2:	MIC [ug/mL]	MIC50[ug/mL]	Conc. [ug/ml]	% INH_1:	% INH_2:	MIC [ug/mL]	MIC50[ug/mL]
128	-97	-98	16-32	16-32	128	-21	-20	>128	>128
64	-98	-99			64	-17	-14		
32	-95	-98			32	-16	-21		
16	-80	-77			16	-7	-13		
8	-34	-28			8	-5	-2		
4	-21	-14			4	-1	-5		
2	-7	-3			2	-5	-5		
1	-10	1			1	-4	-5		
0.5	-6	4			0.5	-2	-4		
0.25	0	3			0.25	-3	-6		

Table S4. Inhibition (%) of phocoenamicin B against *E. faecium* VR (MBB5571), *E. faecium* (VS144754) and *E. faecalis* (VS144492).

	E. faecium VR_MB5571			*E. faecium VS144754*				E. faecalis VS144492			
Conc. [ug/ml]	% INH_1:	% INH_2:	MIC [ug/mL]	% INH_1:	% INH_2:	MIC [ug/mL]	MIC50[ug/mL]	% INH_1:	% INH_2:	MIC [ug/mL]	MIC50[ug/mL]
128	-26	-7	>128	-66	-62	>128	16-32	-74	-77	>128	16-32
64	-22	-19		-63	-59			-75	-81		
32	-23	-23		-54	-56			-72	-65		
16	23	21		-39	-36			-37	-40		
8	57	71		-20	-13			-5	-8		
4	61	69		-5	0			3	4		
2	43	60		0	6			4	4		
1	56	37		1	-1			1	2		
0.5	57	58		0	5			1	4		
0.25	62	61		-2	1			-1	0		

Table S5. % inhibition of the seven spirotetronates against MRSA MB5393, *M. tuberculosis* H37Ra, *E. faecalis* VANS144492 and *E. faecium* VANS144754.

		MRSA MB5393				*M. tuberculosis* H37Ra				*E. faecalis* VANS144492				*E. faecium* VANS144754			
	Conc. [ug/ml]	%INH_1:	%INH_1:	%INH_1:	MIC µg/mL	%INH_1:	%INH_1:	%INH_1:	MIC µg/mL	%INH_1:	%INH_1:	%INH_1:	MIC µg/mL	%INH_1:	%INH_1:	%INH_1:	MIC µg/mL
1	128	-97	-93	-92	64	-88	-81	-93	64	-20	-20	13	> 64	-34	-92	-19	≥ 128
	64	-88	-93	-56		24	-62	-18		7	16	-1		-22	-18	-13	
	32	-32	-30	-17		3	2	-18		1	-10	-4		-11	-8	-6	
	16	-15	-9	-14		-17	-31	2		-4	-4	-2		-3	-3	-6	
	8	-12	-5	-11		11	21	12		-8	-6	-1		-3	-4	-6	
	4	-12	-5	-12		-1	25	18		-6	-5	-3		-4	-6	-9	
	2	-13	-4	-12		13	1	10		-1	-6	-6		-5	-8	-9	
	1	-12	-7	-13		9	20	16		-3	-5	-4		-4	-9	-11	
	0,5	-12	-8	-12		13	19	9		-4	-6	-6		-5	-7	-11	
	0,25	-13	-6	-13		-9	-3	-1		-6	-14	-4		-7	-9	-11	
2	128	-100	-101	-93	32-64	-90	-81	-92	32-64	-31	-35	-38	> 64	-48	-47	-36	> 64
	64	-93	-98	-91		22	-87	-76		-27	-33	-20		-40	-50	-27	
	32	-86	-87	-75		-30	-70	-58		-41	-42	-25		-14	-31	-21	
	16	-57	-61	-51		-42	-21	-8		-13	-18	-12		-3	-13	-13	
	8	-18	-29	-31		16	10	8		-2	-5	-2		4	-7	-9	
	4	-7	-9	-20		1	12	20		5	2	3		6	-5	-6	
	2	-2	-2	-16		10	18	27		5	1	2		17	-7	-4	
	1	-1	0	-15		20	22	28		3	0	-1		9	-7	-7	
	0,5	1	1	-15		20	26	27		3	-3	-2		10	-6	-7	
	0,25	3	2	-12		17	19	21		1	-2	-1		10	-7	-9	
3	128	-102	-101	-103	4	-95	-98	-98	8	-104	-102	-99	8	-101	-102	-94	4-8
	64	-103	-101	-102		-91	-97	-99		-101	-102	-93		-100	-100	-92	
	32	-101	-101	-103		-100	-97	-101		-100	-100	-95		-99	-99	-86	
	16	-100	-101	-101		-98	-99	-100		-91	-97	-78		-96	-99	-71	
	8	-100	-100	-101		-90	-98	-98		-87	-90	-73		-98	-98	-56	
	4	-96	-100	-101		-16	-48	-40		-55	-55	-42		-75	-85	-29	
	2	-52	-60	-63		12	4	-9		-18	-20	-19		-7	-10	-11	
	1	-18	-14	-20		-40	23	2		-2	-4	-5		-4	2	-9	
	0,5	-14	-6	-13		12	24	18		-1	-2	-3		0	3	-6	
	0,25	-10	-3	-11		10	23	13		-3	-4	-4		-1	2	-10	
4	128	-101	-103	-92	8	-21	-97	-98	16	-65	-76	-32	> 64	-84	-81	-45	≥ 64
	64	-101	-101	-98		-10	-91	-93		-65	-65	-34		-78	-79	-42	
	32	-101	-101	-101		-75	-88	-89		-66	-62	-44		-70	-73	-31	
	16	-101	-101	-101		-66	-73	-89		-37	-37	-29		-48	-53	-24	
	8	-101	-98	-96		-23	-12	-69		-16	-17	-14		-12	-11	-13	
	4	-30	-35	-37		19	18	-13		-9	-9	-7		-3	4	-9	
	2	-11	-13	-24		15	-5	14		-1	1	0		0	4	-3	
	1	-5	-9	-14		-41	23	18		1	-1	-1		-1	2	-3	
	0,5	-1	-6	-12		16	18	16		1	1	-3		0	3	-4	
	0,25	-3	-7	-10		10	16	10		0	-1	-2		-2	2	-7	
5	64	4	-2	-101	32	7	-78	-91	32-64	-3	3	-37	> 64	1	4	-48	> 64
	32	3	0	-94		16	-79	-86		-2	2	-22		0	7	-20	
	16	3	0	-41		-23	-6	-37		-2	-1	-12		5	7	-9	
	8	2	2	-14		1	12	-10		-2	2	1		3	9	-4	
	4	1	3	-12		-12	21	3		0	6	1		1	7	-4	
	2	5	3	-11		14	30	13		0	1	-2		3	7	-3	
	1	3	3	-11		18	25	21		-4	4	-4		7	5	-5	
	0,5	3	3	-12		-38	31	18		-1	3	-5		3	5	-6	
	0,25	3	5	-11		18	24	18		1	4	-4		7	5	-6	
	0,125	4	3	-9		24	25	19		2	4	-5		4	5	-5	
6	128	-96	-101	-102	1	-99	-98	-100	1	-102	-101	-103	32	-103	-101	-103	0,5
	64	-100	-100	-101		-99	-97	-99		-103	-101	-8		-101	-100	-102	
	32	-100	-101	-101		-96	-86	-92		-92	-56	-12		-100	-99	-102	
	16	-17	-31	-13		3	11	-14		-4	-9	-5		-96	-84	-5	
	8	-100	-98	-68		-66	-94	-84		-7	-12	-7		-100	-100	-71	
	4	-92	-97	-81		-38	-97	-68		-6	-9	-10		-100	-100	-26	
	2	-42	-58	-13		9	-2	-16		-5	-11	-7		-100	-83	-7	
	1	-6	-3	-9		-44	22	17		-4	-7	-7		-14	-11	-9	
	0,5	-100	-99	-61		-96	-97	-64		-1	-11	-9		-100	-100	-100	
	0,25	-9	-2	-10		16	23	21		-4	-6	-8		-7	0	-8	
7	128	-169	-106	-105	> 0.25	-95	-97	-100	32	-109	-105	-105	1	-103	-103	-105	0,5
	64	-220	-103	-104		-99	-97	-100		-104	-102	-105		-100	-99	-103	
	32	-101	-102	-101		-96	-96	-86		-46	-36	-8		-101	-100	-21	
	16	-101	-101	-101		-73	-81	-61		-100	-99	-8		-100	-100	-103	
	8	-100	-101	-101		-7	-4	-22		-100	-99	-6		-101	-101	-102	
	4	-100	-102	-100		3	14	-20		-100	-59	-6		-101	-100	-102	
	2	-100	-101	-89		14	16	5		-101	-62	-10		-99	-100	-100	
	1	-100	-100	-99		-42	19	6		-31	-31	-10		-43	-49	-18	
	0,5	-100	-101	-50		7	20	5		-100	-32	-13		-100	-100	-4	
	0,25	-101	-101	-50		-3	0	0		-26	-25	-11		-26	-46	-8	

Bibliography

Bibliography

1. Hutchings, M.; Truman, A.; Wilkinson, B. Antibiotics: past, present and future. *Curr. Opin. Microbiol.* **2019**, *51*, 72–80, doi:10.1016/j.mib.2019.10.008.

2. Church, N.A.; McKillip, J.L. Antibiotic resistance crisis: challenges and imperatives. *Biologia (Bratisl).* **2021**, *76*, 1535–1550, doi:10.1007/s11756-021-00697-x.

3. Abushaheen, M.A.; Muzaheed; Fatani, A.J.; Alosaimi, M.; Mansy, W.; George, M.; Acharya, S.; Rathod, S.; Divakar, D.D.; Jhugroo, C.; et al. Antimicrobial resistance, mechanisms and its clinical significance. *Disease-a-Month* **2020**, *66*, doi:10.1016/j.disamonth.2020.100971.

4. Holmes, A.H.; Moore, L.S.P.; Sundsfjord, A.; Steinbakk, M.; Regmi, S.; Karkey, A.; Guerin, P.J.; Piddock, L.J.V. Understanding the mechanisms and drivers of antimicrobial resistance. *Lancet* **2016**, *387*, 176–187, doi:10.1016/S0140-6736(15)00473-0.

5. Martins, A.; Vieira, H.; Gaspar, H.; Santos, S. Marketed marine natural products in the pharmaceutical and cosmeceutical industries: Tips for success. *Mar. Drugs* **2014**, *12*, 1066–1101, doi:10.3390/md12021066.

6. Pereira, F. Have marine natural product drug discovery efforts been productive and how can we improve their efficiency? *Expert Opin. Drug Discov.* **2019**, *14*, 717–722, doi:10.1080/17460441.2019.1604675.

7. Niu, G.; Li, W. Next-Generation Drug Discovery to Combat Antimicrobial Resistance. *Trends Biochem. Sci.* **2019**, *44*, 961–972, doi:10.1016/j.tibs.2019.05.005.

8. Konwar, A.N.; Hazarika, S.N.; Bharadwaj, P.; Thakur, D. Emerging Non-Traditional Approaches to Combat Antibiotic Resistance. *Curr. Microbiol.* **2022**, *79*, 1–15, doi:10.1007/s00284-022-03029-7.

9. Atanasov, A.G.; Zotchev, S.B.; Dirsch, V.M.; Orhan, I.E.; Banach, M.; Rollinger, J.M.; Barreca, D.; Weckwerth, W.; Bauer, R.; Bayer, E.A.; et al. Natural products in drug discovery: advances and opportunities. *Nat. Rev. Drug Discov.* **2021**, *20*, 200–216, doi:10.1038/s41573-020-00114-z.

10. Cragg, G.M.; Newman, D.J. Natural products: A continuing source of novel drug leads. *Biochim. Biophys. Acta - Gen. Subj.* **2013**, *1830*, 3670–3695, doi:10.1016/j.bbagen.2013.02.008.

11. Davison, E.K.; Brimble, M.A. Natural product derived privileged scaffolds in drug discovery. *Curr. Opin. Chem. Biol.* **2019**, *52*, 1–8, doi:10.1016/j.cbpa.2018.12.007.

12. Genilloud, O. Natural products discovery and potential for new antibiotics. *Curr. Opin. Microbiol.* **2019**, *51*, 81–87, doi:10.1016/j.mib.2019.10.012.

13. Harvey, A.L. Natural products as a screening resource. *Curr. Opin. Chem. Biol.* **2007**, *11*, 480–484, doi:10.1016/j.cbpa.2007.08.012.

14. Abdel-Razek, A.S.; El-Naggar, M.E.; Allam, A.; Morsy, O.M.; Othman, S.I. Microbial natural products in drug discovery. *Processes* **2020**, *8*, 1–19, doi:10.3390/PR8040470.

15. Harvey, A.L.; Edrada-Ebel, R.; Quinn, R.J. The re-emergence of natural products for drug discovery in the genomics era. *Nat. Rev. Drug Discov.* **2015**, *14*, 111–129, doi:10.1038/nrd4510.

16. Newman, D.J.; Cragg, G.M. Natural Products as Sources of New Drugs over the Nearly Four Decades from 01/1981 to 09/2019. *J. Nat. Prod.* **2020**, *83*, 770–803, doi:10.1021/acs.jnatprod.9b01285.

17. Murray, C.J.; Ikuta, K.S.; Sharara, F.; Swetschinski, L.; Robles Aguilar, G.; Gray, A.; Han, C.; Bisignano, C.; Rao, P.; Wool, E.; et al. Global burden of bacterial antimicrobial resistance in 2019: a systematic analysis. *Lancet* **2022**, *399*, 629–655, doi:10.1016/S0140-6736(21)02724-0.

18. Singhal, T. Antimicrobial Resistance: The "Other" Pandemic!: Based on 9th Dr. I. C. Verma Excellence Award for Young Pediatricians Delivered as Oration on 19th Sept. 2021. *Indian J. Pediatr.* **2022**, *89*, 600–606, doi:10.1007/s12098-021-04008-9.

19. Christaki, E.; Marcou, M.; Tofarides, A. Antimicrobial Resistance in Bacteria: Mechanisms, Evolution, and Persistence. *J. Mol. Evol.* **2020**, *88*, 26–40, doi:10.1007/s00239-019-09914-3.

20. Mikhaleva, T. V.; Zakharova, O.I.; Ilyasov, P. V. Antibiotic Resistance: Modern Approaches and Ways to Overcome It (Review). *Appl. Biochem. Microbiol.* **2019**, *55*, 99–106, doi:10.1134/S000368381902011X.

21. Davies, J.; Davies, D. Origins and evolution of antibiotic resistance. *Microbiol. Mol. Biol. Rev.* **2010**, *74*, 417–433.

22. Walsh, C.; Wencewicz, T. *Antibiotics: challenges, mechanisms, opportunities*; John Wiley & Sons, 2020; ISBN 1555819311.

23. Sirijan Santajit; Nitaya Indrawattana Mechanisms of antimicrobial resistance in Pasteurellaceae. *PBioMed Res. Int.* **2016**, *2016*, 1–8.

24. Prestinaci, F.; Pezzotti, P.; Pantosti, A. Antimicrobial resistance: A global multifaceted phenomenon. *Pathog. Glob. Health* **2015**, *109*, 309–318, doi:10.1179/2047773215Y.0000000030.

25. Butler, M.S.; Gigante, V.; Sati, H.; Paulin, S.; Al-Sulaiman, L.; Rex, J.H.; Fernandes, P.; Arias, C.A.; Paul, M.; Thwaites, G.E.; et al. Analysis of the Clinical Pipeline of Treatments for Drug-Resistant Bacterial Infections: Despite Progress, More Action Is Needed. *Antimicrob. Agents Chemother.* **2022**, *66*, doi:10.1128/aac.01991-21.

26. Michel, A.L.; Müller, B.; van Helden, P.D. Mycobacterium bovis at the animal-human interface: A problem, or not? *Vet. Microbiol.* **2010**, *140*, 371–381, doi:10.1016/j.vetmic.2009.08.029.

27. Von Wintersdorff, C.J.H.; Penders, J.; Van Niekerk, J.M.; Mills, N.D.; Majumder, S.; Van Alphen, L.B.; Savelkoul, P.H.M.; Wolffs, P.F.G. Dissemination of antimicrobial resistance in microbial ecosystems through horizontal gene transfer. *Front. Microbiol.* **2016**, *7*, 1–10, doi:10.3389/fmicb.2016.00173.

28. Ayukekbong, J.A.; Ntemgwa, M.; Atabe, A.N. The threat of antimicrobial resistance in developing countries: Causes and control strategies. *Antimicrob. Resist. Infect. Control* **2017**, *6*, 1–8, doi:10.1186/s13756-017-0208-x.

29. De Mol, M.L.; Snoeck, N.; De Maeseneire, S.L.; Soetaert, W.K. Hidden antibiotics: Where to uncover? *Biotechnol. Adv.* **2018**, *36*, 2201–2218, doi:10.1016/j.biotechadv.2018.10.008.

30. Chandra Mohana, N.; Yashavantha Rao, H.C.; Rakshith, D.; Mithun, P.R.; Nuthan, B.R.; Satish, S. Omics based approach for biodiscovery of microbial natural products in antibiotic resistance era. *J. Genet. Eng. Biotechnol.* **2018**, *16*, 1–8, doi:10.1016/j.jgeb.2018.01.006.

31. Dias, D.A.; Urban, S.; Roessner, U. A Historical overview of natural products in drug discovery. *Metabolites* **2012**, *2*, 303–336, doi:10.3390/metabo2020303.

32. Shen, B. A New Golden Age of Natural Products Drug Discovery. *Cell* **2015**, *163*, 1297–1300, doi:10.1016/j.cell.2015.11.031.

33. Reverter, M.; Rohde, S.; Parchemin, C.; Tapissier-Bontemps, N.; Schupp, P.J. Metabolomics and Marine Biotechnology: Coupling Metabolite Profiling and Organism Biology for the Discovery of New Compounds. *Front. Mar. Sci.* **2020**, *7*, 1–8, doi:10.3389/fmars.2020.613471.

34. Aharoni, A.; Goodacre, R.; Fernie, A.R. Plant and microbial sciences as key drivers in the development of metabolomics research. *Proc. Natl. Acad. Sci.* **2023**, *120*, 1–11, doi:10.1073/pnas.2217383120.

35. Afoullouss, S.; Balsam, A.; Allcock, A.L.; Thomas, O.P. Optimization of LC-MS2 Data Acquisition Parameters for Molecular Networking Applied to Marine Natural Products. *Metabolites* **2022**, *12*, doi:10.3390/metabo12030245.

36. Aron, A.T.; Gentry, E.C.; McPhail, K.L.; Nothias, L.F.; Nothias-Esposito, M.; Bouslimani, A.; Petras, D.; Gauglitz, J.M.; Sikora, N.; Vargas, F.; et al. Reproducible molecular networking of untargeted mass spectrometry data using GNPS. *Nat. Protoc.* **2020**, *15*, 1954–1991, doi:10.1038/s41596-020-0317-5.

37. Quinn, R.A.; Nothias, L.F.; Vining, O.; Meehan, M.; Esquenazi, E.; Dorrestein, P.C. Molecular Networking As a Drug Discovery, Drug Metabolism, and Precision Medicine Strategy. *Trends Pharmacol. Sci.* **2017**, *38*, 143–154, doi:10.1016/j.tips.2016.10.011.

38. Nothias, L.F.; Petras, D.; Schmid, R.; Dührkop, K.; Rainer, J.; Sarvepalli, A.; Protsyuk, I.; Ernst, M.; Tsugawa, H.; Fleischauer, M.; et al. Feature-based molecular networking in the GNPS analysis environment. *Nat. Methods* **2020**, *17*, 905–908, doi:10.1038/s41592-020-0933-6.

39. Miyawaki, I. Application of zebrafish to safety evaluation in drug discovery. *J. Toxicol. Pathol.* **2020**, *33*, 197–210, doi:10.1293/tox.2020-0021.

40. Zicarelli, G.; Multisanti, C.R.; Falco, F.; Faggio, C. Evaluation of toxicity of Personal Care Products (PCPs) in freshwaters: Zebrafish as a model. *Environ. Toxicol. Pharmacol.* **2022**, *94*, 103923, doi:10.1016/j.etap.2022.103923.

41. Pensado-López, A.; Fernández-Rey, J.; Reimunde, P.; Crecente-Campo, J.; Sánchez, L.; Torres Andón, F. Zebrafish models for the safety and therapeutic testing of nanoparticles with a focus on macrophages. *Nanomaterials* **2021**, *11*, 1–34, doi:10.3390/nano11071784.

42. Ali, S.; van Mil, H.G.J.; Richardson, M.K. Large-Scale assessment of the zebrafish embryo as a possible predictive model in toxicity testing. *PLoS One* **2011**, *6*, doi:10.1371/journal.pone.0021076.

43. Copmans, D.; Rateb, M.; Tabudravu, J.N.; Pérez-Bonilla, M.; Dirkx, N.; Vallorani, R.; Diaz, C.; Pérez Del Palacio, J.; Smith, A.J.; Ebel, R.; et al. Zebrafish-Based Discovery of Antiseizure Compounds from the Red Sea: Pseurotin A2 and Azaspirofuran A. *ACS Chem. Neurosci.* **2018**, *9*, 1652–1662, doi:10.1021/acschemneuro.8b00060.

44. Guarin, M.; Faelens, R.; Giusti, A.; De Croze, N.; Léonard, M.; Cabooter, D.; Annaert, P.; de Witte, P.; Ny, A. Spatiotemporal imaging and pharmacokinetics of fluorescent compounds in zebrafish eleuthero-embryos after different routes of administration. *Sci. Rep.* **2021**, *11*, 1–15, doi:10.1038/s41598-021-91612-6.

45. Malve, H. Exploring the ocean for new drug developments: Marine pharmacology. *J. Pharm. Bioallied Sci.* **2016**, *8*, 83.

46. Santos, J.D.; Vitorino, I.; Reyes, F.; Vicente, F.; Lage, O.M. From ocean to medicine: Pharmaceutical applications of metabolites from marine bacteria. *Antibiotics* **2020**, *9*, 1–30, doi:10.3390/antibiotics9080455.

47. Liang, X.; Luo, D.; Luesch, H. Advances in exploring the therapeutic potential of marine natural products. *Pharmacol. Res.* **2019**, *147*, 104373, doi:10.1016/j.phrs.2019.104373.

48. Elgohary, A.M.; Elfiky, A.A.; Pereira, F.; Mohamed, T.; El-aziz, A. Since January 2020 Elsevier has created a COVID-19 resource centre with free information in English and Mandarin on the novel coronavirus COVID- 19 . The COVID-19 resource centre is hosted on Elsevier Connect , the company ' s public news and information . **2020**.

49. https://marinlit.rsc.org/ (accessed on 5 February 2023)

50. Liu, M.; El-Hossary, E.M.; Oelschlaeger, T.A.; Donia, M.S.; Quinn, R.J.; Abdelmohsen, U.R. Potential of marine natural products against drug-resistant bacterial infections. *Lancet Infect. Dis.* **2019**, *19*, e237–e245, doi:10.1016/S1473-3099(18)30711-4.

51. Krishna M. S., A.; Mohan, S.; Ashitha, K.T.; Chandramouli, M.; Kumaran, A.; Ningaiah, S.; Babu, K.S.; Somappa, S.B. Marine Based Natural Products: Exploring the Recent Developments in the Identification of Antimicrobial Agents. *Chem. Biodivers.* **2022**, *19*, doi:10.1002/cbdv.202200513.

52. Haque, N.; Parveen, S.; Tang, T.; Wei, J.; Huang, Z. Marine Natural Products in Clinical Use. *Mar. Drugs* **2022**, *20*, doi:10.3390/md20080528.

53. Cuevas, C.; Pérez, M.; Martín, M.J.; Chicharro, J.L.; Fernândez-Rivas, C.; Flores, M.; Francesch, A.; Gallego, P.; Zarzuelo, M.; De La Calle, F.; et al. Synthesis of ecteinascidin ET-743 and phthalascidin Pt-650 from cyanosafracin B. *Org. Lett.* **2000**, *2*, 2545–2548, doi:10.1021/ol0062502.

54. Morokutti-Kurz, M.; Unger-Manhart, N.; Graf, P.; Rauch, P.; Kodnar, J.; Große, M.; Setz, C.; Savli, M.; Ehrenreich, F.; Grassauer, A.; et al. The saliva of probands sucking an iota-carrageenan containing lozenge inhibits viral binding and replication of the most predominant common cold viruses and SARS-CoV-2. *Int. J. Gen. Med.* **2021**, *14*, 5241–5249, doi:10.2147/IJGM.S325861.

55. www.marinepharmacology.org. (accessed on 5 February 2023)

56. Roth, P.; Gorlia, T.; Reijneveld, J.C.; de Vos, F.; Idbaih, A.; Frenel, J.-S.; Le Rhun, E.; Sepulveda, J.M.; Perry, J.; Masucci, G.L. Marizomib for patients with newly diagnosed glioblastoma: a randomized phase 3 trial. *Neuro. Oncol.* **2024**, noae053.

57. De Simeis, D.; Serra, S. Actinomycetes: A Never-Ending Source of Bioactive Compounds—an Overview on Antibiotics Production. *Antibiotics* **2021**, *10*, doi:10.3390/antibiotics10050483.

58. Subramani, R.; Sipkema, D. *Marine rare actinomycetes: A promising source of structurally diverse and unique novel natural products*; 2019; Vol. 17; ISBN 3131748311.

59. Sapkota, A.; Thapa, A.; Budhathoki, A.; Sainju, M.; Shrestha, P.; Aryal, S. Isolation, Characterization, and Screening of Antimicrobial-Producing Actinomycetes from Soil Samples. *Int. J. Microbiol.* **2020**, *2020*, doi:10.1155/2020/2716584.

60. van der Meij, A.; Worsley, S.F.; Hutchings, M.I.; van Wezel, G.P. Chemical ecology of antibiotic production by actinomycetes. *FEMS Microbiol. Rev.* **2017**, *41*, 392–416,

doi:10.1093/femsre/fux005.

61. Jagannathan, S. V.; Manemann, E.M.; Rowe, S.E.; Callender, M.C.; Soto, W. Marine actinomycetes, new sources of biotechnological products. *Mar. Drugs* **2021**, *19*, doi:10.3390/md19070365.

62. Zhao, P.; Xue, Y.; Gao, W.; Li, J.; Zu, X.; Fu, D.; Feng, S.; Bai, X.; Zuo, Y.; Li, P. Actinobacteria–Derived peptide antibiotics since 2000. *Peptides* **2018**, *103*, 48–59, doi:10.1016/j.peptides.2018.03.011.

63. Robertsen, H.L.; Musiol-Kroll, E.M. Actinomycete-derived polyketides as a source of antibiotics and lead structures for the development of new antimicrobial drugs. *Antibiotics* **2019**, *8*, doi:10.3390/antibiotics8040157.

64. Hirsch, A.M.; Valdés, M. Micromonospora: An important microbe for biomedicine and potentially for biocontrol and biofuels. *Soil Biol. Biochem.* **2010**, *42*, 536–542, doi:10.1016/j.soilbio.2009.11.023.

65. Mast, Y.; Stegmann, E. Actinomycetes: The antibiotics producers. *Antibiotics* **2019**, *8*, 10–13, doi:10.3390/antibiotics8030105.

66. Genilloud, O. Actinomycetes: still a source of novel antibiotics. *Nat. Prod. Rep.* **2017**, *34*, 1203–1232.

67. Qi, S.; Gui, M.; Li, H.; Yu, C.; Li, H.; Zeng, Z.; Sun, P. Secondary Metabolites from Marine Micromonospora: Chemistry and Bioactivities. *Chem. Biodivers.* **2020**, *17*, doi:10.1002/cbdv.202000024.

68. Boumehira, A.Z.; El-Enshasy, H.A.; Hacène, H.; Elsayed, E.A.; Aziz, R.; Park, E.Y. Recent progress on the development of antibiotics from the genus Micromonospora. *Biotechnol. Bioprocess Eng.* **2016**, *21*, 199–223, doi:10.1007/s12257-015-0574-2.

69. Hifnawy, M.S.; Fouda, M.M.; Sayed, A.M.; Mohammed, R.; Hassan, H.M.; AbouZid, S.F.; Rateb, M.E.; Keller, A.; Adamek, M.; Ziemert, N.; et al. The genusMicromonosporaas a model microorganism for bioactive natural product discovery. *RSC Adv.* **2020**, *10*, 20939–20959, doi:10.1039/d0ra04025h.

70. Trujillo, M.E., Hong, K., Genilloud, O. (2014). The Family Micromonosporaceae . In: Rosenberg, E., DeLong, E.F., Lory, S., Stackebrandt, E., Thompson, F. (eds) The Prokaryotes. Springer, Berlin, Heidelberg. https://doi.org/10.1007/978-3-642-30138-4_196

71. Yan, S.; Zeng, M.; Wang, H.; Zhang, H. Micromonospora: A Prolific Source of Bioactive Secondary Metabolites with Therapeutic Potential. *J. Med. Chem.* **2022**, *65*, 8735–8771, doi:10.1021/acs.jmedchem.2c00626.

72. Braesel, J.; Crnkovic, C.M.; Kunstman, K.J.; Green, S.J.; Maienschein-Cline, M.; Orjala, J.; Murphy, B.T.; Eustáquio, A.S. Complete Genome of Micromonospora sp. Strain B006 Reveals Biosynthetic Potential of a Lake Michigan Actinomycete. *J. Nat. Prod.* **2018**, *81*, 2057–2068, doi:10.1021/acs.jnatprod.8b00394.

73. Lacoske, M.H.; Theodorakis, E.A. Spirotetronate polyketides as leads in drug discovery. *J. Nat. Prod.* **2015**, *78*, 562–575, doi:10.1021/np500757w.

74. Vieweg, L.; Reichau, S.; Schobert, R.; Leadlay, P.F.; Süssmuth, R.D. Recent advances in the field of bioactive tetronates. *Nat. Prod. Rep.* **2014**, *31*, 1554–1584, doi:10.1039/c4np00015c.

75. Braddock, A.A.; Theodorakis, E.A. Marine spirotetronates: Biosynthetic edifices that inspire drug discovery. *Mar. Drugs* **2019**, *17*, doi:10.3390/md17040232.

76. Iorio, M.; Maffioli, S.I.; Gaspari, E.; Rossi, R.; Mauri, P.; Sosio, M.; Donadio, S. Chrolactomycins from the actinomycete actinospica. *J. Nat. Prod.* **2012**, *75*, 1991–1993, doi:10.1021/np300470f.

77. Pérez-Bonilla, M.; Oves-Costales, D.; De La Cruz, M.; Kokkini, M.; Martín, J.; Vicente, F.; Genilloud, O.; Reyes, F. Phocoenamicins B and C, new antibacterial spirotetronates isolated from a marine Micromonospora sp. *Mar. Drugs* **2018**, *16*, doi:10.3390/md16030095.

78. Huang, H.; Song, Y.; Li, X.; Wang, X.; Ling, C.; Qin, X.; Zhou, Z.; Li, Q.; Wei, X.; Ju, J. Abyssomicin Monomers and Dimers from the Marine-Derived Streptomyces koyangensis SCSIO 5802. *J. Nat. Prod.* **2018**, *81*, 1892–1898, doi:10.1021/acs.jnatprod.8b00448.

79. Iglesias, A.; Latorre-Pérez, A.; Stach, J.E.M.; Porcar, M.; Pascual, J. Out of the Abyss: Genome and Metagenome Mining Reveals Unexpected Environmental Distribution of Abyssomicins. *Front. Microbiol.* **2020**, *11*, doi:10.3389/fmicb.2020.00645.

80. Keller, S.; Nicholson, G.; Drahl, C.; Sorensen, E.; Fiedler, H.P.; Süssmuth, R.D. Abyssomicins G and H and atrop-abyssomicin C from the marine Verrucosispora strain AB-18-032. *J. Antibiot. (Tokyo).* **2007**, *60*, 391–394, doi:10.1038/ja.2007.54.

81. Nicolaou, K.C.; Harrison, S.T.; Chen, J.S. Discoveries from the Abyss: The abyssomicins and their total synthesis. *Synthesis (Stuttg).* 2009, 33–42.

82. Riedlinger, J.; Reicke, A.; Zähner, H.; Krismer, B.; Bull, A.T.; Maldonado, L.A.; Ward, A.C.; Goodfellow, M.; Bister, B.; Bischoff, D.; et al. Abyssomicins, inhibitors of the para-aminobenzoic acid pathway produced by the marine Verrucosispora strain AB-18-032. *J. Antibiot. (Tokyo).* **2004**, *57*, 271–279, doi:10.7164/antibiotics.57.271.

83. Sadaka, C.; Ellsworth, E.; Hansen, P.R.; Ewin, R.; Damborg, P.; Watts, J.L. Review on abyssomicins: Inhibitors of the chorismate pathway and folate biosynthesis. *Molecules* **2018**, *23*, 1–25, doi:10.3390/molecules23061371.

84. Song, Y.; Li, Q.; Qin, F.; Sun, C.; Liang, H.; Wei, X.; Wong, N.K.; Ye, L.; Zhang, Y.; Shao, M.; et al. Neoabyssomicins A–C, Polycyclic Macrolactones from the Deep-Sea Derived Streptomyces Koyangensis SCSIO 5802. *Tetrahedron* **2017**, *73*, 5366–5372, doi:10.1016/j.tet.2017.07.034.

85. Wang, Q.; Song, F.; Xiao, X.; Huang, P.; Li, L.; Monte, A.; Abdel-Mageed, W.M.; Wang, J.; Guo, H.; He, W.; et al. Abyssomicins from the South China Sea deep-sea sediment verrucosispora sp.: Natural thioether michael addition adducts as antitubercular prodrugs. *Angew. Chemie - Int. Ed.* **2013**, *52*, 1231–1234, doi:10.1002/anie.201208801.

86. Bonjouklian, R.; Mynderse, J.S.; Hunt, A.H.; Deeter, J.B. Structures of A88696 C,D and F: Gastric ATP-ase inhibitors. *Tetrahedron Lett.* **1993**, *34*, 7857–7860, doi:10.1016/S0040-4039(00)61494-6.

87. Nakai, R.; Kakita, S.; Asai, A.; Chiba, S.; Akinaga, S.; Mizukami, T.; Yamashita, Y. Chrolactomycin, a novel antitumor antibiotic produced by Streptomyces sp. *J. Antibiot. (Tokyo).* **2001**, *54*, 836–839, doi:10.7164/antibiotics.54.836.

88. Imai, H.; Suzuki, K.; Morioka, M.; Numasaki, Y.; Kadota, S.; Nagai, K.; Sato, T.; Iwanami, M.; Sato, T. Okilactomycin, a novel antibiotic produced by Streptomyces species. *J. Antibiot. (Tokyo).* **1987**, *40*, 1475–1482.

89. Zhang, C.; Ondeyka, J.G.; Zink, D.L.; Basilio, A.; Vicente, F.; Salazar, O.; Genilloud, O.; Dorso, K.; Motyl, M.; Byrne, K.; et al. Discovery of okilactomycin and congeners from Streptomyces scabrisporus by antisense differential sensitivity assay targeting ribosomal protein S4. *J. Antibiot. (Tokyo).* **2009**, *62*, 55–61, doi:10.1038/ja.2008.8.

90. Igarashi, Y.; Ogura, H.; Furihata, K.; Oku, N.; Indananda, C.; Thamchaipenet, A. Maklamicin, an antibacterial polyketide from an endophytic Micromonospora sp. *J. Nat. Prod.* **2011**, *74*, 670–674.

91. Igarashi, Y.; Iida, T.; Oku, N.; Watanabe, H.; Furihata, K.; Miyanouchi, K. Nomimicin , a new spirotetronate-class polyketide from an actinomycete of the genus Actinomadura. *J. Antibiot. (Tokyo).* **2012**, 355–359, doi:10.1038/ja.2012.30.

92. Zhang, Z.; Zhou, T.; Yang, T.; Fukaya, K.; Harunari, E.; Saito, S.; Yamada, K.; Imada, C.; Urabe, D.; Igarashi, Y. Nomimicins B-D, new tetronate-class polyketides from a marine-derived actinomycete of the genus Actinomadura. *Beilstein J. Org. Chem.* **2021**, *17*, 2194–2202, doi:10.3762/bjoc.17.141.

93. Matsumoto, M.; Kawamura, Y.; Yoshimura, Y.; Terui, Y.; Nakai, H.; Yoshida, T.; Shoji, J. Isolation, characterization and structures of PA-46101 A and B. *J. Antibiot. (Tokyo).* **1990**, *43*, 739–747.

94. Ochoa, J.L.; Sanchez, L.M.; Koo, B.M.; Doherty, J.S.; Rajendram, M.; Huang, K.C.; Gross, C.A.; Linington, R.G. Marine Mammal Microbiota Yields Novel Antibiotic with Potent Activity Against Clostridium difficile. *ACS Infect. Dis.* **2018**, *4*, 59–67, doi:10.1021/acsinfecdis.7b00105.

95. Jia, X.Y.; Tian, Z.H.; Shao, L.; Qu, X.D.; Zhao, Q.F.; Tang, J.; Tang, G.L.; Liu, W. Genetic Characterization of the Chlorothricin Gene Cluster as a Model for Spirotetronate Antibiotic Biosynthesis. *Chem. Biol.* **2006**, *13*, 575–585, doi:10.1016/j.chembiol.2006.03.008.

96. Schindler, P.W. Chlorothricin , an Inhibitor of Porcine-Heart Malate Dehydrogenases , Discriminating between the Mitochondria1 and Cytoplasmic Isoenzyme. **1975**, *585*, 579–585.

97. Yamamoto, I.; Nakagawa, M.; Hayakawa, Y.; Adachi, K.; Kobayashi, E. Hydroxychlorothricin, a new antitumor antibiotic. *J. Antibiot. (Tokyo).* **1987**, *40*, 1452–1454.

98. Lam, K.S.; Hesler, G.A.; Gustavson, D.R.; Berry, R.L.; Tomita, K.; MacBeth, J.L.; Ross, J.; Miller, D.; Forenza, S. Pyrrolosporin A, a new antitumor antibiotic from Micromonospora sp. C39217-r109-7. I. Taxonomy of producing organism, fermentation and biological activity. *J. Antibiot. (Tokyo).* **1996**, *49*, 860–864, doi:10.7164/antibiotics.49.860.

99. Ching, K.C.; Chin, E.J.; Wibowo, M.; Tan, Z.Y.; Yang, L.K.; Seow, D.C.; Leong, C.Y.; Ng, V.W.; Ng, S.B.; Kanagasundaram, Y. Antibacterial Spirotetronate Polyketides from an Actinomadura sp. Strain A30804. *Molecules* **2022**, *27*, doi:10.3390/molecules27238196.

100. Mazzetti, C.; Ornaghi, M.; Gaspari, E.; Parapini, S.; Maffioli, S.; Sosio, M.; Donadio, S. Halogenated spirotetronates from Actinoallomurus. *J. Nat. Prod.* **2012**, *75*, 1044–1050, doi:10.1021/np300003n.

101. Momose, I.; Hirosawa, S.; Nakamura, H.; Naganawa, H.; Iinuma, H.; Ikeda, D.; Takeuchi, T. Decatromicins A and B, new antibiotics produced by Actinomadura sp. MK73-NF4. II. Structure determination. *J. Antibiot. (Tokyo).* **1999**, *52*, 787–796, doi:10.7164/antibiotics.52.787.

102. Momose, I.; Iinuma, H.; Kinoshita, N.; Momose, Y.; Kunimoto, S.; Hamada, M.; Takeuchi, T. Decatromicins A and B, new antibiotics produced by Actinomadura sp. MK73-NF4. 1. Taxonomy, isolation, physico-chemical properties and biological activities. *J. Antibiot. (Tokyo).* **1999**, *52*, 781–786, doi:10.7164/antibiotics.52.781.

103. Waitz, J.A.; Horan, A.C.; Kalyanpur, M.; Lee, B.K.; Loebenberg, D.; Marquez, J.; Miller,

G.; Patel, M.G. Kijanimicin (Sch 25663), a novel antibiotic produced by actinomadura kijaniata scc 1256 fermentation, isolation, characterization and biological properties. *J. Antibiot. (Tokyo).* **1981**, *34*, 1101–1106, doi:10.7164/antibiotics.34.1101.

104. Gui, C.; Zhang, S.; Zhu, X.; Ding, W.; Huang, H.; Gu, Y.C.; Duan, Y.; Ju, J. Antimicrobial Spirotetronate Metabolites from Marine-Derived Micromonospora harpali SCSIO GJ089. *J. Nat. Prod.* **2017**, *80*, 1594–1603, doi:10.1021/acs.jnatprod.7b00176.

105. Jp, O.; Uosaki, Y.; Kanazawa, J.; Jp, S. (12) United States Patent. **2003**, *2*.

106. Gong, T.; Zhen, X.; Li, X.L.; Chen, J.J.; Chen, T.J.; Yang, J.L.; Zhu, P. Tetrocarcin Q, a new spirotetronate with a unique glycosyl group from a marine-derived actinomycete micromonospora carbonacea LS276. *Mar. Drugs* **2018**, *16*, 2–10, doi:10.3390/md16020074.

107. Tamaoki, T.; KASAI, M.; SHIRAHATA, K.; OHKUBO, S.; MORIMOTO, M.; MINEURA, K.; ISHII, S.; TOMITA, F. Tetrocarcins, Novel Antitumor Antibiotics II. Isolation, Characterization and Antitumor Activity. *J. Antibiot. (Tokyo).* **1980**, *33*, 946–950.

108. Tamaoki, T.; Kasai, M.; Shirahata, K.; Tomita, F. Tetrocarcins E1, E2F, and F-1, new antibiotics fermentation, isolation and characterization. *J. Antibiot. (Tokyo).* 1982, *35*, 979–984.

109. Tan, Y.; Hu, Y.; Wang, Q.; Zhou, H.; Wang, Y.; Gan, M. Tetrocarcins N and O, glycosidic spirotetronates from a marine-derived: Micromonospora sp. identified by PCR-based screening. *RSC Adv.* **2016**, *6*, 91773–91778, doi:10.1039/c6ra17026a.

110. Ding, T.; Yang, L.J.; Zhang, W.D.; Shen, Y.H. The secondary metabolites of rare actinomycetes: Chemistry and bioactivity. *RSC Adv.* **2019**, *9*, 21964–21988, doi:10.1039/c9ra03579f.

111. Euanorasetr, J.; Intra, B.; Mongkol, P.; Chankhamhaengdecha, S.; Tuchinda, P.; Mori, M.; Shiomi, K.; Nihira, T.; Panbangred, W. Spirotetronate antibiotics with anti-Clostridium activity from Actinomadura sp. 2EPS. *World J. Microbiol. Biotechnol.* **2015**, *31*, 391–398, doi:10.1007/s11274-014-1792-z.

112. Ashton, R.J.; Kenig, M.D.; Luk, K.; Planterose, D.N.; Scott-Wood, G. Mm 46115, a new antiviral antibiotic from actinomadura pelletieri. Characteristics of the producing cultures, fermentation, isolation, physico-chemical and biological properties. *J. Antibiot. (Tokyo).* **1990**, *43*, 1387–1393, doi:10.7164/antibiotics.43.1387.

113. Nemoto, A.; Yazawa, K.; Mikami, Y. (12) United States Patent. **2004**, *43*, 1387–1393.

114. Furumai, T.; Takagi, K.; Igarashi, Y.; Saito, N.; Oki, T. Arisostatins A and B, new members of tetrocarcin class of antibiotics from Micromonospora sp. TP-A0316. I. Taxonomy, fermentation, isolation and biological properties. *J. Antibiot. (Tokyo).* **2000**, *53*, 227–232, doi:10.7164/antibiotics.53.227.

115. Shimotohno, K.W.; Furihata, K.; Endö, T. Antibiotic Ac6H A new component of tetrocarcin group antibiotics. *J. Antibiot. (Tokyo).* **1993**, *46*, 682–684, doi:10.7164/antibiotics.46.682.

116. Hegde, V.R.; Patel, M.G.; Das, P.R.; Pramanik, B.; Puar, M.S. A family of novel macrocyclic lactones, the saccharocarcins produced by Saccharothrix aerocolonigenes subsp. antibiotica. II. Physico-chemical properties and structure determination. *J. Antibiot. (Tokyo).* **1997**, *50*, 126–134, doi:10.7164/antibiotics.50.126.

117. Wei, R.B.; Xi, T.; Li, J.; Wang, P.; Li, F.C.; Lin, Y.C.; Qin, S. Lobophorin C and D, new kijanimicin derivatives from a marine sponge-associated actinomycetal strain AZS17. *Mar. Drugs* **2011**, *9*, 359–368, doi:10.3390/md9030359.

118. Zhang, C.; Ding, W.; Qin, X.; Ju, J. Genome Sequencing of Streptomyces olivaceus SCSIO T05 and Activated Production of Lobophorin CR4 via Metabolic Engineering and Genome Mining. *Mar. Drugs* **2019**, *17*, doi:10.3390/md17100593.

119. Chen, C.; Wang, J.; Guo, H.; Hou, W.; Yang, N.; Ren, B.; Liu, M.; Dai, H.; Liu, X.; Song, F.; et al. Three antimycobacterial metabolites identified from a marine-derived Streptomyces sp. MS100061. *Appl. Microbiol. Biotechnol.* **2013**, *97*, 3885–3892, doi:10.1007/s00253-012-4681-0.

120. Braña, A.F.; Sarmiento-Vizcaíno, A.; Osset, M.; Pérez-Victoria, I.; Martín, J.; De Pedro, N.; De La Cruz, M.; Díaz, C.; Vicente, F.; Reyes, F.; et al. Lobophorin K, a New Natural Product with Cytotoxic Activity Produced by Streptomyces Sp. M-207 Associated with the Deep-Sea Coral Lophelia Pertusa. *Mar. Drugs* **2017**, *15*, 4–11, doi:10.3390/md15050144.

121. Jiang, Z.D.; Jensen, P.R.; Fenical, W. Lobophorins A and B, new antiinflammatory macrolides produced by a tropical marine bacterium. *Bioorganic Med. Chem. Lett.* **1999**, *9*, 2003–2006, doi:10.1016/S0960-894X(99)00337-6.

122. Cruz, P.G.; Fribley, A.M.; Miller, J.R.; Larsen, M.J.; Schultz, P.J.; Jacob, R.T.; Tamayo-Castillo, G.; Kaufman, R.J.; Sherman, D.H. Novel Lobophorins Inhibit Oral Cancer Cell Growth and Induce Atf4- and Chop-Dependent Cell Death in Murine Fibroblasts. *ACS Med. Chem. Lett.* **2015**, *6*, 877–881, doi:10.1021/acsmedchemlett.5b00127.

123. Niu, S.; Li, S.; Chen, Y.; Tian, X.; Zhang, H.; Zhang, G.; Zhang, W.; Yang, X.; Zhang, S.; Ju, J.; et al. Lobophorins e and F, new spirotetronate antibiotics from a South China Sea-derived Streptomyces sp. SCSIO 01127. *J. Antibiot. (Tokyo).* **2011**, *64*, 711–716, doi:10.1038/ja.2011.78.

124. Pan, H.Q.; Zhang, S.Y.; Wang, N.; Li, Z.L.; Hua, H.M.; Hu, J.C.; Wang, S.J. New spirotetronate antibiotics, lobophorins H and I, from a South China Sea-derived streptomyces sp. 12A35. *Mar. Drugs* **2013**, *11*, 3891–3901, doi:10.3390/md11103891.

125. Blunt, J.W.; Copp, B.R.; Keyzers, R.A.; Munro, M.H.G.; Prinsep, M.R. Marine natural products. *Nat. Prod. Rep.* **2017**, *34*, 235–294, doi:10.1039/c6np00124f.

126. Elsayed, S.S.; Genta-Jouve, G.; Carrión, V.J.; Nibbering, P.H.; Siegler, M.A.; De Boer, W.; Hankemeier, T.; Van Wezel, G.P. Atypical spirotetronate polyketides identified in the underexplored genus Streptacidiphilus. *J. Org. Chem.* **2020**, *85*, 10648–10657.

127. Wu, T.; Salim, A.A.; Khalil, Z.G.; Bernhardt, P. V.; Capon, R.J. Glenthmycins A-M: Macrocyclic Spirotetronate Polyketide Antibacterials from the Australian Pasture Plant-Derived Streptomyces sp. CMB-PB041. *J. Nat. Prod.* **2022**, *85*, 1641–1657, doi:10.1021/acs.jnatprod.2c00444.

128. Kimura, T.; Umekita, M.; Hatano, M.; Hayashi, C.; Sawa, R.; Igarashi, M. Wychimicins, a new class of spirotetronate polyketides from Actinocrispum wychmicini MI503-A4. *J. Antibiot. (Tokyo).* **2022**, *75*, 535–541, doi:10.1038/s41429-022-00560-4.

129. Park, H.R.; Furihata, K.; Hayakawa, Y.; Shin-Ya, K. Versipelostatin, a novel GRP78/Bip molecular chaperone down-regulator of microbial origin. *Tetrahedron Lett.* **2002**, *43*, 6941–6945, doi:10.1016/S0040-4039(02)01624-6.

130. Toshikazu, K.; Tsutomu, K.; Hiromi, N.; Mari, T.; Atsuko, N.; Tatsuo, O.; Hiroyuki, Y.; Mikio, A. Tetronothiodin, a novel CCKB receptor ligand, antagonizes cholecystokinin-induced Ca2+ mobilization in a pituitary cell line. *Eur. J. Pharmacol.* **1992**, *221*, 99–105.

131. Tsunakawa, M.; Tenmyo, O.; Tomita, K.; Naruse, N.; Kotake, C.; Miyaki, T.; Konishi, M.; Oki, T. Quartromicin1, a complex of novel antiviral antibiotics: I. Production, isolation,

physico-chemical properties and antiviral activity. *J. Antibiot. (Tokyo).* **1992**, *45*, 180–188, doi:10.7164/antibiotics.45.180.

132. He, H.Y.; Pan, H.X.; Wu, L.F.; Zhang, B.B.; Chai, H.B.; Liu, W.; Tang, G.L. Quartromicin biosynthesis: Two alternative polyketide chains produced by one polyketide synthase assembly line. *Chem. Biol.* **2012**, *19*, 1313–1323, doi:10.1016/j.chembiol.2012.07.024.

133. Pérez-Victoria, I.; Martín, J.; Reyes, F. Combined LC/UV/MS and NMR Strategies for the Dereplication of Marine Natural Products. *Planta Med.* **2016**, *82*, 857–871, doi:10.1055/s-0042-101763.

134. Demain, A.L.; Gómez-Ortiz, B.; Ruiz-Villafán, B.; Rodríguez-Sanoja, R.; Sánchez, S. Recent findings of molecules with anti-infective activity: screening of non-conventional sources. *Curr. Opin. Pharmacol.* **2019**, *48*, 40–47, doi:10.1016/j.coph.2019.04.003.

135. Ossai, J.; Khatabi, B.; Nybo, S.E.; Kharel, M.K. Renewed interests in the discovery of bioactive actinomycete metabolites driven by emerging technologies. *J. Appl. Microbiol.* **2022**, *132*, 59–77, doi:10.1111/jam.15225.

136. Bode, H.B.; Bethe, B.; Höfs, R.; Zeeck, A. Big effects from small changes: possible ways to explore nature's chemical diversity. *Chembiochem* **2002**, *3*, 619–627, doi:10.1002/1439-7633(20020703)3:7<619::AID-CBIC619>3.0.CO;2-9.

137. Pluskal, T.; Castillo, S.; Villar-Briones, A.; Orešič, M. MZmine 2: Modular framework for processing, visualizing, and analyzing mass spectrometry-based molecular profile data. *BMC Bioinformatics* **2010**, *11*, doi:10.1186/1471-2105-11-395.

138. Pang, Z.; Chong, J.; Zhou, G.; de Lima Morais, D.A.; Chang, L.; Barrette, M.; Gauthier, C.; Jacques, P.-É.; Li, S.; Xia, J. MetaboAnalyst 5.0: narrowing the gap between raw spectra and functional insights. *Nucleic Acids Res.* **2021**, *49*, W388–W396, doi:10.1093/nar/gkab382.

139. Lever, J.; Krzywinski, M.; Altman, N. Principal component analysis. *Nat. Methods* **2017**, *14*, 641–642, doi:10.1038/nmeth.4346.

140. Worley, B.; Powers, R. Multivariate Analysis in Metabolomics. *Curr. Metabolomics* **2013**, *1*, 92–107, doi:10.2174/2213235x11301010092.

141. Ruiz-Perez, D.; Guan, H.; Madhivanan, P.; Mathee, K.; Narasimhan, G. So you think you can PLS-DA? *BMC Bioinformatics* **2020**, *21*, 1–10, doi:10.1186/s12859-019-3310-7.

142. Chen, Y.; Li, E.M.; Xu, L.Y. Guide to Metabolomics Analysis: A Bioinformatics Workflow. *Metabolites* **2022**, *12*, doi:10.3390/metabo12040357.

143. Caesar, L.K.; Kvalheim, O.M.; Cech, N.B. Hierarchical cluster analysis of technical replicates to identify interferents in untargeted mass spectrometry metabolomics. *Anal. Chim. Acta* **2018**, *1021*, 69–77, doi:10.1016/j.aca.2018.03.013.

144. Holden, P.; Nair, L.S. Deferoxamine: An Angiogenic and Antioxidant Molecule for Tissue Regeneration. *Tissue Eng. - Part B Rev.* **2019**, *25*, 461–470, doi:10.1089/ten.teb.2019.0111.

145. Normant, V.; Josts, I.; Kuhn, L.; Perraud, Q.; Fritsch, S.; Hammann, P.; Mislin, G.L.A.; Tidow, H.; Schalk, I.J. Nocardamine-Dependent Iron Uptake in Pseudomonas aeruginosa: Exclusive Involvement of the FoxA Outer Membrane Transporter. *ACS Chem. Biol.* **2020**, *15*, 2741–2751, doi:10.1021/acschembio.0c00535.

146. Wang, G.Y.S.; Graziani, E.; Waters, B.; Pan, W.; Li, X.; McDermott, J.; Meurer, G.; Saxena, G.; Andersen, R.J.; Davies, J.; et al. Novel natural products from soil DNA libraries in a streptomycete host. *Chemtracts* **2001**, *14*, 223–226.

147. Iijima, M.; Someno, T.; Ishizuka, M.; Sawa, R.; Naganawa, H.; Takeuchi, T. TC202B and C, new siderophores with immunosuppressive activity produced by Streptoalloteichus sp. 1454-19. *J. Antibiot. (Tokyo).* **1999**, *52*, 775–780, doi:10.7164/antibiotics.52.775.

148. Sun, M.Y.; Ye, Y.; Xiao, L.; Rahman, K.; Xia, W.; Zhang, H. Daidzein: A review of pharmacological effects. *African J. Tradit. Complement. Altern. Med.* **2016**, *13*, 117–132, doi:10.4314/ajtcam.v13i3.15.

149. Sharifi-Rad, J.; Quispe, C.; Imran, M.; Rauf, A.; Nadeem, M.; Gondal, T.A.; Ahmad, B.; Atif, M.; Mubarak, M.S.; Sytar, O.; et al. Genistein: An Integrative Overview of Its Mode of Action, Pharmacological Properties, and Health Benefits. *Oxid. Med. Cell. Longev.* **2021**, *2021*, doi:10.1155/2021/3268136.

150. Wang, J.F.; Liu, S.S.; Song, Z.Q.; Xu, T.C.; Liu, C.S.; Hou, Y.G.; Huang, R.; Wu, S.H. Naturally Occurring Flavonoids and Isoflavonoids and Their Microbial Transformation: A Review. *Molecules* **2020**, *25*, doi:10.3390/molecules25215112.

151. Thamchaipenet, A. Maklamicin, an Antibacterial Polyketide from an Endophytic Micromonospora sp. **2011**, 670–674.

152. Daduang, R.; Kitani, S.; Sudoh, Y.; Grace Umadhay Pait, I.; Thamchaipenet, A.; Ikeda, H.; Igarashi, Y.; Nihira, T. 29-Deoxymaklamicin, a new maklamicin analogue produced by a genetically engineered strain of Micromonospora sp. NBRC 110955. *J. Biosci. Bioeng.* **2015**, *120*, 608–613, doi:10.1016/j.jbiosc.2015.04.004.

153. Wang, W.; Qiu, Z.; Tan, H.; Cao, L. Siderophore production by actinobacteria. *BioMetals* **2014**, *27*, 623–631, doi:10.1007/s10534-014-9739-2.

154. Yang, M.; Fazio, S.; Munch, D.; Drumm, P. Impact of Methanol and Acetonitrile on Separations Based on π-π Interactions with a Reversed-Phase Phenyl Column. *J. Chromatogr. A* **2005**, *1097*, 124–129, doi:10.1016/j.chroma.2005.08.028.

155. Ali, I.; Haque, A.; Saleem, K. Separation and identification of curcuminoids in turmeric powder by HPLC using phenyl column. *Anal. Methods* **2014**, *6*, 2526–2536, doi:10.1039/c3ay41987h.

156. Janas, P.; Bocian, S.; Jandera, P.; Kowalkowski, T.; Buszewski, B. Separation of flavonoids on different phenyl-bonded stationary phases-the influence of polar groups in stationary phase structure. *J. Chromatogr. A* **2016**, *1429*, 198–206, doi:10.1016/j.chroma.2015.12.024.

157. Joseph, A.; Rustum, A. Development and validation of a RP-HPLC method for the determination of gentamicin sulfate and its related substances in a pharmaceutical cream using a short pentafluorophenyl column and a Charged Aerosol Detector. *J. Pharm. Biomed. Anal.* **2010**, *51*, 521–531, doi:10.1016/j.jpba.2009.09.002.

158. Apffel, A.; Fischer, S.; Goldberg, G.; Goodley, P.C.; Kuhlmann, F.E. Enhanced sensitivity for peptide mapping with electrospray liquid chromatography-mass spectrometry in the presence of signal suppression due to trifluoroacetic acid-containing mobile phases. *J. Chromatogr. A* **1995**, *712*, 177–190, doi:10.1016/0021-9673(95)00175-M.

159. Shamikh, Y.I.; El Shamy, A.A.; Gaber, Y.; Abdelmohsen, U.R.; Madkour, H.A.; Horn, H.; Hassan, H.M.; Elmaidomy, A.H.; Alkhalifah, D.H.M.; Hozzein, W.N. Actinomycetes from the red sea sponge coscinoderma mathewsi: Isolation, diversity, and potential for bioactive compounds discovery. *Microorganisms* **2020**, *8*, doi:10.3390/microorganisms8050783.

160. Jayasinghe, C.D.; Jayawardena, U.A. Toxicity Assessment of Herbal Medicine Using Zebrafish Embryos: A Systematic Review. *Evidence-based Complement. Altern. Med.* **2019**, *2019*, doi:10.1155/2019/7272808.

161. Guarin, M.; Ny, A.; De Croze, N.; Maes, J.; Léonard, M.; Annaert, P.; de Witte, P.A.M. Pharmacokinetics in zebrafish embryos (Zfe) following immersion and intrayolk administration: A fluorescence-based analysis. *Pharmaceuticals* **2021**, *14*, doi:10.3390/ph14060576.

162. Al Shaer, D.; Al Musaimi, O.; de la Torre, B.G.; Albericio, F. Hydroxamate siderophores: Natural occurrence, chemical synthesis, iron binding affinity and use as Trojan horses against pathogens. *Eur. J. Med. Chem.* **2020**, *208*, 112791, doi:10.1016/j.ejmech.2020.112791.

163. Acquah, K.S.; Beukes, D.R.; Warner, D.F.; Meyers, P.R.; Sunassee, S.N.; Maglangit, F.; Deng, H.; Jaspars, M.; Gammon, D.W. Novel South African rare actinomycete Kribbella speibonae strain SK5: a prolific producer of hydroxamate siderophores including new dehydroxylated congeners. *Molecules* **2020**, *25*, 2979.

164. Bellotti, D.; Remelli, M. Deferoxamine b: A natural, excellent and versatile metal chelator. *Molecules* **2021**, *26*, 1–21, doi:10.3390/molecules26113255.

165. Hamamoto, T.; Beppu, T.; Seto, H. Leptomycins A and B, new antifungal antibiotics ii. structure elucidation. *J. Antibiot. (Tokyo).* **1983**, *36*, 646–650, doi:10.7164/antibiotics.36.646.

166. Zhang, H.; White-Phillip, J.A.; Melançon, C.E.; Kwon, H.; Yu, W.; Liu, H. Elucidation of the kijanimicin gene cluster: insights into the biosynthesis of spirotetronate antibiotics and nitrosugars. *J. Am. Chem. Soc.* **2007**, *129*, 14670–14683.

167. Lin, Z.; Koch, M.; Pond, C.D.; Mabeza, G.; Seronay, R.A.; Concepcion, G.P.; Barrows, L.R.; Olivera, B.M.; Schmidt, E.W. Structure and activity of lobophorins from a turrid mollusk-associated Streptomyces sp. *J. Antibiot. (Tokyo).* **2014**, *67*, 121–126, doi:10.1038/ja.2013.115.

168. Myers, O.D.; Sumner, S.J.; Li, S.; Barnes, S.; Du, X. One Step Forward for Reducing False Positive and False Negative Compound Identifications from Mass Spectrometry Metabolomics Data: New Algorithms for Constructing Extracted Ion Chromatograms and Detecting Chromatographic Peaks. *Anal. Chem.* **2017**, *89*, 8696–8703, doi:10.1021/acs.analchem.7b00947.

169. Wang, M.; Carver, J.J.; Phelan, V. V.; Sanchez, L.M.; Garg, N.; Peng, Y.; Nguyen, D.D.; Watrous, J.; Kapono, C.A.; Luzzatto-Knaan, T.; et al. Sharing and community curation of mass spectrometry data with Global Natural Products Social Molecular Networking. *Nat. Biotechnol.* **2016**, *34*, 828–837, doi:10.1038/nbt.3597.

170. Ono, K.; Demchak, B.; Ideker, T. Cytoscape tools for the web age : D3 . js and Cytoscape . js exporters [version 2 ; peer review : 2 approved]. **2022**, 1–13.

171. Horai, H.; Arita, M.; Kanaya, S.; Nihei, Y.; Ikeda, T.; Suwa, K.; Ojima, Y.; Tanaka, K.; Tanaka, S.; Aoshima, K. J. Mass Spectrom. 2010.

172. Audoin, C.; Bonhomme, D.; Ivanisevic, J.; De La Cruz, M.; Cautain, B.; Monteiro, M.C.; Reyes, F.; Rios, L.; Perez, T.; Thomas, O.P. Balibalosides, an original family of glucosylated sesterterpenes produced by the Mediterranean sponge Oscarella balibaloi. *Mar. Drugs* **2013**, *11*, 1477–1489, doi:10.3390/md11051477.

173. Lauritano, C.; Martín, J.; De La Cruz, M.; Reyes, F.; Romano, G.; Ianora, A. First identification of marine diatoms with anti-tuberculosis activity. *Sci. Rep.* **2018**, *8*, 1–10, doi:10.1038/s41598-018-20611-x.

174. Zhang, J.H.; Chung, T.D.; Oldenburg, K.R. A Simple Statistical Parameter for Use in

Evaluation and Validation of High Throughput Screening Assays. *J. Biomol. Screen.* **1999**, *4*, 67–73, doi:10.1177/108705719900400206.

175. Prabst, K.; Engelhardt, H.; Ringgeler, S.; Hubner, H.; Ates, G.; Vanhaeke, T.; Rogiers, V.; Rodrigues, R.; Chan, L.L.-Y.; McCulley, K.J.; et al. *Chapters 1-4, 8: Cell Viability Assays*; 2017; Vol. 1601; ISBN 978-1-4939-6959-3.

176. Danieau's Solution (30×). Cold Spring Harbor Protocols. 2011. Available online: http://cshprotocols.cshlp.org/content/2011/7/pdb.rec12467.full (accessed on 6 July 2023).

177. Kilkenny, C.; Browne, W.J.; Cuthill, I.C.; Emerson, M.; Altman, D.G. Improving Bioscience Research Reporting: The Arrive Guidelines for Reporting Animal Research. *PLoS Biol.* **2010**, *8*, 6–10, doi:10.1371/journal.pbio.1000412.